Metabolomic analyses of *Drosophila* models for human renal disease

A thesis submitted for the degree of Doctor of Philosophy in the University of Glasgow

By

Yahya Hasan Hobani

0509909h

Institute of Molecular Cell and Systems Biology

College of Medical, Veterinary and Life Sciences

University of Glasgow

2011

The research reported within this thesis is my own work except where otherwise stated, and has not been submitted for any other degree.

Yahya Hasan Hobani

Abstract

Inborn errors of metabolism (IEMs) constitute a major class of genetic disorder. Most of IEMs are transmitted recessively, so consanguinity has a huge impact on disease prevalence, particularly in societies like Saudi Arabia, where consanguineous marriage is common. Understanding and treatment are very important in genetic diseases, and simple models would be helpful. Thus, the feasibility of applying the fruit fly, *Drosophila melanogaster*, as a model for a human renal genetic disease - xanthinuria - was investigated. Xanthinuria is a rare human genetic disease, caused by mutations in xanthine oxidase or molybdenum cofactor sulphurase; in *Drosophila*, the homologous genes are *rosy* (*ry*) and *maroon-like* (*mal*), respectively.

The new Orbitrap technology of mass spectrometry has the potential to determine levels of many metabolites simultaneously by exact mass, and a major part of this thesis was to investigate the utility of Orbitrap technology in metabolomics of both wild-type and *Drosophila* mutant. Repeatable significant differences were identified between *ry* and wild-type flies, which recapitulated painstaking analytical biochemical determinations of the 1950s, but with greater precision. Additionally, completely novel impacts of the *ry* mutation (on pyrimidine metabolism, the urea cycle and osmolyte biosynthesis) were identified.

As expected *mal* mutants showed more similar changes as *ry*, but with widespread metabolic perturbations..

The online resource, FlyAtlas.org, provides detailed microarray-based expression data for multiple tissues and life-stages of *Drosophila*. Downstream genes, such as urate oxidase, are utterly tubule-specific. Accordingly, the utility of Orbitrap technology in elucidating tissue-specific metabolomes was also investigated. Additionally, genetic interventions using designed RNAi constructs were also made and validated by QPCR and metabolomics. As urate is a potent antioxidant, survival of *urate oxidase* knockdowns was tested *in vivo*, and a significant impact on survival identified.

An Affymetrix microarray was performed, comparing *ry506* mutant flies against wild-type and differences were identified in a second experiment, the anti-gout drug allopurinol was used to phenocopy the effects of *ry*.

Overall, the thesis showed that Orbitrap technology was highly suitable for metabolomic analysis of both wild-type and mutant *Drosophila*, and had potential in the analysis of metabolomes of single tissues. The possibility of using Orbitrap-based metabolomics in human diagnosis is discussed.

Acknowledgements

First of all, I thank Allah for finishing and completing this long and hard project.

I am very grateful to my patient supervisor Professor Julian Dow. I consider my self very lucky that I was given the opportunity to be trained in his lab. I also would like to express my gratitude to Professor Shireen Davies who has been a hidden soldier in supporting and motivations.

Also I would like to thank all my colleagues and coworkers in the laboratory for their cooperation, helping, and their entertaining and helpful discussions.

My thanks also flow along the river Clyde to our collaborators in Strathclyde University, Glasgow. Dr. Dave Watson, Anas Mohamad Khamleh and Mohammad Al-Barrati for their help and collaboration.

I also do not forget those whom always considered and worried about my study and carrier, whom I will never ever in my life will fulfill their efforts for me, my mum and dad.

To my small family, wife and children, I say the time has come to our souls to be together back again for ever. I regret I was mentally and physically away but the time has finally come.

The unforgettable Saudi friends whom I have learned a lot form them, I gave my warmest regards.

Finally, I would like to thank the government of Saudi Arabia for funding my studies in the great Glasgow especially the PhD project.

Table of contents

List of tables

List of figures

Abbreviations

3MCC 3	3-methylcrotonyl-coenzyme A carboxylase deficiency.
AMP	adenosine monophosphate
ANOVA	analysis of variance
AO	aldehyde oxidase
APRT	adenine phosphoribosyltransferase
ASD	argininosuccinic Acid Synthetase Deficiency
ASL	Argininosuccinate lyase
ATP	adenosine triphosphate
BKT	Ketothiolase Deficiency
cDNA	complementary DNA
Cho	Chocolate
Cin	Cinnamon
CyO	curly of Oster
DNA	deoxyribonucleic acid
dNTP	deoxyribonucloetide triphosphate
EI	Electron impact
ESI	Electrospray ionization
FDA	Food and Drug Administration
FT-ICR	Fourier transform ion cyclotron resonance
G1P	Glucose 1 phosphate
G3P	Glucose 3 phosphate
G6P	Glucose 6 phosphate
G6PD	glucose 6 phosphate dehydrogenase
GA-I	Glutaric Acidemia Type 1
Gal-1-P	galactose 1 phosphate
Galt	galactose-1-phosphate uridyl transferase
GC-MS	Gas chromatography MS
GTP	guanosine-5'-triphosphate
H2O2	Hydrogen peroxide
HGPRT	hypoxanthine-guanine phosphoribosyltransferase
HMG	3-hydroxy-3-methylglutaryl-coenzyme A lyase deficiency
IEM	Inborn errors of metabolism

IVA	Isovaleric Acidemia
LC-MS	Liquid chromatography MS
LNS	Lesch-Nyhan Disease
Lxd	Low xanthine dehydrogenase
M	molar
Mal	maroon-like
MALDI	Matrix assisted laser desorption ionization
MCAD	Medium-chain acyl-coenzyme A dehydrogenase deficiency
Moco	molybdenum cofactor
MG	Midgut
MgCl2	Magnesium chloride
mM	millimolar
MMA	Methylmalonic Acidemia
Moco	Molybdenum cofactor
MPT	Molybdopterin
MSUD	Maple syrup urine disease
NaCl	sodium chloride
NAD+	Nicotinamide Adenine Dinucleotide
NADH	Nicotinamide Adenine Dinucleotide reduced
NADPH	Nicotinamide adenine dinucleotide phosphate
NO	Nitric oxide
NOS	Nitric oxide synthase
O2	Oxygen
O2-.	Superoxide
PA	Propionic Acidemia
PCR	Polymerase chain reaction
PKD	Polycystic Kidney Disease
PKHD	Polycystic kidney and hepatic disease
PKU	Phenylketonuria
PO	Pyridoxal oxidase
Q-PCR	Quantitative polymerase chain reaction
ROS	Reactive oxygen species
rp49	Ribosomal protein 49
RT-PCR	Reverse transcriptase polymerase chain reaction
ry	*rosy*

GSD-1	Glycogen storage disease type I
SO	Sulphite oxidase
TOF	Time of flight
UAS	Upstream activating sequence
XDH	Xanthine dehydrogenase

Chapter 1 Introduction

1.1 Human genetic disease

Many human diseases are either genetic or have a genetic contribution (Goh et al., 2007). Scientists have classified genetic diseases into subcategories, namely; multi-factorial, chromosomal, mitochondrial and single gene disorders. Multi-factorial diseases are caused by a mixture of environmental factors and mutations (or polymorphisms) in multiple genes. Some examples include diabetes, cancer, and obesity. Because of their nature, management of multifactorial diseases is more complicated than the other types. Chromosomal diseases are caused by abnormalities in chromosomal number or structure. Usually several or many genes are defective, for example in Down syndrome (trisomy 21). In mitochondrial diseases, chromosomal DNA is intact but rather the mitochondrial DNA carries mutations. Each mitochondrion contains 5 to 10 circular pieces of maternally-inherited DNA. An example is Leber's hereditary optic neuropathy (LHON), caused by defects in genes encoding subunits of mitochondrial complex I. The fourth category (single gene disorder) is of particular relevance to this thesis. Single gene disorders are classified into further groups according to mode of inheritance, into autosomal, dominant or recessive, or X-linked recessive.

Diseases of dominant or mitochondrial inheritance are rarely found in the neonatal period; however, autosomal or X-lined recessive inheritance constitute the major causes of disease development (Ellaway et al., 2002).

As previously mentioned, all categories of genetic disease are found worldwide; however, the autosomal recessive mode of inheritance is particularly favoured by factors (for example, geographical isolation, close tribal affiliations, large family size and a culture of consanguineous marriage (Al-Gazali et al., 2006)) that are common in the Arab countries (Figure 1-1).

In Saudi Arabia, for example, certain inborn errors of metabolism (IEM) are far more common than in the western world (Table 1-1), and neonatal screening must thus be more comprehensive. These unique inborn errors of metabolism are attributed to the consanguineous marriages practiced in the Arab world, especially in a country like Saudi Arabia (Al-Odaib et al., 2003).

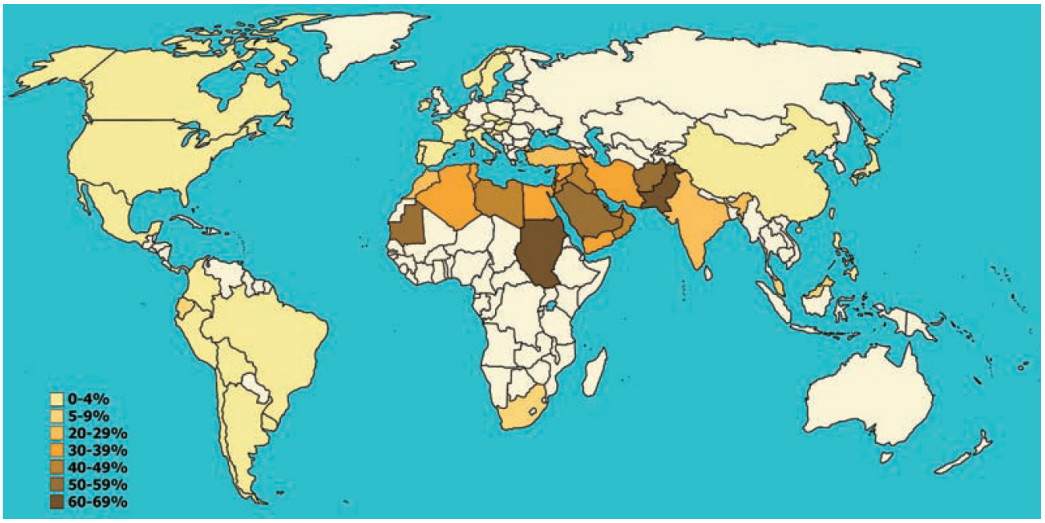

Figure 1-1. Distribution of consanguineous (second cousin or closer) marriages worldwide. (Tadmouri et al., 2009).

Table 1-1. Incidence of selected IEMs in Saudi Arabia compared to Europe and USA. Personal communication from Dr. Hazem Ghneim: (Ghneim, 2010)

Disease	KSA	Germany	USA
PKU	1: 10,528	1:10,400	1: 19,000
MSUD	1: 6,016	1: 250,000	1: 940,000
ASL	1: 8,423	1: 250,000	1: 940,000
ADSL	1: 16,845	No cases	1: 190,000
HMG	1: 42,113	No cases	No cases
IVA	1: 42,113	1: 62,500	1: 130,000
MMA	1: 5,615	1: 125,000	1: 90,000
PA	1: 42,113	1: 250,000	1:300,000
BKT	1:84,226	No cases	1: 470,000
GA-I	1: 42,113	1: 83,300	1:190,000
MCAD	1:1:12,032	1: 20,800	1:13,000
3MCC	1:10,528	1: 125,000	1:36,000
Total screened	84,226	250,000	940,000
Overall incidence	**1: 732**	**1: 2,400**	**1: 4,300**

PKU; Phenylketonuria; MSUD, Maple syrup urine disease; ASL, Argininosuccinate lyase; ADSL, Adenylosuccinate Lyase deficiency; HMG, 3-hydroxy-3-methylglutaryl-coenzyme A lyase deficiency (also known as HMG-CoA lyase deficiency); IVA, Isovaleric Acidemia; MMA, Methylmalonic Acidemia; PA, Propionic Acidemia; BKT, Ketothiolase Deficiency; GA-I, Glutaric Acidemia Type 1; MCAD, Medium-chain acyl-coenzyme A dehydrogenase deficiency; 3MCC, 3-methylcrotonyl-coenzyme A carboxylase deficiency.

1.2 Consanguinity in the Arab world

All humans are heterozygous for several lethal recessive mutations (Consortium, 2010). In an outbred genetic system this is not a severe problem. However, in societies with high levels of consanguineous marriage, the impact will be severe. In Arabic communities for example, first or second cousin marriages are very common (Figure 1-2). Consequently, autosomal recessive disorders, when present, are unsurprisingly going to spread in this community. So when parents are both heterozygous for a given mutation, any child has a 25% likelihood of being affected. In Saudi Arabia, in particular, consanguinity rates are about 50%, of which 60% are at a first-cousin level of consanguinity (El Mouzan et al., 2008); furthermore, the Kingdom is considered to have one of the highest birth rates in the Middle East and North Africa (Saadallah and Rashed, 2007).

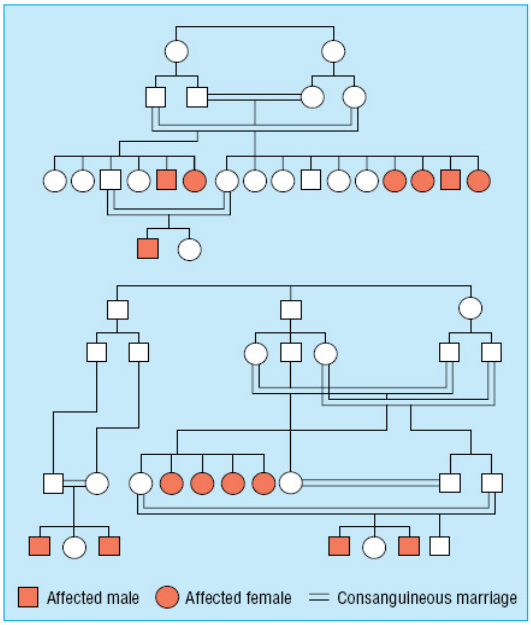

Figure 1-2. High level of consanguinity among Arabs (Al-Gazali et al., 2006). Two Arab family pedigrees, showing intermarriages over several generations.

So premarital screening programmes for congenital diseases could help significantly to limit the incidence and impact of inborn errors of metabolism. In the Jewish population, for example, Tay-Sachs disease incidence is ten times higher when compared with other races (Myerowitz and Costigan, 1988). Thus, an effective premarital screening program (Kaback et al., 1993) and carrier detection (Kronn et al., 1998) are very important (Kaback et al., 1993). At the same time, global population screening-based programs are also indicated (Kaback, 2000) and (Bach et al., 2001).

Although premarital screening is an ideal solution, it is not always practical or economic; so in practice both diagnosis and treatment must also be researched. In order to have better understanding, and to improve management of human genetic disorders, good animal models are desirable. The requirements of such models are discussed further in section 1.5.

1.3 Inborn errors of metabolism (IEMs)

This term was coined by Sir Archibald Garrod, the British physician, to describe a group of disorders which result from failure of steps in a biochemical pathway (Houten, 2009). Inborn errors of metabolism (IEMs) consist of a group of largely monogenic disorders. The clinical manifestations appear as results of an enzyme malfunction a few examples can be seen in Table 1-2 and Figure 1-3.

Table 1-2. Possible impacts of inborn errors of metabolism.

No.	Type of disease	Example	Defective enzyme
1	Lack of immediate product	GSD-I	G6P
2	Accumulation of immediate precursor	Galactosemia	GALT
3	Accumulation of remote precursor	G6PD, PKU	G6PDH, PAH
4	Failure of feedback inhibition	LNS	HGPRT

GSD-I; Glycogen storage disease type I , G6P; Glucose-6-phosphatase, GALT; galactose-1- phosphate uridyl transferase, G6PD; Glucose-6-phosphate dehydrogenase deficiency, G6PDH; Glucose-6-phosphate dehydrogenase, PKU; Phenylketonuria, PAH; phenylalanine hydroxylase, LNS; Lesch-Nyhan syndrome, HGPRT; Hypoxanthine-guanine phosphoribosyltransferase. (Pinksy, 1972).

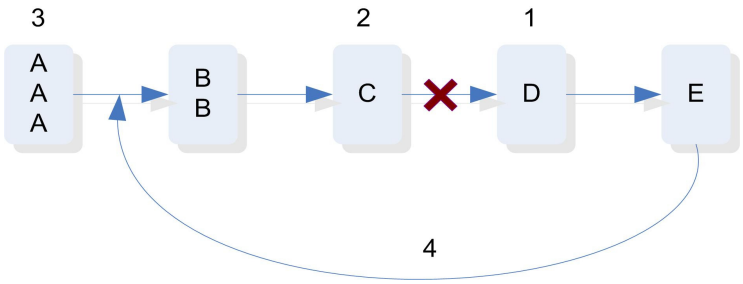

Figure 1-3. Possible impacts of biochemical inhibition (Pinksy, 1972)

In some inborn errors of metabolism, one or more of these biochemical effects produce the final metabolic and pathological picture. For example, in glycogen storage disease type I (GSD-I), glycogen is accumulated in different tissues, namely liver, intestinal mucosa and kidney. This happens as a remote effect of the absence of G6P, the enzyme

responsible for converting glucose-1-phosphate (G1P) to glucose, as shown (number 3) in Figure 1-3. Furthermore, the same enzyme is also responsible from producing glucose from its precursor G3P, which then will be taken into erythrocytes. Absence of the enzyme G6PDH reduces the glucose supply to erythrocytes. This makes the RBCs susceptible to haemolytic anaemia; this is represented as number 1 in Figure 1-3. The GSD disease pathway is summarized in Figure 1-4.

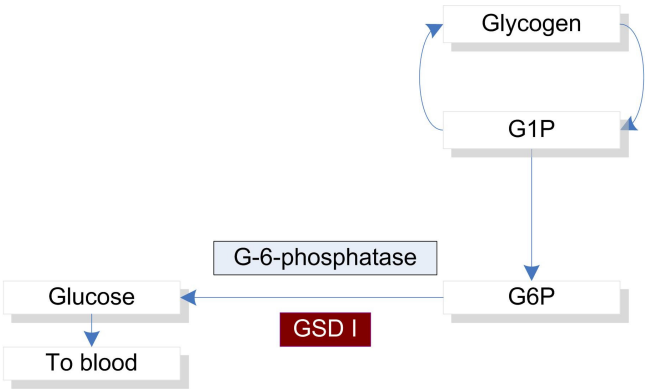

Figure 1-4. Glycogen storage disease type I.

Another example of a metabolic disease that arises as a result of accumulation of an immediate precursor (number 2 in Figure 1-3), is galactosemia. It is an autosomal recessive monogenic metabolic disorder, in which it is not possible to convert galactose to glucose because of the absence of galactose-1-phosphate uridyltransferase (GALT). If not functioning, accumulation of the immediate precursor, which is Gal-1-P, will be obvious. The later, when precipitated within tissues, becomes toxic.

Also, accumulation of chemical compound as a result of a mutated enzyme sometime leads to toxicity. For example, in phenylketonuria, the absence of phenylalanine hydroxylase enzyme leads to accumulation of phenylalanine, which leads to progressive mental retardation.

Metabolic diseases can also result from defects in feedback inhibition Figure 1-5, for example in Lesch-Nyhan syndrome. The defective enzyme is hypoxanthine-guanine phosphoribosyltransferase (HGPRT), which is part of the purine salvage pathway. It inhibits the biosynthesis of purine from hypoxanthine and guanine. Thus in the absence of this inhibition feedback mechanism, excessive uric acid production takes place. This can lead to disorders such as gout.

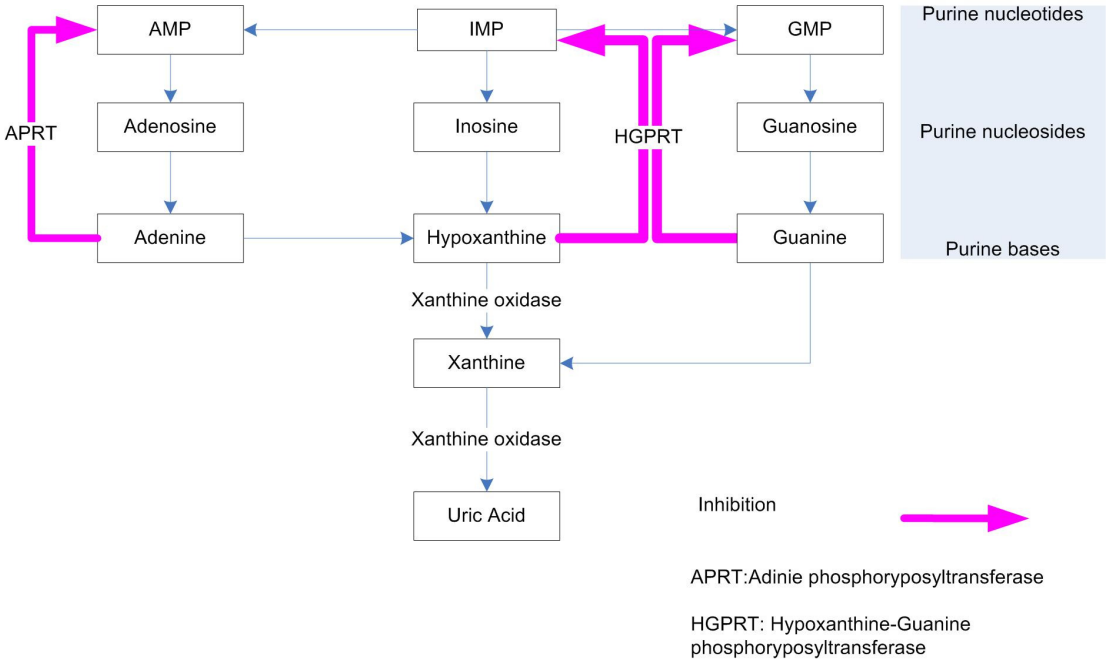

Figure 1-5. Purine biosynthesis -Salvage pathway.

1.3.1 Clinical classification of IEMs

IEMs can be clinically classified into two main categories; I and II (Martins, 1999). Diseases which affect the functional or anatomical system are categorized as category I. The symptoms are clearer and less complicated than category II. Diseases in this category usually affect a specific functional or anatomical system for example the endocrine system, immune system or coagulation factors. The symptoms are consistent and can easily direct the physician to the defective biochemical pathway. For example, a prolonged coagulation time can be a clear indicator of a defect in one of the coagulation factors (Martins, 1999).

On the other hand, category II diseases need careful and thorough investigation. This occurs when the affected metabolic pathway is responsible for a common job in multiple different cells and organs. Diseases from this category have wide clinical diversity, and the disease can manifest as either primary or even as secondary effect of a metabolic pathway. They can be divided into three groups (Figure 1-6). Disturbance of biosynthesis or catabolism constitute the first group. As a result of this disturbance, complex molecules accumulate in some vital sites, such as lysosomes. Thus they are called lysosomal disorders, such as Gaucher disease. Diseases from group two, lead to acute or chronic intoxication. Amino acids related-disorders are the main cause of this

group. Examples are: cystinuria, phenylketonuria and Maple syrup urine disease. The last, group three, is related to energy deficiency or production diseases. This group includes disturbance in the glycolysis and gluconeogenesis defects (Martins, 1999).

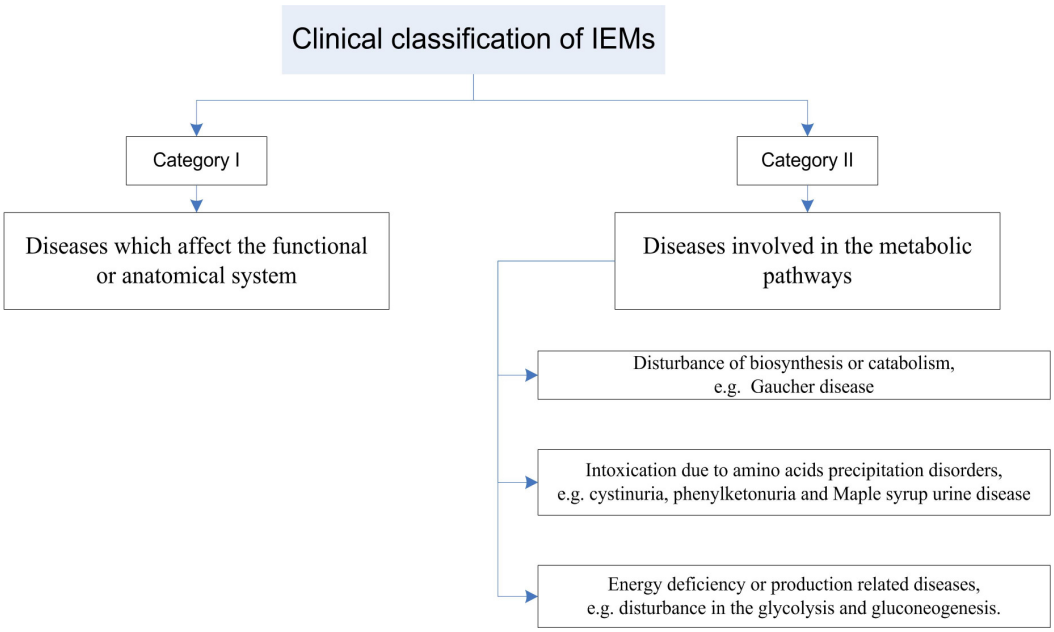

Figure 1-6. Clinical classification of IEMs according to Martins, 1999.

1.3.2 Sample selection for diagnosis

Sample selection varies differently according the metabolic diseases being investigated. Samples could be of whole blood, serum, plasma and even urine. Samples are typically collected into a collection tube with or without anticoagulant. Recently, Guthrie card blood spots for sample collection for inborn errors of metabolism have formed the basis for neonatal screening programs.

The analysis principles and application, later on, varied widely using different detection methods; spectrophotometric, radiochemical, or mass-spectrometric methods. These detection methods provided a powerful selective screening tool for different inherited disorders. However, the above methods for neonatal screening of metabolic disorders have common disadvantages: limited diseases covered by each method, high false-positive rates, and low specificity or sensitivity (Rashed et al., 1997).

All of those and others disorders are nowadays are mostly diagnosed using mass spectrometry. This method is increasingly updated and new analyzers being discovered in order to have better and early diagnosis.

1.4 Congenital kidney disease

Most of the genetic renal diseases in human are related to polycystic kidney disease (PKD). The frequency was estimated to be between 1 in 500 and 1 in 1,000 live births (Rossetti et al., 2007). It is characterized by accumulation of fluids containing cysts in the renal parenchyma. This diseases can be inherited either as dominant or recessive autosomal forms. The dominant form of the disease mainly affects adults and is caused by defective proteins polycystin 1 or polycystin 2, which are encoded by the *PKD1* and *PKD2* genes respectively (Figure 1-7). However, the onset of the recessive form is earlier, either in infancy or in early childhood. It is mainly caused by a defective protein called fibrocytin, which is encoded by polycystic kidney and hepatic disease (*PKHD*) gene (Patel et al., 2009).

Recently, a study suggested that a cellular organelle, the cilium, has a major role in the cause of the PKD in all previously mentioned forms of inheritance (Yoder, 2007). It is located in the top of most body cells and it is hair-like structure. It has an important role in cell proliferation and growth by transducing mechanosensory signals. Thus, any mutation in the genes which are involved in ciliary function will lead to PKD (Figure 1-8). As a result, fluid transport will also affected; and with time, cells become full with fluids. Consequently, with gradual swollen cells become full with fluids and cyst. Finally the whole kidney becomes enlarged and end-stage polycystic diseases arises (Patel et al., 2009). This particular disorder is an example of one that cannot be modelled in *Drosophila* MT, as *Drosophila* cells (with the exceptions of sperm and some sensory cells) lack primary cilia (Zhang et al., 2004).

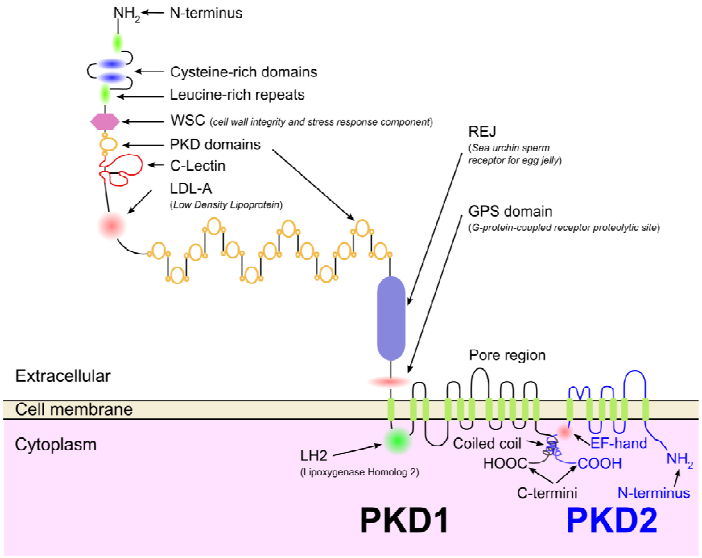

Figure 1-7. Structure of PKD 1and 2 after (Stayner and Zhou, 2001).

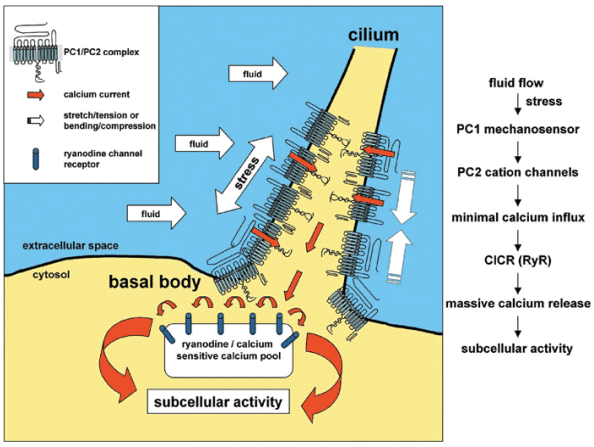

Figure 1-8. Signal transduction by cilium. The function of the cilia is to sense fluid movement. PC1, acts as a sensory molecule for fluid that transmits the signal from the extracellular to PC2, it also produces sufficient Ca^{2+} influx to activate intracellular ryanodine receptors (RyR). This leading to local increase in the cytosolic Ca^{2+} concentration. This increase in the cystolic Ca^{2+}, regulates numerous molecular activities inside the cell that contribute to tissue development (Nauli et al., 2003).

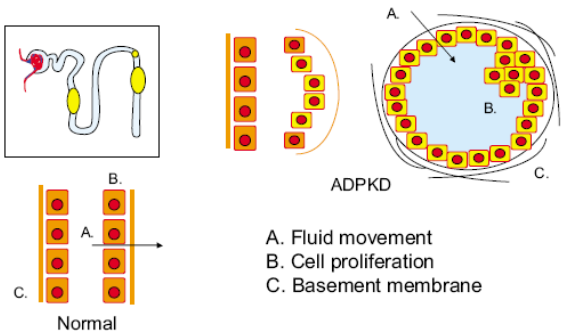

Figure 1-9. Mechanism of progression of PKD. Mutation in *PKD* 1 & 2 genes which encoding the proteins polycystin 1 and 2 leads to abnormalities in tubular fluid secretion (A), cell proliferation (B) and tubular basement membranes (C), all of these are give rises in renal cysts (Bennett, 2009).

However, many IEMs also have renal consequences. This can be because the kidney is unable to clear sufficient quantities of accumulating metabolite; this can typically precipitate to form concretions called kidney stones, and so block the kidney. The term *nephrolithiasis* refers to stone formation within the kidney itself, and *urolithiasis* to formation within the broader urinary tract; both are possible consequences. An example of a congenital inherited disorder which affects the kidneys is Xanthinuria type I. It is an autosomal recessive genetic disease where the enzyme xanthine oxidase is absent. This enzyme is responsible for converting hypoxanthine to xanthine and then to uric acid. In the absence of this enzyme, uric acid production is reduced sharply; and as a result the

substrates, hypoxanthine and xanthine, accumulate. The consequences of this disorder is explained in detail in (Dent and Philpot, 1954).

1.5 Animal models for IEMs

When the human genome project started, it was thought that answers about human hereditary diseases would emerge rapidly (Collins and Mansoura, 2001). However, this massive effort mostly produced the sequence of the genome, and did not of itself cure any human disease (Sachidanandam et al., 2001). It became clear around a third of all genes were entirely novel. How could their function be elucidated?

So for this reason the approach of reverse genetics has emerged. Reverse genetics, unlike forward genetics, is moving from the genotype to phenotype (Lewin, 1986; Orkin, 1986; Ruddle, 1982). This means selecting a target gene, then mutating it either by knockdown or overexpression, then looking for a phenotype. If a suitable model is available, it is possible to perform physiological, behavioural or metabolomic experiments.

1.5.1 Mouse

The mouse is the closest related genetically tractable model to human. It is a mammal, and it has defined body organs such as kidneys, heart, lungs and blood. Transgenic lines are available in several genomic centres around the world (Dow, 2007). All of these characteristics make it a very useful animal model. Furthermore, the whole mouse genome has been sequenced. However, can all of these features make it the exclusive candidate for all research purposes including genetic studies? The answer is not necessarily “yes”.

Different models have different advantages depending on the question to be addressed. For example, when studying DNA replication, *E. coli* is the best model, as it reproduces every 20 minutes. Thus, it is not surprising that the Nobel prize for the study of DNA replication was awarded for work on bacteria (Berg and Lehman, 2007) (Dow, 2007).

Furthermore, in the genetic study, transgenic technique is crucially important to produce mutations of specific genes and to intervene in a tissue-specific way. In mouse, this procedure it must be planned carefully in terms of cost and time. Constructing a transgenic mouse needs several years. There is a huge financial outlay that can reach

$100,000 and continuing cost of $10,000 per year to maintain a single line (Dow, 2007). Therefore, mouse is not automatically always the best choice as an animal model for genetic diseases.

1.5.2 *Drosophila*

So we argue that *Drosophila melanogaster* has clear advantages for studying some human disease genes, applying the reverse genetic approach. This is based on the rich information available for researchers. For example, availability of the completed *Drosophila* genome sequence (Adams MD, 2000), the tens of thousands of available classical mutants in stock centres, RNAi stocks for nearly every gene (Dietzl et al., 2007), and the FlyAtlas.org (Chintapalli et al., 2007) and Homophila (Reiter et al., 2001) websites. The last two web sites are for finding the best tissue to select for studying, and the fly gene homologues to human disease genes respectively.

In contrast with mouse, a transgenic fruit-fly line can be made for approximately $500 in only three months and costs $30 per year to maintain (Dow, 2007). Further details of *Drosophila melanogaster* as genetic model are discussed in section (1.6 Droso. As a genetic model) 1.6.

On the other hand, *Drosophila* as an invertebrate, suffers from some limitations particularly when trying to model genes involved in specifying specifically vertebrate or mammalian characteristics, for example creating the four-chambered heart, ducts of mammary glands or bone calcification diseases (Bier, 2005).

1.5.3 When to choose *Drosophila* vs. mouse

Despite all of this, all experimentally animal models are vitally important for research. However, answering some specific biological questions which will persuade an individual to select one over the other (Figure 1-10). For example, some inherited metabolic disorders, like Xanthinuria type I, cannot be studied in mouse. The reason behind that is the defective xanthine oxidase enzyme, which is responsible for xanthinuria, also interferes with milk production in mouse (Wu et al., 1994), (Vorbach et al., 2002). Thus, mutated female lines are unable to produce the necessary milk to their progenies. While, in *Drosophila*, it is not only easy to find a mutant, but

constructing a transgenic line and targeting the effect specifically to Malpighian tubules can be done relatively easily.

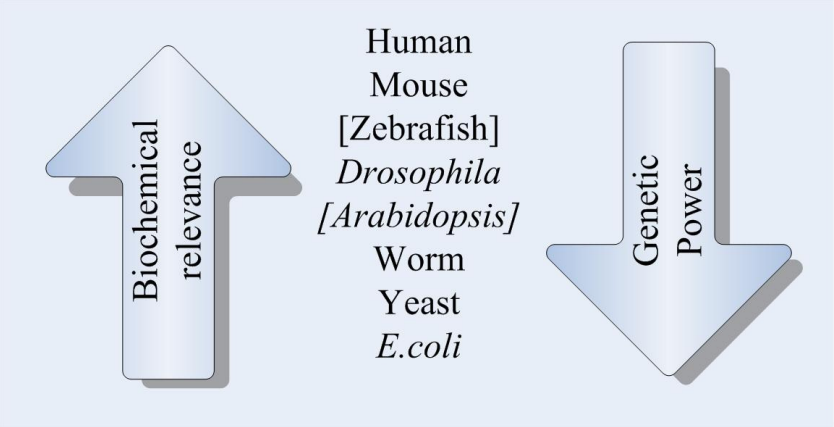

Figure 1-10. Trade-off between genetic power and biochemical relevance (Dow, 2007).

1.6 *Drosophila* as a genetic model

Drosophila melanogaster has drawn scientists' attention for approximately 100 years, since T.H. Morgan described the first ever discovered *white* mutant. Since that time, *Drosophila melanogaster* has been extensively used to research biological status in health and disease conditions.

Drosophila, or fruit fly as others call it, is one of the best and powerful genetic animal models being used; this is due to its short life cycle, which allows multiple generations to be screened quickly. The availability of full *Drosophila* genome sequence is another advantage. The small size of the insect makes it better than many other animal models in terms of space in the lab and food requirements.

At the molecular level, balancers and P-elements provide powerful genetic tools for gene transformation and phenotype selection. Interfering RNA is also one of the important molecular genetic tools which helps in field of functional genomics, specifically reverse genetics.

1.6.1 P-elements

There are many transposon families naturally found in the *Drosophila* genome, the best known of which is the P-element. They are important because they are extensively used in constructing and generating transgenic flies. The P-element normally contains one gene, which encodes the transposase enzyme, required for transposition to take place.

This transposable element is autonomous, and is 2.9 kb in size, so they have the ability to jump from plasmids into the germlines of the fly. At the same time in the genome, smaller incomplete P-elements are present and it is believed that they were generated as a result of deletions in the original P-element. The difference between the two P-elements apart from the size is that the smaller ones are non-autonomous (Rubin and Spradling, 1983).

1.6.2 Enhancer trapping

Enhancer trapping provides a powerful method to map patterns of gene expression in a fly or embryo. It also allows the identification of genes that are expressed in a particular pattern (O'Hare and Rubin, 1983) (Brand and Perrimon, 1993).

In most engineered P-elements, the transposase gene is substituted with a genetic cargo of choice, together with a reporter gene, mini-white, downstream or a ubiquitous promoter, allowing the presence of a P-element to be scored visually in a w^- background. So this line has a non-motile or trapped P-element. These flies are then crossed with another line carrying germline-expressed transposase, mostly from the Δ2,3 line which contains an incompletely excised (and thus immotile) P-element. So in such a cross, the P-element is going to jump only in the germline of the progeny. In subsequent generations, flies with red eyed colour are selected for further experimentation (Guo, 1996).

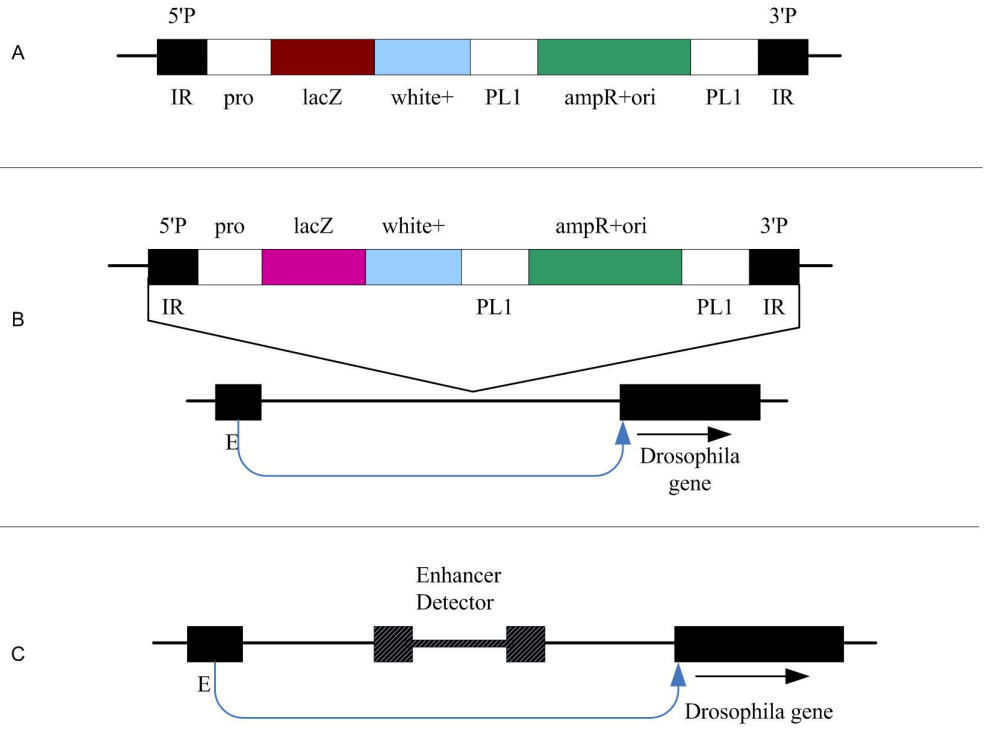

Figure 1-11 Schematic diagram of first generation enhancer trap. A) The main features of the *Drosophila* transposons. B) Transposon could be inserted between the gene regulatory elements and a gene. C)The gene specific regulatory elements can drive the expression of LacZ.

1.6.3 GAL4-UAS system

Using P-elements with a marker gene like white, the transgenes are introduced into the flies with the help of a helper plasmid encoding transposase into w^- flies to visibly identify transgenesis. However, some random insertions show lethality when they were made homozygous. This is because of the insertion of the P-element into an essential place in the genome.
In this case these flies will be made heterozygous using the help of balancer chromosomes that do not allow recombination.

GAL4 is a transcription factor that is naturally found in yeast ((O'Kane and Gehring, 1987)). It has been applied to be used in activating the gene transcription in *Drosophila*. By itself, GAL4 has no target gene in the *Drosophila* but will specifically drive expression of the transgenes under the control of upstream activating sequence (UAS). Both GAL4 and UAS comes in a bipatriate system developed by brand and perrimon

(1993). The GAL4 is either randomly inserted in the genome of the fly or fused downstream of a promoter sequence which constitute one component. The other component is the transgene of interest cloned under the control of UAS.

When these two systems or in other words flies are mated they will give rise to the progeny that have both components. This in turn activate the transgene under the control of UAS by the GAL4-specific expression manner. As the GAL4 expression depend on the upstream elements it was inserted or fused with, this system is useful in elucidating tissue- and cell-specific functions. For example, GAL4 can be placed under the control of the *urate oxidase* gene promoter as this gene is expressed exclusively in the Malpighian tubules, the Uro-GAL4 line drives transgene expression with exquisite precision in these tissues (Terhzaz et al., 2010). This is not as easy as it sounds, it have some problems and do not always work because some gene's promoters not necessarily at the start of the gene , so enhancer trap do not always reflect expression of the gene. Another possibility, inserts may unintentntially disrupt a gene. Also, RNAi may not be effective, or may have off-target effects.

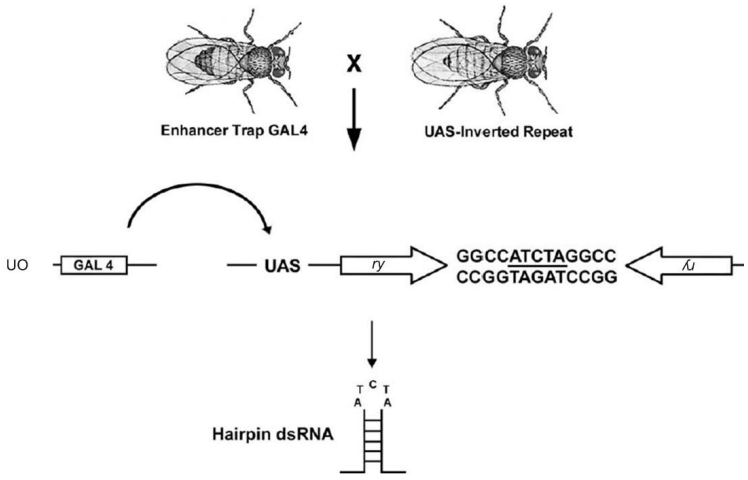

Figure 1-12. The GAL4 UAS system. This diagram showing the GAL4-UAS system in gene expression. The expressed gene in this case is an inverted repeat that gives a hairpin-like dsRNA which silences a targeted gene (Brand and Perrimon, 1993).

1.6.4 Balancer chromosomes

As recessive lethal mutations must be kept alive by providing a functional gene in trans, in most species it is necessary to select for the mutant gene in every generation, so adding hugely to the cost and complexity of genetic research. A key advantage of Drosophila is the relative ease of keeping recessive lethal alleles alive, so allowing large stock centres to be built. Here comes the usefulness of balancer chromosomes. A balancer is a region which prevents recombination between homologous chromosomes during meiosis. This feature is gained from the presence of an inverted region or a series of inversions on it.

Typically, balancer chromosomes in the Drosophila melanogaster contain three important features: (i) multiple inversions to suppress the recovery of viable recombination products over the length of the chromosome; (ii) a dominant visible phenotype that enables the inheritance of the chromosome to be tracked easily in progenies; and (iii) a recessive lethal mutation that eliminates the homozygous balancer from the population of breeding flies.

The inverted regions entirely prevent crossover. The markers also make it very clear where the balancer is, even if it is visually indistinguishable from wild-type. This makes genetic crosses with balancers totally predictable.

Even though mutations are often detrimental, if left in a stock of flies with a wild-type counterpart, after a number of generations they will be lost. Some can be kept on their own, if they are viable enough, but some mutations are poorly viable, or totally lethal. In this case, in order for the stock of flies to persist, a wild-type copy of the gene must be present to rescue the lethality. If present on a wild-type chromosome, the mutation will be lost from the stock as the wild-type chromosome takes over. However, if the wild-type copy is present on a balancer, the balancer cannot take over as they are homozygous lethal.

In the case of a recessive lethal mutation, only files containing the lethal chromosome and the balancer can survive.

1.6.5 Heritable RNAi

The complete sequencing of *Drosophila melanogaster* has encouraged researchers to investigate the function of each gene (Adams MD, 2000). The reverse genetic approach is considered as the best choice of elucidating gene function by generating loss of function phenotype. To cause a gene malfunction, RNA interference (RNAi) technique may be the best choice, because it tends to produce viable hypomorph, rather than (possibly lethal) nulls. This then allows physiological studies. Double-stranded RNAi is widely used to inactivate genes of interest and provide a powerful tool for gene function studies (Fire et al., 1998).

However, gene silencing by injected dsRNA is transient and consequently is not going to be heritable. So heritable dsRNA is highly desirable as an experimental tool. So more advanced methods were developed to construct plasmids that are able to express dsRNA into transgenic fly. Furthermore, those plasmids or vectors after transcription produce inverted repeats or hairpin RNA loops that are substrates for the RISC complex, so generating dsRNA (Kennerdell and Carthew, 2000).

However, cloning long inverted repeats into a plasmid is known to be problematic. This is because of the internal deletions that happened as a result of bacterial culturing. To solve this problem, a short linker (like a functional intron) must be introduced between the repeated sequence (Lee and Carthew, 2003).

A contemporary vector for the efficient construction of RNAi lines is pRISE (Kondo et al., 2006), with the characteristic repeat of the Gateway recombination cassette (Akbari et al., 2009) and (Boy et al., 2010). This vector enables the gene silencing effect to be achieved more easily and with great efficiency (Kondo et al., 2006). Further details are found in (2.7.6 The pRISE vector for RNAi)

1.6.6 Malpighian tubules

Renal function in *Drosophila* is performed by the Malpighian tubules. Part of this thesis is devoted to testing their suitability as a model of mammalian renal dysfunction.

1.6.6.1 History

The tubules are named after Marcelo Malpighi, who was a physician of the Pope, 500 years ago. Beside his work as comparative anatomist, he was a pioneer in the use of

microscopy. This interest allowed him to apply his skills in microscopy to investigate insect anatomy. As a result of this interest he discovered the Malpighian tubules. However, it was not demonstrated until the 20th century, that they can produce urine (reviewed in Dow and Davies, 2003). Since then, tubules have been extensively studied for their excretory and osmoregulatory functions.

1.6.6.2 The *Drosophila* Malpighian tubules

The Malpighian tubules are simple, cylinders, closed at one end. They connect to the junction of mid-gut and hindgut by the ureters. They are two pairs, anterior and posterior and each contribute equally to the function (Figure 1-13) (Dow and Davies, 2003). They are among the smallest insects tubules to be studied. They measure approximately 2 mm long, 35 μm in diameter and consist of nearly 150 cells. Each tubule is divided into multiple segments, namely; initial, transitional and main segments, and lower tubule and upper and lower ureter (Sozen et al., 1997).

Each segment in this simple epithelial tube does a specialised function. The initial segment of the anterior tubule absorbs calcium and stores it. The main segment is a secretory segment heavily involved in fluid transport and other key funcitons of redox homeostasis. The lower tubule involved in the reabsorption of the fluid. The ureter joins two tubules and opens up into the hindgut.

The main segment of the tubules is composed of two cell types; the columnar epithelial principal cells and the star-shaped stellate cells. The principal cells have deep basal infoldings and long apical microvilli, and are more abundant than the stellate cells (Cabrero et al., 2004). The stellate cells are comparatively small and thin, with shallow basal infoldings and short apical microvilli (Wessing, 1978; Wessing and Eichelberg, 1978). Enhancer trapping has been used to investigate the Malpighian tubule's morphology with great insights identifying a distinct lower segment in both the anterior and posterior tubules. Bar-shaped cells and tiny cells in the tubule were discovered by Sozen et al., in 1997. The bar-shaped cells are thought to be the equivalent of stellate cells in the initial segment, and the tiny cells may be stem cells (Sozen et al., 1997).

1.6.6.3 Physiology

The Malpighian tubules perform various physiological roles in *Drosophila*, from the expected renal and hepatic roles, to a surprising role in immune response as well as osmoregulation. Active cation transport by the tubules is described by the Wieczorek model (Wieczorek et al., 1991). The model suggests that the principal cells use the apical proton-pumping activity of the Vacuolar ATPase (V-ATPase) to build a favourable transport gradient. Apical alkali metal-proton exchangers are then able to drive potassium into the tubule lumen, with water following the potassium due to the osmotic gradient. The Wieczorek model seems to fit the tubule experimental data in *Drosophila*, as V-ATPase inhibitors prevent fluid secretion (Dow et al., 1994), and the V-ATPase subunits are highly enriched and expressed in the principal cells (Wang et al., 2004). The principal cells are also involved in the active transport of cations and anions (O'Donnell et al., 1996; Torrie et al., 2004).

The stellate cells appear to be the site of transcellular chloride shunt and therefore water movement (Dow and Davies, 2003). Chloride shunt is controlled by the hormone Drosokinin and the second messenger intracellular Ca2+, which increase transcellular conductance through chloride channels (O'Donnell et al., 1998).

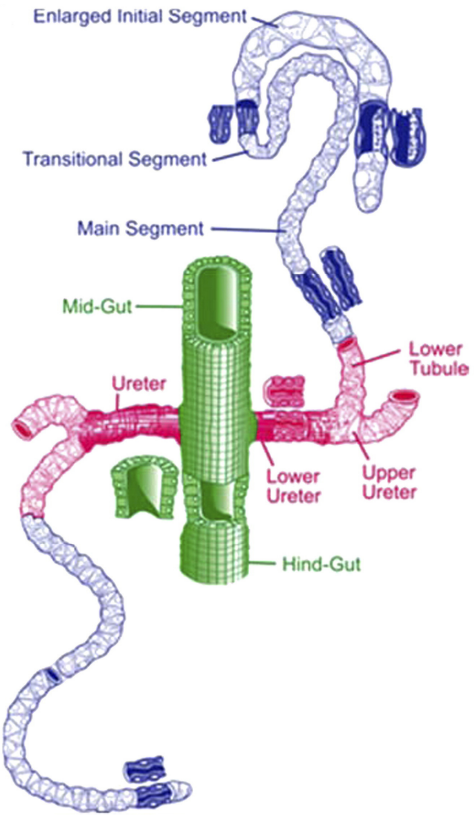

Figure 1-13. Regional differentiation of adult *Drosophila* Malpighian tubules. After (Wessing and Eichelberg, 1978) and (Singh et al., 2007).

1.7 The human kidney

1.7.1 Introduction

The kidneys play a dominant role in regulating the composition and volume of the extracellular fluid (ECF). They normally maintain a stable internal environment by generating the urine and excreting many solutes. These substances include not only waste products and foreign compounds, but also many useful substances that are present in excess as a result of eating, drinking, or metabolism.

The kidneys perform a variety of important functions:

1. They regulate the osmotic pressure (osmolality) of the body fluids by excreting osmotically dilute or concentrated urine, as appropriate, under hormonal control.

2. They regulate the concentrations of numerous ions in blood plasma, including Na^+, K^+, Ca^{2+}, Mg^{2+}, Cl^- , bicarbonate (HCO_3^-), phosphate, and sulphate.

3. They play an essential role in acid–base balance, by excreting H^+ when there is excess acid, or HCO_3^- when there is excess base, to protect against acidosis or alkalosis, respectively.

4. They regulate the volume of the ECF by controlling Na^+ and water excretion.

5. They help regulate arterial blood pressure by adjusting Na^+ excretion and producing various substances (e.g., renin) that can affect blood pressure.

6. They eliminate the waste products of metabolism, including urea (the main nitrogen-containing end product of protein metabolism in humans), uric acid (an end product of purine metabolism), and creatinine (an end product of muscle metabolism).

7. They remove many drugs (e.g., penicillin) and foreign or toxic compounds.

1.7.2 Functional renal anatomy

Each kidney in an adult weighs about 150 g and is roughly the size of a fist. If the kidney is sectioned, two regions are seen: an outer part, called the **cortex (1),** and an inner part, called the **medulla (2)**.

All the glomeruli, convoluted tubules, and cortical collecting ducts are located in the cortex.

The medulla has a striated appearance that results from the parallel arrangement of loops of Henle, medullary collecting ducts, and blood vessels of the medulla.

The medulla can be further subdivided into an **outer medulla (a)**, which is closer to the cortex, and an **inner medulla (b)**.

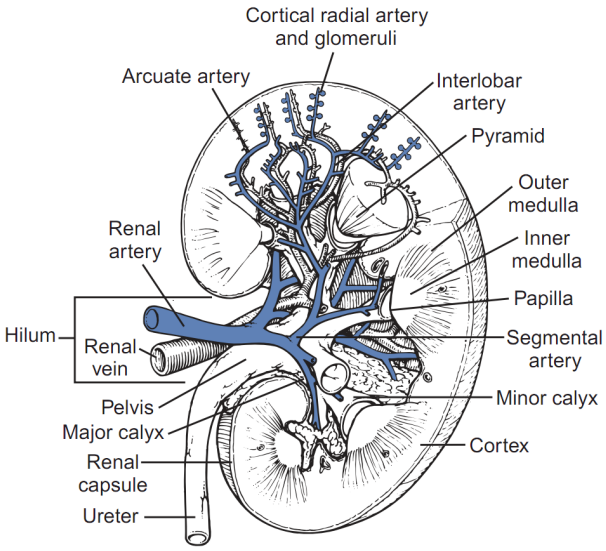

Figure 1-14 Mammalian kidney.

(Modified from Smith HW. Principles of Renal Physiology. New York: Oxford University Press, 1956.

1.7.3 The nephron is the basic unit of renal structure and function

Each human kidney contains about one million **nephrons**, each of which consists of a **renal corpuscle** (1) and a **renal tubule (2)**. The renal corpuscle consists of a tuft of capillaries, the **glomerulus (a)**, surrounded by **Bowman's capsule (b)**. The renal tubule is divided into several segments. The part of the tubule nearest the glomerulus is the proximal tubule (2a). This is subdivided into a **proximal convoluted tubule** (2a1) and **proximal straight tubule** (2a2). The straight portion heads toward the medulla, away from the surface of the kidney. The loop of Henle includes (3) the proximal straight tubule, thin limb, and thick ascending limb. Connecting tubules (4) connect the next segment, the short distal convoluted tubule, to the collecting duct system. Several nephrons drain into a cortical collecting duct, which passes into an outer medullary collecting duct. In the inner medulla, inner medullary collecting ducts unite to form large papillary ducts.

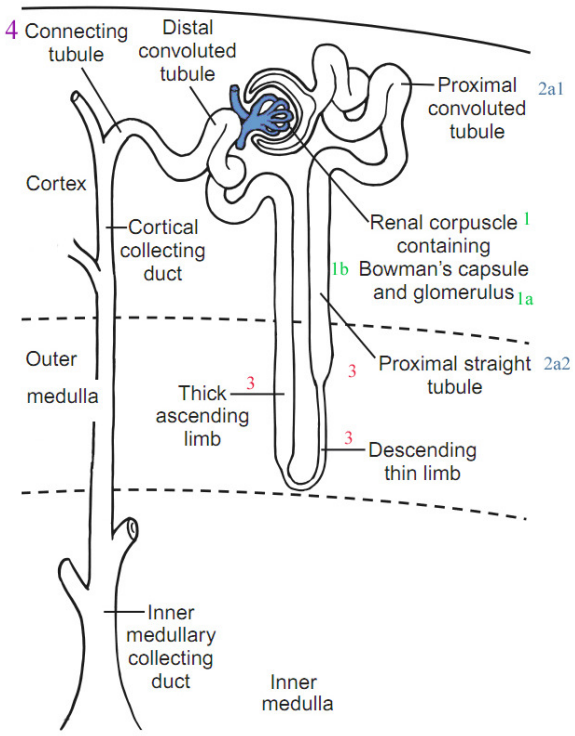

Figure 1-15 Components of the nephron and the collecting duct system. (Modified from Kriz W, Bankir L. A standard nomenclature for structures of the kidney. Am J Physiol 1988;254:F1–F8.)

The glomerulus of the nephron (Figure **1-16**a) in the mammalian kidney is responsible for blood filtration. The filtration barrier is constituted by specialized epithelial cells called podocytes, which surround the glomerular capillaries. These cells are paved on a basement membrane, and arranged closely to each other with 30-50nm spaces or slits (Figure **1-16**b). Theses slits together with the basement membrane control and constitute the filtration barrier. Disruption of this barrier leads to leakage of blood proteins into the urinary space (proteinuria), and is diagnostic of kidney dysfunction.

Insects' excretory systems lack nephrons; however, nephron-like components such filtration cells (nephrocytes) and ducts (MT) are present (Figure **1-16**c). On the other side, insect nephrocytes (Figure **1-16**d), which absorb potentially harmful substances. It has been found by (Weavers et al., 2009), infoldings in the plasma membranes forming small cavities. Similar to the situation in podocytes, the cavities' entrances are narrow gaps, 30 nm width, that are bridged by cell surface proteins forming the nephrocyte diaphragm. The nephrocyte diaphragm and basement membrane both behave as a selectively permeable barrier (Figure **1-16**d), and filtrate is endocytosed from the sides

of the lacunae. Significantly, the anatomies of the nephrocyte and podocyte filtration barriers are remarkably similar, because both contain neprhrin, the characteristic protein of the slit diaphragm. Weavers et al. 2009 have thus postulated that the insect excretory system is an intermediate step towards the formation of a glomerular filtration system. It is not that the insect system is more primitive (both insects and vertebrates are successful classes of organism); it is that the small size of insects has rendered the formation of an elaborate vascular system, and a glomerular kidney, unnecessary.

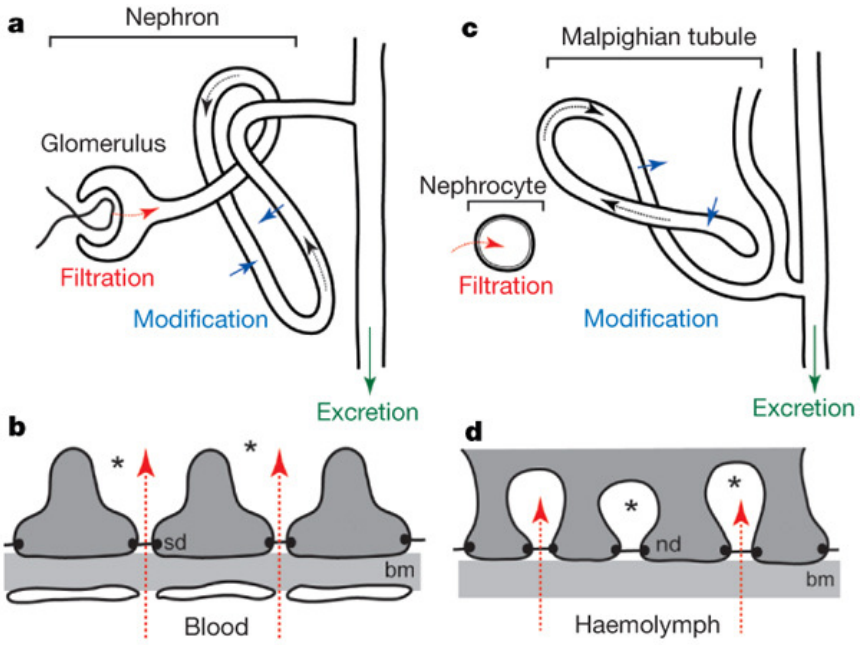

Figure 1-16 The glomerular and nephrocyte filteration barriers. a–d, Diagram of the vertebrate nephron (a), glomerular filtration barrier (b), insect excretory system (c) nephrocyte filtration barrier (d). bm, basement membrane; nd, nephrocyte diaphragm; sd, slit diaphragm.

1.8 Metabolomics

1.8.1 Introduction

Clearly, understanding the impacts of inborn errors of metabolism invites the study of the broader metabolism of an organism or tissue. As a global technique, metabolomics is a new emerging part of the 'omics' approach (Dettmer and Hammock, 2004). Genomics deals with genes, transcriptomics deals with mRNA and proteomics deals with the proteins. The crucial advantage of the metabolome is that it can potentially provide a 'fingerprint' of the entire metabolic status of a cell or tissue and so help in closing the gap between genotype and phenotype. Metabolomics is the "systematic study of the unique chemical fingerprints that specific cellular processes leave behind - specifically, the study of their small-molecule metabolite profiles" (Daviss, 2005).

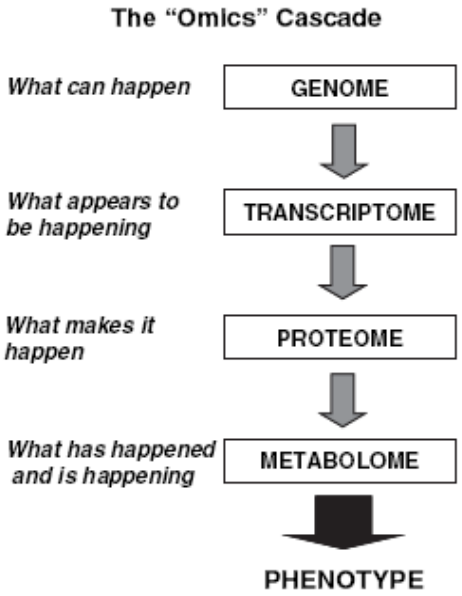

Figure 1-17. The 'Omics' Cascade. (Dettmer et al., 2007)

The metabolome can be considered as the end-point of the OMICS cascade (Figure 1-17). In view of its importance, metabolomics has rapidly developed in the last few years (Figure 1-18) (Oldiges et al., 2007).

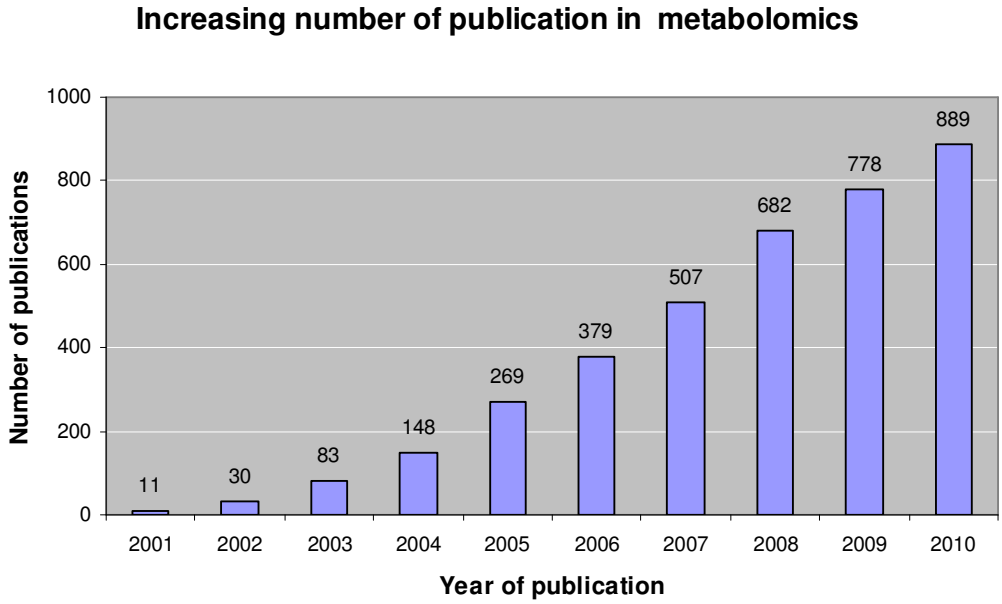

Figure 1-18. This graph shows the rapid increase in publications in the field of metabolomics (Oldiges et al., 2007).

1.8.2 The basic MS principle

Metabolomic analysis can potentially be performed with almost any analytical technique, but the power of mass spectroscopy (MS), means that this has rapidly become the standard for such studies. The basic principle of MS is thus covered here Figure 1-19.

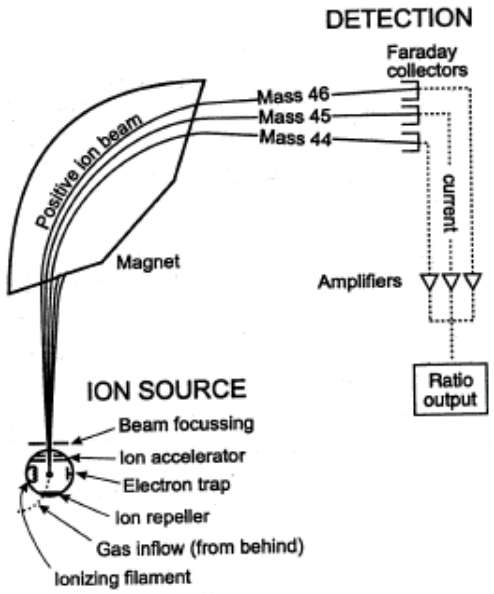

Figure 1-19 Operation of a spectrometer mass analyzer (Revesz et al., 2002).

Consider a sample contains two metabolites A and B that are introduced into the high vacuum of an MS instrument on a "target". Firstly, in the ion source, the sample is converted from the liquid status into gas status i.e. vaporized, for example by heat or laser. Then, with the ionization step, each metabolite becomes electrically charged, and may be fragmented into smaller charged molecules.

In the analyser part of the spectrometer, electrical and magnetic fields are applied as each samples passes through. When an electrical or magnetic current is applied, each metabolite behaves differently from other metabolites according to its mass to charge (m/z) ratio. Thus the electrical force accelerates the particles through the machine, and particles and the magnetic field will affect the ion direction. Finally, the arrival of charged molecules is measured in a detector. There is thus the potential to resolve multiple molecular species from a single specimen.

Metabolomic experiments, utilizing MS, were first performed in 1971 (Horning and Horning, 1971) and (Mamer et al., 1971). Although the first papers did not mention the word "metabolomics", more than 250 metabolites were measured in a single experiment in the same year (Pauling et al., 1971). However, the term metabolomics started to appear in the literature after Oliver and colleagues conducted a systematic functional analysis of the yeast genome (Oliver et al., 1998).

Metabolomics can be applied in many research and diagnostics fields and the analytical samples vary widely depending on the biological question researchers want to address.

The samples studied in metabolomics include dried blood specimens (Chace et al., 2003), serum (Brindle et al., 2002), urine (Salek et al., 2007), wide range of fluids, like seminal fluid, amniotic fluid, cerebrospinal fluid (Lindon et al., 2006), tissue extracts (Kamleh et al., 2008) or microorganisms (Mashego et al., 2007).

In the field of agriculture, plants have been modified genetically or environmentally in order to improve diet, health and nutrition. This leads to alteration in the genomic and metabolomic levels, thus newly produced metabolites should precisely and effectively monitored by metabolomic study (Fiehn et al., 2001).

In the pharmaceutical field, metabolomics has been used in the application of drug discovery, development, toxicology and pathophysiology of diseases (Wishart, 2008).

In bacteriology, the application of metabolomics focuses on the understanding of genetics and physiology of the bacterium to improve human health, drug effectiveness and resistance and bacterial effects on the environmental health (Mashego et al., 2007).

Also these bacteria could be engineered to ordered them to make new compounds or enzymes that are not normally produced by them, this is an emerging field called synthetic biology. It is a relatively new field of study, combining biological science and engineering. A good example for this approach is the bacteria that produce different light in specific status and so called the *Escherichia coli* that can see light (Levskaya et al., 2005).

In the diagnosis of inborn errors of metabolism, metabolic analysis was used many years ago by Sir Archibald Garrod (Lanpher et al., 2006). With the recent technological advances, metabolomic profiling has long been applied with high success in all previously mentioned fields. However, issues like accuracy and reproducibility are still waiting to be addressed.

Metabolic analysis was first used for simple detection of changes in black urine from alkaptonuric patients (Houten 2009). After this and after further advances in sensitivity, it was used to detect more smaller and specific metabolites, such as glucose, from different human biological fluids like serum and plasma samples.

As more metabolites are studied simultaneously, it becomes harder to separate them and resolve them from each other, so it was important to find a method for separating those metabolites. So liquid chromatography was developed and coupled to a range of analyzers in order to improve separation and detection. Coupling the liquid chromatographic column will be explained in detailed later.

1.8.3 Technologies available for metabolomic studies

1.8.3.1 Gas chromatography MS (GC-MS)

GC-MS is a common type of chromatographic detection, applied in the field of analytical chemistry, for volatile metabolites. The basic principle of the technique relies on the mobile phase which in this case is the gas to carry the molecules over the stationary phase, which is the inner side of the glass tube. Helium or nitrogen are the most widely gases used in this method. The inner side of the column is sometimes coated with different materials that interact differently with other metabolites and may delay or increase the retention time for molecules. Molecules are typically ionised by electrospray ionization (ESI).

1.8.3.2 Liquid chromatography MS (LC-MS)

This is another technique for metabolic detection branching from analytical chemistry. Separation principle is based on the physical and molecular mass properties of the molecules being separated. Interfacing the output of this liquid chromatographic column with the MS is usually accomplished by ESI.

LC-MS has been considered as a powerful metabolic technique, and is widely used in field of analytical chemistry. It offers a reasonable extent of sensitivity and specificity for targeted detection molecules.

In the LC-MS the diameter of the separation column, usually 1 mm and the flow rate are both small. This is considered a limitation of this technique, as it thus permits only a limited injection into the MS instrument, and so limits sensitivity.

1.8.3.3 Fourier transform ion cyclotron resonance (FT-ICR)

FT-ICR offers the best resolving power and the best accuracy among all MS analysers (McLuckey and Wells, 2001). In this type of detection, the principle is based on the measuring the frequency of oscillating ions in a spindle-shaped detector. The Orbitrap mass analyser is one of the best of this type, with the potential to measure mass to better than 1 part in 1 million, and will be used extensively in this thesis.

1.8.4 Mass spectrometry technology

1.8.4.1 Ion generation, positive mode electrospray ionization (PIESI)

Samples are to be analysed should be first dissolved into a polar volatile solvent before it can be transported into a high potential electrospray needle. Due to the very high voltage inside the needle, all molecules become charged with the addition of 1 H^+ ion or more; to calculate these adducts, calculations such as those shown in Table 1-3 are used. This additive has the mass of 1.0073, thus adding this mass number to the total mass expected to each molecular species. At the point where the liquid leaves the needle, a cone shape is formed which is called Taylor cone as shown in Figure 1-20 . This Taylor cone slowly bursts into smaller fine sprays due to solvent evaporations under the effect of heat. These smaller sprays droplets, which contain metabolites shrink until they reach the gas phase, with ions moving individually through the mass analyser.

Positive ion electrospray ionisation (PIESI) is the most common ionisation technique, and generally works well for both low and high molecular weights molecules. Although the technique has been improving and developing since its discovery, the basic working principles have remained the same.

The PIESI is the widely method applied and is considered very sensitive for compounds separation containing an amine group, amides, etc. On the contrary, PIESI does not work well for polar acids such as Krebs cycle acids or for neutral sugars.

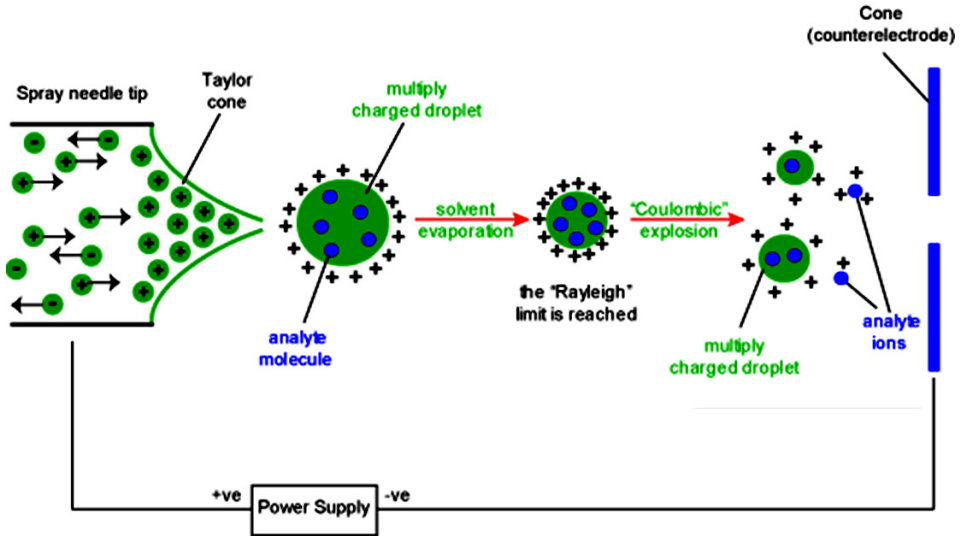

Figure 1-20. Taylor cone. In this diagram a spraying needle tip is shown. Due to the high voltage all molecules are charged. As the sprayed liquid leaving the needle and at just where the liquid leaves the needle a cone shape is formed which is called Taylor cone (Gates, 2004).

1.8.4.2 Ion generation, negative mode electrospray ionization (NIESI)

On the opposite to PIESI, negative ion electrospray ionisation (NIESI) is generally somewhat less sensitive than PIESI and consequently detects fewer compounds. The main groups of compounds which can be detected exclusively in negative ion mode are neutral sugars and organic acids such as the Krebs cycle acids. Table 1-3 is useful table to help in accurately deduce metabolites.

Table 1-3. Expected adducts generated as a result of ionization. Where M = any metabolites detected (Kind, 2010).

Ion name	Ion mass	Charge	Ion name	Ion mass	Charge
1. Positive ion mode			**2. Negative ion mode**		
M+3H	M/3 + 1.0073	3+	M-3H	M/3 - 1.0073	3-
M+2H+Na	M/3 + 8.3346	3+	M-2H	M/2 - 1.0073	2-
M+H+2Na	M/3 + 15.7662	3+	M-H2O-H	M- 19.0184	1-
M+3Na	M/3 + 22.9893	3+	M-H	M - 1.0073	1-
M+2H	M/2 + 1.0073	2+	M+Na-2H	M + 20.9747	1-
M+H+NH4	M/2 + 9.5206	2+	M+Cl	M + 34.9694	1-
M+H+Na	M/2 + 11.9983	2+	M+K-2H	M + 36.9486	1-
M+H+K	M/2 + 19.9852	2+	M+FA-H	M + 44.9982	1-
M+ACN+2H	M/2 + 21.5205	2+	M+Hac-H	M + 59.0139	1-
M+2Na	M/2 + 22.9892	2+	M+Br	M + 78.91889	1-
M+2ACN+2H	M/2 + 42.0338	2+	M+TFA-H	M + 112.9856	1-
M+3ACN+2H	M/2 + 62.5471	2+	2M-H	2M - 1.0073	1-
M+H	M + 1.0073	1+	2M+FA-H	2M + 44.9982	1-
M+NH4	M + 18.0338	1+	2M+Hac-H	2M + 59.014	1-
M+Na	M + 22.9892	1+	3M-H	3M - 1.0073	1-
M+CH3OH+H	M + 33.0335	1+			
M+K	M + 38.9632	1+			
M+ACN+H	M + 42.0338	1+			
M+2Na-H	M + 44.9712	1+			
M+Propanol+H	M + 61.0653	1+			
M+ACN+Na	M + 64.0158	1+			
M+2K-H	M + 76.9190	1+			
M+DMSO+H	M + 79.0212	1+			
M+2ACN+H	M + 83.0604	1+			
2M+H	2M + 1.0073	1+			
2M+NH4	2M + 18.0338	1+			
2M+Na	2M + 22.9892	1+			
2M+K	2M + 38.9632	1+			
2M+ACN+H	2M + 42.0338	1+			
2M+ACN+Na	2M + 64.0158	1+			

1.8.5 Ion separation methods

A very wide range of mass analysers can be used to separate the ions generated by ESI. In this thesis particular attention will be given to the Orbitrap analyser.

1.8.5.1 The Orbitrap mass spectrometer

The Orbitrap analyser was invented in 2005 by Makarov and then was available in the markets by Thermo Electron Corporation (Hu et al., 2005). The detection principle is based on the trapping the injected ions into the trap between the inner spindle-like electrode and the outer barrel like electrode Figure 1-21 (Bateman et al., 2009).

The analyser is consists of an outer barrel-like shape electrode divided into two exact halves, and an inner spindle-like shape electrode.

As group of ions enters the trap, the electric field is switched ON and then attracts the ions between the barrel-like and the spindle-like central electrodes, then the ions will start moving in a circular movement around the spindle-like electrode. This shape of the electrodes give advantages of giving a modified electric field which permits to the ions to move into angular, radial and axial oscillation movements regularly (Makarov et al., 2006). The frequency of this oscillation movement is proportional to the mass over charge ratio (m/z). Then the readings are output as chromatograms (electrographs) (Breitling et al., 2006; Makarov et al., 2006).

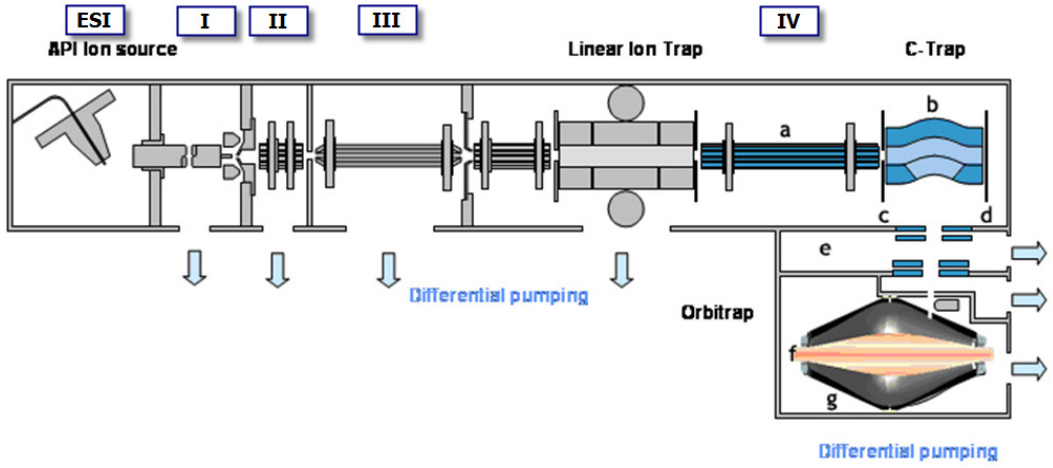

Figure 1-21. The LTQ-Orbitrap working mechanism. A, transfer octopole; B, curved RF-only quadrupole (c-trap); C, gate electrode; D, trap electrode; E; ion optics, F; inner orbitrap electrode (centeral electrode), G; outer orbitrap electrode. In ESI, the analytes is pumped into the source in solution via the eluent flow LC that interfaced with mass spectrometer. The analyte solution flowing through the electrospray needle to form droplets. These droplets travel between needle tip and counter electrode to evaporate solvents before sample injected into mass spectrometer. When a high voltage is applied, Taylor cone is produced and spray charged droplet is formed. Then charged ions pass through stages of differential pumping through RF only multipoles into a curved RF only quadruple then to the C-trap. Ions in the C-trap accumulate and their energy is dampened using nitrogen gas. They are then injected by a curved lens system which provides further areas of differential pumping before being passed into Orbitrap detector. Then mass spectra are acquired by image current detection. The Orbitrap mass spectrometer consists of : ESI ionization source, (I) heated capillary, followed by (II)

multi-pole focusing devices, (III) a gating lens, followed by a focusing octapole, linear ion trap (LTQ) following by focusing multi-pole (IV) which leads to new bent quadrupole (C-trap), and finally the Orbitrap mass analyser (Makarov et al., 2006).

Because of this working principle, this Orbitrap analyser ensures vary high mass accuracy; with internal lock mass, it can resolve to better than 2 parts in 1,000,000. This makes it the most precise mass spectrometry currently available (Olsen et al., 2005).

The Orbitrap has several advantages, when compared with other analysers, as it is relatively cheaper and with lower maintenance cost. It also, does not have a huge magnetic sector and consequently a complicated cooling system is not required.

To explain this high mass accuracy, molecules having the same integer mass but with different molecular formulae will have slightly different exact masses. For example ethanol (C_2H_4O) and methyl hydrazine (CH_4N_2) both have the same mass of 44, but the exact masses are 44.02622 and 44.03744 respectively (Figure 1-19). The Orbitrap, but not the other analysers, has sufficient precision to differentiate between them (Breitling et al., 2006).

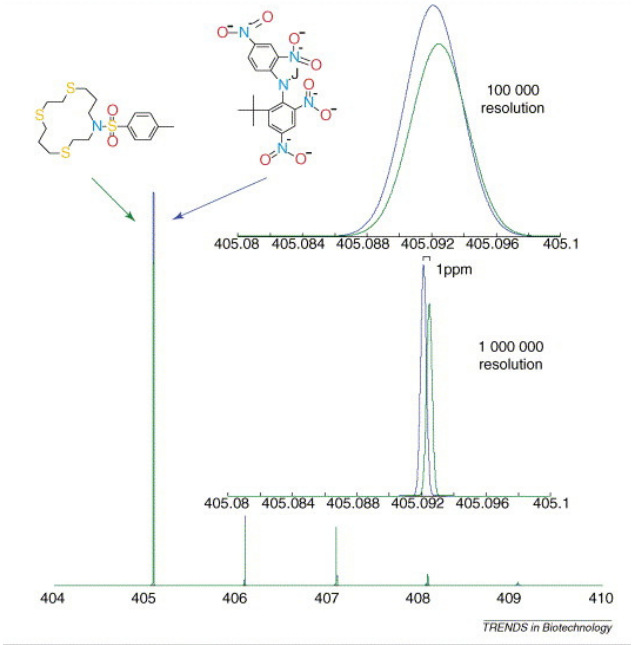

Figure 1-22. Ultra-high accuracy and resolution are required to discriminate metabolites of near-identical mass. The masses of metabolite A (blue) and metabolite B (green) differ by only 0.004 Da (1 ppm). This is one of the most extreme cases observed in small-molecule databases. No other organic chemical has a similar mass; therefore, accurate mass measurement enables unambiguous assignment of a molecular formula. If the Orbitrap analyzer was set at high enough resolution (around 1 000 000 full-width half-maximum resolution), the two compounds could even be distinguished in the same mixture.

1.8.6 Further separation methods

In order to have accurate metabolite detection, and isomers to be accurately distinguished, an efficient chromatographic separation is highly recommended.

Generally, a chromatographic step minimizes the risk of ion suppression effects and can help distinguish between isomers. Thus, an extra separation method at the beginning of the process, can decrease of interfering compounds, and can help in identifying a larger number of metabolites.

1.8.6.1 Hydrophilic Interaction Chromatography (HILIC)

HILIC provides an excellent separation chromatographic method. On the zwitterionic (ZIC-HILIC) column, the water layer associated with column surface acts as a pseudo stationary phase Figure 1-23. The zwitterion coating in theory is charge neutral thus minimising ion exchange interactions with the analyte and the chain length separating the positive and negative charges of the ZICHILIC column is optimised so that the charges on the column surface can fold round and interact to neutralise each other. The column is used with a high organic solvent content in the mobile phase which favours ionisation under ESI conditions (Watson, 2010) and (Alpert, 1990).

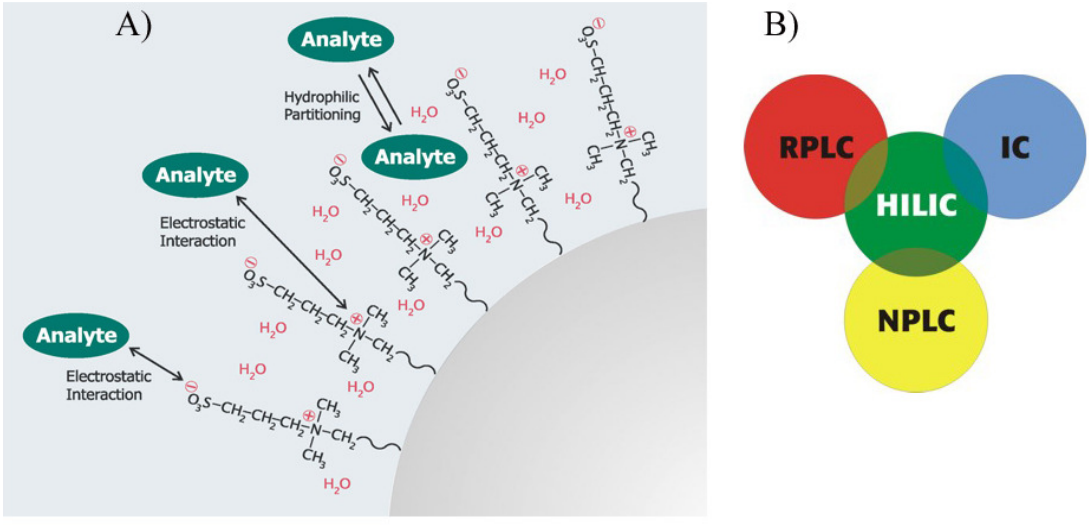

Figure 1-23 The chemistry of the ZIC-HILIC column. A) HILIC is a high-performance liquid chromatographic (HPLC) technique for separation of polar and hydrophilic compounds. It is based on the HILIC retention, which is based on partitioning of the

injected analyte solute molecules between the mobile phase eluent and a water-enriched layer in the hydrophilic HILIC stationary phase. The more hydrophilic the analyte is, the more is the partitioning equilibrium shifted towards the immobilized water layer in the stationary phase, thus the more is the analyte retained. The hydrophilic surface holds water when exposed to mixtures of organic solvent and water. Compounds such as, acids, bases, ions, sugars, and other charged and neutral hydrophilic compounds that are annoying to separate in ordinary separation techniques. They are much easier to be separated in HILIC due to the different separation selectivity. Some compounds are possible to separate by more than one chromatographic technique, and HILIC does them all. B) HILIC partly overlap with RPLC (reverse phase liquid chromatography), NPLC (Normal Phase Liquid Chromatography) and IC (Ion Chromatography) and it fills the gap in the chromatographic toolbox and perfectly fits in-between other separation techniques (Appelblad et al., 2008).

Analytical method	Advantage	Disadvantage
NMR	• Rapid analysis • High resolution • No derivatization needed • Non-destructive	• Low sensitivity • Convoluted spectra • More than one peak per component • Libraries of limited use due to complex matrix
GC–MS	• Sensitive • Robust • Large linear range • Large commercial and public libraries	• Slow • Often requires derivatization • Many analytes thermally-unstable or too large for analysis
LC–MS	• No derivatization required (usually) • Many modes of separation available • Large sample capacity	• Slow • Limited commercial libraries
CE–MS	• High separation power • Small sample requirements • Rapid analysis • Can analyse neutrals, anions and cations in single run • No derivatization (usually)	• Limited commercial libraries • Poor retention time reproducibility
FTIR	• Rapid analysis • Complete fingerprint of sample chemical composition • No derivatization needed	• Extremely convoluted spectra • More than one peak per component • Metabolite identification nearly impossible • Requires sample drying

Figure 1-24 Comparison of advantages and disadvantages for different MS techniques (Shulaev, 2006).

1.8.7 Data Processing

The greatest amount of time in metabolomic experiments is devoted to data processing.

1.8.7.1 Sieve Software

Most commercial data processing software aims to plot extracted ion chromatograms across the full scan range of the mass spectrometer. In order to do this the Sieve software is widely used. Sieve is a software developed by a collaboration between Vast Scientific and Thermo Scientific (Vast_Scientific_Inc., 2010). It takes the data generated by the Orbitrap mass spectrometers and aligns it, extracts the relative ion chromatograms (RICs) and tabulates them. Further details of the software analysis used in this thesis are provided in chapter 2.

1.8.8 Microarray

The function of a cell depends on the genes which it expresses. Measurement of gene expression, for example by Northern blot, is a cornerstone of molecular biology. Most recently, microarray technology has allowed the simultaneous measurement of tens of thousands of genes from a single sample. The reconciliation of microarray and metabolomic data is thus potentially extremely powerful.

1.8.8.1 Technology

Microarray principle is highly dependent in its work on the principle of hybridization following the reverse Northern blot principle. In other words, oligonucleotide probes, corresponding to every gene or transcript that is to be measured, are arrayed on a solid substratum in a known pattern. Labelled mRNA is hybridised to the slide, and the signal attached to each probe is measured- typically by confocal microscopy or some variant thereof. This will tell researchers which genes are being expressed in each sample, and at what levels the transcripts are found. A typical microarray chip contains tens of thousands of probes attached to the glass slide. In the Affymetrix system (Figure 1-25), each gene has multiple probes, each of approximately 28 nt length. Half the probes are perfect matches to the known sequence (PM probes), and half (MM probes) have single base changes from the corresponding PM probes. The proprietary analysis software uses

the difference between PM and MM signals to control for nonspecific hybridisation, and so potentially yield more quantitative results (Wu and Irizarry, 2004)

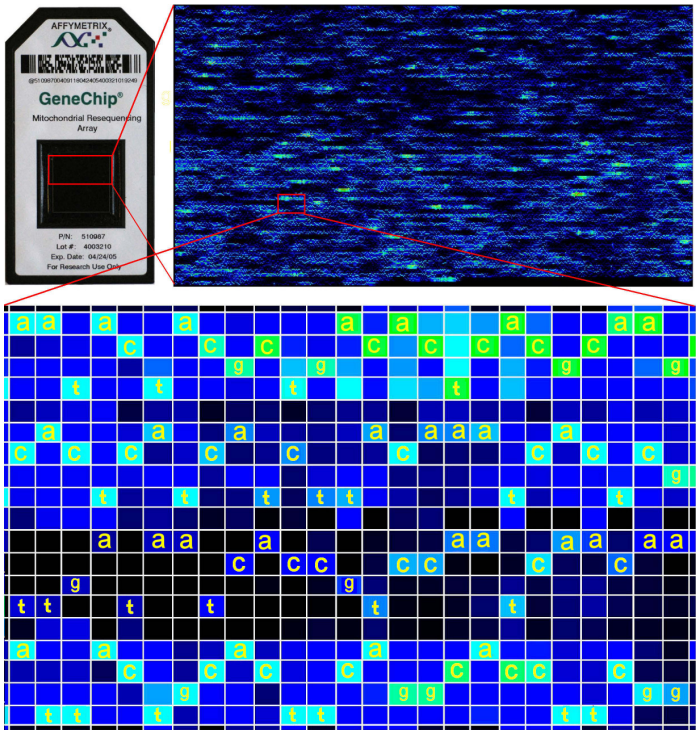

Figure 1-25. Probe distribution on an Affymetrix gene chip. From http://www.mun.ca/biology/scarr/Human_mtDNA_re-sequencing_microarray.html

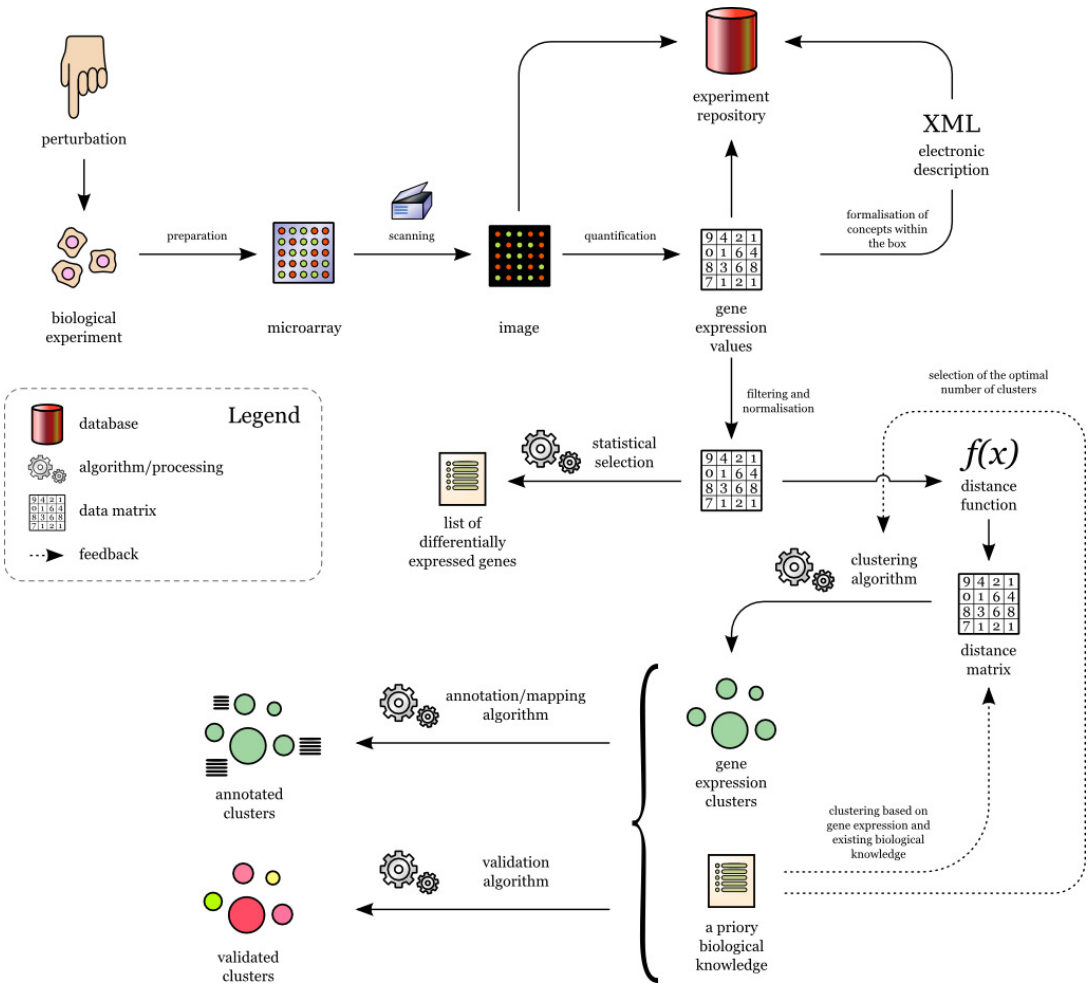

Figure 1-26. A typical microarray workflow for the identification of clusters of differentially expressed genes. http://www.stathis.co.uk/art/infographics/infographics-gallery/?pid=96

The availability of Affymetrix microarrays has helped the *Drosophila* community hugely. Among applications of the technology, the FlyAtlas.org resource has clearly helped in closing the phenotype gap between human diseases and *Drosophila* (Chintapalli et al., 2007) by directing researchers to the specific *Drosophila* tissues in which their genes of interest are mostly expressed. This is particularly useful when looking for the best fly tissues to start investigating for human disease homology.

Microarrays are widely employed to explore differences between samples (healthy vs. diseased, experimental vs. control, etc.), as shown in Figure 1-26. In this work, we will be using microarrays to analyse the differences between *rosy* and wild type flies, and additionally to perform a time-course gene expression analysis of drug action.

1.8.8.2 Validation of microarray results

Although Affymetrix arrays are considered to be highly reliable, it is considered prudent to validate changed expression of genes of particular interest before publication. This could be by several techniques (for example Northern blotting, or Western blotting for protein levels); but is usually performed by quantitative reverse transcriptase PCR (Q-RT-PCR).

1.8.9 Aims of the thesis

The main aims of this thesis is to

- Test the feasibility of *Drosophila melanogaster* 'kidney' (Malpighian tubules) as genetic model.
- Applying the *Drosophila* to give insights informative information about inborn errors of metabolism.
- Test the *Drosophila* as a model for disease related to congenital renal diseases.
- How beneficial this would be to the field resulting from the powerful genetic tools that *Drosophila* acquired over the years.
- Integrating the omics approach; genomics, transcriptomics and maybe metabolomics may provide novel insights into the disease state or even its amelioration.

Chapter 2 Materials and Methods

2.1 *Drosophila melanogaster*

2.1.1 *Drosophila* stocks

Name	From	Used for	Phenotype
Oregon R	Bloomington stock center (BSC)	Control for all studies	wild type
Canton S	BSC	control for all studies	wild type
w^{1118}	(Hazelrigg et al., 1984)	background for P-element insertions	white eyes
mal ^{37}	BSC	Metabolomics	brown eyes
cho	BSC	Metabolomics	brown inclusions in tubules
ry ^{506}	BSC	Metabolomics	brownish eyes
w^{1}	BSC	Alternative *white* allele	white eyes
w^{93}	BSC	Alternative *white* allele	white eyes
5' HIUH	VDRC	UAS-RNA line	Carries mini-w^{+}
uro- GAL 4	Made in lab, (Terhzaz et al., 2010)	Drives expression in principal cells	Carries mini-w^{+}
Actin-GAL 4/*CyO*	BSC	Drives ubiquitous expression	Carries mini-w^{+} and *CyO* balancer
TM3, *Sb*, (*Ser*)	BSC	Balancer for Chromosome 3	Stubbly bristles; (some variants have serrate wings)
w^{1118}; {w^{+mC}=WH}PBac *uro*^{f04888}	Bloomington	Survival assay	Normal
CyO	Bloomington	Balancer for Chromosome 2	Curly wings

2.1.2 *Drosophila* rearing

All flies were kept in small ventilated plastic vials on standard *Drosophila* medium (at section 8.1) (Ashburner, 1989). The room temperature was between 20 – 22 ºC in a 12:12 light: dark cycle and between 35 – 40 % relative humidity. When large quantities of *Drosophila* were needed, large bottles were used under the same conditions. Flies were tipped as required on to new medium, approximately every two weeks.

2.1.3 Dissection of *Drosophila*

Adult flies, usually 5 to 7 days old, were first anaesthetized on ice before they were transferred to a Petri dish containing an appropriate volume of Schneider's medium. Fly Malpighian tubules can be easily dissected intact without complicated equipment (Dow et al., 1994). For dissecting Malpighian tubules, a fly is firmly held by a forceps from the thorax region and with the other hand, forceps pulling the very end part of the fly gently and slowly. At this point the Malpighian tubules will start to appear - attached, however, to the midgut (MG). Then they need to be freed by using the forceps with great care, gently hold the tubules from the ureter by separating them from the MG at the ureter (Figure 2-1). In case of head sampling, the head was separated from the body by applying two forceps on the neck and pulling in opposite directions. The number of flies dissected varied depending on each experiment. This method was adopted after (Dow et al., 1994; Sullivan and Sullivan, 1975).

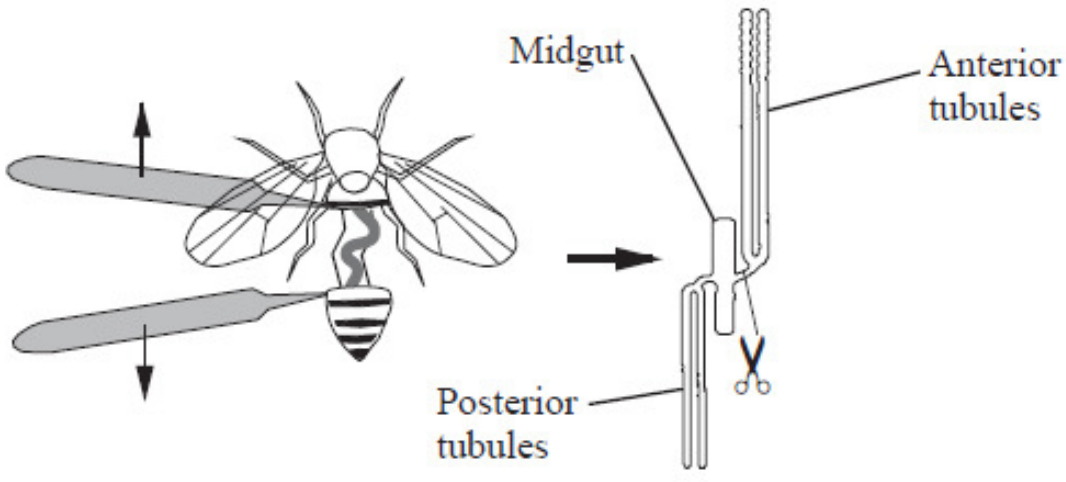

Figure 2-1 Malpighian tubule dissection method (Dow et al., 1994).

2.1.4 Generation of transgenic flies

After constructing appropriate plasmids and providing the required amount of at least 50 µg, DNA samples were sent to Bestgene *Drosophila* Injection Services, USA. for microinjection into white background (w^{1118}) flies along with a helper plasmid supplied by Bestgene. The newly generated flies (G0) were crossed with w^{1118} again. This service included microinjection, transfomant identification and –optionally- balancing.

2.1.5 Characterization of transgenic flies

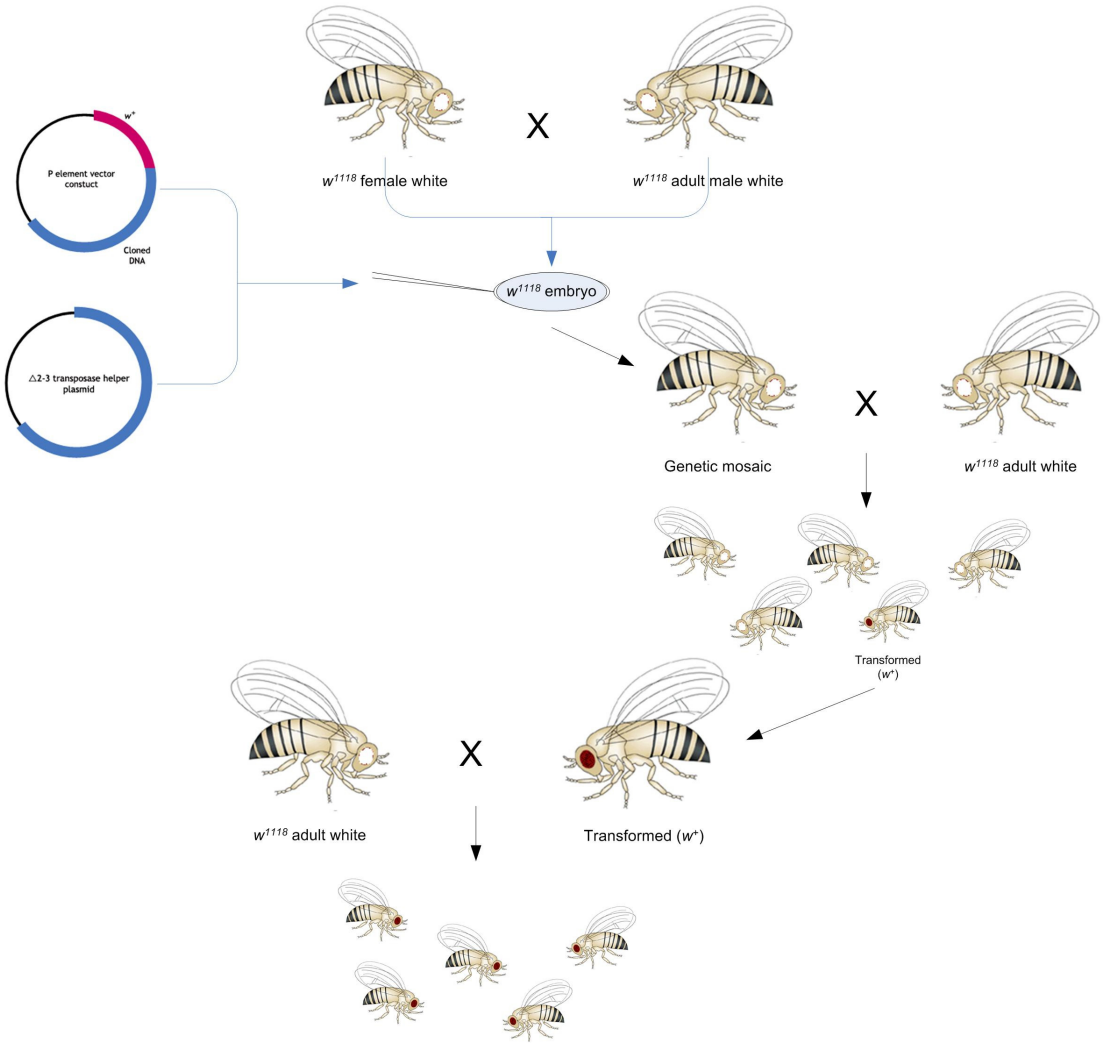

Figure 2-2. Germline transformation of *Drosophila*.

The germline transformation process is conducted by injecting embryos from the w^{1118} strains with a P-element shuttle vector that contains the gene of interest and a marker *mini-white* gene, along with a Δ2-3 helper plasmid. Emerged flies from these embryos are crossed with w^{1118}. Progeny of this cross are then screened for red eyes, implying

that they carry *mini-white*, and thus transgenes. Only those red-eyed adult flies are backcrossed again to w^{1118}, and selected to produce a stably transformed line. Figure is after (Guo, 1996).

2.1.6 Crossing and rearing crosses

The GAL4/UAS system provides a powerful tool for cell-specific expression of transgenic payloads (Sentry and Kaiser, 1992). Typically, a UAS-RNAi line was tested for effectiveness by crossing to the Actin-GAL4 driver, to determine whether ubiquitous expression of the construct has an effect on fly development, survival, or any other detectable phenotype. For finer spatial control, UAS lines were also crossed to the *uro*-GAL4 driver, which directs expression to only tubule principal cells of only third instar and adult flies (Terhzaz et al., 2010). This was achieved by collecting between 20 to 30 virgin flies of the *uro*-GAL4 into small vials. Each vial contained one virgin fly and was kept for 2 to 3 days, to ensure that fertilized eggs were not being laid. Any vial containing fertilized eggs was discarded. After making sure only virgins were present, each was crossed to *uro* or *ry* RNAi lines males. The reciprocal crosses were also made, to test for sex-specificity of expression, though this was not observed in this project.

Example: UAS line on Chromosome III

$$w^{-};\ \frac{uro\text{-}GAL4}{uro\text{-}GAL4};\ +\qquad \text{X} \qquad w^{-};\quad +\quad ;\quad \frac{P}{TM3}$$

Uro GAL4 expression driver

Flies carrying the designed content (P) with red eyes, short bristles phenotype.

↓

$$w^{-};\ \frac{uro\text{-}GAL4}{+};\ \frac{P}{+}\qquad \& \qquad w^{-};\ \frac{uro\text{-}GAL4}{+};\ \frac{+}{TM3}$$

Use for experiments

Flies with long bristles were only selected from this cross.

Example: UAS line on Chromosome II

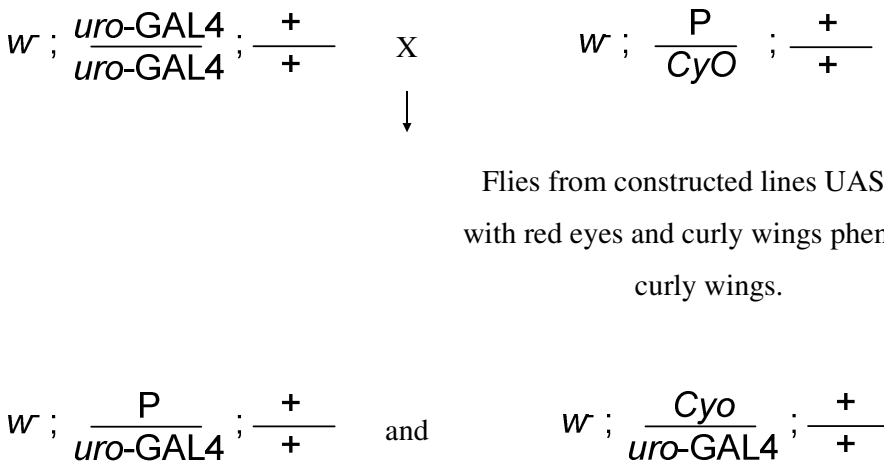

Figure 2-3 Some typical examples of GAL4-UAS crosses and selection of appropriate progeny.

After mating took place and sufficient eggs were laid, adults were transferred into new fly food bottles leaving the first bottles with only larvae. The newly transferred flies were left for several days until sufficient eggs were laid then again transferred as desired. This process took approximately between five to ten days.

2.1.7 Survival food preparation

To test for survival under oxidative stress conditions, a special peroxide diet was prepared. The food contained 1% agarose, 1% sucrose and 1% H_2O_2 into a final volume of 10 ml per vial.

2.1.8 Oxidative stress survival assays

Freshly emerged adults were placed in mixed-sex groups of 20 flies on normal diet in tubes, until egg-laying was established, then transferred to vials with H_2O_2, freshly prepared as described above. To ensure that the oxidative challenge was maintained, flies were transferred to fresh H_2O_2 vials every 2 days. The time to emergence of adult progeny was carefully noted. Then the percentage of survivors were calculated using the

(GraphPad) using the Kaplan-Meier survival curve as means ± SEM. Experiments were always performed in which progeny of a cross (typically a GAL*4*/UAS cross) were compared with each parental line, i.e. two different parents and the progeny.

2.2 RNA extraction

Messenger RNAs (mRNAs) were extracted using the Qiagen RNeasy Mini extraction kits following the manufacturer's instructions. For Malpighian tubules, mRNA was extracted from 25 to 35 flies, depending on the experiment. Tubules were then collected into 2.0 ml eppendorf tubes with 350 µl lysis (RLT) buffer containing 10% β-mercaptoethanol, prepared freshly. For long-term storage, lysates were immediately frozen in liquid nitrogen and then transferred to a -80 ºC freezer, where it could be stored for several months until needed. Once extracted according the manufacturer's protocol, mRNA concentration and purity were checked using the Nanodrop^{TM} 1000 spectrophotometer. First strand cDNA synthesis

Complementary DNA (cDNA) was prepared from mRNA with the help of the Superscript II reverse transcriptase (Invitrogen) according to the manufacturer's protocol. Then the DNA concentration and purity were checked using the Nanodrop^{TM} 1000 spectrophotometer.

2.3 Quantification of nucleic acid

Quantification of mRNA and DNA are important steps in any molecular experiment. This was carried out using the Nanodrop^{TM} 1000 analyzer. At the same time sample purity was also monitored. The measurements were based on the assumption that an OD of 1 at 260 nm corresponds to 50 µg/ ml for DNA and 40 µg/ ml for RNA. The analyzer was zeroed by the same elution solution used in the samples.

The purity was calculated by the ratio of A260/280. Values of 1.8 for DNA and 2.0 for RNA were considered pure.

2.4 Oligonucleotide synthesis

All primers in this thesis were designed using MacVector 10.0 software. The selected pairs were then sent to the MWG Biotech where they were synthesized. Primer quality was controlled and assessed by MWG Biotech using Trityl monitoring, OD

measurement and MALDI-TOF MS. Primers were supplied as lyophilized pellets, and reconstituted with the appropriate volume of ultrapure sterile water to produce a stock of 100 pmol/μl. Further dilution was needed to produce a working PCR primer concentration of 6.6 µM. When not in use, primer stocks were stored at -20 ºC.

2.5 Polymerase chain reaction (PCR)

2.5.1 Standard PCR using Taq DNA polymerase

Volumes (in µl) for a typical PCR reaction are shown below:

10 x PCR buffer	5
$MgCl_2$	1.5
dNTPs	2
Forward primer	1
Reverse primer	1
Taq DNA polymerase	0.4
cDNA	2 (or as needed to yield 50-100 ng template)
H_2O	To 20 μl

2.5.2 Reverse-transcription (RT) PCR

Reverse transcription PCR (RT-PCR) is a technique to measure abundance of expression. It is a two-step process, in which mRNA is first reverse transcribed to cDNA, then amplified with gene-specific primers. Reverse transcription was carried out using Superscript II reverse transcriptase kit (Invitrogen), dNTPs and oligo-dT. The reaction volumes were 20 µl following the company instruction's protocol. Then appropriate aliquots were made and stored at – 20 ºC for further use.

2.5.3 Quantitative (Q)-PCR

Quantitative PCR technique is a powerful tool for gene expression analysis. In this thesis the analysis was carried out into a 96 well plate. Each tube contains mixture solution of 12 µl of Sybr green, 1 µl of each forward and reverse primers. Water was

added to a final volume of 24 μl/ sample. Then in each qPCR tube an equal concentration of cDNA template was added. A no-template blank was included to ensure the integrity of the master mix.

The absolute quantitation of gene expression method used to measure the gene expression. For this method, a standard curve was generated to estimate the sample copy number. This led to make a serial dilution of the corresponding gene being analyzed. At the same time, an internal quality checking was also analysed using the α-tubulin housekeeping gene (Chintapalli et al., 2007) with specific primer set. After aliquotting the master mix and the addition of samples, tubes were carefully covered with special caps. To ensure the content is completely mixed together and it is at bottom of the tubes, centrifugation for each strip was necessary .

The protocol used was the following:

	Denaturation	95 ºC	10 min
30-40 x	Denaturation	95 ºC	10 s
	Annealing	50-60 ºC	30 s (according to primers)
	Extension	72 ºC	30 s
	Absorption reading	76 ºC	10 s
	Incubation	72 ºC	5 min
	Melting curve	63 - 90 ºC	read every 0.2 ºC

2.5.4 Agarose gel electrophoresis

Agarose gel electrophoresis is historically the method of choice for DNA detection in research labs. The principle of DNA separation relies on the negative charge that DNA possesses and its size. Small DNA fragments migrate faster towards the positive anode.

The mixture prepared in 1% agarose in 0.5x TBE and ethidium bromide. After certain period of time the visualization took place under the UV light, the gel was photographed and the fragment sizes were compared with 1kb ladder (Sambrook and Russell, 2001).

2.5.5 PCR purification

When the DNA generated from a PCR run is needed for further experiments (such as cloning), it is necessary to remove any unutilized dNTPs, primers or Taq enzyme to leave only pure DNA fragments. For this task, the Qiagen DNA purification kit was used according the manufacturer's instructions.

2.5.6 Gel purification

After running a gel and observing a DNA fragment of the desired size, it is sometimes necessary to select that particular fragment for further analysis. For such needs, one specific band was excised using a scalpel blade under UV illumination on the transilluminator, taking care to protect the eyes from UV. This fragment would be transferred to an eppendorf tube, weighed, then processed according to the Qiagen Gel Extraction Kit manufacturer's instructions.

2.6 DNA cloning

2.6.1 *E. coli* strains and plasmids

One Shot® Top 10 chemically competent *E. coli* were used for the pENTR directional TOPO cloning.

The DH5α ™ were used for general transformation, for example with the pRISE2 dsRNA vector.

E.coli	
Strain	**Genotype**
One Shot® Top10	(F- mcrA Δ(mrr-hsdRMS-mcrBC) φ80lacZΔM15 ΔlacX74 recA1 araD139 Δ(ara-leu) 7697 galU galK rpsL (StrR) endA1 nupG λ-)
DH5α™ subcloning efficiency competent cells (Invitrogen)	(F- ϕ80d*lac*Z ΔM15, Δ(*lac*ZYA-*arg*F), U169, *deo*R, *rec*A1, *end*A1, *hsd*R17 (r_K-,m^K+), *pho*A, *sup*E44,λ-, *thi*-1, *gyr*A96, *rel*A1).
Plasmids	
Name	**Purpose**
pRISE (Invitrogen)	Used to clone DNA fragment of interest downstream of the UAS sequence, to generate RNAi. Also contains the Amp^R gene to confer ampicillin resistance when transformed into *E.coli.*
pENTR Gateway cloning system (Invitrogen)	Plasmid used to express the effects of RNA interfering. Also contains the Amp^R gene to confer ampicillin resistance when transformed into *E.coli.*

2.6.2 Topo cloning of PCR products

The Invitrogen Topo-Directional cloning kit was used. It allows efficient directional cloning into a vector. Many issues should be taken into account. This starts with the primers design, where CACC bases at the 5' end of the forward primer should be added. Then the blunt-end PCR product generated should be used freshly, and cloned into

Topo-D vector in 1:1 molar ratio. To complete the cloning, this then needed to be transformed into One Shot Top 10 chemically competent *E. coli* and incubated with SOC medium for an a hour then plated overnight onto L-amp X-GAL IPTG agar (Katzen, 2007).

2.6.3 Restriction digests

New England Biolab restriction enzymes were used in this project. Generally 1-10 μg of DNA was digested with 1 µl of a particular enzyme in 20 μl of the corresponding buffer for 1 h at 37 ºC. If purification of the resulting DNA was required, this was accomplished either by DNA pruficaton (2.5.5.) or gel excision (2.5.6).

2.6.4 DNA ligation

DNA ligation was required when cloning a DNA fragment into a vector was needed. Before this, both vector and insert had to digested with appropriate compatible restriction enzymes, and the resulting DNAs purified and quantified. To prevent the vector from religating to itself, a treatment with alkaline phosphatase at the end of the restriction digest incubation period was occasionally performed; this need was reduced by designing directional cloning strategies with two enzymes that produced incompatible sticky ends. Then a specific molar ratio of insert to vector was used according to the instruction's manual according to Roche rapid DNA kit ligation kit.

2.6.5 Transformation into *E. coli*

Two µl of plasmids were transformed into *E. coli* competent cells by incubating on ice for 5 to 30 min. The mixture was then heat-shocked for 30 sec at 42 ºC then placed on ice immediately. The reaction volume then added into 250 µl of SOC medium before incubated at 37ºC for one hour with shaking at 250 rpm. The final step of transformation 100 µl was spread on selective bacterial plates containing 50 µg/ml kanamycin or 60 µg/ml ampicillin, as appropriate.

2.6.6 The pRISE vector for RNAi

Several "RNAi" vectors for constructing RNA inverted repeat sequence are available, and some are designed for germline transformation into *Drosophila*. One of them is pRISE II. The pRISE II vector contains two *attR1*-ccdB-*attR2* recombination cassettes in inverted orientation separated by a functional intron from the *ftz* gene. So this will help to insert any DNA sequence into two different orientations with the help of another vector contains the recombination sites like the pENTR/D from Invitrogen. This pENTR/D contains *attL*1 and *attL*2 recombination sequence. So when we clone our DNA into the pENTR vector, between the *attL*1 and *attL*2 positions, it can be easily transferred into the pRISE vector by an enzyme called LR Clonase Figure 2-4. This enzyme recognizes the *attL* and *attR* target sites (Kondo et al., 2006).

The pRISE also contains the UAS promoter region which allows the cell-type specific expression of dsRNA under the control of appropriate GAL4 drivers.

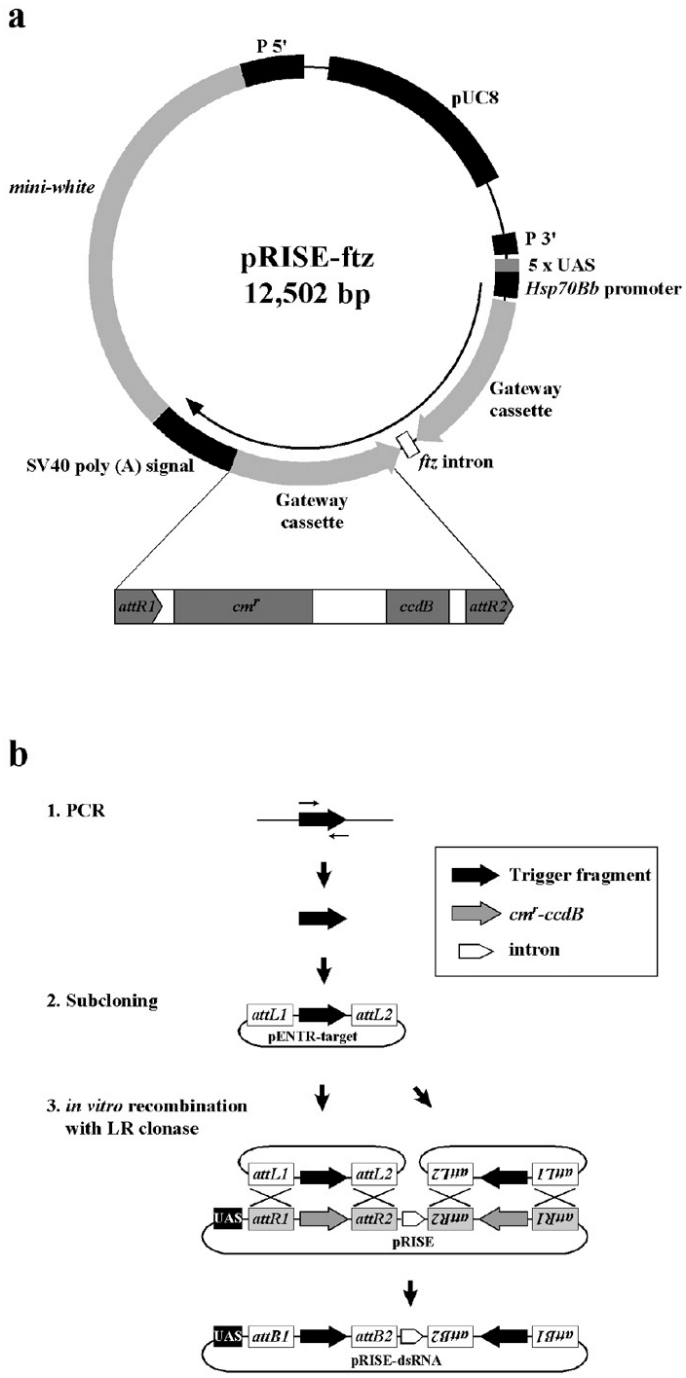

Figure 2-4 The pRISE plasmid vector and principle of generating an inverted repeat for gene silencing construct generation. a) The pRISE vector. b) Steps of constructing an inverted repeat using pENTR and pRISE vectors with the help of LR Clonase enzyme. After (Kondo et al., 2006).

2.6.7 Gateway™ cloning

The first step in gene cloning for gene silencing with the Gateway kit, the DNA fragment of interest must me first cloned into an entry clone. This enter clone will

contain the gene of interest flacked by *attL* sequences, which later can be easily recombine with the destination victor particularly in the *attR* sequences.

This technology insures fast, efficient directional cloning that ligates the DNA fragment with desired orientation for gene expression (Figure 2-5).

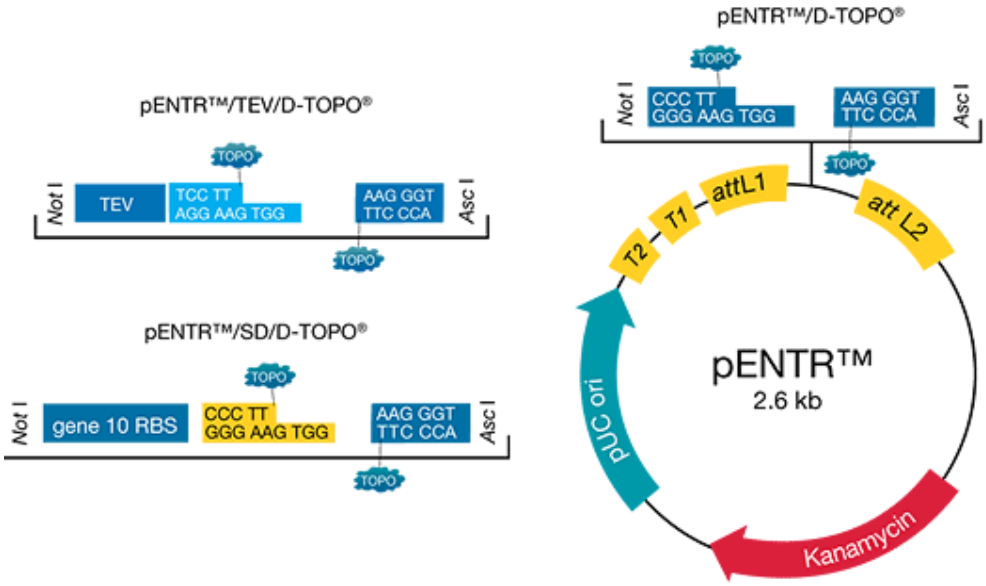

Figure 2-5 The pENTR vector (Invitrogen, 2002).

2.6.8 LR Clonase

The Gateway LR Clonase enzyme mix is an enzyme responsible for the facilitating the recombination between an entry clone into a destination vector. In this thesis it was responsible to transfer the DNA sequence in the pENTR to the destination vector pRISE to constructing an inverted repeat to produce RNAi effects when driven by GAL4.

This based on the site recombination between the *attL* and *attR* site in each vector.

An equal molar ratio (1:1) of the insect entry clone was added to the destination vector with LR Clonase buffer. TE buffer (pH 8), was added to a final volume of 16 µl. Then 4 µl LR Clonase^{TM} enzyme was added to the reaction and mixed by brief vortexing. All previous steps were carried out at room temperature. Then the reaction tube was incubated at room temperature for 60 min before the Proteinase K was added. This was incubated for further 10 min at 37 ºC. The next step was transform it to DH5α as in section 2.6.1 .

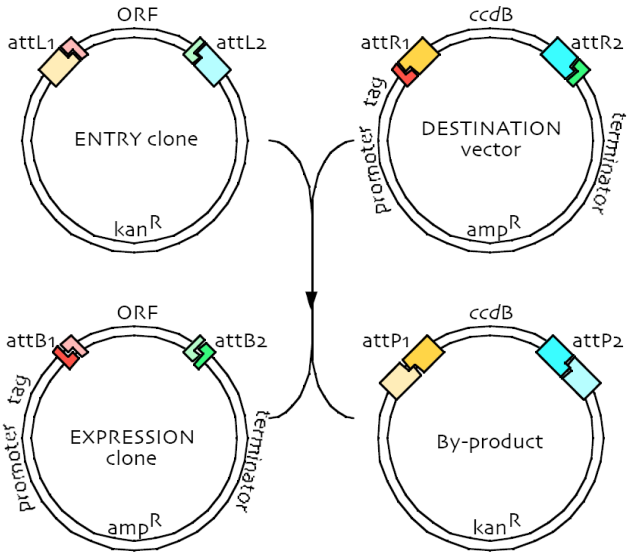

Figure 2-6 The Gateway LR in vitro recombination reaction (Invitrogen, 2010).

2.6.9 Colony screening and selection

2.6.9.1 Plasmid selection

The DNA plasmids utilised during this study contained either the ampicillin or kanamycin resistance genes, which were used as transformation selection factors. Colonies transformed with the plasmid were selected by the addition of ampicillin (100 μg ml^{-1}) or kanamycin (50 μg ml^{-1}) to the L-Agar or L-Broth growth medium. Ampicillin was stored as a 100 mg ml^{-1} stock solution (w/v) in 50% H_2O, 50% ethanol, at -20 °C. Kanamycin was purchased in a 50 mg ml^{-1} solution (Sigma-Aldrich, UK) and stored at 4 °C.

2.6.9.2 Diagnostic PCR for plasmid selection

To identify the presence and orientation of a DNA insert in a vector, bacterial colonies on a plate were tested using PCR (before overnight cultures were set up). PCR reactions were sat up with one primer that bound to the insert and one primer that bound to the vector (facing into the cloning site). The colony was touched with a sterilised tip and then the tip was used to pipette the PCR solution up and down several times.

2.6.9.3 Preservation of selected bacterial cultures

Equal amounts of bacterial cultures and 30 % glycerol were added to a screw-top cryovial tube with gentle stirring with the pipette tip. This was immediately snap- frozen in liquid nitrogen before the stocks were stored in the – 70 °C freezer.

2.7 Affymetrix microarray experiments

2.7.1 Fly preparation and Allopurinol treatment scheme

Fly food used in this experiment was freshly prepared and all vials used were from the same fly food stock. Allopurinol was added in the concentration of 110 µg/ml as it was found in pilot experiments that this concentration can phenocopy the *ry* mutant. The drug was added on the surface of the fly food. To prevent evaporation, vials was immediately closed with cotton and left for overnight to dry. Four different time course samples were prepared as zero, 6, 24 and 48 hours along with the ry^{506} mutant.

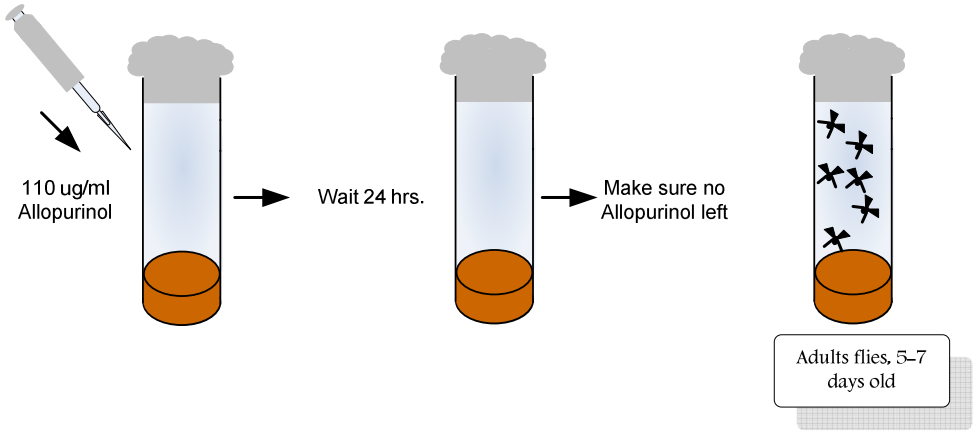

Figure 2-7 Schematic diagram for preparation of fly food with Allopurinol. In this sample preparation, allopurinol was added to fly food. The drug concentration was 110 µg/ml (Keller and Glassman, 1965) . After adding the drug, vials were left for 24 hours to make sure that all was absorbed by the food and that no residue remained to cause the fly to stick to the diet, and thus die. Was drawn by me.

2.7.2 Sample preparation

Malpighian tubules were dissected from flies aged between 5 to 7 days after emergence. Tubules from between 25 to 30 flies were used for each sample. Malpighian tubule dissection was followed as described in section 2.1.3 and as in Figure 2-1. In order to minimize the chance of RNA degradations, each dissected MT were immediately

transferred into the RLT buffer that was kept on ice. For total-RNA extractions the Qiagen-RNeasy Mini Kit was used following the manufacturer protocol. The goal of this experiment was to test the transcriptomic changes elicited on the MT by allopurinol, and to compare with the authentic *rosy* mutation. For reasons of cost, the experiment was designed as a time course, with samples taken in triplicate at 0 h (control), and at six, twenty four and forty eight hours, together with a t=0 h *rosy*^{506} mutant for comparison.

2.7.3 RNA target preparation

Total RNA was extracted with Qiagen minicolumns according to the manufacturer's protocols, and quality verified using the Agilent Bioanalyzer, which is a computer assisted nanogel electrophoresis for total or complementary RNA. A GeneChip® IVT Expression Kit, based on linear RNA amplification and T7 in vitro transcription technology, was used to prepare cRNA for microarray.

In this process, the total RNA undergoes reverse transcription to synthesize the first strand cDNA, this then converted into a double strand DNA template for transcription. In vitro transcription synthesis an amplified RNA (aRNA) and incorporates a biotin-conjugated nucleotide, washing step taken place to remove unconjugated NTPs , salt and enzymes. Next is fragmentation of the biotin-labelled aRNA in preparation for hybridization onto the array chip.

2.8 Metabolomics

2.8.1 The control animal model strains

An Oregon R wild type strain was used as a control in these experiments. These flies were cultured on standard food at 25 C° and 55% r.h. on a 12:12 photoperiod as described in the section on *Drosophila* rearing 2.1.2.

2.8.2 Chemicals

The allopurinol used for this study was purchased from Sigma Chemical Co. (St Louis, MO, USA). Acetonitrile was from Fisher Scientific (Leicestershire, UK), formic acid (UWR, Pool, UK) and methanol. All chemicals used were analytical reagent grade. A Direct Q-3 water purification system (Millipore, Watford, UK) was used to produce the HPLC water that was in all of the analyses. All other chemicals used were obtained from Sigma Chemicals (Poole, Dorset), or Fisher Scientific Co.

2.8.3 Dissection and sample preparation

Different fly tissues were dissected the same way as in section 2.1.3 except where otherwise mentioned. Then all following steps were carried out on ice. Next in order to homogenize the contents, each sample were then sonicated very well for 2-3 s for three times.

Samples then were centrifuged at 10,000 rpm at 4ºC for 10 min in a cooled microcentrifuge, and the supernatants were collected into new 2.0 ml eppendorf tubes and kept at – 80 ºC (Figure 2-8).

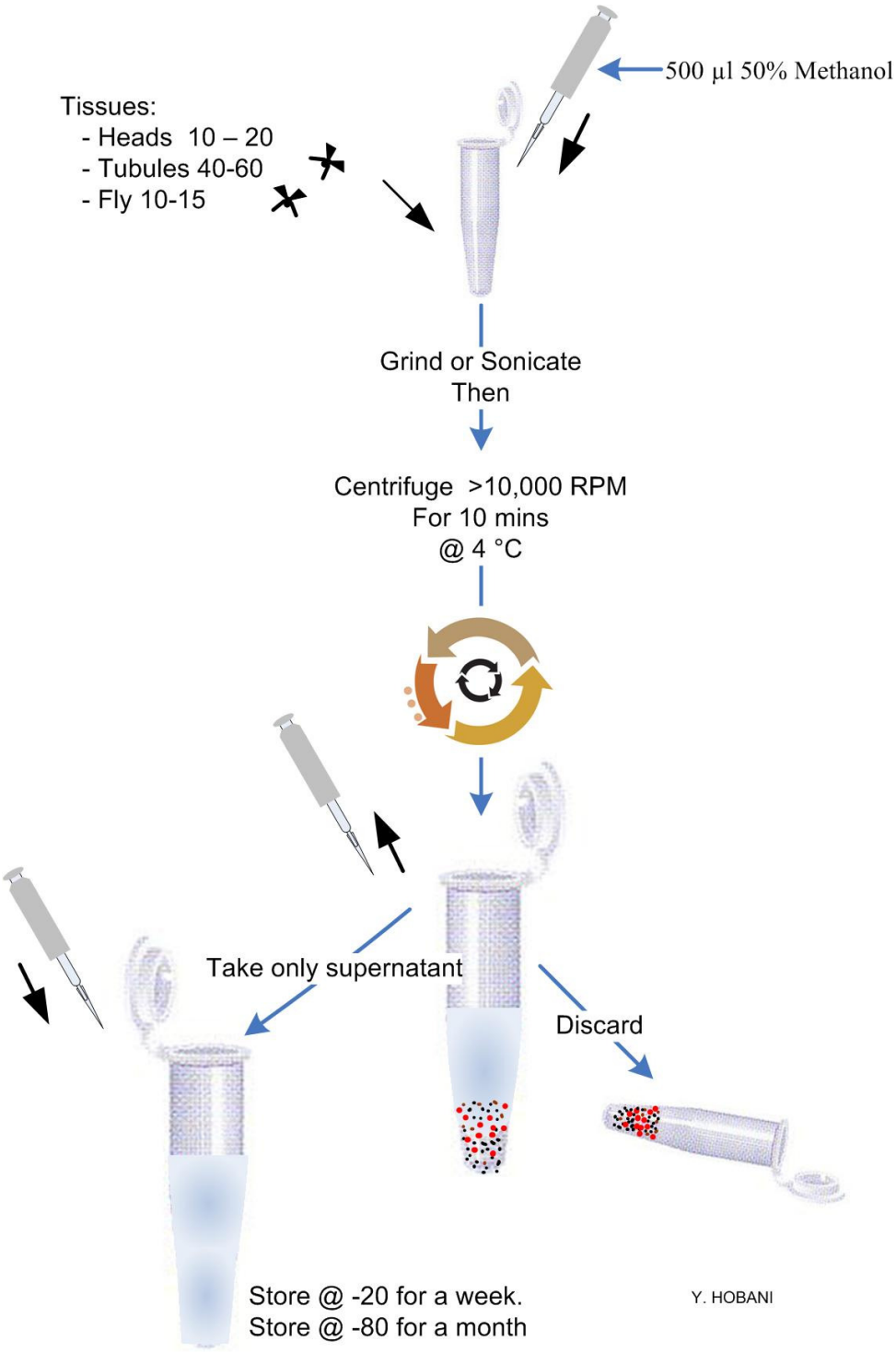

Figure 2-8 Metabolite sample preparation methodology. Was drawn by me.

2.8.4 Operation of the Orbitrap

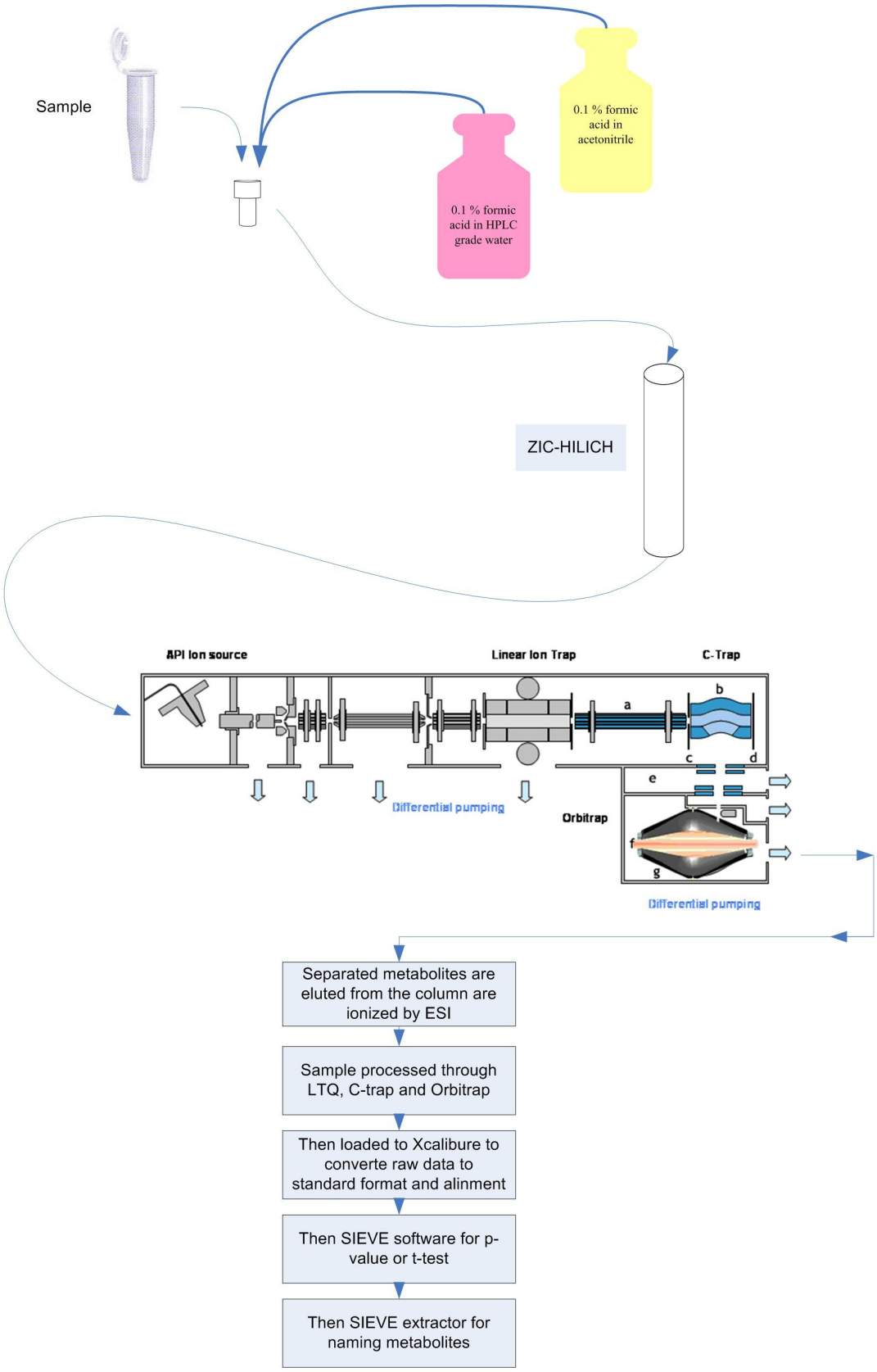

Figure 2-9 Diagram showing the steps taken for metabolomic investigation. Was drawn by me.

2.9 Metabolite extraction strategies

2.9.1 Methanol-water (MW) solvent

Solvent used in this experiment was a mixture of methanol and water in the ratio (1:1), which was suggested by (Kamleh et al., 2008). Ten whole flies (male and female) were added into 500 µl of the mixture solvent in eppendorf tubes and then homogenized by sonication for 2-3 seconds for three times; the mixtures tubes were then spun in a cooled microcentrifuge at 10 000 rpm at 4 ˚C. The filtered extracts were then kept in the freezer at -80 ˚C prior to analysis. On the day of analysis, samples were brought to RT temperature and placed into chromatograph glass vials.

2.9.2 Chloroform-methanol-water (MCW) solvent

An alternative method method of extraction was also tested. Methanol/chloroform/water solvents were also used in the sample extraction method in the ratio was 3:1:1. Ten adult flies from both genders were collected and anesthetized under CO_2, they were then transferred into the mixed solvents and well homogenized for 2-3 seconds by sonication for three times. The sample was then centrifuged for 10 minutes at 4˚C, and supernatants were then transferred into new eppendorf tubes and then were stored in the freezer at -80˚C until required. Prior to analysis, samples were kept at room temperature and were placed into chromatograph glass vials.

2.10 Allopurinol containing-fly food preparation

This was prepared as described for the microarray experiments, to allow comparison between corresponding transcriptomes and metabolomes of the tubule.

2.11 Software and applied libraries used

In the following, all software used and applied libraries are listed in table 4

Software	Description
Excel 2007	Microsoft spreadsheet
Xcalibur v. 2.0	Analysis of LC/MS data
Sieve software v.1.2	Converts raw data to appropriate format
Sieve Extractor	Automates metabolites identification
SIMCA-P+11	Evaluates and displays LC/MS data
KEGG Encyclopaedia	Works as identifier to provide metabolite names
(http://www.genome.jp/kegg/)	Works as identifier to provide metabolite names
PubMed (http://www.ncbi.nlm.nih.gov/pubmed	Works as identifier to provide literature for metabolite names
Metlin (http://metlin.scripps.edu/) database	Works as identifier to provide metabolite names
Human Metabolome Database (http://www.hmdb.ca/)	Works as identifier to provide metabolite names

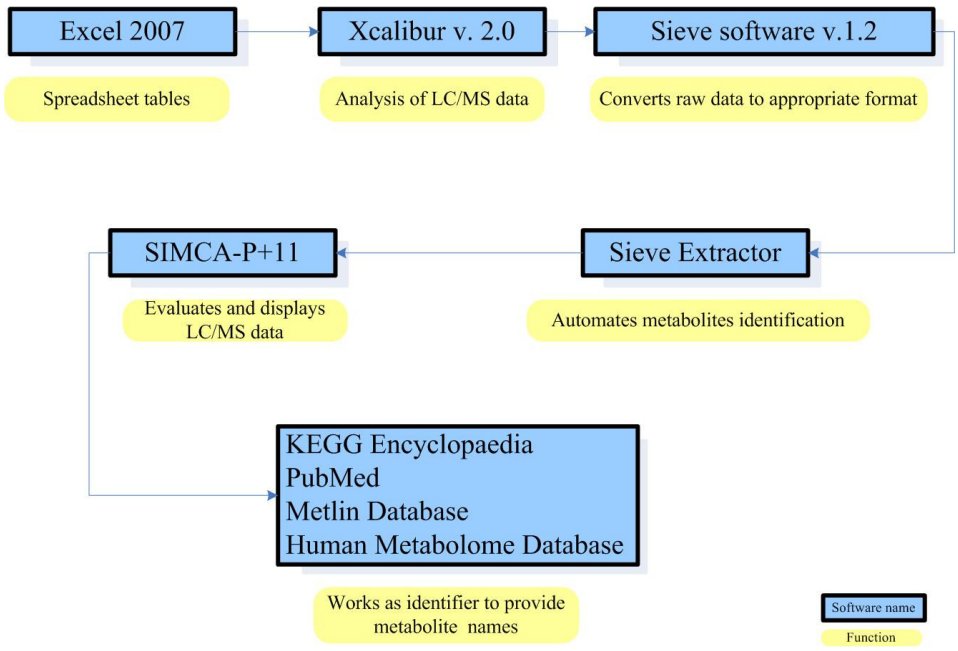

Figure 2-10 Workflow of metabolic software used.

2.12 High resolution mass spectrometry adjustments

LC-MS data were obtained from experiments that were carried out at Strathclyde University (Department of Pharmaceutical Analysis) using a Finnegan LTQ Orbitrap (Thermo Fisher, Hempstead, UK). Orbitrap analyser resolution was set up at 30000. Samples was analysed in positive mode with a capillary temperature of 250˚C, Sheath gas flow 40ml/min and auxiliary gas was 10, while the mass scanning range was (50-1250) m/z. The whole instrument was controlled by Xcalibur software version 2.0 (copyright© Thermo Fisher Co).

ZIC–HILIC column 5µm (150 × 4.6mm) was used in all analyses and a method was developed which produced good separation for a broad spectrum of metabolites. Solvent A was 0.1 % formic acid in HPLC grade water, and solvent B was 0.1 % formic acid in acetonitrile. A flow rate of 300 µl/min was used and the injection volume was 10 µl. Samples were in a vial tray which was set at constant temperature at 3 ˚C to avoid any possible degradation of samples.

2.13 Metabolite identification

Samples within an experimental set were analysed on the same day and in a single run. This means that the differences in instrument response from run to run due to independent manual tunings were limited.

LC-MS data obtained from Xcalibur software version 2.0 composed of retention time and the mass/charge ratio of metabolite. Several steps of the metabolite identification and data analysis were carried out in this thesis and are worth describing here.

2.14 Step by step data analysis

2.14.1 Xcalibur

Firstly, the Xcalibur sample files were loaded into Sieve software 1.2 (Thermo Fisher Co) to convert raw data obtained from Xcalibur software to a common format that allows use for further data processing.

The software shows only 2 dimensions.

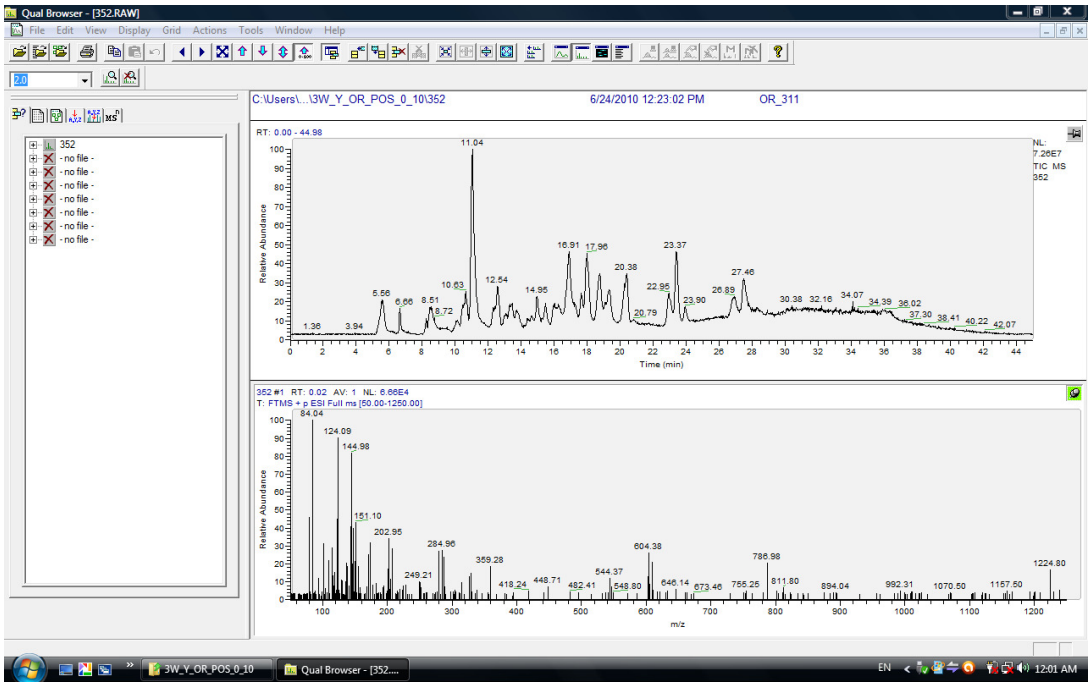

Figure 2-11 Typical raw data produced by the Xcalibur software. The upper trace shows total current chromatograms, and the lower trace, mass spectrogram peaks from 50 – 1200 dalton. Was captured by me.

2.14.2 Sieve software

Secondly, samples are uploaded to the Sieve program as two groups: control and test samples. Sieve software was tasked with the alignment and framing of chromatograms. The software shows retention time, observed mass, ratio for the mean peak areas, mass intensity and *P*-value or *t*-test between ion chromatograms of the control group (normal wild type) and those of the test group.

The importance of this program is mainly to align data obtained from the Xcalibur. Data alignment is important to bring peaks widths within the limit of reading range, and to minimise the analyser's reading errors.

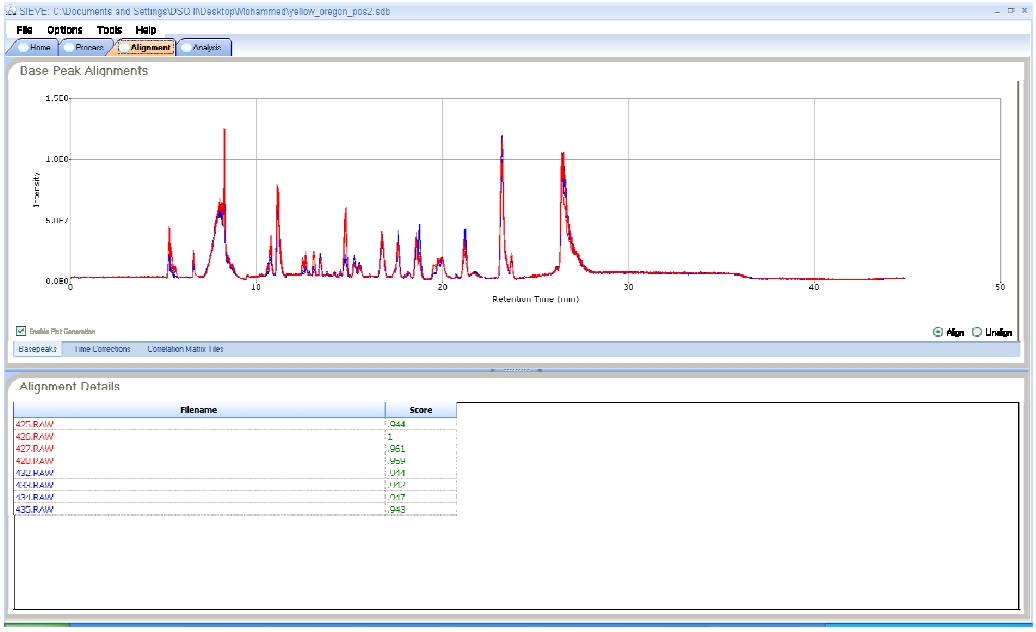

Figure 2-12 Typical screenshot of the alignment step in Sieve. The control and experimental traces are coloured blue and red. Was captured by me.

The second step of the Sieve software is to analyse the aligned peaks Figure 2-13.

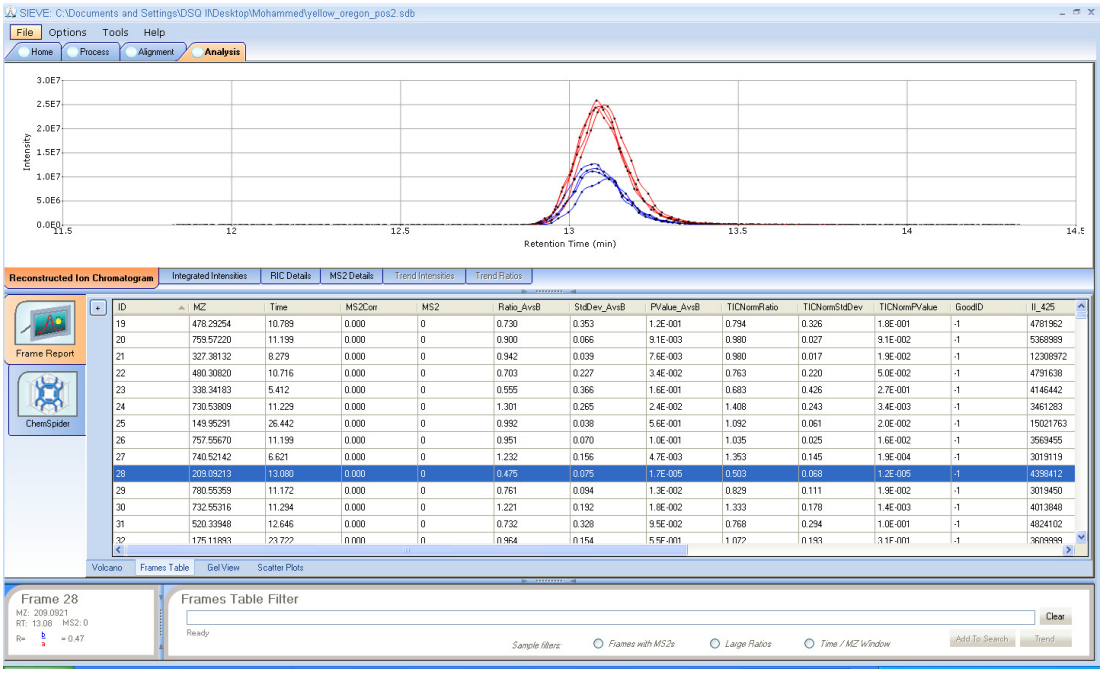

Figure 2-13 Detail of aligned peaks in Sieve. Each trace represents an individual experimental sample. In this case, the record is for the metabolite kynurenine its molecular weight, compared with the m/z ratio, retention time , P-value. (Five dimensions).

2.14.3 Sieve Extractor

Thirdly, a large number of extracted mass results from the Sieve program were not annotated automatically with the name of the metabolite. Sieve Extractor software can help in naming metabolites. Following classification by Sieve software, data obtained were copied and pasted into Sieve Extractor (SE), a programme designed by Strathclyde University – Pharmaceutical Analysis Department in-house for automated metabolite identification. Briefly, Sieve data were manipulated by SE according to ion chromatogram mass width and R.T Width. Two chemical structure databases, Metlin and KEGG were searched to establish identity for peaks by exact mass. New identifications were manually curated for specificity and plausibility before being accepted (discussed below).

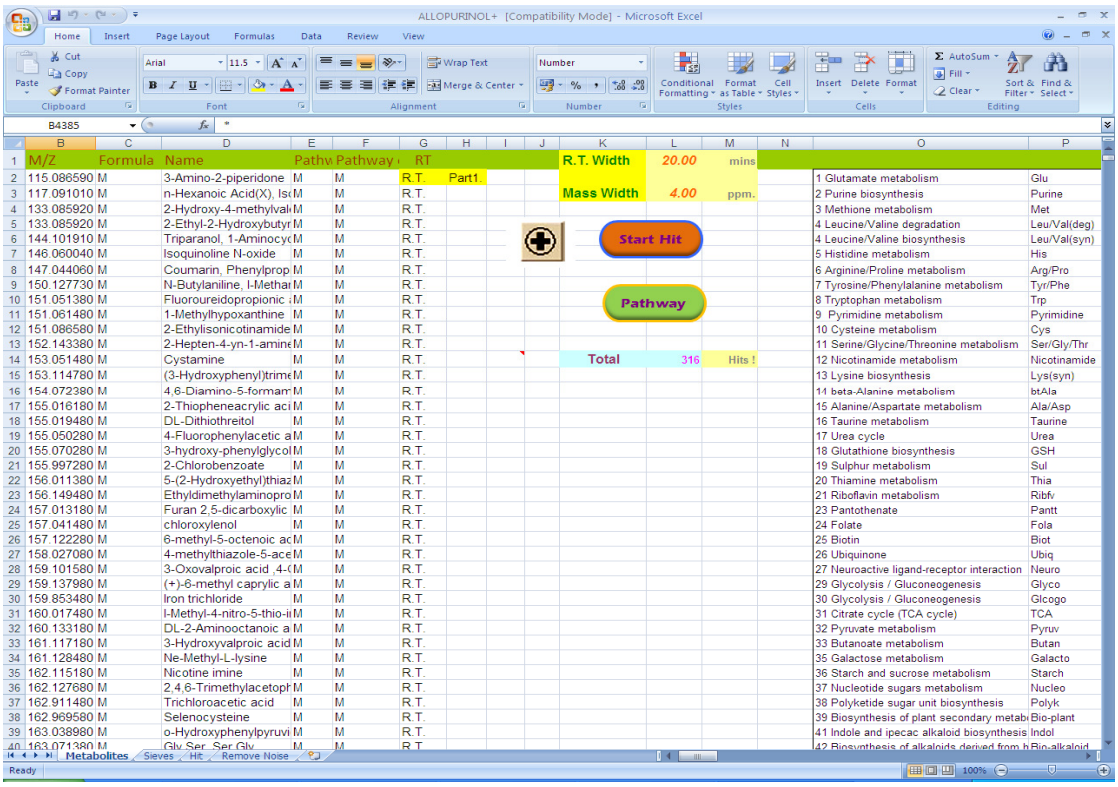

Figure 2-14 Sample output from Sieve Extractor (SE) Programme. Was captured by me.

In a few cases some metabolites suggested by the software make no sense, thus manual checking is always required. In most cases several formula are possible but one or more of these do not make sense in biological classification and can be rejected. Chemical databases such as PubChem, Human Metabolome and Metlin database were associated with metabolite naming when the possible formula within mass accuracy limit was used.

Misidentification or incomplete identification of metabolites was occurring during data analysis for several different reasons. In such cases, MS^2 fragmentation is one of the metabolite identification approaches that can help in confirming the identity of compounds especially when distinguishing structurally similar constituents such as isomers. Loss of the lower mass range occurs during the fragmentation mechanism. An additional approach for distinguishing isomer ions is possible on the basis of the retention time of metabolites in the ZIC-HILIC column stationary phase. Metabolite identification based on retention time depends on understanding of the chemical properties of a metabolite which reacts with ZIC-HILIC column. In HILIC columns, metabolites which are classified as cations are retained more than anions.

In this thesis, hypoxanthine and allopurinol are isomer compounds. Although the Orbitrap and Xcalibur showed no difference in mass and elemental composition between hypoxanthine and allopurinol, a separation between them was observed by chromatographic column according to physicochemical properties. An example is shown in Figure 2-15.

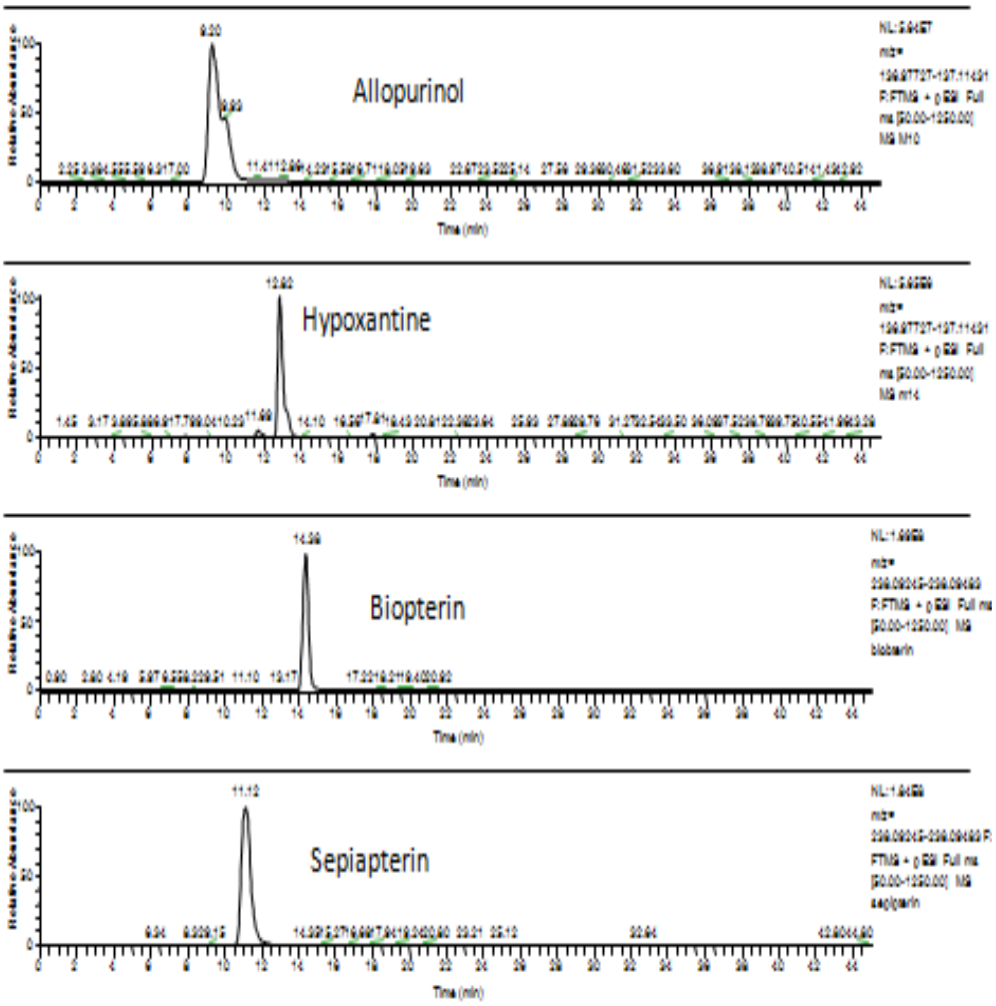

Figure 2-15 Extraction chromatograms from TIC of isomeric compounds using the HILIC-column.

Sometimes differences in retention times do not tell the whole story. Thus MS/MS fragmentation is mandatory to get an informative answer for some isomeric compounds, for example hypoxanthine and allopurinol or oxypurinol. Another step is using standards to differentiate between metabolites which produce the same observed molecular mass in the analyzer.

2.15 Microscopy

2.15.1 Polarizing microscope

Is a simple bright field microscope equipped with polarizer, located between light source and specimen, and analyzer, placed in the optical pathway before the eyepieces. Although polarizing microscopy has a range of uses, it was particularly useful in this thesis for the visualization of uric acid crystals in situ. Uric acid is a metabolite of Xanthine, and so presence of urate crystals implies a functional purine metabolism pathway. Uric acid crystals are brightly birefringent (that is, they appear bright under crossed polaroizing filters).

See the chapter 5 on *uro* 5.4.1 for more details.

Chapter 3 The *rosy* (*ry*)

3.1 History

The mutant *rosy* (*ry*) is the second *Drosophila* mutant ever identified, just after the *white* mutant was discovered by T.H. Morgan in 1910. Although the exact date is not clear, it is likely that *rosy* was first isolated in 1912 (Dow, 2007). The *rosy* mutant is characterized by a red-dull eye colour (Figure 3-1), due to the absence of the enzyme Xanthine dehydrogenase (XDH) (Hadorn and Schwinck, 1956). This enzyme has an important role in the eye pigmentation reaction in *Drosophila*. Chemically, flies lacking this enzyme possess high levels of 2-amino-4-hydroxypteridine, which is a precursor of isoxanthopterin (Glassman and Mitchell, 1959). Moreover, *ry* flies show high levels of hypoxanthine and xanthine, which are precursors of uric acid, so *rosy* clearly affects the purine metabolism pathway. The r*y* mutants are sensitive to purine-rich diet; *ry* mutants' life span is shown to be directly reduced by a purine enriched diet when compared to wild type flies (Collins et al., 1970).

Strikingly, this phenotype is not found only in *ry*. Several other mutants, like *mal*, *cin*, *lxd*, are described having the same eye colour defects, and subsequent investigation has shown that they encode other genes which impinge on the purine metabolism pathway (Table 3-1).

Table 3-1. Comparison between selected *Drosophila* mutants with defective eye-colour.

Gene	**sym**	**chr**	**Eye colour**	**Enzyme activity**	**References**
rosy	*ry*	3	Brown, Red dull	Absent or low XDH	(Hadorn and Schwinck, 1956)
maroon-like	*mal*	1	Brown red dull	Present, inactive Co-F.	(Forrest et al., 1956) (Wahl et al., 1982)
cinnamon	*cin*	1	Reddish-brown	AO, PO, XDH, SO.	(Baker, 1973)
chocolate	*cho*	1	Brown	2-amino-4-hydroxypteridine absent	(Sturtevant, 1955) (McKay, 1972)

AO; Aldehyde oxidase, PO; pyridoxal oxidase, XDH; xanthine dehydrogenase, SO; sulfite oxidase.

There is also a renal phenotype; in the *ry* mutants: as an result of XDH absence, the enzyme's substrates, xanthine and hypoxanthine are found at much higher levels than

normal. Consequently, xanthine calculi form in the Malpighian tubules (MT), which become enlarged and malformed (Figure 3-2).

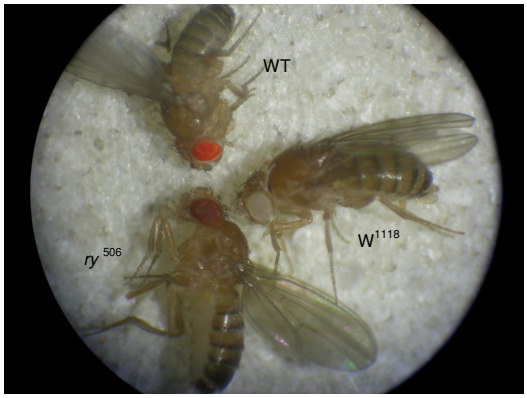

Figure 3-1. Showing the characteristic red-dull eye colour of *ry* mutant against white-eyed flies (w^{1118}) and Canton S wildtype (WT).

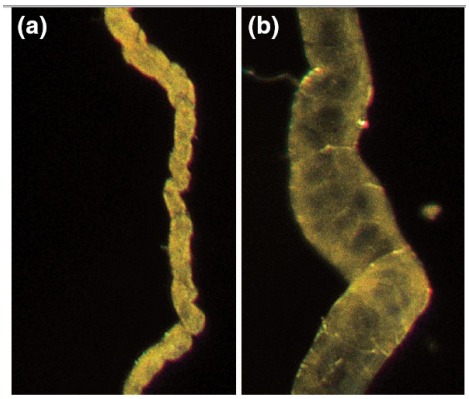

Figure 3-2. Inflated MT in *ry* and compared with WT (Wang et al., 2004).

A; MT from a wild type fly, B; shows inflated MT from homozygous *ry* mutant blocked with xanthine orange particles.

As the mutant is best known for its dull-red eye colour (Figure 3-1), one might expect that the main location of the XDH enzyme is in the eyes. Reaume et al (1989) stated that XDH enzyme is transported to the eye but not expressed; however by looking at the Flyatlas.org one can see the gene is expressed almost everywhere in the fly, including the eyes, but mainly in the MT. Also, XDH is mainly cytoplasmic, so transportation is unlikely.

3.2 Xanthine dehydrogenase vs. oxidase

Xanthine oxidoreductase is the generic name for the house keeping gene enzyme; namely Xanthine dehydrogenase (XDH) and Xanthine oxidase (XO) (Meneshian and Bulkley, 2002).

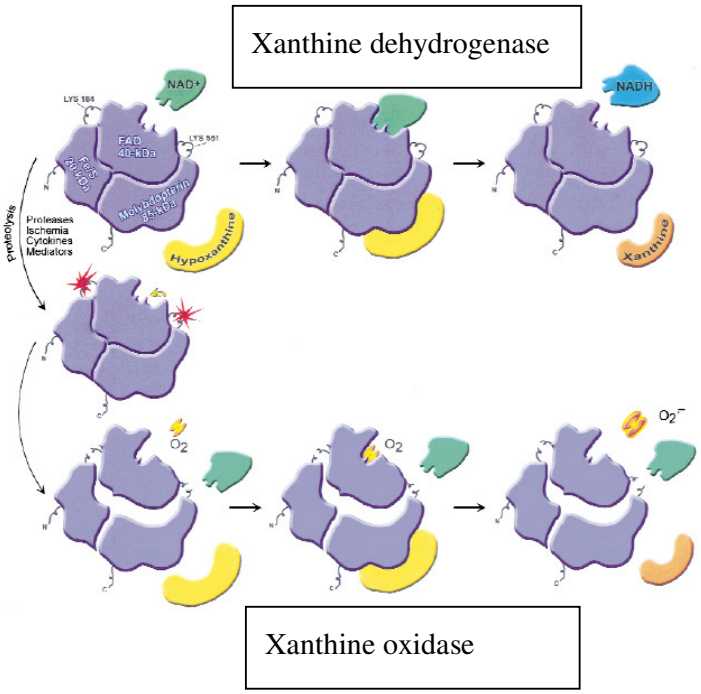

Figure 3-3. Xanthine Oxidoreductase (XOR) structure and interchangable mechanism (Meneshian and Bulkley, 2002).

Both the dehydrogenase and oxidase use hypoxanthine and xanthine as substrates to produce uric acid; however, different cofactors are utilized in each reaction. The dehydrogenase uses NAD^+ as an electron acceptor and produces NADH. However, the oxidase utilizes O_2 as a cofactor and produces more reactive oxygen species (ROS), namely H_2O_2 and O_2^-. These in turn can form further radicals. So the XO is known to be a source of free radicals as seen in the reaction (A) in (Figure 3-4).

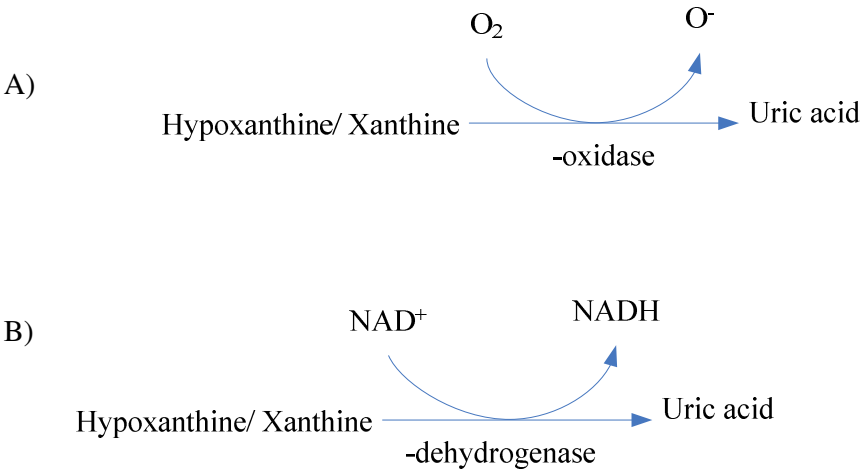

Figure 3-4. Xanthine dehydrogenase and oxidase reactions.

Furthermore, both enzymes are encoded by the same gene and exist as interchangeable forms. Usually it is found in the dehydrogenase form; however under some pathophysiological conditions or in injuries such as ischemic reperfusion, it is converted into the oxidase form, using the excessive O_2 present as a cofactor and thus producing ROS as a result of the oxidative stress. This switch could thus be thought of as a defence mechanism in ischemia, where the body suffers from severe O_2 loss; on recovery, the body is trying to provide an immediate supply of O_2 to the affected tissue. This huge supply of O_2 gained into cells, from increased blood flow, can causes sometimes unwanted effects like cellular damage of proteins, DNA and plasma membrane (Martin et al., 2004). Thus, in order to prevent cell death, conversion of XDH to XO helps to utilize the excessive O_2 present. However, although this mechanism rescues the body from oxidative stress, it is at the cost of generating high levels of ROS.

This interconversion can also be either reversible when sulfhydrylated; or irreversible, when proteolysed (Figure 3-5) (Chung et al., 1997).

Thus, the enzyme XDH/OX has an important role in cellular defence against oxidative stress.

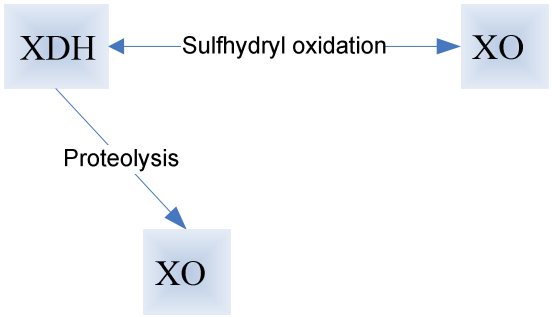

Figure 3-5. Interconversion between XDH and XO (Modified from Chung et al., 1997).This figure shows the interconversion between XDH and XO. The original form is the dehydrogenase form, which can be converted to the oxidised form by sulfoxidation and converted back to the dehydrogenase form by reduction. However, conversion to XO by proteolysis is irreversible.

Furthermore, XO plays an important role against free radicals, because its main product is uric acid, a very well known reducing agent (electron donor). Urate can thus act as a free radical scavenger by donating electrons to be coupled to ROS. Moreover, XDH/XO could modulate the immune response, as ROS, in the form of O_2^-, OH^- and H_2O_2; and

RNS, in the form of NO, in the presence of bacteria, can act as antibacterial and cytotoxic agents against various pathogens and tumour cells (Vorbach et al., 2003).

In humans, the interconversion between XDH and XO is known to occur, leading to its naming as XOR. Such interconversion has not been demonstrated in *Drosophila,* where the gene product has been called XDH since 1956. Thus, to avoid misunderstanding, in this thesis I am going to call the enzyme XDH in *Drosophila* and XOR when discussing in mammal particularly humans.

3.2.1 Basic biochemistry

Both enzymes are composed of two identical subunits with a total size of 300 kDa. Each subunit consists of one molybdenum (85kDa), two non-identical Fe_2S_2 centres (20kDa) and flavin adenine dinucleotide (FAD) (40kDa), producing a total molecular weight of 150kDa (Chung et al., 1997).

3.3 Results

3.3.1 Tissue-specific knockdown of XDH activity

Although a wide range of *rosy* alleles have been characterised, and many are still available in stock centres, we wished to investigate the role of *rosy* in further detail, dissecting its enzymic and defence roles in individual tissues – for example, the Malpighian tubules, the tissue in which *ry* is most abundantly expressed. As both *rosy* and the corresponding human disease (Xanthinuria type I) both show similar defects, this would allow a more detailed modelling of the human condition in flies, and so test the implicit hypothesis of the thesis (that human renal disease could usefully be modelled in *Drosophila*). Accordingly, we tried to develop new alleles of *rosy*, and new analytical techniques to study their impact.

3.3.2 RNA interference (RNAi)

RNAi is a method widely used as a powerful tool for reverse genetics in gene silencing. The method first was used in *C. elegans*, then was adapted into *Drosophila melanogaster* for gene silencing (Kennerdell and Carthew, 2000). Since then, many elegant RNAi vectors have been developed. For our purposes, the RNAi inducing silencing vector (pRISE) is an effective tool to generate constructs that can be used in *Drosophila* RNA silencing technique (Kondo et al., 2006).

This approach is based on constructing a plasmid including an inverted repeat of the *ry* target sequence separated by a functional intron to form double stranded RNA (Figure 2-4 B). This plasmid also uses a characteristic repeat sequence of the Gateway recombination cassette which helps in avoiding multiple restriction digest and ligation steps. To accomplish the *ry* gene silencing, our DNA fragment has first to be cloned into an appropriate entry vector, which is the pENTR/D-TOPO from Invitrogen. Once the cloning is done then this will be transferred or subcloned easily into the pRISE by the help of an enzyme recognising the Gateway cassette site by recombination reaction (Figure 2.6 LR clonase). This enzyme is the LR Clonase, also from Invitrogen.

In principle, the use of clonase rather than ligase offers very high frequency of ligation, and the approach was successful elsewhere in this project. However, after several attempts, it proved impossible to clone the open reading frame for *ry* into pENTR in-house (Figure 3-6).

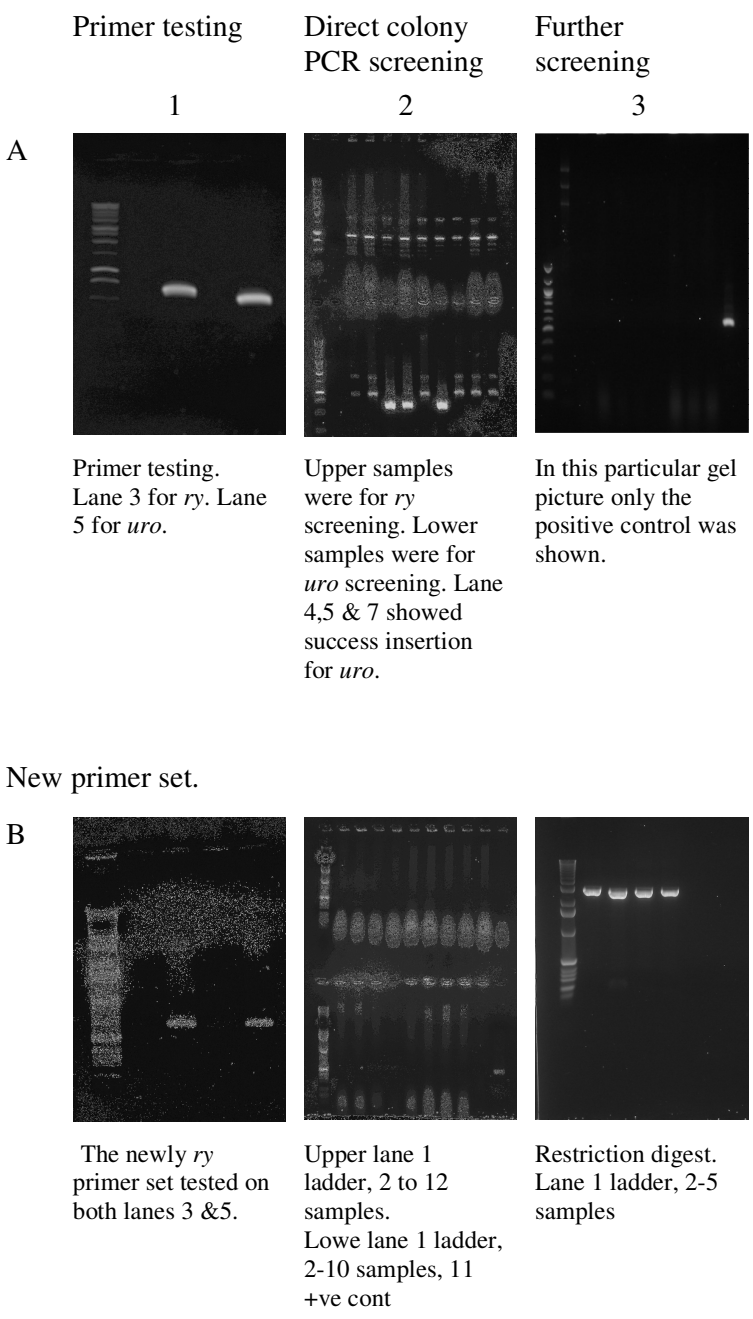

Figure 3-6 Gel pictures showing *ry* cloning.

All column 1 gel pictures are for primer testing. A1 *ry* and *uro* primer testing. While in B1 a new *ry* primer set was used. Column 2 gel pictures were for direct colony screening. Same steps in row B were repeated several times.

During the course of the project, comprehensive libraries of transgenic *Drosophila* containing RNAi constructs downstream of UAS, have become available from several stock centres. Accordingly, the transformant 25172 was also ordered from the *Drosophila* Genomic Resource Centre in Vienna.

3.3.2.1 Validation by qPCR.

Flies were crossed with *urate oxidase*-GAL4 line, which drives RNAi expression exclusively in the principal cells of the main segment of the tubules of third instar larvae and adults (Terhzaz et al., 2010). Then week-old adult progeny were selected, tubules were dissected, total mRNA were extracted, cDNA were also generated and then gene expression validation of the knockdown took place.

QPCR method is considered the method of choice for gene expression validation. So primers were designed to amplify a DNA fragment of 196 bp (primers qPCR *ry* II F and R see appendix 9.5) in the *ry* gene. Then the annealing temperature was optimised. Results were normalized against the housekeeping gene, α-tubulin (Chintapalli et al., 2007).

Malpighian tubules were dissected from both parents and progeny then total mRNAs were checked for quality as well as for quantity. Then cDNA was generated and then checked for quality and quantity, next this was used as a template for the gene expression validation reaction. It was found that the RNAi line, when driven by the tubule-specific driver *uro*-GAL4, reduced expression of the *ry* in the tubules significantly, by 70 % compared to parental lines (Figure 3-7).

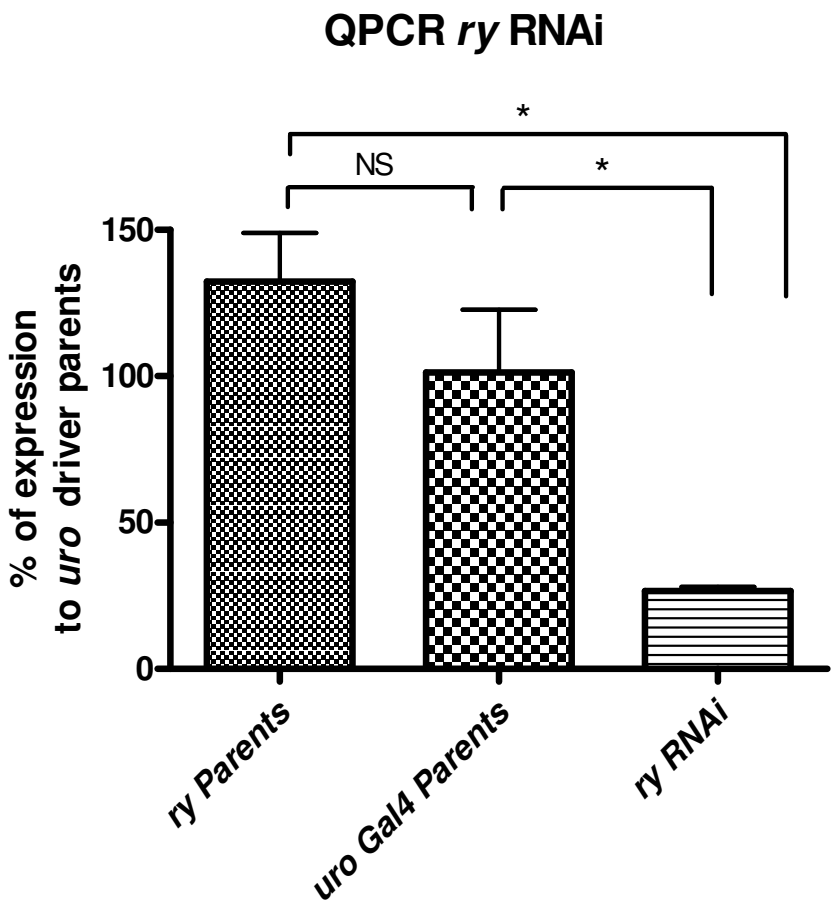

Figure 3-7. The *ry* RNAi knockdown validated by qPCR

The *ry* gene knockdown expression is compared to *uro*-GAL4 and *ry* RNAi parents. Data mean ± SEM, N=4. Significance of changes was assessed by Student's *t*-test (two tailed) taking *P*=0.05 as the critical level: significant changes are marked with *.

Accordingly, it was concluded that the Vienna UAS-*ry*(RNAi) line provided a suitable resource – a strong, cell-specific hypomorphic allele of *ry* – and in-house cloning efforts were discontinued.

3.3.3 Metabolomics

The metabolomic approach has emerged as a new branch of the omics era. With the advances in bioinformatics and unparalleled sensitivity in detection, it has potential applications for simple model organisms like *Drosophila*.

The Orbitrap was known to be able to detect relevant metabolites, from manufacturer standards. However, we set out to establish whether they could be resolved with sufficient sensitivity in real extracts of flies.

Thus we tried to use the *Drosophila rosy* mutant to find out whether metabolomics, and specifically the Orbitrap, are useful tools in flies. Oregon R also was used as a control. In a brief pilot study 10 flies were grind up and run. As it can be seen in (Figure 3-8) the desired peaks of purine metabolism related metabolites were seen.

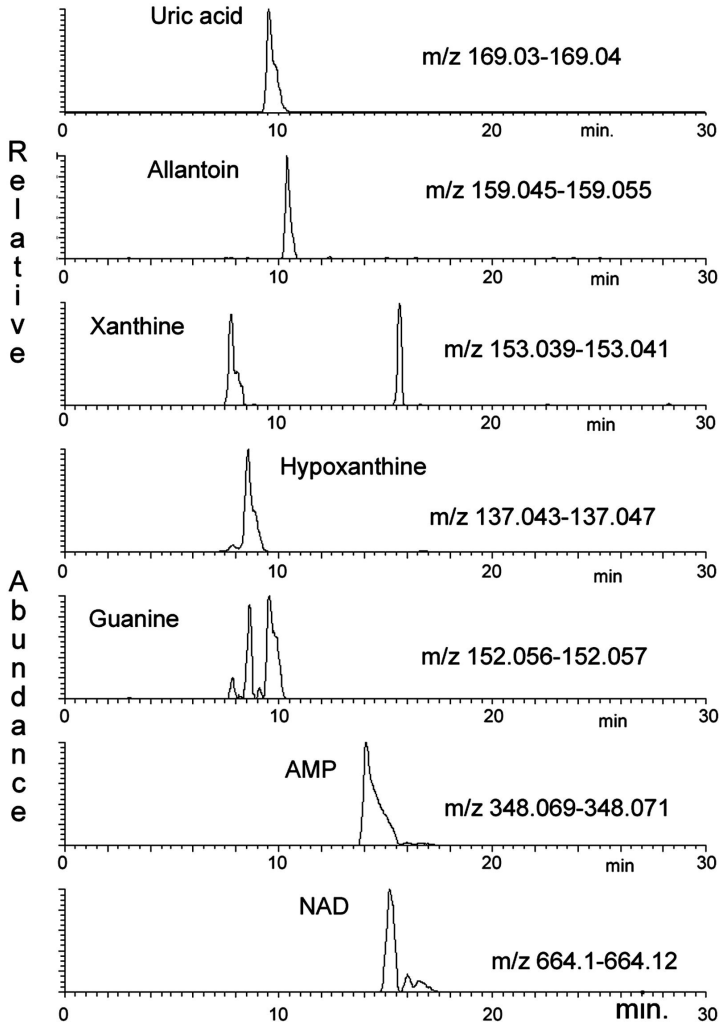

Figure 3-8 Narrow-range extracted ion traces extracted across a range of 0.02 amu showing the metabolites related to uric acid biosynthesis from female wild-type *Drosophila*. Along with their retention time as well as mass/charge ratio.

3.3.3.1 Validation by Orbitrap

For further validation, and as a new method for gene knockdown validation, we tried to apply metabolomics to measure relevant metabolites that should be directly affected by *ry* gene silencing.

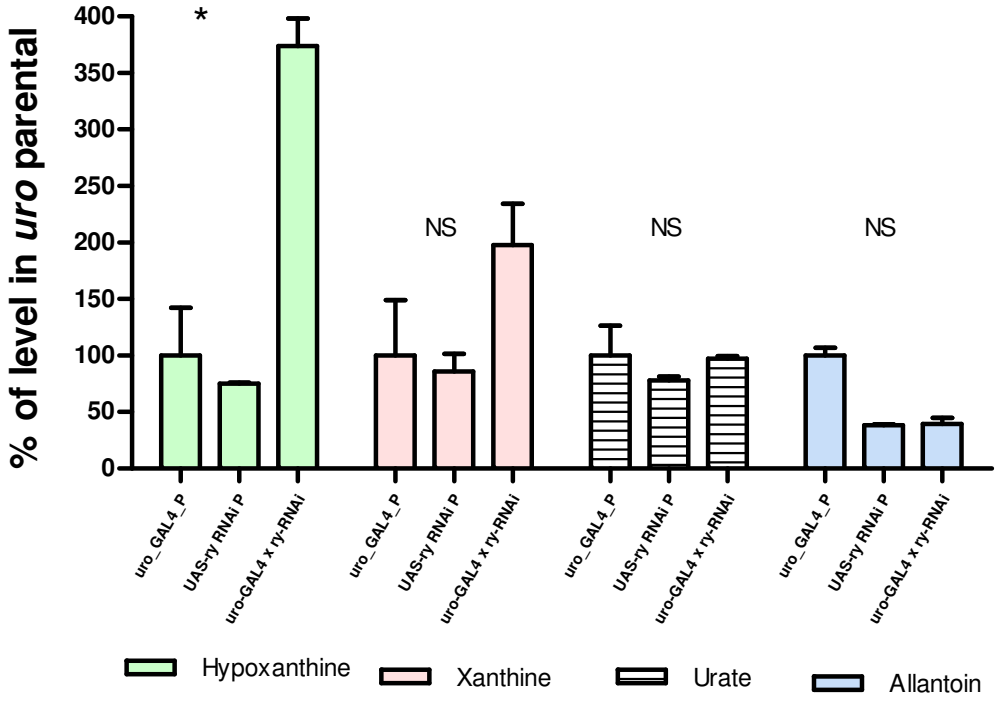

Figure 3-9. RNAi knockdown of *rosy* phenotypically validated by Orbitrap. It shows comparisons between the major metabolites involved in the absence of XDH in different lines. *Uro*-GAL4 drivers parents, *ry* RNAi parents and progenies. Data are shown as mean ±SEM for N=3 independent experiments. Data that differ significantly are marked with asterisks are analyzed by Student's *t*-test two tailed.

So from the data presented, the RNAi line produces a useful knockdown of *rosy*, assessed both by gene expression and metabolomic pathway disruption; and the Orbitrap technology provides a useful screen for knockdown of a metabolic enzyme.

3.3.4 Whole fly metabolomics

Could this technology also be useful for classical mutations (of which there are many thousands in stock centres worldwide)? A pilot experiment was performed on extracts

pooled from 10 flies. Male and females were kept separate using the *ry*^{506} mutant, known for as XDH enzyme deficient and Oregon R wild type as a control. Initially we were looking for key metabolite changes like xanthine, hypoxanthine and urate, a targeted rather than global metabolomic approach (Figure 3-10).

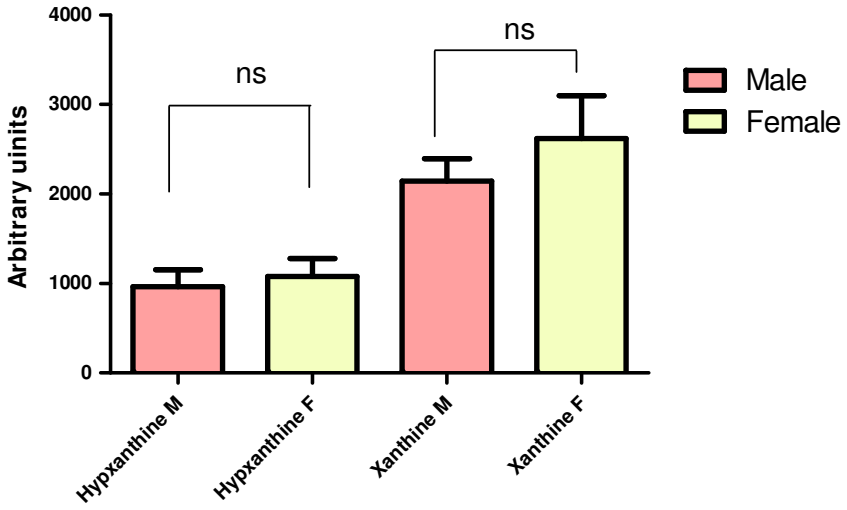

Figure 3-10 A pilot study for male and female *rosy* mutant. It shows no differences between male and female involved the two main metabolites in purine metabolism pathway. Data are shown as mean ±SEM for N=5 independent experiments. Data that differ significantly analyzed by Student's *t*-test two tailed are marked with asterisks.

From classical biochemistry, it was expected to find that both xanthine and hypoxanthine are elevated in the *ry*^{506} mutant (Hadorn and Schwinck, 1956) and (Glassman and Mitchell, 1959). This was clearly observed in both males and females, with both producing similar results. These results both confirm the classical data, and validate the accuracy of the Orbitrap in reproducing similar results with a fundamental technology. The Orbitrap is thus a useful tool for targeted metabolomics in *Drosophila.*

Having obtained the expected results, the analyzer was challenged further, to see to what extent that it would be useful in specific fly tissues. This experiment is much more demanding in terms of low metabolite concentrations. Consequently, we carried out another experiment using different fly tissues, like heads and Malpighian tubules.

Empirically, 15-20 heads and tubules for 20-30 flies were found to give good results (Figure 3-11).

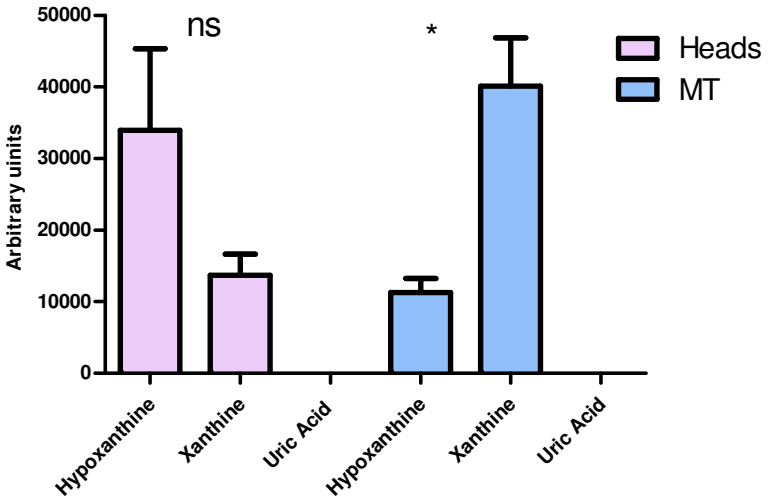

Figure 3-11. Comparison in the *rosy* mutant between heads and MT. Uric acid levels in both head and tubule were too low to be measured. Data are shown as mean ±SEM for N=5 independent experiments. Data that differ significantly are marked with asterisks are analyzed by Student's *t*-test two tailed. This graph shows that xanthine is much more significantly higher than hypoxanthine in the MT. While in the heads samples, although hypoxanthine level is higher than xanthine, it is not statistically significantly.

Accordingly, tissue-specific differences were analysed in more detail, as shown in (Figure 3-12) and (Figure 3-13). In both heads and tubules, hypoxanthine and xanthine levels were strongly elevated, and uric acid and allantoin depleted; but these effects were much more marked in the tubules. This is consistent with microarray expression data, as *ry* is expressed in the whole fly, with higher levels particularly in MT. The metabolites viewed in different tissues thus reflect gene expression level in those individual tissues (Chintapalli et al., 2007), suggesting that it may ultimately be possible to build models linking transcriptome and metabolome.

The results were encouraging, as they showed that the Orbitrap is very useful tool not only in fly metabolomics but also in small tissues as well. Very clear metabolite differences were seen between *ry* and WT in tubules as well as in the heads (Figure

3-11). Thus metabolomics of individual tissues can provide more detailed insights than whole-organism studies, in a manner exactly analogous with the single-tissue microarrays that underpin the FlyAtlas.org resource (Chintapalli et al., 2007).

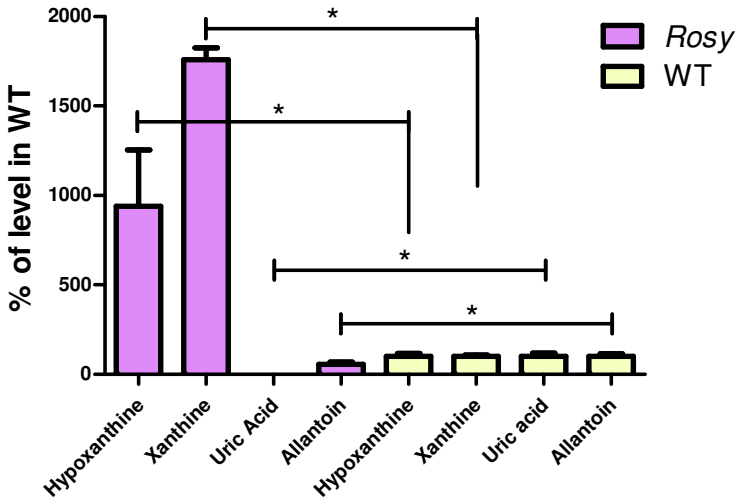

Figure 3-12. Wild type vs. *rosy* heads. Comparisons between key metabolites in purine metabolism pathway to their counterpart in WT in heads samples. Data for each metabolite are expressed as a percentage relative to the wild-type levels. Data are shown as mean ±SEM for N=5 independent experiments. Data that differ significantly are marked with asterisks are analyzed by Student's *t*-test two tailed.

.

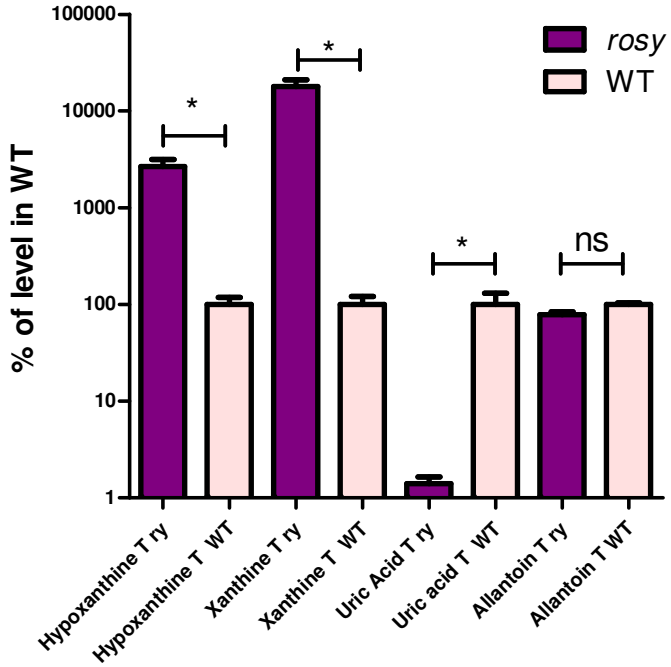

Figure 3-13. Wild type vs. *rosy* Malpighian tubules. This graph shows the comparisons between key metabolites in purine metabolism pathway to their counterpart in WT in MT samples. Data for each metabolite are expressed as a percentage relative to the wild-type levels. Data are shown as mean ±SEM for N=5 independent experiments. Data that differ significantly are marked with asterisks are analyzed by Student's *t*-test two tailed..

3.3.5 Global metabolomics of *rosy* and wild-type flies

After validating the technology, by looking for specific metabolites in *ry*, (so called 'targeted' analysis,) and by comparison with historical data, the approach was extended to all metabolites that could be resolved in the Orbitrap, the so-called 'global metabolomic analysis'.

Initially we broadened our analysis to those metabolites associated with purine metabolism biosynthesis and metabolism (Table 3-2). This confirmed the classical findings for *rosy*, but also extended it to several further metabolites.

Table 3-2. A broader view of the purine metabolism pathway.

Metabolite	P Value (Paired t-Test)	Ratio *ROSY*/WT	Remarks
Allantoin	0.00	0.002	
Uric acid	0.00	0.0041	
Leucylarginine	0.00	0.1107	
Thymine	0.12	0.2296	NS
Uridine	0.02	0.2996	
Aspartic acid	0.02	0.5576	
Valineyl valine	0.41	0.5734	NS
Uracil	0.00	0.7721	
Guanine	0.01	0.8169	
Guanosine	0.07	0.8713	NS
Glutamine	0.75	1.0403	NS
Inosine	0.59	1.0565	NS
Glutamic acid	0.41	1.0895	NS
Cytosine	0.14	1.4403	NS
Adenosine	0.00	2.1464	
Deoxyguanosine	0.00	2.1464	
Cytidine	0.18	2.2857	NS
Amp	0.00	2.3137	
Xanthine	0.00	19.870	
Hypoxanthine	0.00	36.006	

NS, non significant. P-value less than 0.05 is significant.

3.3.6 The main study (male and female)

As the approach was clearly working well, the analysis was extended globally. Table 3-3 shows all significantly changed metabolites detected, arranged into putative metabolic pathways.

Table 3-3 Significantly changed metabolites seen in ry^{506} males and females. Analyzed by Student's *t*-test two tailed.

Metabolite/Metabolic pathway	Formula	Recorded Mass	HITS IN METLIN (Filtered)	Female		Male	
				ratio ry/WT	P.value	ratio ry/WT	P.value
Purine / uric Acid related							
Uric Acid	$C_5H_4N_4O_3$	169.0356	1	5.65E-04	7.62E-04	2.5E-09	5.96E-04
Allantoin	$C_4H_6N_4O_3$	159.013	1	0.047	1.19E-04	0.018	0.002
Hypoxanthine	$C_5H_4N_4O$	137.0458	1	15.66	1.92E-04	10.844	4.90E-05
Xanthine	$C_5H_4N_4O_2$	153.0407	1	25.2	3.19E-04	20.665	5.5E-07
Guanine	$C_5H_5N_5O$	152.0567	3	2.83	0.001	1.325	0.073
Guanosine	$C_{10}H_{13}N_5O_5$	284.0989	1	2.89	0.003	1.119	0.527
6-pyruvoyltetrahydropterin (6-PTP) , biopterin	$C_9H_{11}N_5O_3$	238.0935	5	3.03	4.10E-09	1.576	5.18E-04
Dihydrobiopterin	$C_9H_{13}N_5O_3$	240.1091	3	5.47	1.20E-06	5.188	1.2E-07
Dihydropterin	$C_7H_9N_5O_2$	196.0829	1	0.13	0.013	0.214	0.006
Inosine	$C_{10}H_{12}N_4O_5$	269.088	2	4.69	0.005	2.023	0.011
AMP	$C_{10}H_{14}N_5O_7P$	348.0704	2	1.46	0.055	1.075	0.43
Tryptophan pathway Metabolites							
Tryptophan	$C_{11}H_{12}N_2O_2$	205.09715	2	0.53	0.005	0.36	6.4E-07
Hydroxytryptophan	$C_{11}H_{12}N_2O_3$	221.0921	1	1.87	0.028	0.509	0.004
Kynurenine	$C_{10}H_{12}N_2O_3$	209.921	1	3.35	5.5E-08	0.64	0.004
Hydroxykynurenine	$C_{10}H_{12}N_2O_4$	225.0921	1	0.405	2.5E-07	0.345	7.1E-07
Osmolytes							
Choline glycerophosphate	$C_8H_{21}NO_6P$	258.1101	1	14.57	4E-11	9.56	1.8E-11
Glycerophosphoethanolamine	$C_5H_{14}NO_6P$	216.1101	1	16.16	2E-10	9.672	8.7E-08

Choline	$C_5H_{14}NO$	104.107	1	1.33	0.006	0.792	0.09
Pyrimidines							
Cytosine	$C_4H_5N_3O$	112.0505	1	14.31	0.002	2.571	0.016
Uracil	$C_4H_4N_2O_2$	113.0346	1	0.921	0.6	0.402	0.002
Uridine	$C_9H_{12}N_2O_6$	245.0768	2	0.9	0.617	0.5	0.209
Arginine Pathway Metabolites							
Citrulline	$C_6H_{13}N_3O_3$	176.103	1	0.299	0.004	0.348	0.042
Ornithine	$C_5H_{12}N_2O_2$	133.0972	1	0.376	0.147	0.128	0.036
L-Homocitrulline	$C_7H_{15}N_3O_3$	190.11862	1	0.011	1.9E-07	0.00009	0.00031
Misc Metabolites							
Alanine	$C_3H_7NO_2$	90.055	2	1.93	8.4 X 10-8	1.259	0.075
Glutamic acid	$C_5H_9NO_4$	148.0604	4	1.75	3.14E-04	0.871	0.094
Glutamine	$C_5H_{10}N_2O_3$	147.0764	5	1.32	5.66E-04	1.11	0.233
Threonine	$C_4H_9NO_3$	120.0655	2	0.526	0.000032	0.578	2.21 E-04
Nicotinamide	$C_6H_6N_2O$	123.0553	1	1.55	1.60E-04	0.732	0.081
Valine	$C_5H_{11}NO_2$	118.08613	5	1.06	0.494	0.76	0.016

As well as finding what was expected from metabolomic studies in the *rosy* mutant, many further changes in metabolites were obtained, some of which were quite unexpected, and not known from the extensive classical literature on *rosy*. I will now focus on each affected pathway in detail. Red colour readings indicate conflict between male and female.

3.3.7 Purine metabolism pathway

As can be seen in (Figure 3-14), the changes shown in (Table 3-3) are very sensible. Significantly, changes in metabolite levels can be detected several metabolites further from the genetic lesion than had been detected by classical analytical biochemistry. This means that the Orbitrap technology can provide more information in a single experiment than can be obtained by classical techniques.

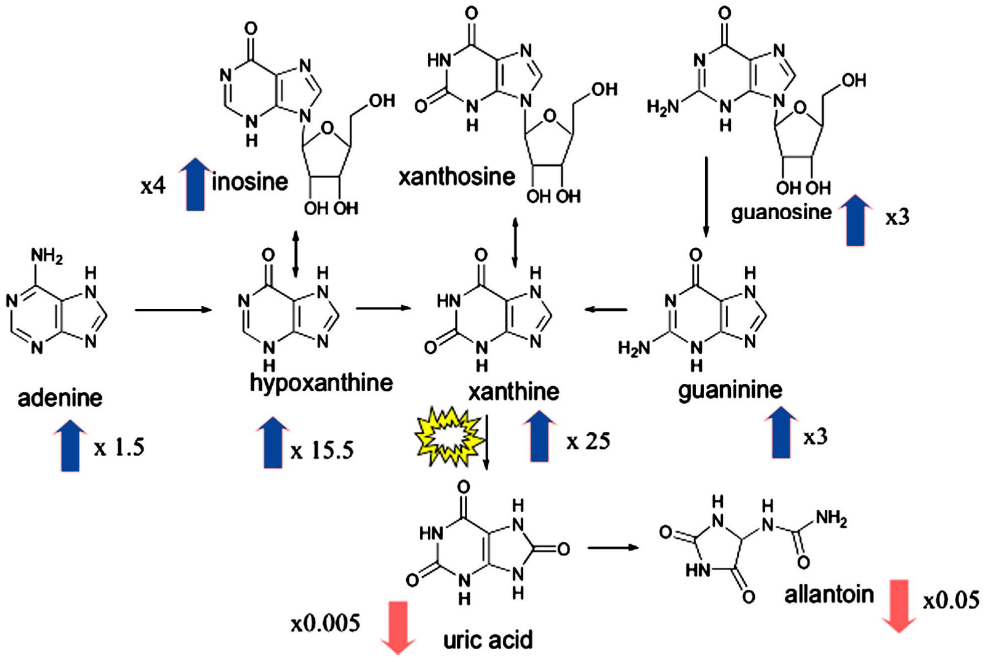

Figure 3-14. Part of purine metabolism pathway in *Drosophila*, with significant changes in whole-fly metabolite levels shown (Kamleh et al., 2008).

3.3.8 Tryptophan pathway metabolites

It was, also found that 3-hydroxykynurenine levels were lower in *ry* (Table 3-2) and (Table 3-3), while kynurenine was elevated. This suggests that the enzyme responsible for converting 3-hydroxykynurenine to kynurenine is reduced in activity; and so explains how the *ry* eye red-dull colour is generated. Generally, the *Drosophila* eye colour is constituted as a result of a mixture of two pigment colours, namely, brown (xanthommatin or ommochrome) and red (drosopterin). Each colour is generated from a distinct pathway (Figure 3-15). Thus, any disruptions in either pathway will impact on the *Drosophila* eye colour. The ommochromes are metabolites of tryptophan pathway, via kynurenine and 3-hydroxykynurenine.

(A)

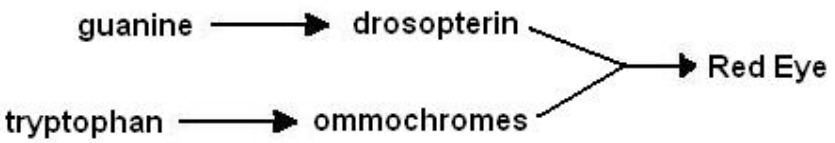

(B)

Tryptophan

↓

N-formylkynurenin

↓

Kynurenin

↓

3-hydroxy kynurenin

↓

Xanthommatin

Figure 3-15 (A) Overview of eye pigment formation in insects. (B) Detailed view of conversion of tryptophan to xanthommatin.

How could Xanthine dehydrogenase impact on the tryptophan metabolism pathway? One possibility is through a reduction in cofactors necessary for enzymatic metabolism of tryptophan. The structure of flavin adenine dinucleotide (FAD) is shown in (Figure 3-16). Adenosine is linked through two phosphate units to a riboflavin; so the idea here is that flavin is very important part in the FAD; so when it is defective, vital metabolic biosynthesis, like hydroxylation of kynurenine will be disrupted. It was observed that levels of riboflavin (vitamin B_2), which is necessary for the biosynthesis of the FAD co-factor required for hydroxylation of kynurenine, were much lower in *ry*. This may be due to malabsorption of the vitamin in *ry* and could provide an explanation for the important of XO on the kynurinine pathway.

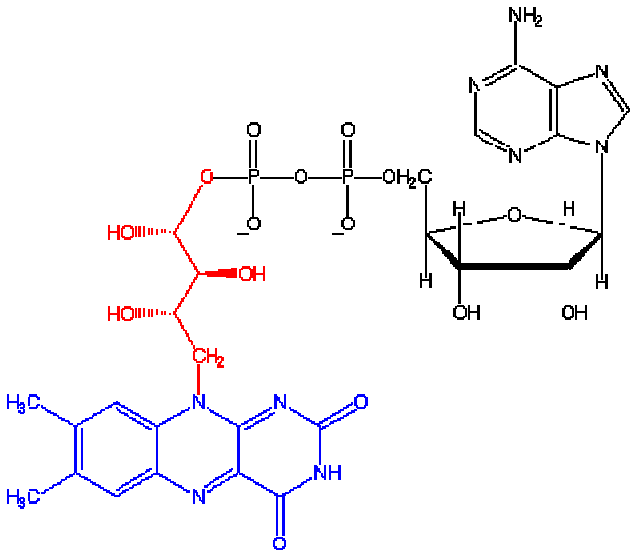

Figure 3-16 Chemical structure of FAD.

The black molecule is **adenosine dinucleotide**, The red is **ribitol**, and the blue **flavin**.

3.3.9 Osmolyte biosynthesis

Changes were also observed in the glycerophospholipid pathway. Both choline glycerophosphate (CGP) and glycerophosphoethanolamine (GPEA) -related to osmolyte biosynthesis- were elevated.

In other organisms, this pathway is triggered or activated when excessive amounts of NaCl or nitrogenous wastes (urea) accumulate in the mammalian renal medullary cells. This occurs as a result of the animal trying to maintain the osmotic balance. How are these metabolites changing in *rosy*? Rather than a direct enzymatic effect on phospholipids, it is possible that defective purine metabolism may result in osmotic stress – as outlined below – and so induce osmolyte biosynthesis.

Nitrogenous waste products are highly toxic and need to be eliminated immediately from insects. To do so these wastes are must be metabolized to lesser toxic products, like uric acid in *Drosophila*. Uric acid is water insoluble so its excretion is sparing of organismal water (Chapman and Chapman, 1998). However, if urate formation is blocked, purine metabolism may result in the accumulation of water-soluble metabolites, thus they must be diluted to reduce its toxicity until they excreted. As *ry*

mutants are unable to make uric acid in the absence of XDH, they excrete the nitrogen waste in other forms, perhaps as water-soluble xanthine. This process would be wasteful of water, leading to osmotic stress. This could explain the observation of CGP and GPEA in higher levels in comparison to WT fly in the osmolyte biosynthesis (Figure 3-17).

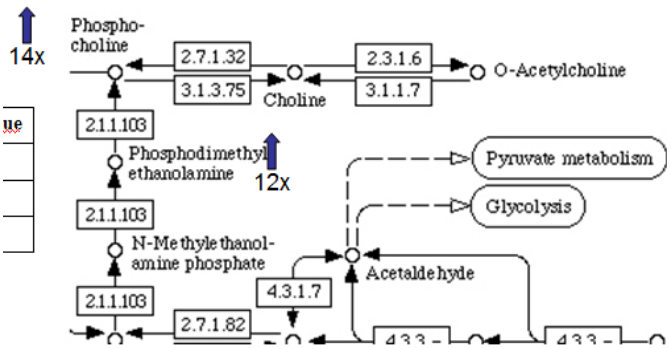

Figure 3-17. Osmolyte biosynthesis: extract from the KEGG pathway map, with fold changes superimposed.

Thus all previous effects of on the osmolyte pathway are not directly an effects of *ry*, it is rather a secondary impact of the XDH enzyme on phospholipid synthesis.

A corollary of this model is that *rosy* flies might be under baseline osmotic stress, and so might be more susceptible to external stress – for example – hyperosmotic diets. It would be interesting to test this model experimentally, if time allowed.

3.3.10 Arginine metabolism

Arginine metabolism (the urea cycle) is also affected in *ry,* with significantly lower levels of ornithine, citrulline and L-homocitrulline (Table 3-2). L-homocitrulline does not actually feature on a KEGG map; but it is synthesised from carbamoyl phosphate (a precursor of citrulline), and lysine. So its depression could link to the observed reduction in levels for citrulline (Figure 3-19). One explanation could be that an observed accumulation of dihydrobiopterin (DHBT) causes an inhibition of tetrahydrobiopterin (THBT) recycling (Figure 3-18). One of the isomers of DHBT is

known to be an inhibitor of THBT regeneration (Thony et al., 2000) and THBT is required as a co-factor in arginine oxidation which results in the formation of NO and citrulline. Accumulation of DHBT in vascular tissue may have a role in insulin resistance where it inhibits vasodilation through inhibiting NO production (Shinozaki et al., 1999).

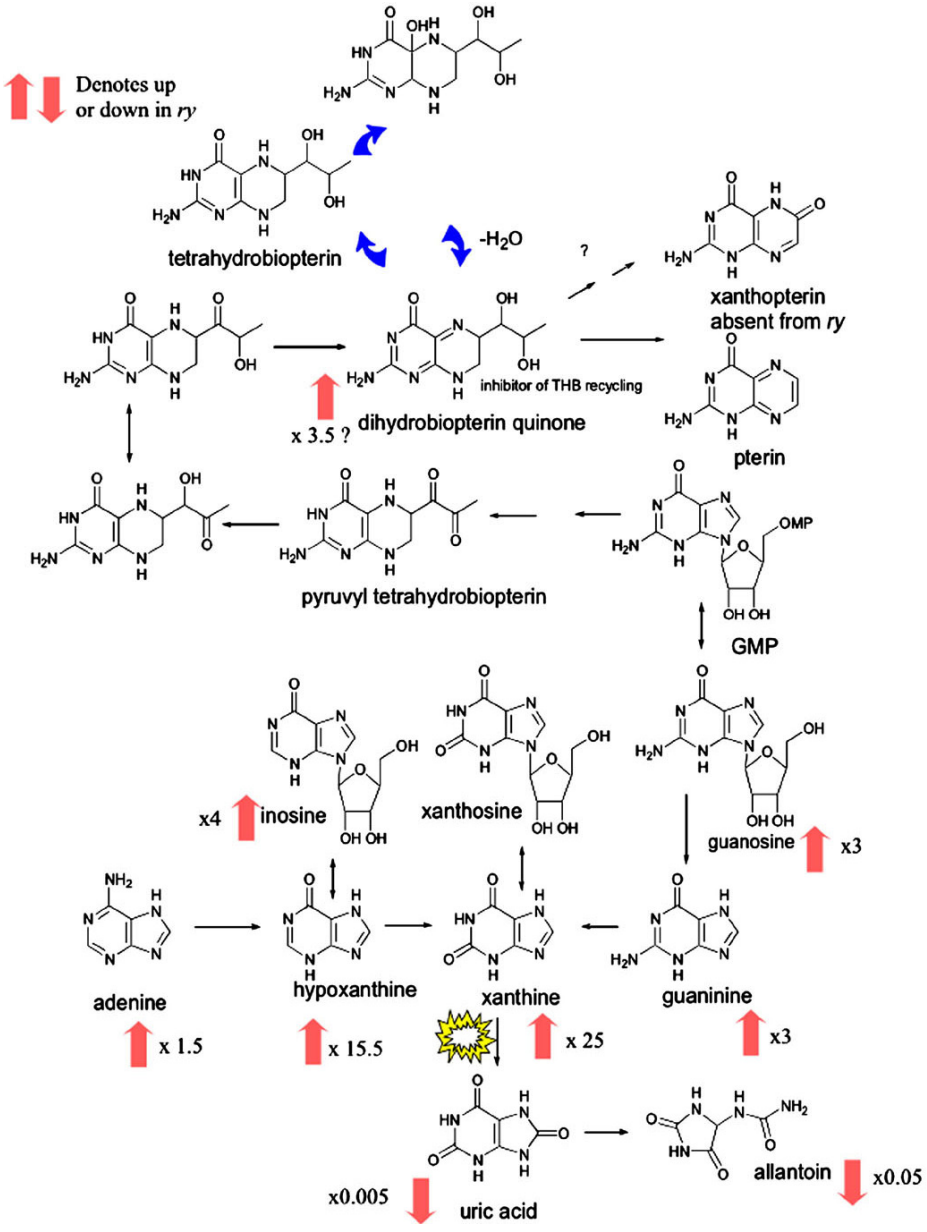

Figure 3-18 Impact of *rosy* mutation on the purine and biopterin metabolic pathway. Although the primary lesion is a disruption of xanthine dehydrogenase, the impact on the dehydrobiopterin pathway might be explained by the increase in guanosine levels. Red arrows denote significantly changed metabolites; fold changes are shown alongside each arrow. After (Kamleh et al., 2008).

More simply, a lesion in purine metabolism increases the pressure on other routes for nitrogen excretion, and urea production is a key by-product of the arginine (urea) cycle (Figure 3-19). Even if *rosy* exerted a relatively focused effect on purine metabolism, it could still perturb this remote part of the metabolic map.

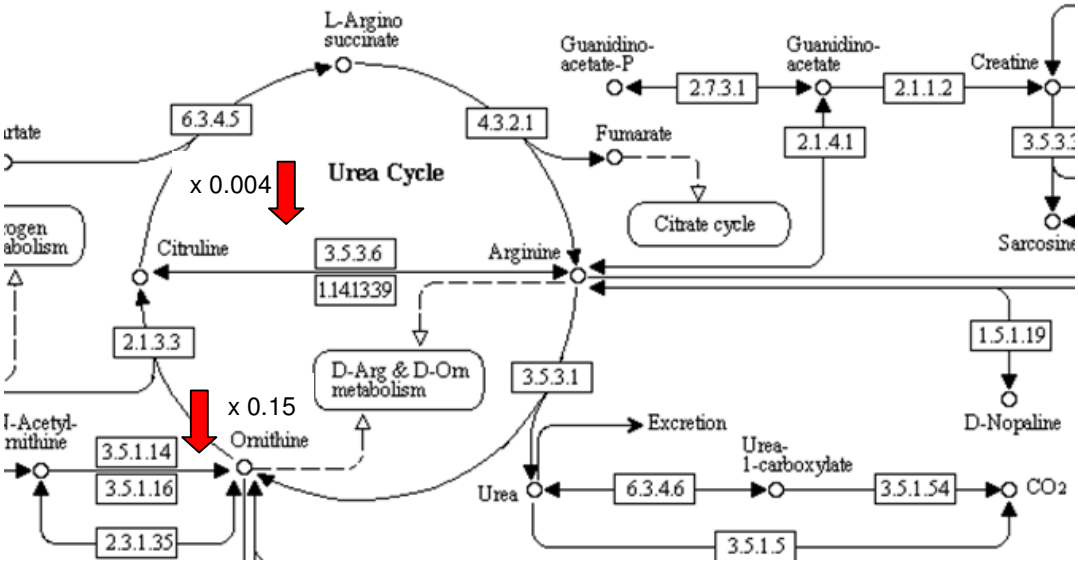

Figure 3-19. Arginine pathway: extract from the KEGG pathway map, with fold changes superimposed.

3.3.11 Pyrimidine metabolism

Cytosine is strongly increased, and uracil decreased in *rosy* compared to wild-type, although the uracil depression was male specific (Table 3-2). Cytosine and uracil are neighbouring metabolites in the pyrimidine metabolic pathway (Figure 3-20). By contrast, their neighbours (cytidine and uridine) are not significantly changed. The pyrimidine compounds can also be degraded into urea. For example cytosine can be catabolized into uracil and then catabolized further to β-Alanine.

The reason why cytosine is the only metabolite elevated is not clear, however – as for the arginine explanation above- this could be possibly as a secondary effect of the fly

trying to compensate for a shortfall in nitrogenous compound excretion through the purine metabolism pathway.

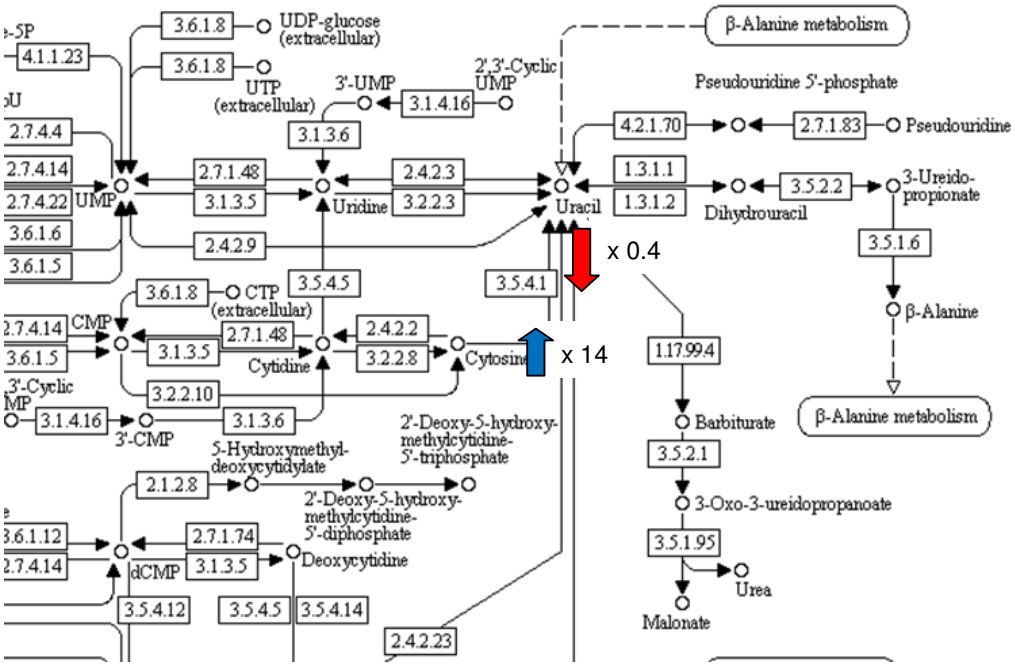

Figure 3-20. Pyrimidine pathway: extract from the KEGG pathway map, with fold changes superimposed.

3.4 The mutant *rosy*, allopurinol and gout

3.4.1 Introduction

Gout is an inflammatory disease condition characterized by a recurrent attacks of inflammatory arthritis, redness, tenderness and swollen joints, as a result of sodium urate or uric acid crystals precipitating in joints and soft tissues (Figure 3-21) and (Figure 3-22).

For example, in the UK it is estimated 1.4 % of the adult population are affected with gout. The disease is mainly seen in the elderly people over 65 years (Patel et al., 2010).

Gout can be caused by either dietary habits; high sugar and protein intake, or could be happens as a result of secondary effects of metabolic syndrome. It may also result from renal failure.

The exquisitely painful nature of gout has been described by several prominent writers:

"People wish their enemies dead, but I do not; I say give them the gout, give them the stone!" (Mary Worley Montagu)

"Be temperate in wine, in eating, girls, and sloth; Or the gout will seize you and plague you both" (Benjamin Franklin)

Figure 3-21. A cartoon illustrating the painful inflammatory effects of gout in man can be. (From: The Gout, James Gillray, 1799.)

(A) (B)

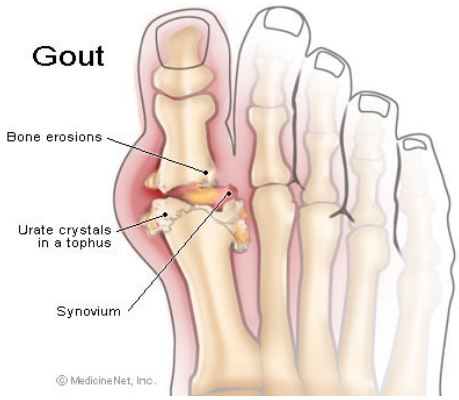

Figure 3-22 (A) Diagram of disruption of the big toe (the most common locus for gout) by urate crystals. (From medicinenet.com) (B) an affected joint, with a tophus of urate crystals clearly visible through the distended skin. (From news.bbc.co.uk).

At first sight, therefore, it would seem that urate formation is undesirable, and that circulating levels of urate should be kept as low as possible (Figure 3-23). However, (Hilliker et al., 1992) suggested that urate is an important antioxidant agent; as urate-null mutants, like *ry*, are extremely sensitive to oxidative stress agents like paraquat and die quicker than wild types. Thus they suggested that urate is playing an important role in longevity (this will be discussed further in the *uro* chapter). The human body is thus

likely actively maintain a preferred level of circulating urate, and gout can be seen as an unfortunate long-term side-effect of setting this level too high.

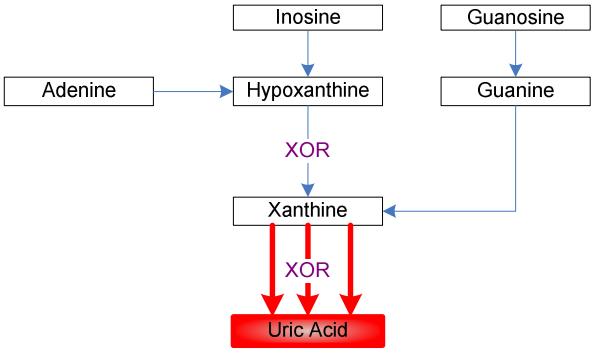

Figure 3-23. Part of purine metabolism showing the key role of Xanthine oxidoreductase in urate formation, and thus in gout.

Nonetheless, treatments for gout have been found, and revolve around reducing urate levels, by reduced nitrogen in the diet (low protein), higher fluid intake, and allopurinol, a pseudosubstrate inhibitor of XOR.

Hypoxanthine

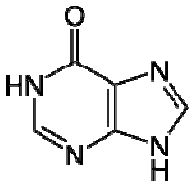

Allopurinol

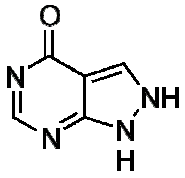

Figure 3-24 Hypoxanthine vs. allopurinol chemical structures.

Its chemical structure is very similar to hypoxanthine with a slight difference in the carbon and nitrogen atoms arrangement (Figure 3-24). Furthermore, the enzyme does not differentiate between the two chemically similar compounds: allopurinol is rapidly metabolized byxanthine oxidase, to its active metabolite oxypurinol (Figure 3-25), which is also an inhibitor of xanthine oxidase. Allopurinol is almost completely metabolized to oxypurinol within two hours of oral administration, whereas oxypurinol is slowly excreted by the kidneys over 18-30 hours. For this reason, oxypurinol is believed to be responsible for the majority of allopurinol's effect.

Oxypurinol

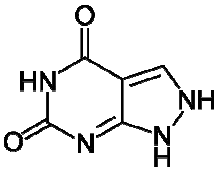

Xanthine

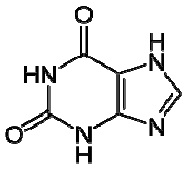

Figure 3-25 Xanthine vs. oxypurinol chemical structure.

Crucially, however, oxypurinol can interact with XOR to block urate production from xanthine (Spector, 1988).

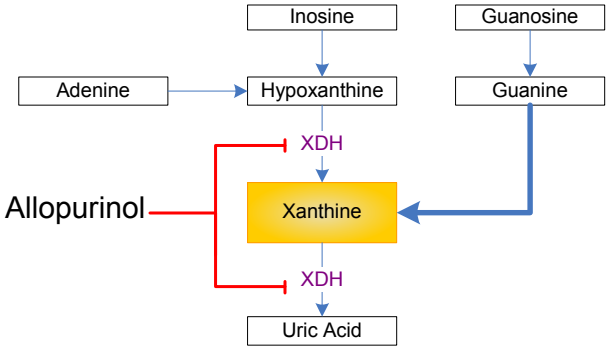

Figure 3-26. Allopurinol drug effect.

Consequently, free hypoxanthine concentration will feedback inhibit the XOR production and oxypurinol prevent urate production. Consequentially producing lesser amount of uric acid and accumulating of the precursors, hypoxanthine and xanthine. The accumulation of these two metabolites will lead to accumulation of adenine and guanine, precursors of hypoxanthine and xanthine respectively. Increased levels of adenine and guanine have an inhibitory feedback effect on a rate-limiting enzyme in the purine biosynthesis pathway. So allopurinol not only reduces uric acid by inhibiting its conversion from its precursor, xanthine, but also by inhibiting the purine biosynthesis (Figure 3-26). Allopurinol is also used with cancer patients as prophylaxis treatment with chemotherapy as a treatment for stomatitis (mouth ulceration), though its mode of action is unclear (Yokomizo et al., 2004).

The effect of allopurinol is not only to reduce urate formation, but it could also lead to accumulation of the urate precursors, xanthine and hypoxanthine to high levels. It might thus be predicted that high levels of, or sustained treatment with, allopurinol could lead to xanthinuria; and indeed, xanthinuria type I can arise as a secondary effect of therapy with allopurinol. In *Drosophila,* allopurinol was reported to phenocopy the *rosy* mutant (Keller and Glassman, 1965). So we wanted to validate this concept by using the Orbitrap (Figure 3-27). Importantly, allopurinol has the potential to allow the acute effects of XDH inhibition to be studied over time; by contrast studies of *ry* mutants can only follow relatively long-term adaptations to the lesion in XDH.

3.4.2 Experimental procedure

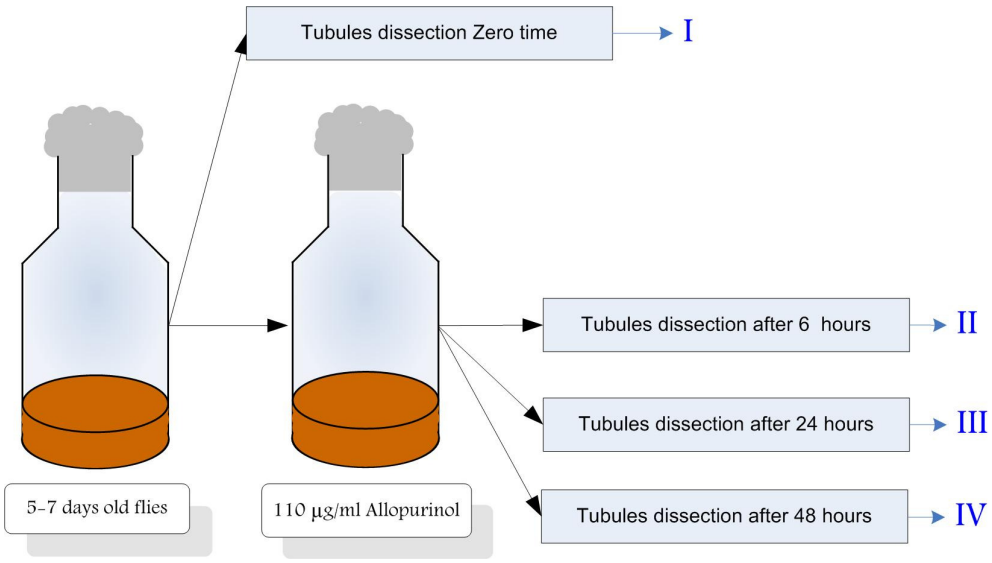

Figure 3-27. Allopurinol experiment overview. Was drawn by me.

Allopurinol-treated flies were tested in a time-course experiment. Keller and Glassman, (1965) found that 110 µg/ml allopurinol was sufficient to give *ry* phenotype. Three different times were selected to conduct the experiment; zero, 6, 24 or 72 hours. Replicate samples were taken for microarray analysis.

3.4.3 Results

Initially, the treatment of Oregon (WT) with allopurinol led to dramatic changes in metabolite concentration of hypoxanthine, xanthine, allantoin, uric acid and oxypurinol when compared with the control group (Table 3-4). Expressed graphically (Figure

3-28), it can be seen that levels of hypoxanthine and xanthine increase immediately upon exposure to allopurinol, but build steadily to maximum levels over two days. Urate, however, declines only very slowly. This is probably because the tubules, fat body and eyes of the fly contain major deposits of urate as insoluble uric acid crystals. Accordingly, these deposits are likely to have very long half-lives and so deplete very slowly. By contrast, allantoin decreases quickly and rather erratically, perhaps reflecting that its major pool is as soluble allantoin in the tubules. Accordingly, there is a dynamic sub-pool of urate and allantoin in tubules (independent from the insoluble urate pool) which is more sensitive to the activity of XDH, and thus the instantaneous metabolism of xanthine.

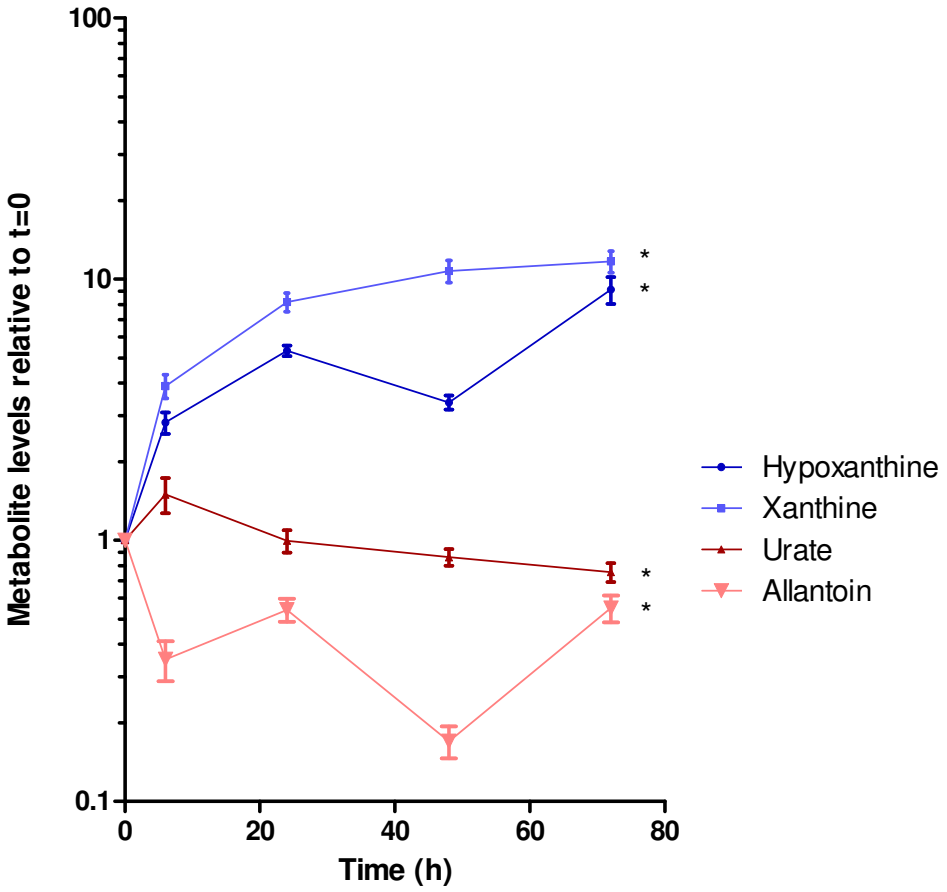

Figure 3-28 Timecourse of major metabolites in the purine metabolism pathway after feeding allopurinol to Oregon R (WT) flies at *t*=0. In this log scale graph, dramatic changes in metabolite concentration of hypoxanthine, xanthine uric acid and allantoin are visible. Hypoxanthine and xanthine levels were increased immediately upon exposure to allopurinol and then were built steadily to maximum levels over two days (blue lines). By contrast, urate and allantoin (red lines) were both decreased. Urate declined very slowly. This is probably because the tubules, fat body and eyes of the fly

contain major deposits of urate as insoluble uric acid crystals. Accordingly, these deposits are likely to have very long half-lives and so deplete very slowly. By contrast, allantoin decreases quickly. Data are shown as mean ±SEM for N=5. Metabolites that differ significantly from t=0 are marked with asterisks are analyzed by Student's *t*-test two tailed.

Other pathways are impacted by allopurinol (Table 3-4), though in general the changes are less marked than for the purine metabolism pathway. As with the previous metabolomic analysis of *rosy* mutants, there is impact on the pigment precursor (kynurinene and typtophan) metabolism pathways, serving to confirm the broad accuracy with which allopurinol phenocopies the *rosy* mutation.

Table 3-4. Metabolic pathways significantly affected by allopurinol. (F.C.; Fold change, P.V.; P value). Red means down regulated, blue means up regulated. Analyzed by Student's *t*-test two tailed.

	M_r	Elution time	6 h		24 h		48 h		72 h	
			F.C.	P.V.	F.C.	P.V.	F.C.	P.V.	F.C.	P.V.
Purines/pterins										
Hypoxanthine	137.0460	11.5	**2.3**	0.0036	**5.2**	0.012	**3.1**	0.0035	**6.0**	0.0025
Xanthine	153.0407	10.9	**3.2**	0.0077	**7.8**	0.0082	**12**	0.010	**12.3**	0.0001
Urate	169.0357	14.04	**1.1**	0.38	**1.1**	0.085	**0.85**	0.14	**0.72**	0.002
Allantoin	159.0514	15.1	**0.25**	0.00073	**0.52**	0.007	**0.10**	0.0011	**0.40**	0.0028
Pterin	164.0568	12.7	**1.3**	0.035	**1.7**	0.000006	**1.6**	0.0024	**1.4**	0.0016
Isoxanthopterin	180.0517	13.0	1.1	0.32	1.0	0.9	1.2	0.64	1.0	0.70
Inosine	269.0882	12.7	**0.84**	0.19	**1.0**	0.91	**0.74**	0.0012	**0.67**	0.0026
Drosopterin	369.1534	19.2	1.1	0.26	1.1	0.13	**1.3**	0.012	1.0	0.43
Oxidative stress										
Methionine S-oxide	166.0532	19.1	0.99	0.98	**2.77**	0.00072	**1.5**	0.0019	1.4	0.83
Ascorbic acid	175.0248	13.7	ND	-	ND	-	ND	-	ND	-
GSH	308.91	17.0	**0.51**	0.0054	0.40	0.01	**0.52**	0.0077	**0.45**	0.0059
Riboflavin	377.1458	10.2	1.0	0.84	**0.47**	0.0067	**0.31**	0.0084	**0.26**	0.0048
GSSG	613.1592	21.5	1.4	0.12	**2.9**	0.011	**1.8**	0.022	1.4	0.06
Pentose phosphate pathway										
Deoxyribose	133.0506	8.4	0.42	0.033	0.30	0.11	0.6	0.087	0.36	
Sedoheptulose 7-phosphate	289.0331	20.3	0.73	0.022	1.0	0.33	**0.75**	0.0031	**0.71**	0.0075
Aldose reductase										
Gulonolactone	177.0405	12.2	**0.30**	0.029	**0.32**	0.034	**0.26**	0.026	0.52	0.090
glucitol	181.0718	16.3	**0.29**	0.031	0.50	0.073	**0.42**	0.048	**0.43**	0.048
Gulonic acid	195.0511	16.9	**0.46**	0.020	**0.44**	0.020	**0.36**	0.012	**0.42**	0.021
Kynurenine pathway										
Niacin/Nicotinate	124.0393	8.2	**0.72**	0.029	**0.79**	0.034	**0.44**	0.0016	**0.44**	0.002
Oxoadipic acid	159.0300	12.2	**0.28**	0.003	**0.31**	0.029	**0.24**	0.0027	0.54	0.1
dihydroxyquinoline	162.0548	9.1	**1.4**	0.039	**1.7**	0.00066	1.2	0.090	0.94	0.65
Xanthurenic acid	206.0448	11.7	**0.86**	0.011	0.96	0.47	**0.70**	0.001	**0.80**	0.0011

L-Kynurenine	209.0922	13.4	**0.71**	0.00088	0.69	0.012	**0.62**	0.0019	**0.41**	0.0019
3-Hydroxy-L-kynurenine	225.0868	15.1	0.90	0.15	0.83	0.027	**0.85**	0.00069	**0.63**	0.00069
N-Formylkynurenin	237.0871	13.9	1.1	0.58	0.45	0.30	**0.23**	0.0027	**0.53**	0.0027
Miscellaneous										
L-Tyrosine	182.0812	15.7	**0.73**	0.024	0.87	0.043	**0.61**	0.0069	**0.75**	0.0069
AHMDHP	196.0831	11.1	**5.6**	0.029	23.9	0.21	199	0.025	**4.0**	0.025
5-Hydroxy-L-tryptophan	221.092	13.6	**0.41**	0.0043	0.18	0.00021	**0.19**	0.0023	**0.32**	0.0023
Linolelyl carnitine	424.3421	10.1	**0.66**	0.003	0.95	0.5	**0.63**	0.0023	**0.57**	0.0013
oleylcarnitine	426.3576	10.1	**0.81**	0.0088	1.1	0.21	**0.75**	0.0084	**0.73**	0.0020

ND; metabolite not detected in sample group. AHMDHP; 2-Amino-4-hydroxy-6-hydroxymethyl-7,8-dihydropteridine

3.4.4 Conclusion

Allopurinol is one of the best inhibitors of XOR and is rapidly converted to oxypurinol by oxidation process: both allopurinol and its oxidized metabolite oxypurinol inhibit XOR activity (Spector, 1988). Accordingly, as in humans, oral administration of allopurinol induced a blockade of the purine pathway in *Drosophila*. Interestingly, the data provide dynamic data on the relative mobility of different pools of purine metabolites in the fly; it would be interesting to test the resulting model (that there is a dynamic pool of urate and allantoin in the tubules, independent of the insoluble urate crystals). It is reasonable to posit a key role for tubules, because –as will be discussed later- the enzyme *urate oxidase* is expressed absolutely specifically in tubules, so this is where allantoin formation will occur.

Inconveniently, oxypurinol has precisely the same molecular weight as xanthine, and so the rise in xanthine levels could be attributed to an accumulation of oxypurinol. However, the dietary concentration of allopurinol (at 110 μg/ml) is so low that in practice, the peak is likely to represent endogenous xanthine.

Allopurinol use as an inhibitor of XO ramifies into several branches that result in several impacts on different biochemical pathways, for following the metabonomic field requires a full understanding of biochemistry as well as an open mind.

Indeed, the present study is the first to utilize the technique of HILIC-LC-ESI-MS for the analysis of allopurinol.

3.5 General Discussion

The *rosy* mutation is a triumph of the *Drosophila* paradigm. It is the second mutation ever discovered in *Drosophila* (almost a hundred years ago) (Dow, 2007), and yet the original mutant stocks still exist today. Although many workers in the *Drosophila* field are presently energetically pursuing even tenuous models for human disease, *rosy* recapitulates rather precisely its corresponding human genetic disease (Chintapalli et al., 2007) . It is even possible to phenocopy the *rosy* mutations in flies (Keller and Glassman, 1965), and the xanthinuria symptoms in humans (Gok et al., 2003), with the XOR inhibitor allopurinol.

- In this chapter, the Orbitrap technology was brought to bear on *Drosophila*, and there were several key findings:
- Orbitrap and flies are compatible: a simple homogenate allows the identification of hundreds of metabolites in a single experiment
- The Orbitrap is sufficiently sensitive to allow metabolomes of single fly tissues to be measured
- Single gene mutations have significant impact on the organismal metabolome
- The Orbitrap not just reproduces findings from years of classical, painstaking biochemistry in a single experiment, but its amazing sensitivity allows these classical findings to be greatly extended.
- The Orbitrap also allows the pharmacological impact of drugs on the metabolome to be followed.

As a result of this work, there are several intriguing lines of further investigation suggested. How does XDH knockdown impact on osmolyte biosynthesis? How about oxidative stress- is this a result of urate deficiency? And are there separate labile and stable pools of urate in specific tissues, like the tubules? Although time did not allow the study of these new theories, it is hoped that it will one day be possible to follow them up.

Chapter 4 *Maroon-like* (*mal*)

4.1 Introduction

4.1.1 History

Similarities among *Drosophila* mutants have long drawn the attention of Drosophilists. Similarities like body size and shape or eye colour, could result from either different alleles for the same locus or different genes in the same pathway. There has thus been a long tradition of crossing together mutants with similar phenotypes, to test for allelism (two mutants in the same gene) or for epistasis (the effects of one gene are modified by one or several other genes upstream in an enzyme series). Until the advent of DNA sequencing, such complementation analysis and epistatic analysis was a cornerstone of experimental genetics (Ashburner, 1990).

In 1959, it was noted that several *Drosophila melanogaster* mutants shared a dull red eye colour. Those mutants are *ry* (Forrest et al., 1956), *mal* (Hadorn and Schwinck, 1956) and later cinnamon (*cin*) (Baker, 1973).

Similarities between *rosy* and *maroon-like* are remarkable. Both of them have the same dull red eye colour; and both, also, are deficient in uric acid and have excesses of hypoxanthine and xanthine. Mutants in either are unable to convert 2-amino-4-hydroxypterdine to isoxanthopterin, or to oxidise hypoxanthine to xanthine then to uric acid, reactions catalyzed by the xanthine oxidase. This is due to the absence of the enzyme. However, the genetic lesion is different, as the *ry* gene is located on the third chromosome, while *mal* is on the X chromosome (Glassman and Mitchell, 1959). The *mal* mutant, in addition to the malfunction of XDH, is also defective in aldehyde oxidase (Courtright, 1967) and pyridoxal oxidase (Forrest et al., 1961). Thus, this suggested a link between the previous two enzymes and XDH, namely that *mal* was essential for the activity of all three different enzymes. As *mal* is epistatic to those three enzymes, it is likely to play a common role in their synthesis or function.

It is known that conversion of 4-hydroxypteridine to 2,4-dihydroxypteridine needs an oxidative-type reaction. The same reaction type occurs in both wild type and *rosy* mutant flies, but not in the *mal*. This implies that *mal* is different from *ry* by the activity of the oxidases, which are suggested to be absent in the *mal* (Forrest et al., 1961).

Furthermore, specific antibodies for xanthine dehydrogenase showed that the protein was found in higher levels in extracts from *mal* than *ry*, which implicates that the enzyme in *ry* is either absent or reduced, while in *mal* it is present but is inactive (Glassman and Mitchell, 1959). This was subsequently found to be because ROSY is one of a small group of enzymes which use molybdenum at their active site, and Mal is the enzyme which inserts the molybdopterin prosthetic group into the maturing XO enzyme (Ichida et al., 2001).

Molybdenum cofactor biosynthesis is a conserved pathway among bacteria, fungi and humans (Schwarz and Mendel, 2006). This synthesis pathway consists of five important steps summarized in (Figure 4-1), starting with guanosine triphosphate (GTP). The GTP is converted to compound originally known as precursor Z, later called cyclic pyranopterin monophosphate cPMP. Then the latter is converted to molybdopterin (MPT) and finally to the mature molybdenum cofactor, MoCo (Figure 4-1).

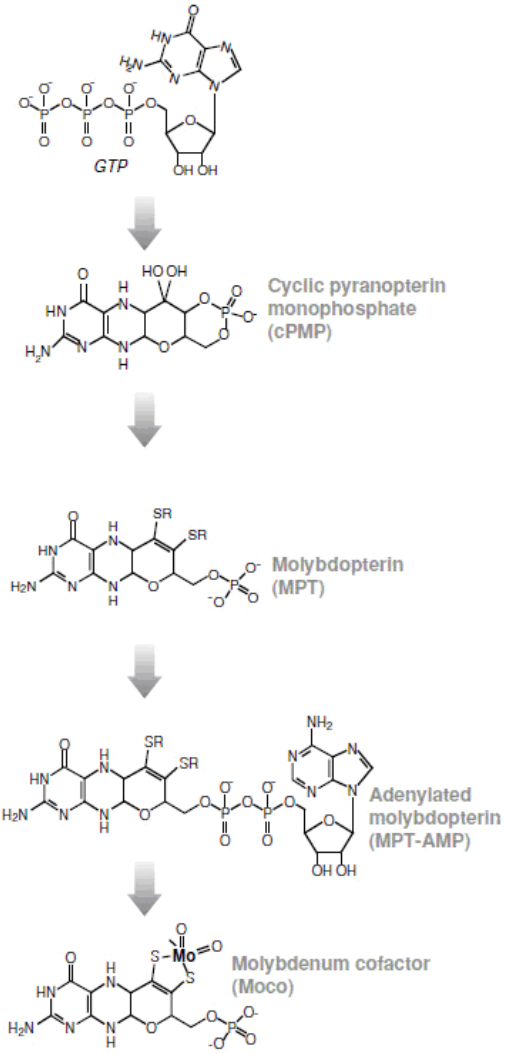

Figure 4-1 Molybdenum cofactor biosynthesis. After (Schwarz and Mendel, 2006).

4.1.2 Molybdenum- containing enzymes of *Drosophila* and their synthesis

The main molybdenum-containing enzymes; XDH, AD and SO in *Drosophila* are all dependent on MoCo synthesis for their activity. Thus any defects in MoCo production leads to multiple *Drosophila* mutant phenotypes (Kamdar et al., 1997). This is summarized in (Figure 4-2). The *ry* mutant is mutated in the XDH gene, consequently no enzyme produced to oxidize hypoxanthine to xanthine and then to uric acid. This in human, is called xanthinuria type I. Second, *mal* mutants suffer from dual enzyme loss; in addition to XDH, an AO is also absent. However the XDH enzyme is still present, but in inactive form. This is due to failure of an enzyme called sulphurase to add a sulphur to the prosthetic site of the MoCo. This enzyme also affect the purine metabolism pathway in *Drosophila* as well as in human and are causing a disease called xanthinuria type II. Lastly, *cin* mutants suffer from the complete absence of the MoCo production, thus affecting not only XDH and AO, but also SO. This in human causes the MoCo deficiency disease which leads to neurological effects.

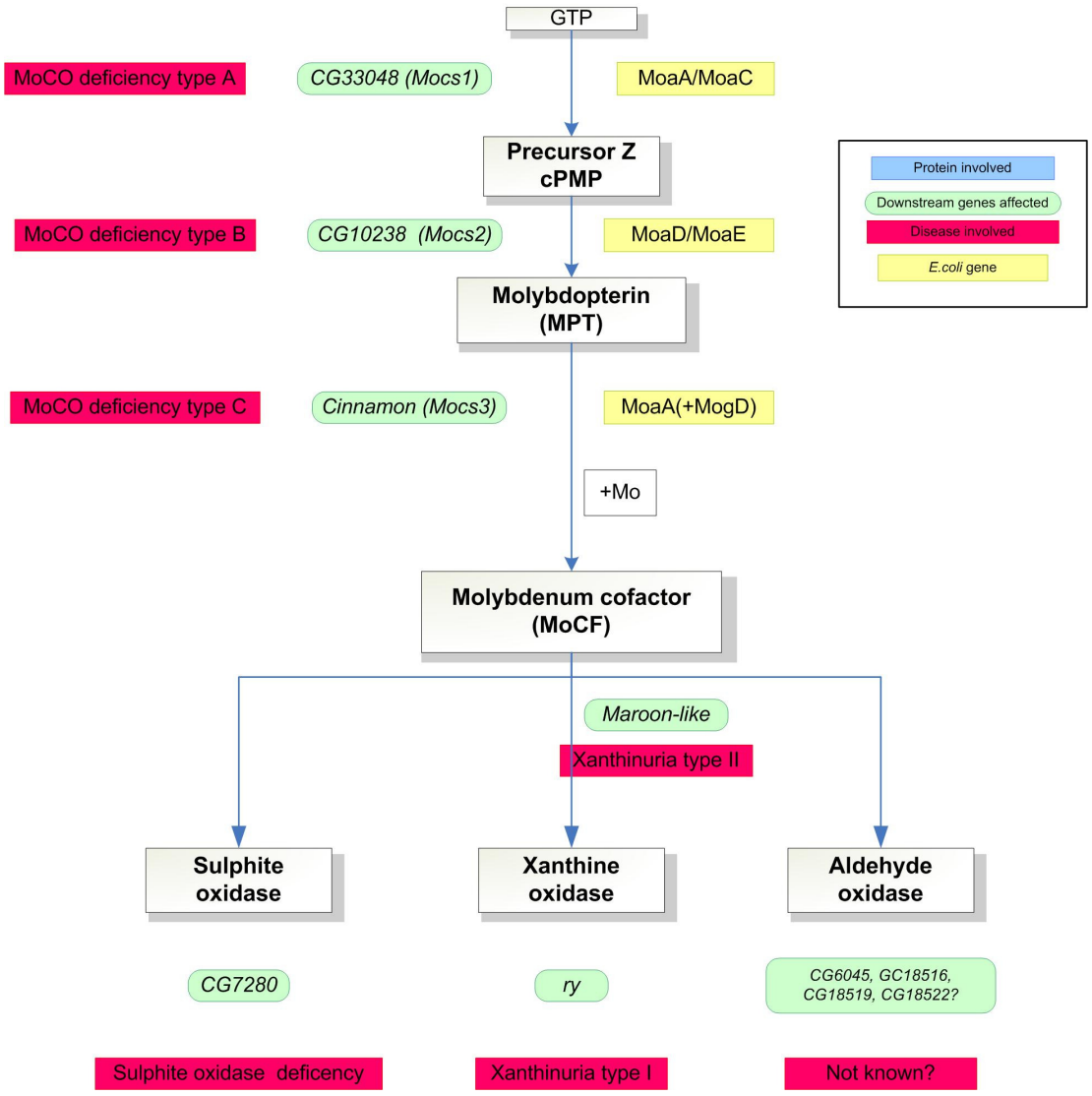

Figure 4-2 MoCo containing enzymes in *Drosophila*. This figure was drawn by me. GTP; Guanosine triphosphate, MPT; molybdopterin, MoCo; molybdenum cofactor , SO; sulphite oxidase, XDH; xanthine dehydrogenase, AO; aldehyde oxidase, *cin*; *cinnamon, ry*; *rosy*, *mal*; *maroon-like*. This figure was drawn by me.

Because of their similarities in the chemical structures , both XDH as well as AO are classified in the same sub-group. Both, in order to be in the active form, are require post-translational sulphuration of the MoCo. On the other hand this post-translational sulphuration is not necessary for the other molybdoenzymes,, i.e. SO. This important reaction is carried out by an enzyme called sulphurase, which substitutes one of the oxo-groups of the MoCo with a sulpho double bond (Figure 4-3).

Failure in this sulphuration with sulphurase enzymes leads to defects in both enzymes , XDH and AO that leads to the rare inborn error of metabolism, xanthinuria type II (Garattini et al., 2008).

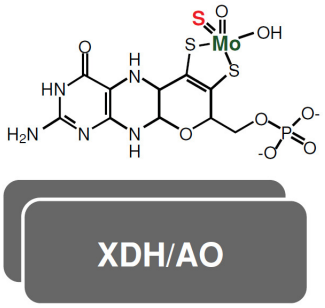

Figure 4-3. The effect of the sulfurase enzyme. substitution of an oxo group of MoCo with sulpho- double bond (red).

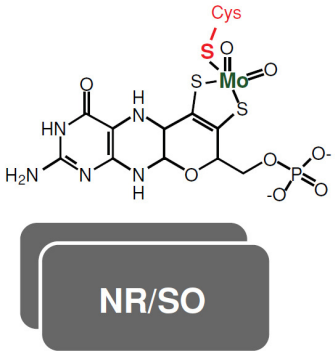

Figure 4-4. Instead of sulphuration, a Cys is added.

So deficiencies in any of the molybdopterin biosynthetic enzymes should produce a maroon-like phenotype, which is a super set of the *rosy* phenotype as all molybdoenzymes will be defective.

So in flies, *mal* should produce a phenotype more severe than *ry* because more than one metabolic pathway is impacted.

4.1.3 Links to human molybdoenzyme deficiency

The molybdenum cofactor (MoCo) is an essential component of molybdoenzymes. So deficiency in MoCo is known, but rare in humans. It is autosomal recessive inborn error of metabolism, caused by defects in the biosynthesis of molybdenum-complexed pterin cofactor (Ichida et al., 2001).

This defects lead to deficiency of the previously mentioned three molybdenum-requiring enzymes: sulphite oxidase (SO), xanthine dehydrogenase (XDH) and aldehyde oxidase (AO). Affected individuals typically display severe neurological dysfunction in the newborn period or at early infancy along with renal impairment and high plasma concentration of xanthine.

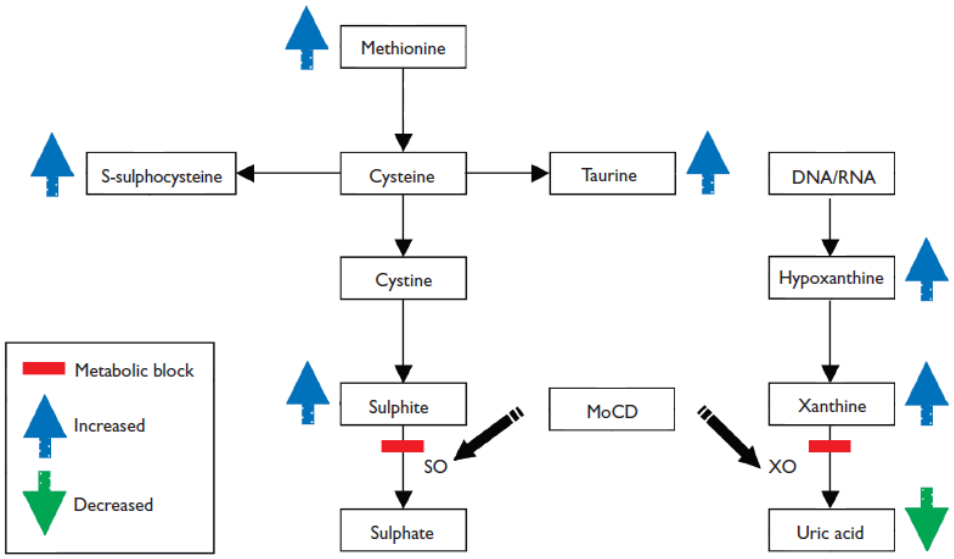

Figure 4-5. This chart show the metabolic pathways affected by molybdenum deficiency in human. SO; sulphate oxidase, XO; xanthine oxidase, MoCo; molybdenum cofactor deficiency. Due to absence of the MoCo, activity of XO and SO will be decreased. Figure after (Ngu et al., 2009)

Affected individuals typically display intractable seizures, metabolic acidosis, intracranial haemorrhage, feeding difficulties, dysmorphic facial features, profound developmental delay, alterations in muscle tone, microcephaly, lens dislocation and renal stones. Because of these varied features and the very rare occurrence, the disease can be easily misdiagnosed. The prognosis is poor: most of the infants die in the first days or weeks of their lives, and this could be the reason why it is rarely diagnosed: not because it is rare but because the it shares many of the clinical features with other diseases and its onset is in the early infancy period and it is also fatal, so newborn babies die before proper diagnosis.

As *mal* is a clear homologue of the human sulphurase, it is likely that it recapitulates to some extent the human disease. It may thus provide (as *rosy* does for xanthinuria type I), a model for xanthinuria type II. This chapter seeks to study the closeness of the model using metabolomics to profile the broader metabolic impact of the mutation.

4.2 Aims

So, we selected mal for metabolomic analysis study because, we wanted to have better understanding of this mutant as human homolog xanthinuria type II animal model.

In humans, xanthinuria type II produces additional defects and is more severe than type I. Would additional metabolic pathways also affected in *Drosophila*?

All previous studies and research indicated that the molybdenum cofactor is deficient, thus all molybdoenzymes are present but are not functioning. Could this investigation lead to discovery of novel effects of the molybdenum co-factor deficiency?

In addition in this chapter, I compare two different major wild type strains to compare inter-strain differences with mutant phenotypes.

4.3 Results

We conducted another comprehensive metabolic analysis profiling for *mal* using the methods described in the previous chapter. The investigation took place between the *maroon-like* mutant as a sample and as a control we used the wild type flies, Oregon R (OR). The impact of the mal mutation can be seen summarized in (Table 4-1).

Table 4-1. Major metabolomic differences between *mal* and OR. Reduced metabolites are in red coloure while blue colour indecates the incresed metabolite level. The test was repeated twice, separated by five months and with *N*=5 biological replicates. . Analyzed by Student's *t*-test two tailed.

Compound	m/z	Ratio 1	P value	Ratio 2	P value 2
I. Purine metabolism pathway					
GABA	104.0707	0.53	0.00000030	0.731	0.00963
Adenine	136.0759	3.7	0.00045	5.138	0.0019
Hypoxanthine	137.0459	6.4	0.000014	21.816	0.079634
Guanine	152.057	0.43	0.0019	0.656	0.086113
Xanthine	153.041	75.0	0.000032	18.051	0.016686
Allantoin	159.0516	0.027	0.00026	0.134	0.071928
Uric acid	169.0358	0.0010	0.00028	0.021	0.001168
Guanidine	284.0993	0.57	0.025	0.262	0.000145
II. Eye pigmentation pathway					
Drosopterin	369.1531	0.22	0.000280	0.466	0.002149
Xanthopterin	180.0518	0.0030	0.0030	0.021	0.018049
Xanthommatin (met of Drosopterin)	424.0648	12	0.0057	2.165	0.000374
Pterin (Benzene ring) the cofactor	164.0568	6.2	0.011	6.911	0.030468
III Melanin pigments					
Tyrosine (is a precursor of melanin pigments)	182.0814	3.2	0.00056	11.586	0.006997
Dihydrobiopterin	236.0783	2.0	0.058	3.330	0.001336
IV Arginine and proline metabolism					
Proline betaine	144.1022	0.12	0.000034	0.572	0.0346
Acetyl arginine	217.1297	2.8	0.0035	3.658	0.020833

4.3.1 Purine metabolism pathway

As with *rosy* (and with allopurinol treatment), changes are observed in the purine metabolism pathway, consistent with the inhibition of XDH (Figure 4-6) not (Fig. 4-7).

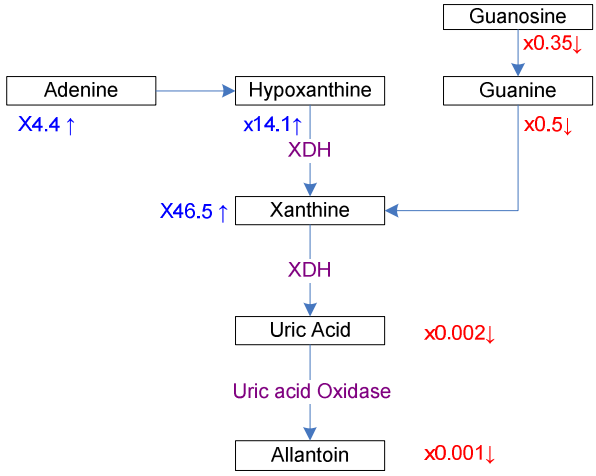

Figure 4-6. Major metabolite changes in purine metabolism pathway using the *mal* mutant.

Accordingly, *mal* behaves as expected, and the Orbitrap technique is implicitly validated for identifying common metabolic fingerprints between mutants of related genes. But are there further, or more severe, changes, consistent with the pathology of human xanthinuria type II?

4.3.2 Eye pigmentation

The normal *Drosophila* eye pigments are composed of two important pathways, ommochrome and pteridines. The ommochromes, which are synthesized from the tryptophan pathway, give rise to the brown pigments. By contrast, the pteridines are synthesized from guanine and produce the red pigments. Thus, any mutation to the ommochrome pathway will affect the *Drosophila* eye colour, and by reducing the amount of brown pigments, make the eye appear redder. Conversely, mutations affecting the pteridine pathway will make the brown colour in the eye predominant so the eye will appear darker.

The ommochrome biosynthesis pathway is well understood, and is less complicated compared to the pteridine pathway. Three pteridine pigment types are present in the

Drosophila eye, Drosopterin, isoxanthopterin and sepiapterin (Evans and Howells, 1978). Drosopterin in particular is produced from two precursors; pyrimidodiazepine PDA and dihydropterin DHP (Wang et al., 2008).

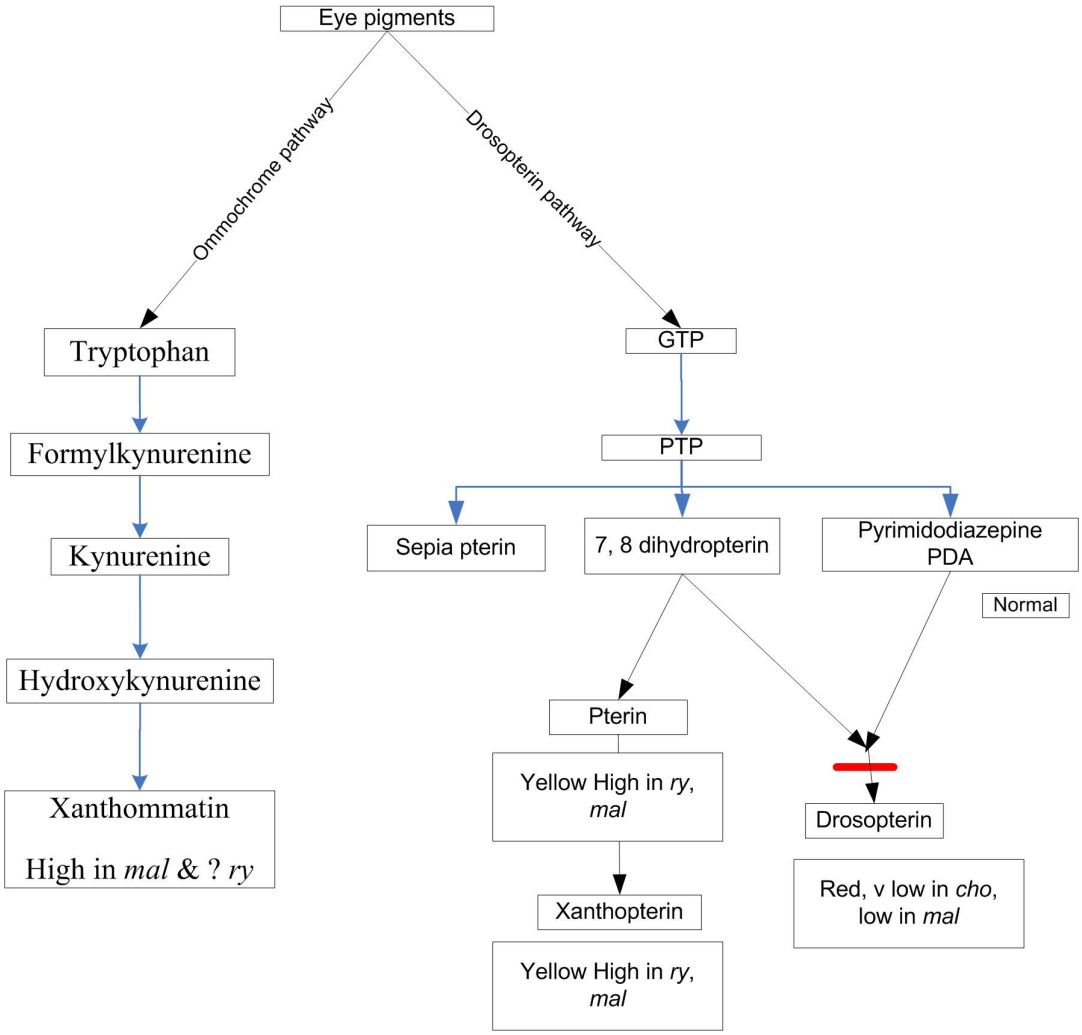

Figure 4-7. Visual pigment biosynthesis. (is the enzyme converting 7, 8 dihydropterin to Drosopterin is the same that converting pterin to xanthopterin? And this could be why both Drosopterin and xanthopterin are reduced? Even though their precursors are high in concentration?)

4.3.3 Major metabolites differences between OR and CS wild types

As a further control, two widely-used wild type lines, namely Oregon-R and Canton-S, were compared to each other. The full list of metabolites resolved in Oregon R is presented in (Table 4-2).

Table 4-2 Metabolites in *Drosophila* OR strain observed by HILIC chromatography in combination with LC-MS

Metabolite	Observed Mass	Rt min	Metabolite	Observed Mass	Rt min
Linoleamide	280.264	5	Oleoamide	282.28	5.4
Hydroxy phenylacetic acid	151.04	6.3	*Pyruvic acid	87.0088	6.9
*Hydroxyketoglutaric acid	161.009	6.4	Niacin	124.039	7.4
*Lactic acid	89.0244	6.8	Succinic acid*	117.019	7.6
Pantothenic acid	220.118	6.8	Fumaric acid*	115.004	7.7
N-acetylglutamate	190.071	6.9	Ketobutyric acid*	101.025	8.1
Aminohexadecanediol	274.274	7.7	Pyroglutamic acid	130.05	8.3
* Ascorbic acid	175.025	7.8	Dihydrobiopterin 1	236.078	8.4
Dopa quinone	196.061	8	Kynurenic acid	190.05	8.5
Diacetyl ornithine	217.118	8	Formyl val-gly	203.103	8.7
Hydroxybutyric acid*	103.04	8.1	Deoxyadenosine	252.109	8.9
4-amino-4-deoxychorismate	226.071	8.8	Myristamide	230.248	9
*Ribose	133.051	9.1	N-acetylaspartate	176.056	9.1
Pyridoxate	184.06	9.3	Riboflavin	377.146	9.4
Xanthurenate	206.045	9.5	Linolenylcarnitine	424.343	9.8
Linolylcarnitine	426.359	9.8	Oleoylcarnitine	428.374	9.8
Pyrimidodiazopterin	222.099	9.9	Dihydrobiopterin 1	240.109	9.9
Dihydrobiopterin 2	236.078	9.9	Biopterin 1	238.094	10.2
Histidine lipid	338.244	10.6	Xanthine	153.041	10.3
Hypoxanthine	137.046	10.7	Hydromethyldeoxyhydropterin	196.047	10.5
Succinyladenosine	384.115	10.7	Uridine	245.077	10.5
Xanthosine 1	285.083	10.8	Uracil	113.035	10.6

Metabolite	Observed Mass	Rt min	Metabolite	Observed Mass	Rt min
Butoctamide semisuccinate	316.212	10.9	Histidine lipid	362.244	10.6
Acetylcholine 1	146.118	11.6	Histidine lipid	364.26	10.6
Inosine	269.088	11.6	C12 sphinganine	218.212	10.7
Pterin	164.057	11.9	Glycolic acid*	105.019	10.8
Leucineproline isomer 1	229.155	11.9	Methylguanosine	298.115	10.8
Ethyl n-acetylarginate	245.161	11.9	Valineleucine	231.171	11.3
*Malic acid	133.014	12	Leu-leu	245.186	11.3
Xanthopterin	180.052	12.1	Xanthosine 2	285.083	11.8
Dihydroxanthopterin	182.068	12.1	Methyl tyrosine	196.097	12
§*Hexose isomer1	179.056	12.2	Guanine 1	152.057	12.2
Propylcarnitine	218.139	12.2	Cyclothionine	206.048	12.2
*Deoxyhexose	163.061	12.4	Narigenin	273.075	12.2
Phenylalanine	166.086	12.4	*Hexitol	181.072	12.4
Butanedione	87.0441	12.5	Indospicine	174.124	12.6
Kynurenine	209.092	12.7	Glycyl-dopa	255.098	12.6
Biopterin 2	238.094	12.7	Adenosine	268.104	12.6
Xanthommatin	424.079	12.7	Hydroxyindole acetic acid	192.066	12.7
Tetrahydrofolate	446.179	12.7	Hydroxytryptophan	221.092	12.7
Leucine	132.102	12.8	Hydroxyketoglutaric	163.06	12.9
Guanine 2	152.057	12.8	Leucineproline isomer 2	229.155	12.9
*Ketoglutaric acid	145.014	12.9	Isoleucine	132.102	13
Leu-ala	203.139	12.9	Tryptophan	205.098	13.1
Uric acid	169.036	13	§*Hexose isomer 2	179.056	13.2
Dihydromethylguanosine	300.13	13	N-succinyl-2,6-diaminoheptanedioate	291.119	13.6
Acetyl carnitine	204.124	13.1	Acetyl choline 1	146.118	13.7
Pyridoxal	168.066	13.3	Tetrahydrothiophene carboxylic acid	133.032	13.8
Dihydrobiopterin 2	240.109	13.3	Aminoadipic acid	162.076	13.8
Guanosine 1	284.099	13.3	*Gluconolactone	177.04	13.9
Methylproline 1	130.086	13.4	Allantoin	159.052	14
Acetyl serine	148.097	13.4	N2-(d-1-carboxyethyl)-l-lysine	219.134	14

Metabolite	Observed Mass	Rt min	Metabolite	Observed Mass	Rt min
Acetyllysine	189.124	13.5	Guanosine 2	284.099	14.1
Methionine	150.059	13.8	* Erythrose	119.035	14.2
N2-acetyl-l-aminoadipate semialdehyde	188.092	13.8	Adenine	136.062	14.2
Formylkynurenic acid	237.087	13.8	*Pentose	149.046	14.2
Spermidic acid isomer 1	176.092	13.9	Hydroxy kynurenine	225.087	14.2
Pro-val/dethiobiotin	215.139	14	Valine	118.086	14.4
§*Hexose isomer 3	179.056	14.2	Thioproline	134.027	14.4
Leucineproline isomer 3	229.155	14.2	Proline betaine	144.102	14.4
Camp 1	330.06	14.4	Tyrosine	182.081	14.5
Ectoine	143.082	14.5	Spermidic acid isomer 2	176.092	14.8
Guanidine butanoate	146.093	14.6	Ala-pro	187.108	14.8
Propionylarginine	231.146	14.6	Methylproline 2	130.087	14.9
N-acetyl-l-glutamate 5-semialdehyde	174.076	14.7	Camp	330.06	15
Oxidized biopterin	254.089	15.1	Methyladenine	150.078	15.1
Ala-glu	219.098	15.2	Methionine s-oxide	166.053	15.1
N-acetylhistamine	154.098	15.3	Thymine	127.05	15.2
Octopine	247.14	15.3	Gsh	308.092	15.3
Proline	116.071	15.4	N-acetylhistamine isomer	154.098	15.8
Uridine monophosphate	325.043	15.4	Cgmp	346.055	15.8
Glycine betaine	118.086	15.5	Imp	349.054	15.8
Carnitine	162.113	15.5	N6-(1,2-dicarboxyethyl)-amp	464.082	15.9
Methylphosphate	113	15.6	Carnitine isomer	162.113	16
Dihydrothymine	129.066	16.1	Acetylarginine	217.13	16
Hydroxyproline 1	132.066	16.1	Ornithine acetate	175.108	16.2
Taurine	126.022	16.3	Methyl adenosine 1	282.12	16.2
Alanine	90.0549	16.4	Glutamic acid	148.061	16.3
Meso-2,6-diaminoheptanedioate	191.102	16.5	4-hydroxyphenylacetylglycine	210.076	16.3
Acetylhydroxylysine	205.119	16.5	GABA	104.071	16.4
Threonine	120.066	16.6	Glu-gln	276.119	16.7

Metabolite	Observed Mass	Rt min	Metabolite	Observed Mass	Rt min
Amp	348.071	16.6	Hydroxyproline 2	132.066	16.8
* Gluconic acid	195.051	16.7	Glucosamine phosphate	260.053	16.8
Aspartic acid	134.045	16.8	Phosphoethanolamine	216.064	16.9
Dopa	198.076	16.8	Glutamine	147.077	17
Phosphoric acid	98.9843	16.9	Beta-alanine	90.055	17.1
Aminopentanamide	117.102	17.1	Methylguanidino inositol	236.125	17.1
Asparagine	133.061	17.4	Diaminocyclohexane tetraol	179.103	17.2
Nicotinate d ribonucleotide	335.064	17.4	Guanidino inositol	222.109	17.3
Glycine	76.0393	17.5	*Pentose-hexose	311.098	17.3
Choline	104.107	17.5	Cytosine	112.051	17.6
Serine	106.05	17.5	Hydroxyguanine	168.049	17.7
Cytidine	244.093	17.6	Tyrosine phosphate	262.048	17.9
Methyl adenosine 2	282.12	17.6	Phosphoethanolamine	142.026	18.2
Citrulline	176.092	17.7	Cytidine monophosphate	324.059	18.4
*Methoxyhydroxyphenyle thyleneglycol	185.08	17.7	Glutathione disulphide	615.13	18.8
Arginylglycine	232.141	17.7	Methylhydroxyproline	146.081	18.9
Drosopterin	369.153	17.7	*Citric acid	191.02	19.6
Nad	664.117	17.8	Cysteine	241.031	20
Glucose phosphate	261.037	17.9	Phosphocholine	184.073	20.1
Gmp	364.065	18.1	*Tetrahexose	665.212	20.4
Glycerophosphocholine	258.11	18.3	Acetylhydroxylysine	205.119	20.8
* Trihexose	503.162	19.6	Arginine related	229.13	21
Cystathione	223.075	20.2	Dimethylarginine	203.15	21.3
Methyldihydroinosine	285.12	20.6	Histidine related compound	168.077	22
*Pentahexose	863.242	20.6	Methylhistidine	170.092	22
Phosphoarginine	255.086	20.8	Aminobutyraldehyde	88.0756	22.7
Argininosuccinate	291.13	21	Ornithine	133.097	23
Histidine	156.077	22	Galactosylhydroxylysine	325.161	23.3
Arginine	175.119	22.7	S-adenosylmethionine	399.145	24.3
Lysine	147.113	22.9	N-acetylspermidine	188.176	25.2

Metabolite	Observed Mass	Rt min	Metabolite	Observed Mass	Rt min
Fructosyl lysine	309.165	23	Putrescine	89.1072	26.2
Thiamine	265.112	24.5	Phenol phosphate	171.992	28
Histamine	112.087	25.9			
Glyceraldehyde phosphate	171.006	28			

* Observed in negative ion mode

These data, reflecting increased resolution as our skill in analysis increased, shows that the Orbitrap is clearly a very powerful machine for global metabolomic analysis.

Investigations showed that both strains are fairly similar, however a few metabolites showed differences (Table 4-3).

Table 4-3**.** Significant metabolite differences between OR and CS wild type flies.

The test was repeated twice, separated by five months and with *N*=5 biological replicates.

Metabolite	m/z	Ratio 1	P value 1	Ratio 2	P value 2
aminooxopentanoate	132.0656	3.5	0.0000048	9.3	0.067221
ornithine	133.0972	1.6	0.0002134	3.3	0.037372
Indospicine isomer	174.1239	12	0.0000033	10	0.000749
N-acetylornithine	175.1079	23	0.0000706	87	0.000807
Arginine	175.1191	0.77	0.0067336	0.59	0.000039
Spermidic acid ?	176.0919	2.4	0.0000778	0.4	0.014783
Spermidic acid?	176.0919	185	0.0000224	ND	
citrulline	176.1031	3.8	0.0005660	14.8	0.005540
Hydroxyindole acetic acid	192.0657	0.62	0.0082408	0.22	0.000725
Kynurenine	209.0923	0.62	0.0088140	0.17	0.000245
Dihydrobiopterin	240.1094	0.59	0.0180132	0.48	0.001517
AMP	348.0707	0.55	0.0034903	0.83	0.032279

The results are spread fairly broadly across the metabolic map, and there does not appear to be a particular concentration of metabolic changes within a particular part of the map. It is thus possible that some of these changes are false positives; at $P<0.05$, one would expect one false positive per 20 metabolites, and with more than 250 metabolites determined in each run, there is scope for most of these to be false positives. This is why in our earlier analysis, it was important to look for more than one change in a particular metabolic pathway.

In principle, further experimentation and more replicates could resolve the issue, and increase confidence in the changes observed. One change, however, that did seem consistent, and that survived repeated sampling, was in the arginine metabolism pathway (Figure 4-8).

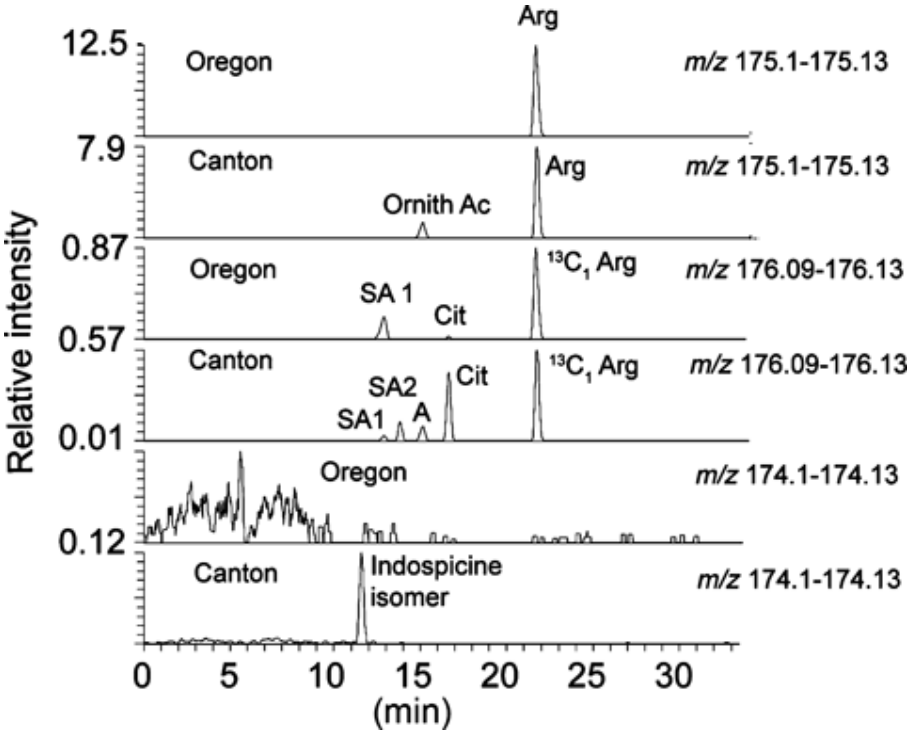

Figure 4-8 Metabolic signatures of OR and CS showing variations in the extracted ion chromatograms representing compounds in the arginine/ornithine pathway. A, 13C isotope peak of ornithine acetate; SA, spermidic acid. After (Kamleh et al., 2009).

Arginine levels are slightly lower in CS. Assuming that the urea cycle is not fully functional in *Drosophila*, in that conversion of arginine to ornithine via the loss of urea does not occur, citrulline and ornithine function as the precursors of arginine. Ornithine, ornithine acetate and citrulline are all elevated in CS. In addition to functioning as a precursor of arginine, ornithine enters the polyamine pathway, and two compounds, which are isomers of the spermidine metabolite spermidic acid (Kawase et al., 1994) are

present in high abundance in CS. Only one of these compounds could correspond to spermidic acid; the other would have to be a compound such as aminoheptadioic acid. Neither of these compounds appears in the Metlin or KEGG databases, although spermidic acid has been reported as a metabolite of spermine (Kawase et al., 1994). Although further experimentation would be required to validate this theory, the data show that the Orbitrap has the potential to resolve and identify entirely new metabolites.

4.4 Discussion and conclusion

4.4.1 How similar are different wild-type strains of *Drosophila*?

All previously carried out experiments were done along with control samples. The fly wild type lines are the OR and CS. These fly lines are considered as the wild type flies and are used extensively, world wide. Despite all the years, no studies have been conducted to investigate the deference or the similarities between them.

It has been observed from the previous *ry* experiment that the Orbitrap is a powerful analyser in which can be applied to generate new hypothesis in investigating new mutants or even wild types. As it has not been reported before, a comparison between the two wild type strains are not exactly the same. This dose not mean they are both not wild types. The differences among the OR and CS are much fewer than comparing any of them to *ry* or any other mutant. Furthermore, the significant difference in metabolites are not consistently in the same pathway which suggested the increase in false positive results. In any dataset with hundreds of data points, their will be some false positives. However, changes that occur in nearby metabolites are more likely to represent real changes than false positives.

4.4.2 How similar are the metabolomic footprints of lesions in *ry* and *mal*?

Similarities between *ry* and *mal* are not only in the phenotypes, but also in some metabolites. The main affected pathway is in the purine metabolism pathway, where the impact of XDH is clearly revealed. This is reflected in the excessive levels of hypoxanthine and xanthine and their precursors, like adenine and inosine. By contrast, downstream metabolites such as urate and allantoin are both sharply reduced or sometimes even not detected. While the *ry* mutant mimics the xanthinuria type I inborn

error of metabolism, *mal* mimics the xanthinuria type II. Although *ry* and *mal* are phenotypically similar, they are genetically very different; the lesion in *ry* is in chromosome 3 whereas in *mal* it is in the X chromosome. In *rosy* only one enzyme is defective namely, XDH. While in *mal* the lesion is due to deficiency in both XDH and AO. This is attributed to a defect in sulphurase enzyme which adds a sulphur atom to the cofactor binding site.

What was interestingly different from the *ry* mutant is on the tyrosine levels.

The cause of defect in the purine pathway in *mal* mutant is that the lesion is not because the absence of the XDH enzyme, it is rather present, but the molybdopterin co-factor, which is require for the XDH functioning is defective. This co-factor is required not by the XDH only, but by a wide range of enzymes like aldehyde oxidase and sulphite oxidase. And this may explain the secondary effects on the tyrosine metabolism.

Also, the aldehyde oxidase enzyme oxidises pyridoxal to pyridoxate. Accordingly, pyridoxate was seen in both OR and *ry*, but not in *mal* (Figure 4-9). Thus this is clear indication that this must be due to the molybdopterin co-factor defect.

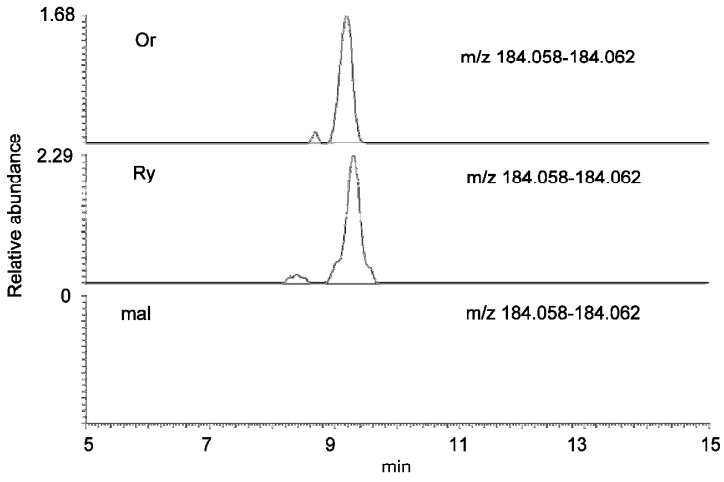

Figure 4-9 This diagram shows the electrogram of the traces of pyridoxate in OR, *ry* and *mal*. After (Kamleh et al., 2009).

4.4.3 *Maroon-like* as a model for xanthinuria type II

This work also allows the comparison of the models offered by *Drosophila* mutants *ry* and *mal*, for the human diseases xanthinuria type I and type II, respectively. Both types are characterised by lower plasma uric acid concentrations, and higher plasma xanthine concentrations; whereas urinary excretion of uric acid is low or undetectable, and that of xanthine is elevated. As discsussed above, both fly mutants recapitulate these symptoms rather closely.

Figure 4-10 This picture shows darker eye colour in *mal* mutant compared with WT. This picture was taken by me.

Although both types of hereditary xanthinuria in human are clinically similar, but there are some differences. Whereas patients with type I can metabolise allopurinol to oxypurinol, those with type II cannot. Unfortunately, we did not test this finding in *maroon-like* flies.

4.4.4 How consistent are metabolomes over time?

The wild-type flies OR and CS were compared at two time points, 5 months apart. On both occasions, there were a number of differences in the metabolites listed in (Table 4-3); however, the differences were not the same on each occasion. Thus, variation in time must be a criterion for establishing stable differences. In addition, there is variation

which occurs on extraction, as it is virtually impossible to stop biologically labile metabolites altering, because metabolism cannot be stopped instantaneously. There are of course some instrumental variations, but analysis of batches, e.g. 5 × OR against 5 × CS, in randomized order eliminates these. Biological variations are a difficult area and represent a major challenge in the extraction of useful metabonomic data. At best, all that is possible at the moment is to state that significant differences must be observed on at least two occasions to be considered significant.

4.4.5 Conclusions

- The Orbitrap is capable of resolving over 250 metabolites in even a small sample, and of identifying potentially novel metabolites.
- The two wild-type strains, Oregon R and Canton S, show highly similar metabolomes, but with consistent differences in arginine metabolism.
- Metabolomes are very labile, and repeated biological replicates need to be taken over an extended period to minimise variation.
- The *rosy* and the *maroon-like* are both excellent models of xanthinuria types I and II, respectively. Maroon-like shows changes in a wider range of metabolites, reflecting the impact on more than one enzyme.

Chapter 5 *Urate oxidase* (*uro*)

5.1 Introduction

As any living organism nitrogenous waste products can be highly toxic and need to be eliminated immediately either in the form of UA or other forms of metabolic forms (Vogels and Van der Drift, 1976). To do so these wastes are must be metabolized to lesser toxic products, like uric acid in *Drosophila*. Uric acid is also water insoluble, so its excretion wastes less water volume. Such uricotelic excretory systems are found in terrestrial insects and birds. Excretion of urea or ammonia is found in large animals and water living animals.

In some cases the wastes are metabolized to water soluble metabolites, thus they must be diluted to reduce its toxicity until they excreted. Consequently, excessive water volume is highly demanded in this process.

Uro encodes a structural gene for urate oxidase enzyme (URO); this enzyme is important in oxidation of urate to 5-hydroxyisourate (5HIU) or allantoin in *Drosophila melanogaster* (Kral et al., 1986). It is exclusively expressed in the *Drosophila* Malpighian tubules, and only in the third-instar larvae and adults (Friedman, 1973) and (Chintapalli et al., 2007). Its activity is rapidly reduced in the late period of the third-instar larvae and disappears in the pupal stage; then it regains its activity again at the early adult stage as shown in (Figure 5-2) (Friedman, 1973). This disappearance is controlled by an intercellular clock-like mechanism which at specific life period stops the expression of *uro* (Friedman and Johnson, 1977). Although others have different opinion (Jackson, 1978), this remarkable disappearance of the enzyme activity does not apply to all *Drosophila* species. For example the *uro* gene in *Drosophila virilis* is expressed only in the MT and the enzyme activity is shown in the third-instar larvae only. Whereas in *Drosophila pseudoobscura* the mRNA abundant is also in the MT but the enzyme activity is shown only during the adult stage (Figure 5-1) (Wallrath and Friedman, 1991).

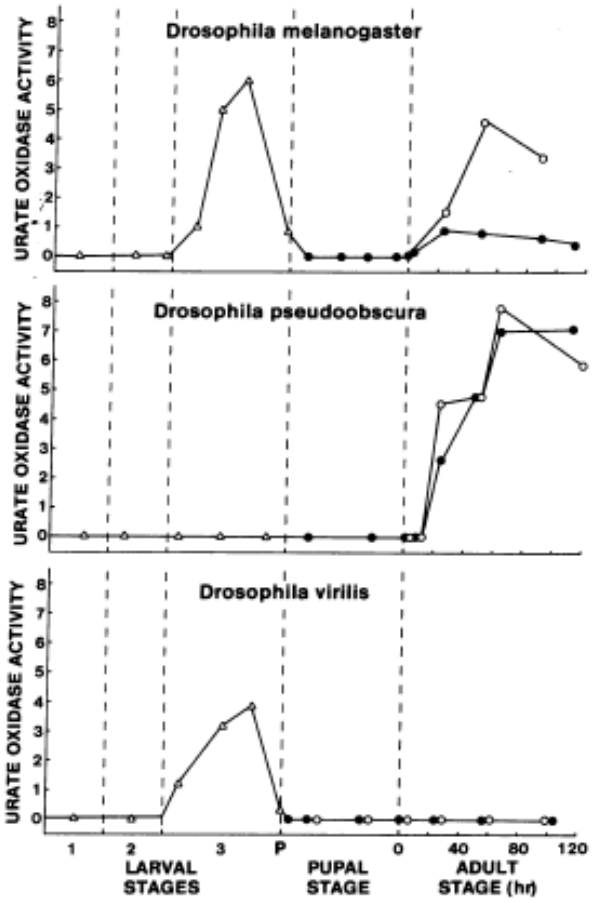

Figure 5-1 Comparison between three different species of *Drosophila* showing the URO enzyme activity during different life span. Dark circles represents males, whereas opened circles represent females (Wallrath and Friedman, 1991).

It is puzzling that this gene should be controlled so precisely, and so differently, in three closely related species. The reason is not known; but it could be because the need for the protective antioxidant properties of urate differs between the species.

The end product of purine metabolism varies between human and *Drosophila.* In *Drosophila,* like other insects, the final purine product is a mixture of uric acid and allantoin, depending on expression levels of urate oxidase. On the other hand, urate oxidase is absent in human; and as a result, urate is not metabolized into allantoin (as in *Drosophila*) as the end product of purine metabolism. The absence of this enzyme has some beneficial effect on mammals (Chapman and Chapman, 1998), as UA, plays an important role as an antioxidant of ROS in plasma and excreted through urine as urate.

5.2 Urate and oxidative stress

Several diseases have been suggested to be caused by toxicity due to free oxygen radicals, like cancer, heart diseases and aging.

It has been shown that an increased lipid peroxidation is found in heavy exercise and is accompanied by increased levels of urate. Free oxygen radicals rise as a result of the aerobic metabolism of metabolic reactions. Consequently, exposure to these active oxygen species will react with electrons from lipids in cell membrane, varieties of important molecules like DNA, RNA, proteins and leading to cell damage. Ultimately, such products will lead to products that are able to be cytotoxic, mutagenic, and carcinogenic and may be lethal to the organism.

Antioxidants are thus important defences against oxidative stress, and have been asserted to protect against cancer and ageing. Urate is a potent free radical scavenger (Ames et al., 1981), which binds to these radicals and keeps them in a more stable form and causing less cellular damage (Hilliker et al., 1992).

5.3 Urate and gout

Although urate plays a vital role in detoxification and free radicals scavenging in disease and normal status (Ames et al., 1981), high levels of uric acid, by contrast can be damaging and lead to inflammatory disease. Gout is an inflammatory human disease that arises due to excessive uric acid levels in blood, and also due to the lack of urate oxidase enzyme to further metabolise uric acid to 5HIU (Maloley and R.Westfall, 2000).

The levels of circulating urate are thus a compromise between two opposing needs. As humans lack a urate oxidase enzyme, they are predisposed to higher levels of urate. By contrast, in *Drosophila melanogaster*, uric acid, is not always not end product of purine metabolism, and can be further metabolized to 5-hydroxyisourate (5HIU), by urate oxidase, and then to allantoin by 5-hydroxyisourate hydrolase (Figure 5-3). Nonetheless, a potential role for urate as a protection against oxidative stress in *Drosophila* can be inferred from the discovery that *rosy* mutants are hypersensitive to oxidative stress, induced by the weed killer paraquat. Paraquat is a redox cycling compound, it is reduced by NADPH to form a relatively stable radical species (Pq^{+})which then racts with O_2 to generat ROS (Hilliker et al., 1992), it is also inhibites microchnodrial electron transport (Franco et al., 2010).

5.4 Control of *urate oxidase* expression

Unlike microorganisms, uric acid oxidase enzyme in *Drosophila melanogaster* is not induced by uric acid, since *ry* and *mal* mutants have higher URO enzyme concentration higher than the Oregon-R wild type mutant. This interest, in both *ry* and *mal* mutants, came from the fact that both of them lack detectable levels of the xanthine dehydrogenase enzyme, which is responsible for hypoxanthine to xanthine then to uric acid conversion (Friedman and Johnson, 1977).

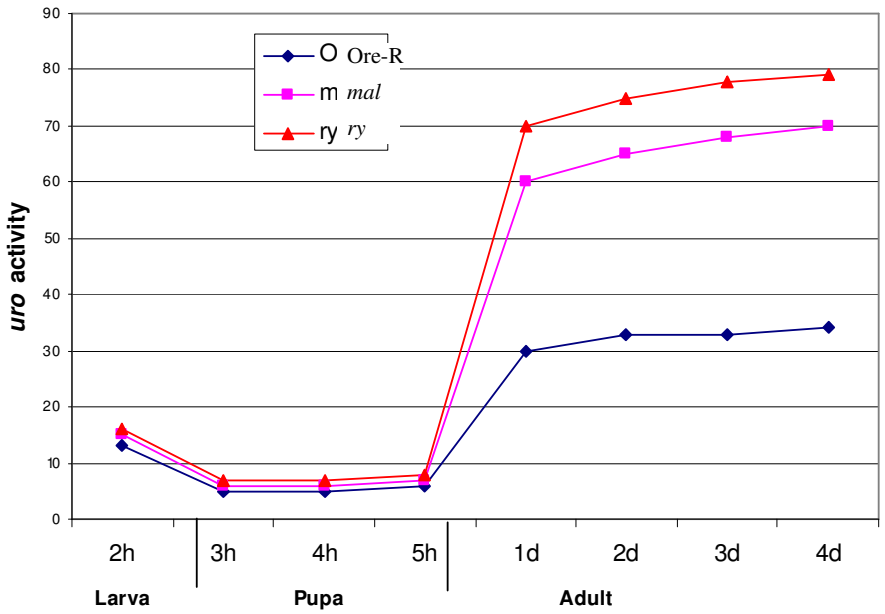

Figure 5-2 The *uro* activity pattern in wild-type *mal* and *ry* in *Drosophila*. Modified after (Friedman, 1973).

Urate oxidase activity is not detected in the first, second instar larvae and pupal stages. However, it is present in third instar larvae and adults. So it seems there is a temporal control of the enzyme activity during different fly stages. However, molecular mechanism of reactivation of the *uro* gene in the adults *Drosophila* is poorly understood. However, (Friedman and Johnson, 1977) have proposed two phenomena for urate oxidase activity. First an inducing factor, closely located to the gene that stimulate the production of enzyme, suggested to be found in the haemolymph. The second is that an autonomous intracellular clock-like mechanism, found in the adult Malpighian

tubules, may be responsible for controlling the time of changes to take place (Friedman and Johnson, 1977).

The inducing factor was found in *ry* and *mal* 5-10 times higher than *uro* -mRNA and *uro* proteins than in wild type adult. (Wallrath et al., 1990). However, studies by (Ramazzina et al., 2006) and (Tipton, 2006) suggested that urate oxidase is converting UA to 5HIU but not allantoin, as it was thought.

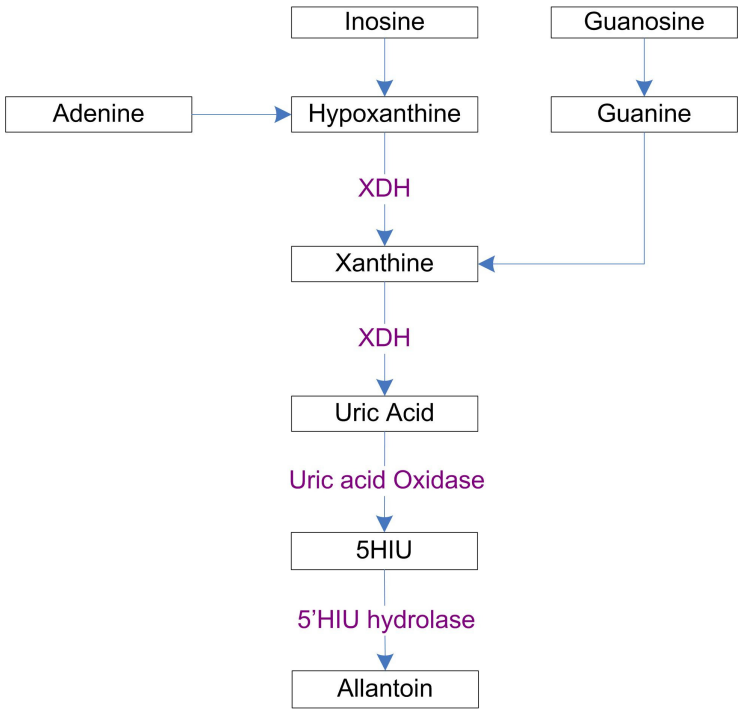

Figure 5-3 Part of purine metabolism pathway, emphasising the downstream metabolism of urate.

5.4.1 Principle of Polarizing microscope assay for uric acid crystals

As well as using metabolomic approaches, it is possible to visualize urate directly, as it is birefringent (Ainsworth et al., 2000). The polarized light microscope is designed to observe and capture specimens that are visible primarily due to their optically anisotropic character. In order to accomplish this task, the microscope must be equipped with both a polarizer, positioned in the light path somewhere before the specimen, and an analyser (a second polarizer; Figure 5-4), placed in the optical pathway between the objective rear aperture and the observation tubes or camera port.

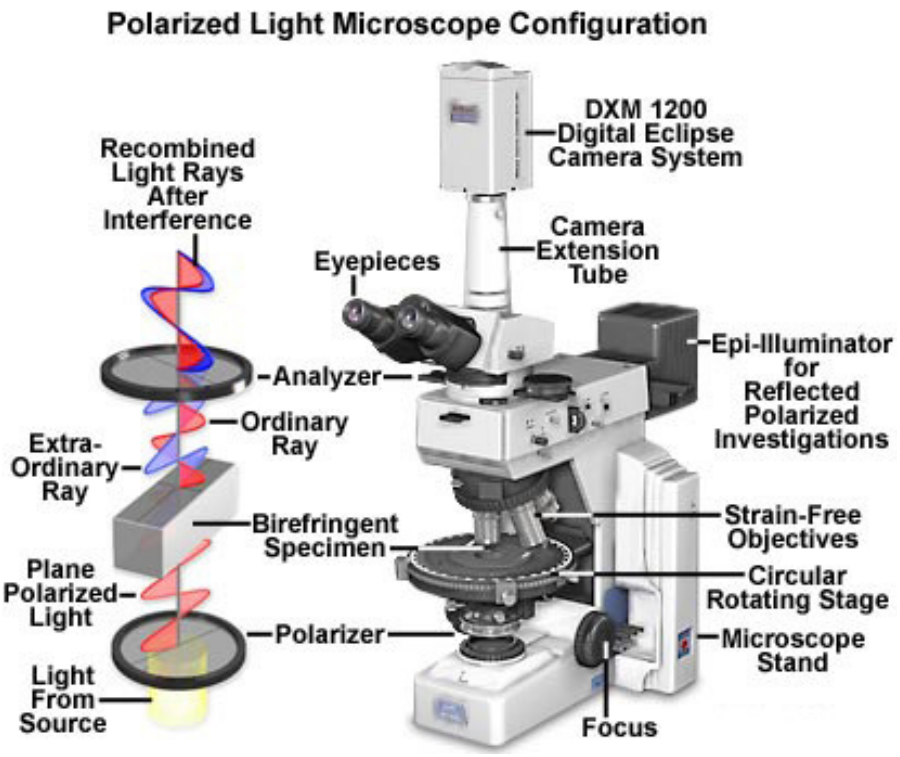

Figure 5-4. The light polarizing microscope.

http://www.microscopyu.com/articles/polarized/polarizedintro.html

This polarizing effect depends on the properties of the specimen, including the thickness difference between the refractive index and the birefringence of the two mutually perpendicular beams, which has a maximum value dependent on the specimen and on the direction of light propagation through the specimen.

As the analyzer plate is rotated, the intensity of the polarization light varies cyclically, from zero (extinction; Figure 5-5 (d)) up to a maximum brightness at 45 degrees (Figure 5-4 (a), and then back down to zero after a further 90-degree rotation.

That is why rotating the plate is crucial in polarized light microscope for determining of the specimen.

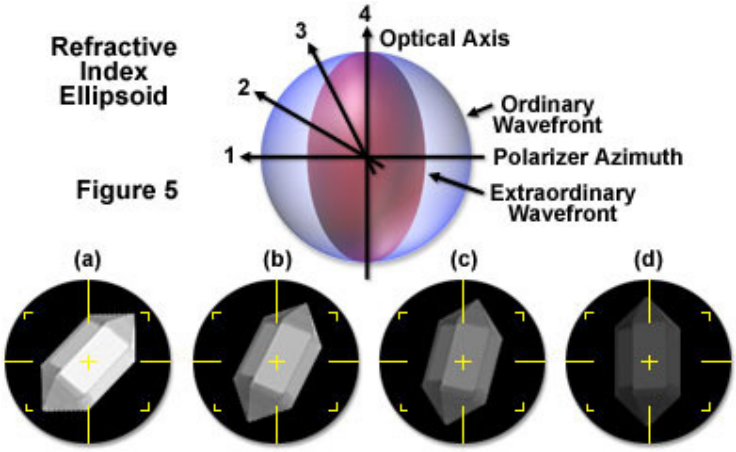

Figure 5-5. Principle of polarizing imaging of birefringent crystals. From:

http://www.microscopyu.com/articles/polarized/polarizedintro.html

One of the most common medical applications for polarized light microscopy is the identification of gout crystals (monosodium urate). Thus, shiny urate crystals are indicated as high levels of crystals under polarizing microscope (e.g. Figure 5-6).

5.5 Aims

We aimed to perturb the *uro* in the *Drosophila melanogaster* specifically in the Malpighian tubules in order to investigate the effects of this gene. As the *uro* is involved in complex biological activities in the human as well as in the *Drosophila*, we wanted to see the effects on longevity, response to oxidative stress and changes in the metabolome. Another interesting point is to investigate whether the nitrogen was being shunted to other pathway, for example proline and glutamine pathways.

5.6 Results

5.6.1 RNAi

The RNAi is a method widely used as a powerful tool for reverse genetics in gene silencing. The method first was used in *C. elegans*, was quickly adopted for gene silencing in *Drosophila melanogaster* (Kennerdell and Carthew, 2000).

In order to intervene a specific gene in the *Drosophila,* an inverted repeat DNA sequence must be constructed to target a specific gene, in our case, *uro,* and to be placed under the control of the UAS promoter. This was carried out with help of the pRISE II transgenic vector (Kondo et al., 2006). Then this construct was sent to be injected into white background fly embryos, w^{1118} and was balanced over the homozygous lethal *CyO* on the second chromosome.

5.6.2 Testing the effectiveness of RNAi against *urate oxidase*

UAS-*uro* (RNAi) flies were crossed to *uro* -GAL4 virgin flies. Then 5 to 7 day old adult progeny were dissected in a Petri dish containing Schneider's medium. Once the MT were separated, they were carefully transferred with a glass rod to be screened for both, uric acid crystals precipitation using the polarizing microscope (Figure 5-6) and gene expression knockdown with both quantitative expression analysis (Figure 5-7) and Orbitrap metabolomics (Figure 5-8).

5.6.3 Polarizing microscope assay

5-7 days old adult progeny of a cross between UAS-*uro* RNAi line and *uro* -GAL4 driver, were selected for the analysis. Dissected MT were immediately transferred using a glass rod onto a microscope slide which also containing a few drops of Schneider's medium. A coverslip was applied, using four dots of high vacuum grease to maintain a gap. This slide was then immediately inspected under the polarizing filter microscope.

As a result of knocking down *uro,* UA crystals would be expected to accumulate in the *Drosophila* MTs. These crystals should be visible as birefringent under the polarizing filter.

In (Figure 5-6), two pictures are shown for the same tubule. The one in the left, used as control as it was taken under the classical light microscope. It was shown the

background is lighter than the object and it is not signs for crystals precipitations. Whereas in the right side picture, the background was dark as well as parts of the tubules as they do not contain crystals. However, the main segments were full of the uric acid crystals; thus they were seen as shining under the polarizing filter.

This provides us with a clear indication that polarizing microscopy is capable of visualizing urate crystals effectively.

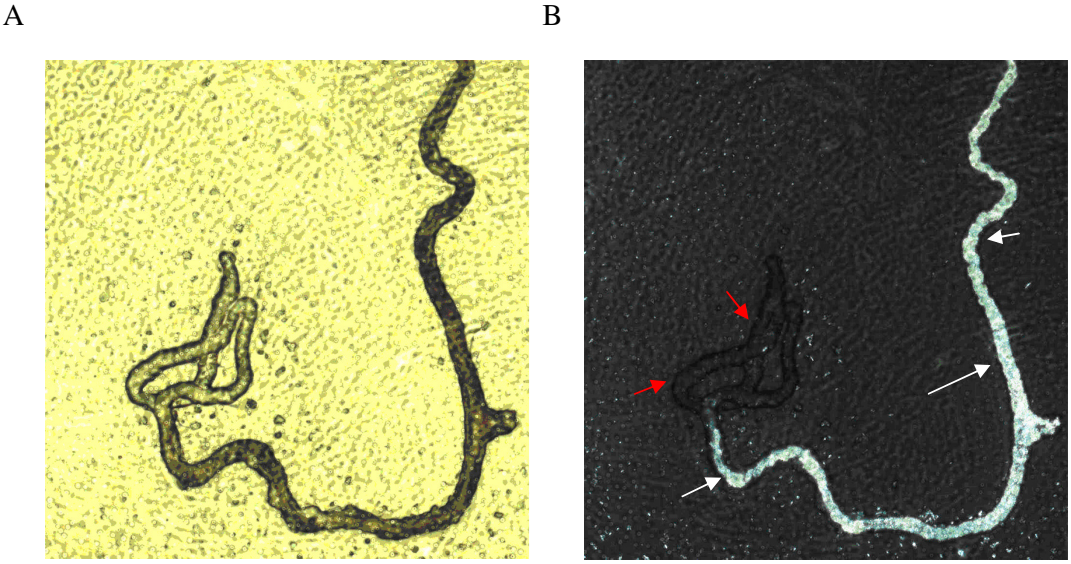

Figure 5-6. Demonstration of uric acid accumulation in tubules. The same picture is shown what it looks like the uric acid crystals under the polarizing microscopy. Transmitted (A) and polarizing (B) views of *uro* knockdown tubules. White arrows denotes uric acid crystals precipitations, while red arrows pointing to areas where no crystals were seen. Wild type vs mutant comparison pictures are shown in Figure 5-9.

5.6.4 Validation by qPCR

As the polarization test suggested that the *uro* knockdown was working, gene expression validation was taken place in order to measure the efficiency of the knockdown. For this MT from parents and the progeny were dissected in a Petri dish containing Schneider's medium. Then the MT were immediately transferred by a glass rod into RLT buffer in preparation for RNA extraction. In the case when the extraction was not going to be immediate, RLT buffer containing the MT were preserved at the -80 ºC. After mRNA extraction, quality and quantity of mRNA were measured. Then after,

cDNA were generated, using the mRNA as a template, and again were checked to quality and quantity.

As a statistical control, four technical replicates were applied for each of three biological replicates. Each tube contained 12.5 µl SYBR green, 2 µl primer set, approximately 500 ng cDNA template and finally made up to 25 µl of nuclease-free water.

As can be seen (Figure 5-7) there is a substantial decrease in the amount of expressed *uro* gene in knockdowns when compared with the other two parents. Approximately 80% gene expression reduction was seen in the dissected MT as compared to the same number of parental tubules dissected. It must thus be concluded that this is a relatively successful knockdown.

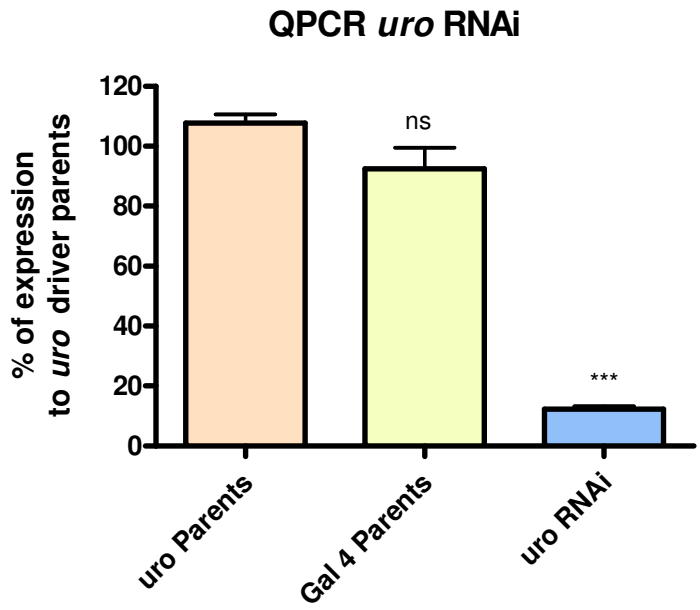

Figure 5-7 This figure shows *uro* RNAi knockdown validated by qPCR. It shows *uro* gene knockdown expression dissected from the MT compared to *uro* GAL4 and *uro* UAS-RNAi parental lines. Approximately eighty per cent *uro* lower expression was seen as determined by Student's *t*-test. Data are expressed as a percentage, compared with the average parental expression levels.

5.6.5 Validation by Orbitrap

Further studies were performed to determine key metabolites as a result of the *uro* knockdown on MT using the Orbitrap. The UAS-*uro* RNAi lines with their parents were used. Around 20 adult flies aged between 5 to 7 days old were used for the MT to be dissected. Fly dissection took place in a Petri dish containing Schneider's medium. After the desired number of tubules was dissected, they were immediately transferred into ice-cold 50% methanol/ 50% water solvent. Samples were kept at -20 ºC for short-term less than one week, or at -80 ºC for longer periods, until the day of analyses. Each fly line was repeated in three biological replicates.

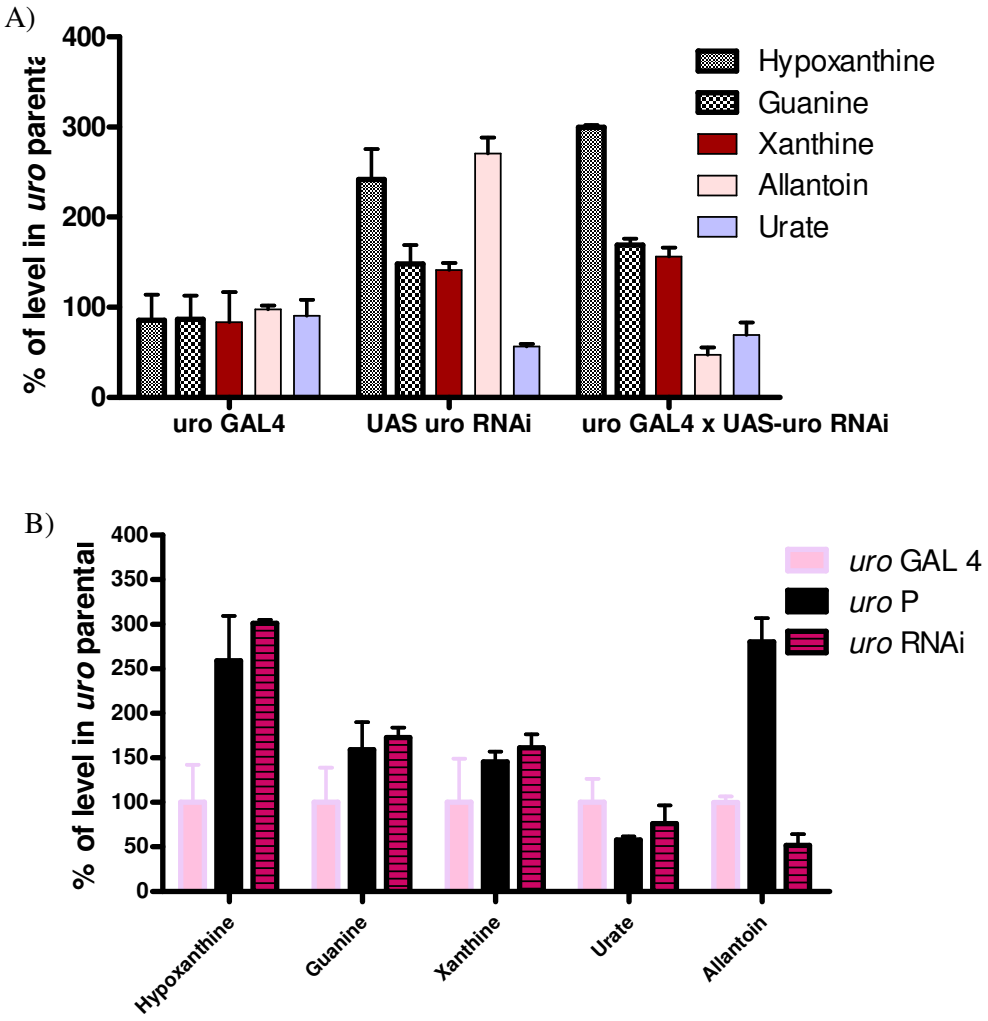

Figure 5-8. Impact of *uro* knockdown on purine metabolite levels in tubule using the Orbitrap. Data are shown as mean +/- SEM of three biological replicates. A) Plotted by genotype. B) The same data plotted by metabolite. UAS may show some leaky expression even when not driven. This would explain why the UAS-*uro* resembles *uro*-GAL4 x UAS *uro*.

It is nice to note that these results also show the ability to produce good metabolic data from isolated single tissues, rather than whole flies.

5.6.6 Crystals under the polarizing microscope

As another validation method in the *uro* knockdown we used the polarizing filter microscope. Usually uric acid crystals shine when seen under crossed polarizing filters, allowing their rapid visual identification in the MT. The MT from the *uro* -RNAi progenies and their parental lines were dissected under the light microscope in a Petri dish containing Schneider's medium. After dissection, a glass slide was marked with the designated line's name and one drop of Schneider's medium added; then with a glass rod the whole tubules were carefully transferred to the slide. As the eye view field was limited, and the whole MT was relatively wide, several pictures were taken then were merged together to form composite pictures showing the whole tubules (Figure 5-9).

In this figure tubules in A and B were for *uro* -GAL4 parent and UAS-*uro* RNAi parent respectively; consistent with normal expression of *uro,* only sparse uric acid crystals were seen. Whereas in C, the UAS-*uro* RNAi progeny, an obvious and aberrant accumulation of uric acid crystals was seen.

Although there was no significant difference in the levels of urate between the three lines in the metabolomic analysis, it was clear in the polarizing microscope and in the quantitative PCR. The results from the three techniques are thus slightly contradictory, but could be explained if most of the uric acid crystals were spun down into the pellet during methanol/water extraction for metabolomic sampling. The protocol used would favour sampling of the soluble urate.

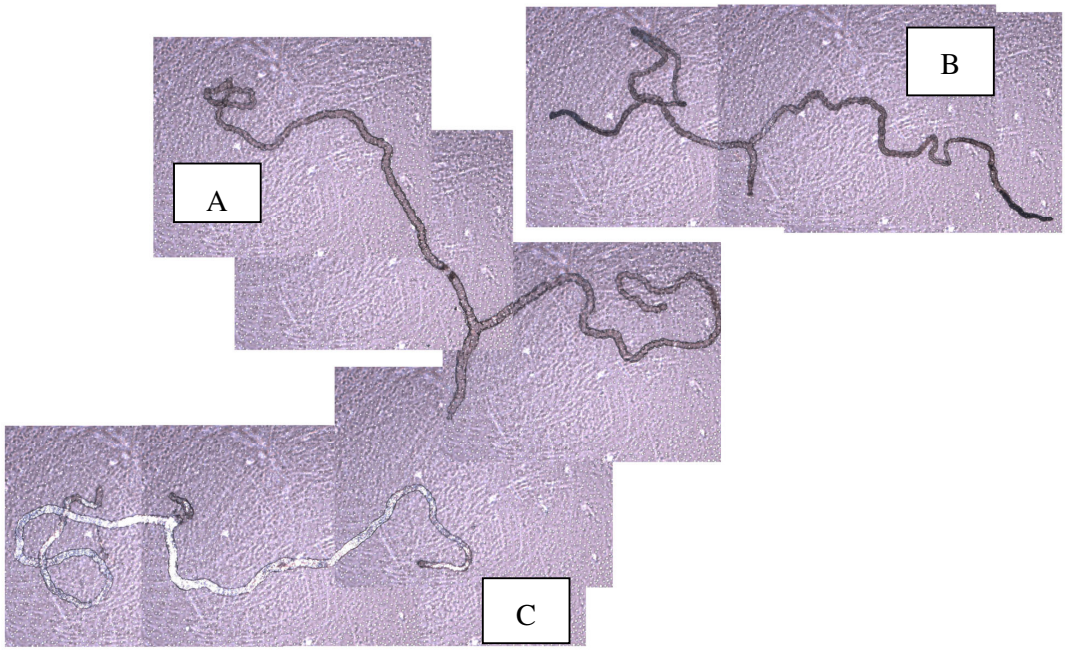

Figure 5-9. Impact of *uro* knockdown on uric acid accumulation in adult tubules. *Uro* -GAL4 parent (A), UAS-*uro* (RNAi) parent (B) and progeny of *uro* -GAL4>*uro* (RNAi) (C). The RNAi knockdown of *uro* was functionally effective, and resulted in an abnormal accumulation of uric acid.

5.7 Survival assay

Furthermore, this line was used to determine the effects on the fly survival and see the effects on aging and longevity.

5.7.1 No additive to the fly food

Longevity has been linked directly to urate concentration. Thus the Malpighian tubule specific gene, *uro,* was tested to see if it has an effect on fly survival. So experiments involved several fly lines were conducted including both the *uro* -GAL4 and UAS-*uro* (RNAi) parents and their progeny. Adult flies were collected and transferred to newly prepared fly food vials, and kept under medium crowding (10 males +10 females per vial). The number of dead flies were recorded twice a week. Flies were tipped weekly into newly-prepared vials. As seen in (Figure 5-10), survivorship curves were plotted. The UAS-*uro* RNAi cross fly line showed a slight improved in longevity compared to both parents, which differed markedly in their survivorship. The UAS-*uro* (RNAi) parent line was the fastest to die, while the other parent, *uro* -GAL4, was very similar to the progeny.

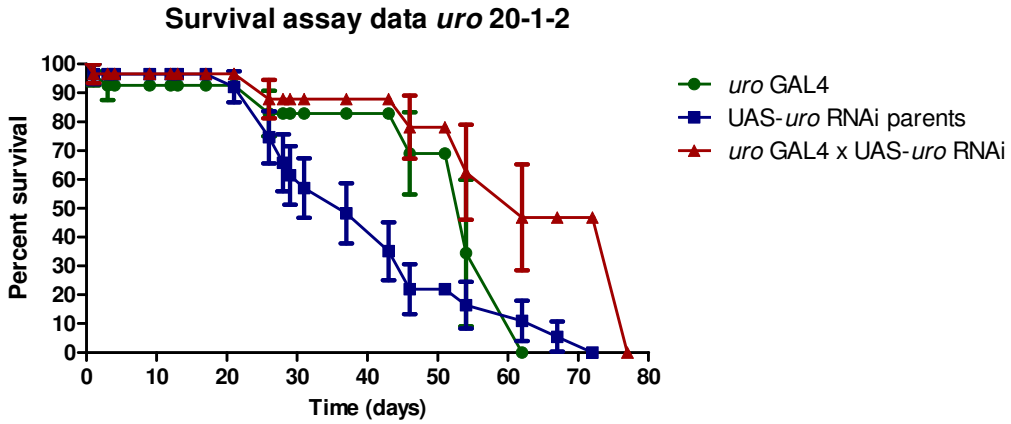

Figure 5-10 Survival assay for *uro* RNAi lines under normal conditions. When *uro* is knockdown it shows more urate, which is antioxidant, this means the fly is better protected, this suggested the flies are healthier. Significant changes were seen *P*-value 0.0018, Log-Rank (Mantel-test).

.

5.7.2 Survival assay under oxidative stress

Unfortunately, our UAS-*uro* RNAi line was lost, so the oxidative stress experiments were performed with the *uro* insertional knockdown line from Bloomington w^{1118}; {w^{+mC}=WH}PBac uro^{f04888} (Mamer et al., 1971).

It is important to increase the efficiency of transposon mutagenesis in *D. melanogaster*, to emphasis on generating stronger loss-of-function alleles. In this line the most promising, pBac transposon was used for more effective gene disruption. When this technique was discovered by (Thibault et al. 2004) eighty-nine percent of the lines yielded unique flanking sequence by inverse PCR. In addition, 97 of 100 pBac lines analyzed by genomic Southern blotting had single insertions. And the unlinked background mutations screens of pBac stocks contained only 0.3 -0.5 %. Finally, they also found the insertion and transposase strains have been stable for 4 years with no observed breakdown. Taken together, these data support the conclusion that pBac acts as an effective mutagen and that the mutations observed are directly caused by the transposon insertion.

The uro gene contain only one small intron (60 bp) in the middle of the gene, and the pBac is 7.2 kb is large enough which was landed in the middle of the gene, and so is highly likely have disrupted the gene reducing the transcription of the normal mRNA as seen in Figure 5-11.

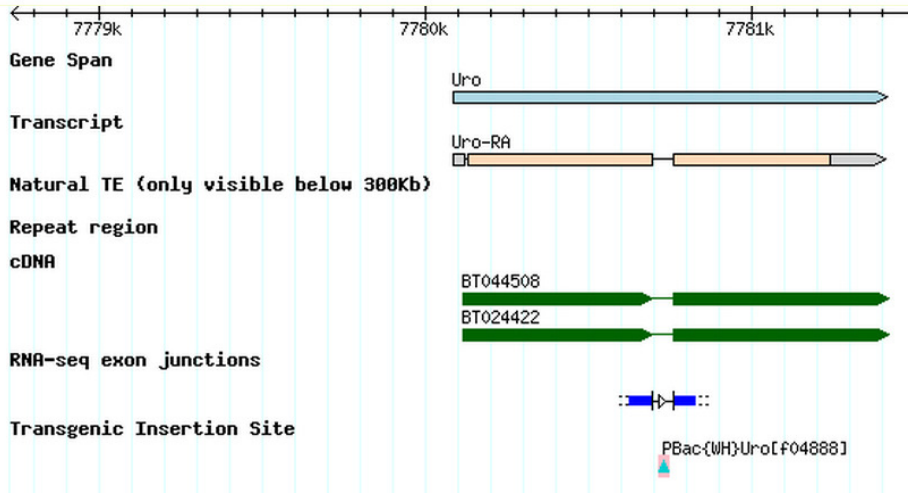

Figure 5-11 The pBac transgenic insertion site on the uro gene.

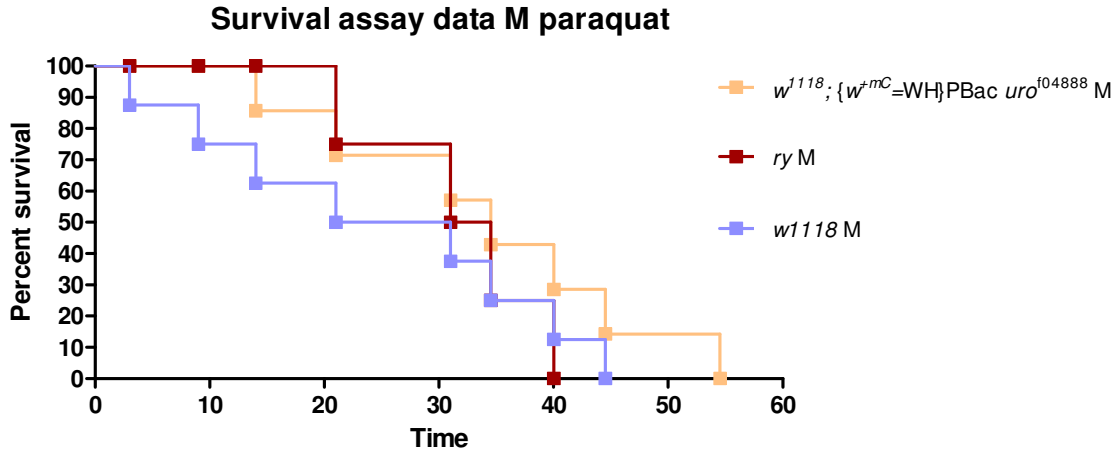

Figure 5-12 Survival assay showing the effects of parquat on male specific into three different mutants. Three tubes of 10 flies.

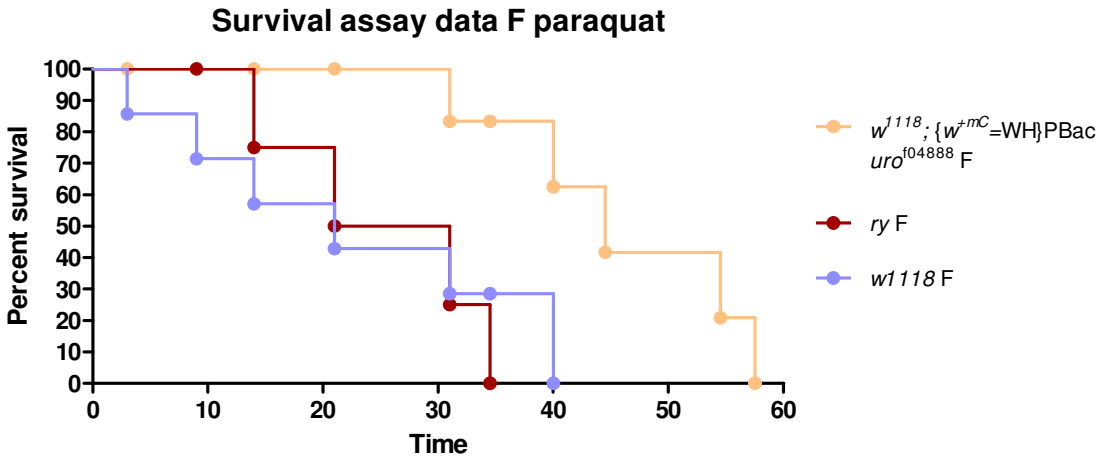

Figure 5-13 Survival assay showing the effects of parquat on female specific into three different mutants. Three tubes of 10 flies.

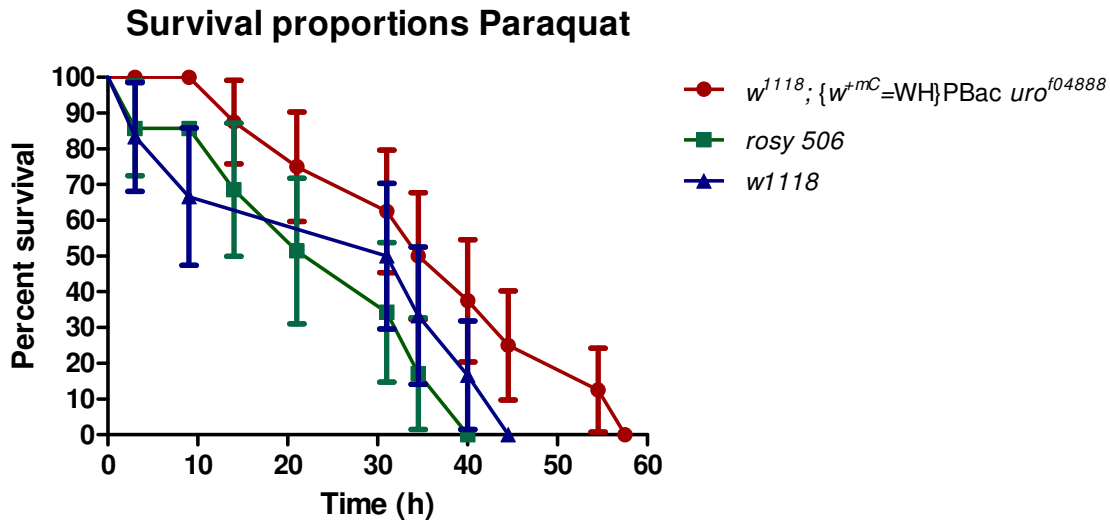

Figure 5-14 A survival assay showing the effects of 20mM parquat on three different lines w^{1118}; {w^{+mC}=WH}PBac uro^{f04888}, $rosy^{506}$ and w^{1118}. No significant changes were seen, *P*-value 0.25, Log-Rank (Mantel-test).

5.8 Discussion

From the interfering RNA work (Figure 5-7), it can be seen that a significant < 0.001 knockdown, of approximately 80% of the uro expression, was achieved. This can be also confirmed by the condensation of the uric acid crystals in the MT of the organism as compared to the other parents (Figure 5-9). This gave enough confidence that it worked.

However, when applying metabolomics, the results were a puzzling and confusing (Figure 5-8 A and B). The explanation to this could be that although there were an approximately 80% knockdown, the other 20% perhaps was enough to produce enough UA to be seen by the Orbitrap. This small percentage (20%) is the residual expression, or what is sometimes called leaky expression, would be capable of producing some protein. An alternative explanation for the UA crystals seen in the MT, are that these are of insoluble urate. This insoluble urate was pulled down in the sample preparation for the metabolomic experiment. So, even if urate production had ceased entirely, carry-over of insoluble urate would result in a relatively slow depletion of urate levels, much as was observed.

Then the effects of uro on the Drosophila lifespan was also needed to be investigated, thus a survival assays were important to be carried out.

Thus a survival assay was conducted to investigate the uro effects on Drosophila's lifespan in comparisons with uro-GAL4 parental line and UAS-uro RNAi parental line as it can be seen in (Figure 5-10). Lifespan was significantly increased, P-value 0.0018 in the progenies of the uro-RNAi line crossed with the uroGAL4.

Moreover, these interesting results have encouraged us to further survival testing using an oxidative stress agent. Sadly, the UAS-uro parental line were lost and this rendered us from carrying out the experiments. However, a Bloomington stock of uro knockdown insertional line were used (w1118; {w+mC=WH}PBac urof04888).

This time survival assay under the 20 mM oxidative stress parquat was conducted. Beside the uro w1118; {w+mC=WH}PBac urof04888 line, rosy506 and w 1118 were also compared. (check if there is Oregon-R)

The limited time during my PhD and the family bereavement happened have prevented me to test the uro w1118; {w+mC=WH}PBac urof04888 line to validate the gene knockdown by qPCR or to visualize the uric acid crystals under the polarizing microscopy.

If the time allowed, it would be nice to continue these experiments in order to get insights in the future for the effect of parquat on the Drosophila lifespan.

In particular, it would have wanted to confirm these exciting results by :

- Re-transforming Drosophila with my RNAi construct.
- Validating knockdown of w1118; {w+mC=WH}PBac urof04888 line by QPCR.
- Validating knockdown of the w1118; {w+mC=WH}PBac urof04888 line by visualising uric acid crystal accumulation (as seen in Figure 5-9); and perhaps
- Validating knockdown of the w1118; {w+mC=WH}PBac urof04888 line by Orbitrap analysis.

In addition, it would be interesting to test the hypothesis that there are both soluble and insoluble pools of urate in tubule.

Chapter 6 *Drosophila* microarray analysis investigation

6.1 Introduction

Gene-expression microarrays have become widely used as measurement tools in biological research (Lamy et al., 2011). Designing the experiment has a direct impact on the efficiency of the results interpretations and test validity (Leung and Cavalieri, 2003). From the experimental and technical point also, the biological replicates of samples are another important point must be carefully considered. In microarray analysis, two types of replication can be carried out: the technical replication, is when mRNA sample is used on multiple microarrays, and the biological replication, is when measurements are taken from multiple sample (Kerr et al., 2000).

However, data analysis is considered the most challenging part of it. A wide range of methods for microarray data analysis have been used .

Microarrays are considered among the most attractive techniques for high-throughput transcriptional profiling with metabolomics. This technique draws its power from the simultaneous detection of tens of thousands of genes at the same time. The cost is dropping constantly and it is not only being used exclusively in the research field, but in screening for cancers, and for disease diagnosis and monitoring. In time, next generation sequencing (NGS) technologies are likely to supplant microarrays for expression profiling; but at present microarrays are the mature platform of choice.

6.1.1 General principle

Generally in any microarrays, probes are fixed to a surface, usually glass. Each probe is complementary to a particular cognate mRNA. From each biological sample, mRNA is used to generate cRNA in order to hybridize to the probes. These cRNAs are usually labelled with fluorescent dyes for hybridization.

After hybridization, laser light is used to excite the fluorescent dye; the amount of florescence is proportional to the intensity of the hybridization, thus reflects the abundance of transcript (Figure 6-1).

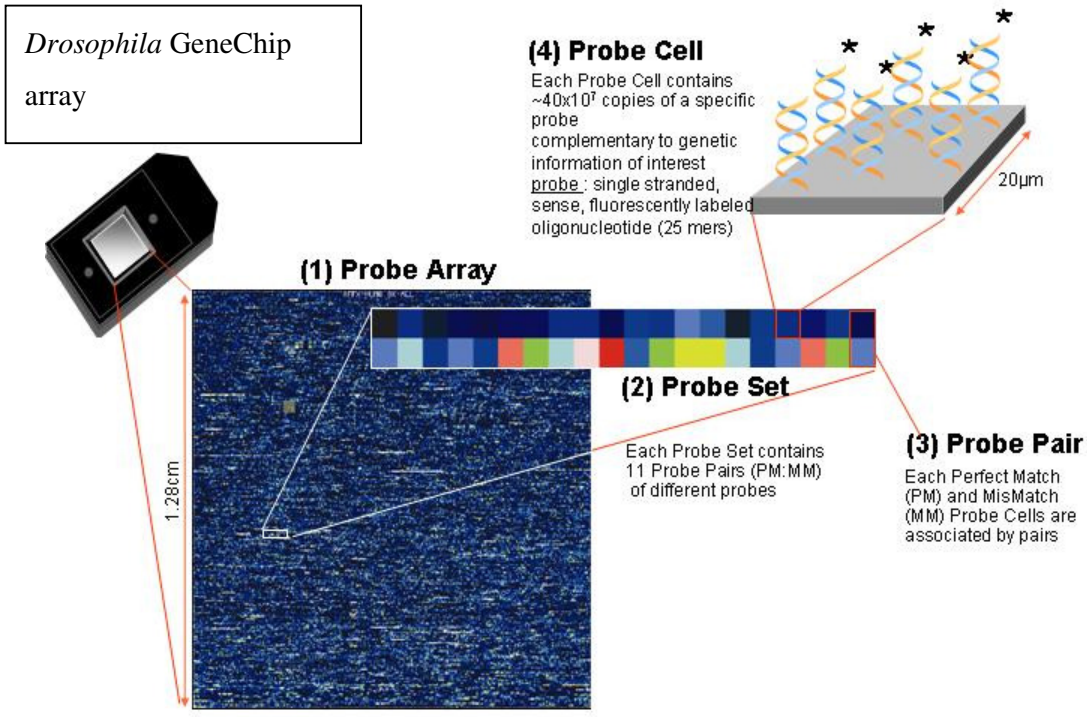

Figure 6-1 Schematic overview of the Affymetrix GeneChip, taken from www.affymetrix.com.

6.1.2 Affymetrix

Affymetrix one of the most popular microarray platforms used (Figure 1.21). In only a small square (1.28 cm^2) glass, more than 1,000,000 different probes are synthetically attached (Lipshutz et al., 1999).

Each probe is 25 nucleotide long, between 16-20 probe pairs representing one particular gene. These probes are synthesized in a basis of perfect match (PM) and mismatch (MM) basis. The PM is designed to complementary hybridized to cRNA, while the MM is the same sequence as the PM except that only one single base in the middle is changed.

The probe lengths should not be exceeded 25 nucleotides as problem of non specific hybridization are expected to be found (Fodor et al., 1991) and (McGall et al., 1996).

6.1.3 RNA quality control

All RNA extracted samples should meet the highest quality standards to ensure the best hybridization on the gene-chip array to be achieved. In order to inspect the RNA quality a small amount of each sample must be assessed by the RNA 6000 Nano assay on the Agilent Bioanalyzer (Agilent Technology UK. Ltd) to examine the ribosomal RNA bands. The more intact the ribosomal RNA, the less RNA degradation has occurred.

Sample absorbance should also be read at 260/280: acceptable readings are between 1.8 to 2.1 for RNA. Readings below 1.8 indicate possible protein contaminations while readings above 2.1 indicate likely RNA degradation.

6.2 Affymetrix microarray experiment

Total 2 µg of RNA was reverse-transcribed and *in vitro* transcribed according to the standard Affymetrix protocol to produce biotinylated complementary RNA (cRNA). Prior to the reverse transcription, poly-A RNA controls were added into the RNA samples before target labeling. Poly-A controls (lys, phe, thr and dap) function is to monitor the target labeling process from the beginning of the experiment to finish. They act as indicators of target preparation and labeling efficiency. The cRNA was then purified and checked for integrity (see section 6.1.3 RNA quality control) and fragmented. Fragmented cRNA was hybridized to *Drosophila* genome 2 expression arrays (4 biological replicates per tissue). Hybridized probes were then stained using streptavidin phycoerythrin conjugate and scanned with an Affymetrix GeneChip Scanner 3000 7G. The overview of the GeneChip 3' IVT express kit labelling assay is shown in Figure 6-2. An additional amplification step was used as necessary for RNA samples less than 2 µg in the two-round amplification protocol; the starting amount of RNA for the two-round amplification was typically 100 ng.

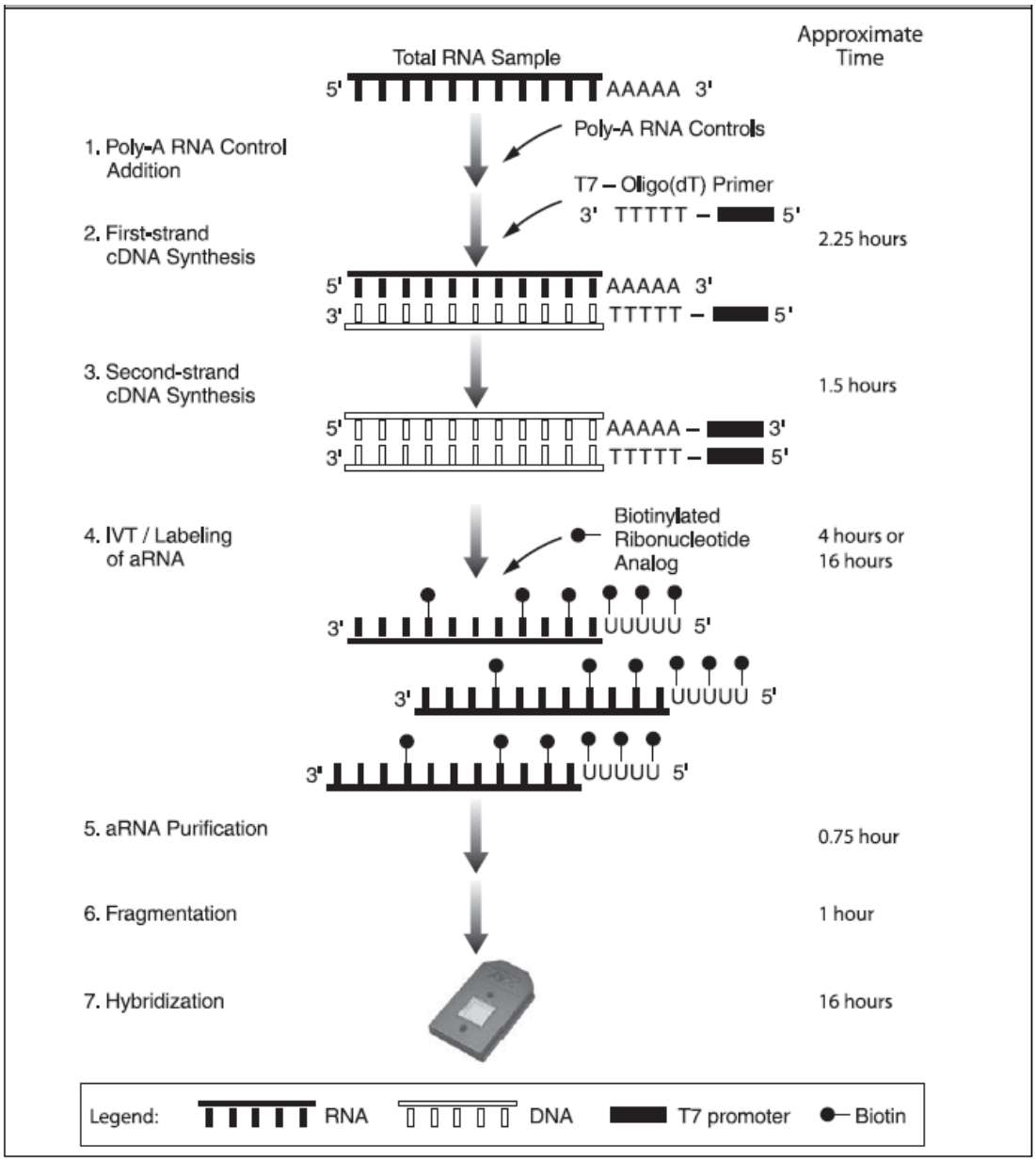

Figure 6-2 Overview of the GeneChip 3' IVT express labelling assay (taken from www.affymetrix.com).

6.2.1 Statistical analysis

Experimental trascriptomes compared against the relevant controls to obtain *t*-test *P*-values for the statistical significance for differential expression.

For the advanced analysis and annotation, GeneSpring GX10 (Agilent UK) was used. Raw data (signal intensity) CEL files were obtained from the Affymetrix GCOS and uploaded into the GeneSpring for further data processing and analysis. In GeneSpring, data was analyzed in several sequential steps which include data processing,

normalization, grouping, interpretation, quality control, statistical analysis and functional annotation.

6.2.2 Functional annotation

The DAVID Gene Ontology (GO) package was used to represent the data on an intuitive heat map and to functionally annotate using ontology terms.

6.2.3 Fold change (FC) analysis

Fold Change Analysis was used to identify genes with expression ratios or differences between a treatment and a control that are outside of a given cut-off or threshold. Where Fold change was used, it was calculated between a condition (Condition 1) and one or more other conditions (Condition 2) treated as an aggregate. The ratio between Condition 2 and Condition 1 is calculated (Fold change = Condition 1/Condition 2). Fold change gives the absolute ratio of normalized intensities (no log scale) between the average intensities of the samples grouped. The entities satisfying the significance analysis are passed on for the fold change analysis.

6.3 Allopurinol drug

Allopurinol, was one of the drugs discovered at Burroughs Wellcome program that started in 1940s and was awarded the Nobel Prize in Physiology and Medicine in 1988 (Pacher et al., 2006). The drug discovery project was meant to find potential antitumor drugs. However, subsequent experiments showed effective control of serum and urinary uric acid by allopurinol; and its direct metabolite, oxypurinol, showed promise for the treatment of hyperuricemia. In 1966, allopurinol was Food and Drug Administration (FDA) approved as treatment for gout and until now it is an important cornerstone in primary and secondary hyperuricemia management (Pacher et al., 2006).

Many researchers have also suggested additional important roles for that XO in different types of ischemic and tissue and vascular injuries, inflammatory diseases, and chronic heart failure. Beneficial effects on the previously mentioned conditions were seen not only due to allopurinol but also from its metabolite, oxypurinol. Reviewed in (Harrison, 2002) , (Harrison, 2004) and (Berry and Hare, 2004).

6.3.1 Pharmacokinetics

When administered orally, allopurinol is rapidly absorbed and reaches peak concentration in plasma within 30 to 60 min. On the other hand oxypurinol has lower oral bioavailability than allopurinol.

In terms of half-life, allopurinol has relatively short time in plasma approximately (2–3 h), whereas the half-life of oxypurinol is much longer (14–30 h) due to renal reabsorption (Pea, 2005).

Gastrointestinal pain, hypersensitivity reactions as well as skin rash are the most common side effects of allopurinol and it may vary from individual to individual (Pacher et al., 2006).

6.3.2 Mechanism of action

Allopurinol is known inhibitor for the enzyme xanthine oxidase, which blocks the metabolism of hypoxanthine and xanthine to uric acid. It acts by interfering with the catabolism of purines resulting in lowering uric acid production.

Also its metabolite, oxypurinol acts as in a competitive inhibitor as it is an isomer of xanthine. Thus preventing the conversion of xanthine to uric acid. Also as indirect inhibition , oxypurinol inhibits the purine biosynthesis by stimulating negative feedback (Pacher et al., 2006).

6.4 Aim

We applied the Affymetrix Gene-chip array in a way to identify the effects of allopurinol drug on the MT of wild type OR *Drosophila melanogaster* in a time-course experiment.

Allopurinol was intended used to phenocopy the *rosy* mutant and to test any metabolic effects on the *Drosophila melanogaster* tubular transcriptome.

Furthermore, the classical *rosy* mutant MT was also analyzed in comparison with the WT OR tubules.

6.5 Results

6.5.1 Microarray results for *rosy* compared to wild type

The main purpose of the microarray experiment was to compare the transcriptome of 5-7 day adult *Drosophila melanogaster* wild type against *rosy* Malpighian tubules. The total numbers of genes significantly (*P*-value 0.05) changed were 8720, where 3368 were up regulated while 5352 genes were down regulated. In order to narrow down the list, only genes two times fold changed up and/or down were selected. This gave a list of total 1189 on both directions. To focus the analysis more tightly, only genes significantly changed five times were only listed in (Table 6-1 and Table 6-2).

Table 6-1 Genes significantly down regulated in *rosy* compared to wild type. Genes shown here are ranked by their fold changed down regulated expression in MT compared to WT, $P < 0.05$.

Gene Symbol	*P*-value	FC Absolute	Gene ontology biological process
ry	7.3E-20	160.1	Determination of adult life span
CG13313	8.2E-18	159.4	
CG14957	3.4E-06	37.3	Chitin metabolic process
CG2781	2.9E-16	30.4	Fatty acid elongation
DnaJ-1	6.0E-07	29.3	Protein folding
CG9981	3.7E-16	19.9	Atp biosynthetic process
Hsp70Ba, Bb, bb and Bc	4.3E-02	18.4	Response to stress
RFeSP	1.6E-12	18.3	Mitochondrial electron transport
Map205	3.1E-10	17.6	Microtubule-based process
Hsp27	2.3E-02	14.2	Response to stress
CG10924	4.8E-12	12.6	Gluconeogenesis
CG18673	4.6E-06	12.5	One-carbon compound metabolic process
CG12910	9.4E-12	11.6	
Hsp26	3.5E-02	11.2	Response to stress
1636495_at	4.7E-08	10.7	
CG13397	3.2E-15	10.5	Metabolic process
Pepck	2.8E-05	10.4	Gluconeogenesis
ninaD	1.7E-03	10.3	Defense response
CG9149	2.8E-21	9.8	Metabolic process
CG4288	7.0E-11	9.7	
CG32103	2.9E-06	9.1	Transport
CG7968	2.6E-04	8.9	
alpha-Est7	1.6E-09	8.6	
CanA1	1.1E-08	8.3	Protein amino acid dephosphorylation
CG3292	4.9E-08	8.0	Metabolic process
CG14688	4.8E-11	7.7	
CG10657	1.2E-06	7.2	Transport

CG14872	1.1E-04	7.0	Transport
CG9360	1.2E-09	7.0	Metabolic process
1624819_s_at	2.1E-13	6.9	
CG15202	1.5E-13	6.6	
1623349_x_at	1.4E-13	6.5	
CG14298	1.3E-11	6.4	
CG12734	2.0E-05	6.2	
CG14120	2.7E-07	6.1	Metabolic process
1639729_s_at	1.6E-13	5.9	RNA-dependent DNA replication
Cyp4e1	8.3E-08	5.9	Oxidation reduction
Ugt86Dd	3.7E-10	5.8	Metabolic process
Hsp22	5.4E-03	5.7	Response to stress
CG6495	5.0E-11	5.6	
CG32750	2.0E-06	5.5	Nitrogen compound metabolic process
Lox	3.4E-06	5.4	Protein modification process
Nha1	9.7E-05	5.4	Transport
CG8147	4.6E-02	5.2	Metabolic process
CG6448	3.5E-15	5.2	
mthl8	3.0E-11	5.0	Response to stress
CG9989	2.9E-07	5.0	

Table 6-2 Genes were up regulated in *rosy* compared to WT.

Gene Symbol	p-value	FC	Gene Ontology Biological Process
CG10140	3.8E-16	72.7	Chitin metabolic process
Cht4	6.3E-10	60.0	Carbohydrate metabolic process
AttD	2.4E-06	59.9	Antibacterial humoral response
CG12009	1.6E-23	56.4	Chitin metabolic process
CG30031	2.4E-07	55.3	Proteolysis
Arc1	2.7E-07	38.4	
Adh	2.6E-15	36.1	Cellular alcohol metabolic process
CG30090	9.7E-20	35.5	Proteolysis
RpL35	1.1E-22	28.0	Mitotic spindle elongation
TyrR	5.4E-25	27.8	Signal transduction
regucalcin	2.3E-19	23.5	
CG6330	6.7E-13	22.4	Nucleoside metabolic process
CG5091	3.5E-20	22.0	Protein amino acid N-linked glycosylation
His4r	1.9E-20	20.0	Chromatin assembly or disassembly
Act42A	3.6E-08	19.6	Cytokinesis
Arc1	2.4E-19	18.9	
CG30154	6.3E-19	18.7	
CG14687	3.9E-11	17.5	
lectin-37Db	8.6E-06	17.0	
CG31997	8.1E-09	16.7	
CG9336	5.2E-10	16.4	
Rab40	1.0E-16	16.3	Intracellular signaling cascade
CG9691	3.6E-09	15.2	
CG11671	6.0E-08	14.7	

cib	6.6E-14	14.5	Cytoskeleton organization
CG15210	4.8E-07	14.0	
alpha-Man-I	2.1E-15	13.9	
yellow-d	7.5E-07	13.8	Protein amino acid N-linked glycosylation
CG5541	1.6E-15	13.6	
CG8768	3.9E-13	12.9	
1625050_s_at	5.6E-09	12.7	Metabolic process
CG7191	9.3E-10	12.7	
CG6643	2.2E-06	12.6	
insc	2.0E-15	12.2	RNA localization
unc-13	1.6E-16	12.2	Intracellular signaling cascade
norpA	3.7E-23	11.7	Lipid metabolic process
Tsp42Eh	2.7E-09	11.7	
1627236_s_at	3.0E-16	11.6	
Mlp60A	2.4E-11	11.5	Multicellular organismal development
CG7447	9.6E-19	11.4	
RpS29	3.4E-16	11.3	Translation
CG9072	1.1E-22	11.0	Tubulin complex assembly
CG7778	3.9E-06	10.6	
cib	7.4E-14	10.5	Cytoskeleton organization
CG5011	2.3E-09	10.0	
Idgf1	4.9E-05	9.6	Carbohydrate metabolic process
CG30026	6.3E-06	9.5	
fau	2.1E-13	9.5	Response to stress
Pvf2	2.1E-07	9.0	Salivary gland morphogenesis
CG13075	7.1E-07	9.0	Chitin metabolic process
CG12780	1.1E-07	8.9	
CG5910	6.4E-05	8.7	
Sema-2a	1.5E-09	8.7	Multicellular organismal development

Nrg	3.4E-11	8.4	Cell adhesion
Bsg	4.2E-05	8.4	Spermatid development
DptB	4.1E-04	8.4	Antibacterial humoral response
Hsp60B	1.5E-16	8.2	Protein folding
Cht8	3.4E-17	8.1	Carbohydrate metabolic process
CG3973	4.8E-14	8.1	Cell cycle arrest
CG7267	4.5E-15	8.1	
Mef2	8.3E-15	8.0	Transcription
CG4757	4.3E-04	7.7	
fax	1.9E-08	7.6	Axonogenesis
CG13117	5.2E-09	7.6	
CG12310	8.6E-06	7.5	
RpII215	2.1E-15	7.5	Transcription
CG16743	9.3E-06	7.2	
Tsp42El	1.1E-09	7.1	
CG9784	5.3E-12	7.1	Dephosphorylation
CG1077	1.4E-13	7.0	
CG1572	2.2E-07	7.0	
Akt1	2.0E-09	6.7	Protein amino acid phosphorylation
CG1146	3.8E-07	6.5	
CG31158	6.9E-12	6.3	Regulation of ARF protein signal transduction
PGRP-SA	1.9E-06	6.3	Defense response
Sucb	9.0E-09	6.3	Tricarboxylic acid cycle
Dcp2	5.2E-13	6.3	Nuclear-transcribed mRNA catabolic process
trol	4.1E-12	6.2	DNA methylation
Eip75B	3.7E-07	6.2	Transcription
CG15347	2.0E-06	6.2	
lea	4.1E-10	6.1	Neuron migration
smi35A	4.5E-14	6.1	Protein amino acid phosphorylation

CG34104	3.5E-11	6.1	Chitin metabolic process
HLHm3	3.6E-14	6.0	Negative regulation of transcription from RNA polymerase
W	1.1E-10	6.0	Embryonic development via the syncytial blastoderm
CG32687	4.9E-10	6.0	
CG9672	4.8E-12	6.0	Proteolysis
Stlk	2.5E-14	6.0	Protein amino acid phosphorylation
msn	2.5E-09	6.0	Activation of MAPKKK activity
Ect4	5.2E-12	5.9	Immune response
Ste12DOR	1.0E-14	5.9	Spermatogenesis
Btd	5.4E-04	5.8	Nitrogen compound metabolic process
CG12112	3.1E-13	5.8	
CG6959	4.6E-10	5.8	
CG9021	6.4E-16	5.8	
eIF-4B	1.1E-11	5.8	Translational initiation
shi	1.1E-14	5.7	Cytokinesis
sls	3.1E-07	5.7	Somitogenesis
1641367_at	7.9E-09	5.7	
1635258_s_at	5.9E-10	5.7	
RpS30	1.3E-17	5.6	Mitotic spindle elongation
CG5804	1.5E-05	5.5	Cellular acyl-coa homeostasis
Pka-C1	2.4E-06	5.4	Protein amino acid phosphorylation
Nrg	9.2E-12	5.4	Cell adhesion
Tm1	3.3E-11	5.4	Muscle contraction
Flo-2	2.7E-10	5.3	Cell adhesion
1625336_s_at	1.2E-15	5.3	
Imp	3.3E-12	5.2	Spermatogenesis
CG32626	1.2E-10	5.2	Purine base metabolic process
CG5630	7.0E-08	5.2	
MtnB	1.2E-11	5.2	Cellular metal ion homeostasis

Eip93F	5.6E-06	5.1	Phagocytosis, engulfment
CG7920	1.9E-09	5.1	Acetyl-coa metabolic process
CG32512	5.0E-14	5.1	
Mctp	1.1E-10	5.1	
Scamp	7.5E-16	5.1	Protein transport
CG42329	5.8E-15	5.1	
Sox100B	1.4E-18	5.1	Male gonad development
CG31004	1.9E-10	5.0	Cell-matrix adhesion
baz	3.1E-10	5.0	Cytokinesis

6.5.2 Reconciling array and metabolomic data for *rosy*

Perhaps the key finding of the thesis is the attempt to reconcile these related, but distinct datasets. Metabolite changes were brought from the *rosy* chapter three, while genes annotations and pathway were from the KEGG website and finally the microarray datasets from this chapter (Figure 6-3).

The purine metabolic pathway is shown, along with changes occurring on the levels of metabolome and transcriptomic (Figure 6-3). As it is known that *rosy* is defective in xanthine oxidase, its precursors accumulate, while urate is lowered. Consistent with the known lesion in *rosy*, the array data show, *ry* was down regulated 160 times, this allowed to xanthine to accumulate 25 times. This accumulation has a concomitant impact on levels of xanthine precursors; hypoxanthine (15 times) and guanine (3 times).

Upstream expression changes ionclude the *guanine deaminase* (3.5.4.3) was found down regulated 2 and half times. Further above the *CG16758* gene was found to be twice as normal indicating the perhaps as a result of urate low concentration, demanding for more urate. The *CG11883* was lowered more than halved time as normal, and that could be hypothesized due to increased levels of adenine, hypoxanthine and guanine, the activation of the feedback inhibition of the enzyme by APRT and HGPRT (Figure 6-3) (Kamleh et al., 2008).

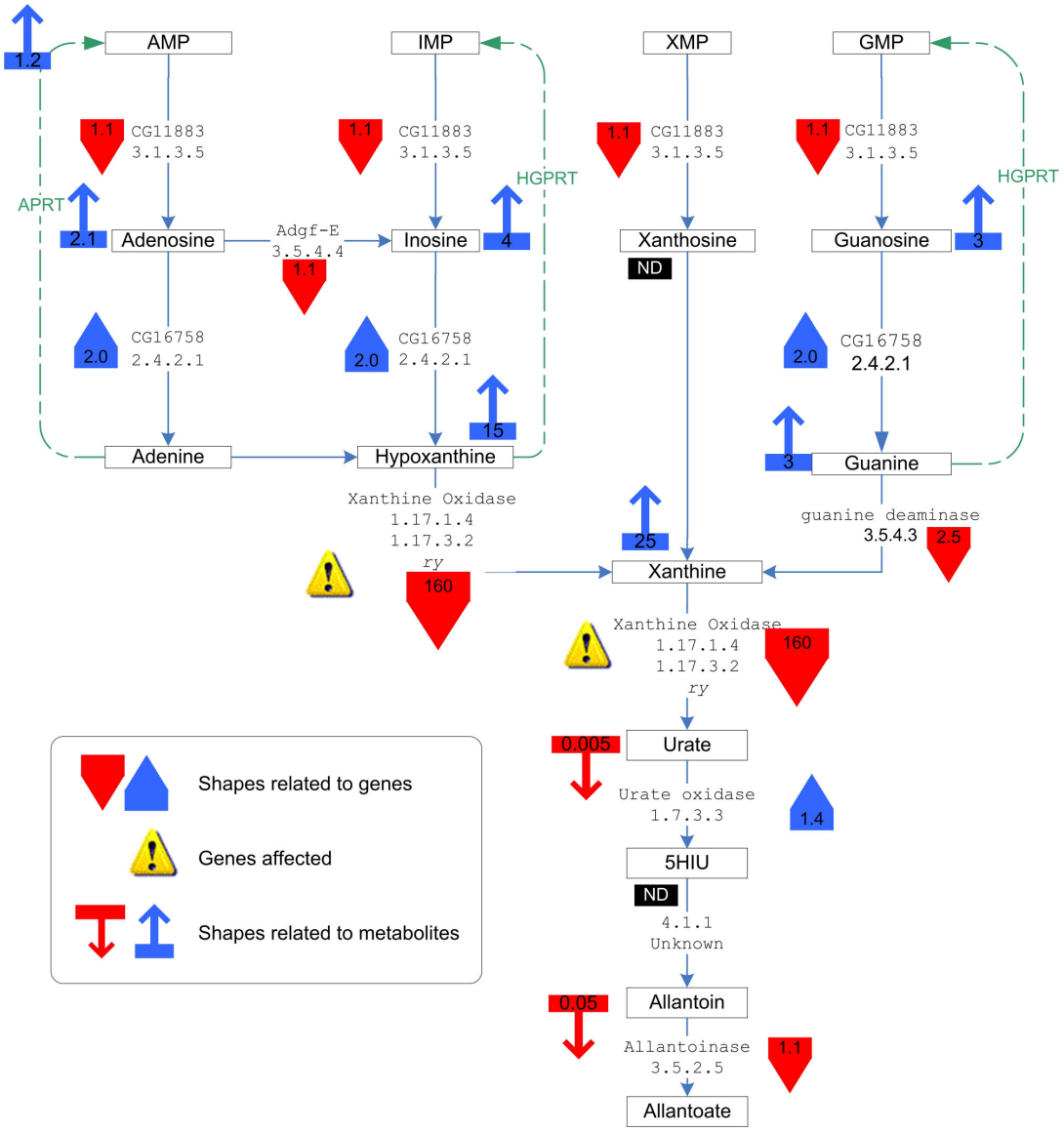

Figure 6-3 A combination of different datasets. This novel compined figure represents the purine metabolism pathway with respect to integrated metabolomic as well as transcriptomic. Triangl shaped denotes or represents gene affeted, while arrows represent metabolites changed. Red colour means reduced in level or downredulated and blue cloure means incresed in level or upregukated. The impact of *rosy* on the xanthine oxidase, urate is reduced, which proved by orbitrap. Consequently *urate oxidase* gene was 1.4 upregulated, this could be as a masage from allantoin ordering the the fly to produce more urate in order to be later converted to allantoin. Futher effect of the enzyme are accumulation of xanthine and hypoxanthine which shown by orbitrap to be 25 and 15 fold increased repectevely. The effects do not soley on xanthine and hypoxanthine, it impacted further up the pathway as it reaches their immediate precursers, for example adenine and guanin and futher up like adenosine, inosine and guanosine with a slightely leasser increas.

6.5.3 Microarray results for Allopurinol

It has been thought phenocopying the *rosy* with allopurinol drug might have interesting effects on the metabolomic and/or transcriptomic levels. Allopurinol is known to phenocopy *rosy* (Keller and Glassman, 1965).

In the microarray dataset for allopurinol experiment, although 374 genes showed changed expression, there was no clear pattern, and there were no significant effects on the key enzymes in the purine metabolic pathway Table 6-3.

This may be because the effect of the drug was only transient on the metabolic level. By contrast, the *rosy* mutant is lacking xanthine oxidase enzyme since birth. Thus no beneficial effect found on the transcriptomic level when applying allopurinol on WT.

Table 6-3 Significantly downregulated grouped genes in six hours allopurinol treated flies.

Top changed groups	**Group members**	**Changed members**	***P*-value changed**	**Percent changed**
Blood coagulation	3	2	8.9e-05	66.67
Reduced folate carrier activity	3	2	7.4e-05	66.67
Determination of adult lifespan	98	2	6.6e-05	2.04
Response to stress	82	7	5.6e-12	8.54
Response to unfolded protein	7	3	4.4e-08	42.86
Heat shock-mediated polytene chromosome puffing	7	3	4.4e-08	42.86
Response to hypoxia	18	4	3.5e-09	22.22
Protein refolding	7	2	2.3e-05	28.57
Cell morphogenesis involved in neuron differentiation	4	4	1.7e-04	100.00
Folic acid binding	4	2	1.5e-04	50.00
Response to heat	81	7	1.2e-11	8.64

WT vs 6h upregulated

Top Changed Groups	Group Members	Changed Members	*P*-Value Changed	Percent Changed
Immune response	98	7	9.7e-06	7.14
RNA-directed DNA polymerase (reverse RT)	12	2	9.6e-05	16.67
Regulation of protein import into nucleus	10	2	9.4e-06	20.00
Eclosion rhythm	12	3	8.6e-07	25.00
Innate immune response	98	8	7.9e-07	8.16
Glutathione peroxidase activity	9	2	6.8e-05	22.22
Circadian rhythm	42	4	6.0e-07	9.52
Antibacterial humoral response	28	6	5.7e-08	21.43
Gns1/sur4 membrane protein	3	2	5.3e-05	66.67
Protein import into nucleus	23	2	5.2e-05	8.70
Regulation of circadian sleep	20	3	4.4e-06	15.00
Tata box binding protein associated factor	8	2	4.1e-05	25.00
Negative regulation of oskar mRNA translation	9	3	4.0e-05	33.33
Structural molecule activity	88	5	3.8e-05	5.68
Locomotor rhythm	37	4	3.6e-07	10.81
Rhythmic process	18	3	3.2e-06	16.67
Vitellogenesis	9	3	3.1e-06	33.33
Rhythmic behavior	20	4	2.7e-08	20.00
Protein heterodimerization activity	58	4	2.2e-06	6.90
Photoperiodism	2	2	2.1e-07	100.00
Negative phototaxis	2	2	2.1e-07	100.00
Circadian behavior	5	2	2.1e-06	40.00
Mating behavior	15	3	1.8e-06	20.00
Negative regulation of histone modification	2	2	1.5e-06	100.00
Entrainment of circadian clock	14	3	1.4e-06	21.43
Acyl carrier activity	9	2	1.4e-04	22.22
Regulation of circadian sleep/wake cycle	4	2	1.3e-06	50.00
Defense response to bacterium	20	3	1.3e-04	15.00
L-phenylalanine catabolic process	4	2	1.3e-04	50.00
Copulation	13	3	1.1e-06	23.08
Perinuclear region of cytoplasm	27	3	1.1e-05	11.11
Sleep	11	2	1.1e-05	18.18
Sex differentiation	27	3	1.0e-04	11.11

6.6 Conclusion

As it can be seen in this experiment, allopurinol did not elicit consistent significantally reliable effects on the wild type fly in the microarray experiment. However, when microarray data were analyzed using the MT of *rosy* mutant against the MT wild type , as expected the *rosy* gene came on the top of the list of the upregulated.

What needs to be addressed here is the question why does allopurinol induce changes in the metabolome, but not in the transcriptome under the same conditions?. Experimental error or high variability in analysis are possibilities. Alternatively, the short-term blockade of the purine metabolism pathway may not induce the same transcriptomic changes as the lifelong knockdown associated with $rosy^{506}$ deletion.

Several genes and metabolites were affected as a direct impact of *rosy*, both in the transcriptomic and on the metabolomic levels respectively. These changes are shown in Table 6-1, Table 6-1 and Table 3-2 and Figure 6-3. Pleasing, to my knowledge it was first time a mutant has been studied with both techniques.

The 'list of genes' resulting from a microarray analysis should not be viewed as an end in itself; its real value increases only as that list moves through biological validation, ranging from the numerical verification of expression levels with alternative techniques. Sadly, time has limited us from further array analysis.

Chapter 7 Summary and discussion

7.1 Introduction

IEMs are a group of diseases with a much higher incidence in some areas more than others, due to factors like consanguinity. Because of their early onset, severity and frequently devastating consequences, good animal models are highly demanded. Investigations of IEMs in animal models might be very helpful in exploring insights in these types of diseases, mode of transmission and the way of tackling them and finding the best screening and / or efficient diagnosis methods. However, most IEMs have vanishingly low incidence in the Western world, and so are considered 'orphan diseases' – the investments in mammalian models or in drug therapy research is not considered justified. Simpler models, and rapid and efficient development pipelines, are thus highly important goals. *Drosophila melanogaster* is well known as a powerful genetic model, and has excellent genetic tools - for example RNAi, UAS-GAL4 system. Other key benefits include its small size, the short reproduction time and fully sequenced genome.

Another bottleneck is provided by screening technologies in humans, which historically have been ad hoc, and based on single disease diagnoses. The newly developed mass analyzer, the Orbitrap, has great potential in neonatal screening, because of its ability to identify 300-500 small metabolites in a single run from a single sample. This provides the opportunity both to streamline neonatal testing, and to expand the range of diseases that can be screened.

In this thesis, I addressed both issues, by using the new Orbitrap to test *Drosophila* mutants homologous to IEM genetic loci in humans, for example xanthinuria type I.

7.2 What was achieved?

At the outset of the project, the Orbitrap was a brand-new instrument, and metabolomics was almost unknown in *Drosophila*. A pilot experiment was performed on extracts pooled from 10 flies, male and females using the ry^{506} mutant. Initially we were testing the validity of the technology by looking for key metabolite changes in the purine metabolic pathway which was a targeted rather than global metabolomic validation.

As expected, the *rosy* mutant revealed what was historically was found. Having obtained the expected results, the analyzer was challenged further, to see to what extent that it would be useful in specific fly tissues. Consequently, we carried out another experiment using different fly tissues, like heads and Malpighian tubules. Empirically, 15-20 heads and tubules for 20-30 flies were found to give informative results.

Findings were again consistent with microarray expression data, as *ry* is expressed in the whole fly, with higher levels particularly in MT.

Then we decided to take one step forward in the analysis, after validating the technology, the approach was extended to all metabolites that could be resolved in the Orbitrap. Thus,

all significantly changed metabolites detected were arranged into putative metabolic pathways. Changes shown in (Table 3-3) were very sensible. Significantly, changes in metabolite levels can be detected several metabolites further up from the genetic lesion than had been detected by classical analytical biochemistry. This provided that the Orbitrap technology with great confidence has provided more information in a single experiment than could be obtained by classical techniques.

Remarkably, some of significantly metabolic changes were quite unexpected, and not known from the extensive classical literature (over 500 papers) on *rosy*. For example, effects on the tryptophan pathway, which involved in *Drosophila* eye pigmentation, were also noticed. This explained how the *ry* eye red-dull colour is generated. Generally, the *Drosophila* eye colour is constituted as a result of a mixture of two pigment colours. Each colour is generated from a distinct pathway. Thus, any disruptions in either pathway will impact on the *Drosophila* eye colour.

Another unexpected finding, was the impact on osmolyte biosynthesis. This was explained on the basis that *ry* mutants are unable to make uric acid in the absence of XDH, they excrete the nitrogen waste in other forms, perhaps as water-soluble xanthine. This process would be wasteful of water, leading to osmotic stress.

These results were extended to a second mutant, *maroon-like*, which is necessary for the activation of both *rosy* and other molybdoenzymes. *Maroon-like* is thus epistatic to *rosy*, and we accordingly observed a broader range of metabolic changes than in *rosy*. The work thus showed that it was possible not just to characterize a known mutant in *Drosophila*, but to extend the phenotypic description usefully, and to follow an epistatic series.

We also applied the Orbitrap technology to characterise a genetic lesion for which the underlying gene was not known – the eye and tubule colour mutant *chocolate*. In the limited time available, a definitive metabolomic fingerprint was not identified. However, with more work, it should be possible to perform such identifications more easily, and thus to provide a useful phenotype for reverse genetics of novel genetic loci.

In summary, then, *Drosophila* is highly compatible with Orbitrap technology, and the results are highly informative for analysis of both known and novel loci.

7.3 Drug action

This technology was also challenged not only with mutants or specific tissues, but also to follow and unravel the pharmacological effects of drug actions. It again proved successful. We used the anti-gout drug allopurinol, which is considered to phenocopy the *rosy* mutant both in humans and flies. Confidently, effects on purine pathway were seen, however we also uncovered interference with isomers - an important issue in metabolic analysis. We found unexpected behaviour of what was believed to be hypoxanthine and xanthine levels. However, later on we concluded these changes were as results of the hypoxanthine and xanthine isomers, the original drug allopurinol and its oxypurinol metabolite, respectively.

7.4 Utility of Drosophila

All of those experiments would not be conducted without the availability of an excellent genetic animal model like *Drosophila melanogaster*. It has clear advantages for studying some human disease genes, based on the rich information available for researchers. For example, availability of the completed *Drosophila* genome sequence (Adams MD, 2000), the tens of thousands of available classical mutants in stock centres, RNAi stocks for nearly every gene (Dietzl et al., 2007), and the FlyAtlas.org (Chintapalli et al., 2007) and Homophila (Reiter et al., 2001) websites.

A transgenic fruit-fly line can be made for approximately $500 in only three months and costs $30 per year to maintain (Dow, 2007). It is also one of the best and powerful genetic animal models being used; this is due to its short life cycle, which allows multiple generations to be screened quickly. The small size of the insect makes it better than many other animal models in terms of space in the lab and food requirements.

At the molecular level, balancers and P-elements provide powerful genetic tools for gene transformation and phenotype selection. Interfering RNA is also one of the important molecular genetic tools which helps in field of functional genomics, specifically reverse genetics.

Also, these findings have encouraged us to think of applying the technology to unlock the mysteries for thousands of *Drosophil*a mutants in captivity in stock centres. Thus, we subjected the *chocolate* mutant to for further metabolic investigations. Moreover, the list could be expanded widely to other mutants in stock centres world wide.

This new technology had helped us in addressing scientific questions fairly quickly and easily. It costs few dollars to run the samples which takes the technician less than 30 minutes in sample preparations and analyzers set-up. Then the analyzer might be left overnight to carry the job. Then a few days of further analysis (depending on the depth of the needed detail) can finalize the results.

The *Drosophila*, as genetic model, has its limitations as it is not mammalian; however with all the new technology and techniques continually emerging, the Orbitrap with great certainty will help in closing the phenotype gap between human and *Drosophila*. In particular, this thesis has shown the usefulness of *Drosophila* in modelling rare, Mendelian diseases of humans that might otherwise be considered too rare to attract major research funding.

Moreover in the utility of this technology, one can integrate the wealth of *Drosophila* genetics and metabolomics in other branches that will be great impact to it. This is to measure the changes in development, drugs mode of actions and newly discovered drug usages and might also be used in insecticide and detoxifications studies.

7.5 Utilization in humans

Certain inborn errors of metabolism (IEM) are far more common in some parts of the world than other places in the world, and neonatal screening must thus be more comprehensive. These inborn errors of metabolism, which are recessively inherited, are attributed to the consanguineous marriages practiced in the Arab world, especially in a country like Saudi Arabia (Al-Odaib et al., 2003).

In Saudi Arabia, in particular, consanguinity rates are about 50%, of which 60% are at a first-cousin level of consanguinity (El Mouzan et al., 2008); furthermore, the Kingdom is considered to have one of the highest birth rates in the Middle East and North Africa (Saadallah and Rashed, 2007).

So premarital screening programmes for congenital diseases could help significantly to limit the incidence and impact of inborn errors of metabolism.

Although premarital screening is an ideal solution, it is not always practical, socially acceptable or economic; so in practice both diagnosis and treatment must also be researched. In order to have better understanding, and to improve management of human genetic disorders, good metabolic screening and fairly fast and reliable analyzer, like the Orbitrap, is desirable. Although we did not assay human samples in this project,

we showed that the Orbitrap is ideal for detecting the metabolic changes associated with such mutations, and in samples far smaller than are likely to be available from human patients.

The consanguinity has played an essential role which made the genetic diseases are certainly important, if not, the most important health problem in this part of the World. The most sensible way to combat this problem is prevention. Thus we found the Orbitrap is very sensitive, quick, and cost-effective when applied to investigate *Drosophila* mutants in metabolic detections. So we concluded that the analyzer is a powerful technique that could be applied in the routine and as a screening for genetic diseases preventions in the Arab world where consanguinity constitutes a major problem especially in country like Saudi Arabia where it reaches up to 50% of all marriages.

Usually, inborn errors of metabolism causing clinical manifestations in the neonatal period are severe and often lethal if early detection was not done and proper therapy is not initiated. Clinical findings in this period are usually non-specific and similar to those seen in infants with sepsis. However, it has been shown that if detected early, complications in these disorders could be easily prevented with restricted dietary programmes or with early drug intervention.

With the advanced mass spectrometer analyzers available today, like tandem MS and GC-MS , a proper diagnostic revolution may not be far away. The tandem MS alone can detect 35-40 metabolic disorders and has revolutionized the concept of newborn screening in the developed countries (Roa. et al, 2009).

It is now possible to screen rapidly, simultaneously, and inexpensively for a number of very rare disorders with the use of tandem mass spectrometry, but some metaboloites would missed with such lower sensitivity when compaired to Orbitrap.

For this reason, assessment for the diagnostic potential of this technology is required. To evaluate the technology fully, studies of the clinical effectiveness of screening and a detailed cost analysis will be necessary, compared with what already available in the medical field.

Recently, new techniques involving the IEM are creating many possibilities for clinical applications. Although theses techniques might still be years away from practical use, it certainly will join the field of expanding genetic applications. These technologies, will have a great impact on carrier screening, which is an integral part of preventive genetics

programs. However, before commencing such programs, diseases should be carefully selected.

For example, in Saudi Arabia (Table 7-1) various rare metabolic diseases are screened at King Faisal Specialist Hospital and Research Centre, Riyadh, KSA (Al Odaib. et al 2003). In the last year, standard Guthrie cards (heel prick blood samples) collected from every newborn in Saudi Arabia (200 000+ annually), are sent to King Faisal, and subjected to a battery of tests (including two MS runs), specifically to identify IEMs. If the Orbitrap could simplify or streamline this testing, it could have a major impact.

Table 7-1 Major IEMs seen at the King Faisal Specialist Hospital and Research Centre. Riyadh, Kingdom of Saudi Arabia (1998-2002)

Disease category	Disease name
Organic acidemias (n= 294)	Methylmalonic acidemia (n=72) Propionic acidemia (n= 56) Glutaric aciduria type 1 (n= 29) 3-Hydroxy-3-Methyl Glutaryl CoA Lyase Deficiency (n=26) Other organic acidemias (n=111)
Amino acid disorders (n= 223)	Maple syrup urine disease (n=58) Classical phenylketonuria (n=33) Biopterin dependent phenylketonuria (n=29) Homocystinuria (n=33) Other amino acid disorders (n=70)
Lysosomal storage disease (n=172)	Niemann-Pick disease type B (n=36) Multiple sulfatase deficiency (n=30) Morquio's disease (n=25) Sandhoff's disease (n=19) Hurler-Scheie disease (n=18) Gaucher disease (norbottnian type) (n=8) Other lysosomal storage disease (n=36)

The medications required for the management of certain inborn errors of metabolism are so costly that few can afford them. For example, the available injectable enzymes for Gaucher and Niemann-Pick diseases cost approximately $30,000 per year for an infant. Since the dose is according to body weight, it increases proportionally with growth. The

same is true for the tetrahydrobiopterin cost for biopterin dependent PKU and for the Betaine required for homocystinuria (Al Odaib. et al 2003).

Thus, the carrier screening for rare genetic screening with a powerful analyzer like the Orbitrap, should take the lead over others in the Arabian Peninsula, especially in society like Saudi Arabia.

7.6 Metabolic modelling and systems biology

Although the Orbitrap is important in diagnosis, the other aim is to improve treatment. How could *Drosophila*, and the easy availability of mutants, help here? Firstly, mutant flies could provide a sensitized background for a genetic screen to identify modifiers of the severity of the disease – this is a very standard *Drosophila* technique. Secondly, the same sensitized background could be used to screen for compounds which improve survival .Although this is not a high-throughput screen, it is much less expensive than working with mice or humans. Thirdly, our work in *Drosophila* could allow us to build systems biology metabolic models that could predict the impact of mutations, and potentially predict possible therapies.

This lead us to integrate the metabolites, viewed in different tissues with gene expression level in those individual tissues (Chintapalli et al., 2007), suggesting that it may ultimately be possible to build models linking transcriptome and metabolome.

However, this is not easy as it sounds, as metabolomic analysis consists of different stages. The hardest part is the data analysis; it requires up-to-date speedy computers as well as continuously cutting-edge computational skills along with very strong biochemistry background knowledge.

7.7 Recommendations

The metabolomic studies are very helpful and a powerful method, along with what is available from the transcriptomic datasets, in the biological fields, in the normal as well as in the disease status. There are tens of thousands of *Drosophila* mutants in stock centres all over the world. Many of these fly lines are kept for several years without knowing the genetic makeup or the metabolomic profiling.

Thus we argue that using the power of the metabolic analysis (especially using the Orbitrap analyser) along with the transcriptomic data, scientists would be able to unlock the genetic mystery of many of the lines and perhaps human genetic diseases.

Furthermore, there is a huge pressure for cost-effective programmes for rare but lethal genetic diseases (like IEMs) in the neonatal and perhaps the premarital periods,

especially in a society like the Kingdom of Saudi Arabia. For this we argue that the Orbitrap analyzer is sensitive, fast, cost effective and high throughput enough analyzer that could be applied both in diagnostics as well as in screening; it is not yet been used in the Kingdom.

Chapter 8 Appendices

8.1 *Drosophila* media

Reagent	composition
Standard fly food	Per 1 litre of water 10 g agar 15 g sucrose 30 g glucose 35 g dried yeast 15 g maize meal 10 g wheat germ 30 g treacle 10 g soya flour
S.O.C Medium	2% Trypton 0.5 % Yeast Extract 10 mM NaCl 10 mM Mg Cl_2 10 mM $MgSO_4$ 20 mM glucose
Schneider's medium	

8.2 Plasmids and vectors

Item	Conceteration
pENTR/D TOPO vector	15-20 ng/µl linerized plasmid DNA in : 50 % glycerol 50 mM Tris-HCL, Ph 7.4 1 mM EDTA 2 Mm ddt 0.1 % Triton x-100 100 µl / ml BSA

	30 μM bromophenol blue
dNTP Mix	12.5 mM dATP 12.5 mM dCTP 12.5 mM dGTP 12.5 mM dTTP In water , pH 8
TE buffer is a commonly used buffer solution in molecular biology, especially in procedures involving DNA or RNA. "TE" is derived from its components: Tris, a common pH buffer, and EDTA, a molecule chelating cations like Mg^{2+}. The purpose of TE buffer is to protect DNA or RNA from degradation.	

8.3 Primers used in this thesis

no	Plasmid used	Gene name	F or R	Primer name to paplo	Full primer seqence incl res.t site	Restic. Enzyme used	Ann. Temp	Seg. Size
1	pWIZ	ry	F	ROSY F1	**GCATTCTAGA**CTACACAGATGACATTCCCCGC	Xba I	58.6	556
2	pWIZ	ry	R	ROSY R1	**GCATTCTAGA**AAACGCTTGGCACGACAGAC	Xba I		
3	pWIZ	ry	F	ROSY F2	**GCATTCTAGA**TCGGAACTGATTCACATTTCGG	Xba I		
4	pWIZ	ry	R	ROSY R2	**GCATTCTAGA**TTCACCCACTGCCTTGGAAGAG	Xba I		
5	pWIZ	uro	F	URO pWIZ F1	**GCATTCTAGA**TCACAATGTTTGCCACGCCC	Xba I	58.6	489
6	pWIZ	uro	R	URO pWIZ B1	**GCATTCTAGA**TGAAGTCGCAGTTCCCTTGGAC	Xba I		
7	pRISE	uro	F	URO pRISE F1	TCACAATGTTTGCCACGCCC		58.6	489
8	pRISE	uro	R	URO pRISE B1	**CACC**TGAAGTCGCAGTTCCCTTGGAC			
9	pWIZ	uro	F	URO pWIZ F2	**GCATTCTAGA**GCAAAAAGGATTACTACCAGGGC	Xba I		
10	pWIZ	uro	R	URO pWIZ B2	**GCATTCTAGA**ACCACGGTGCTAAAGATGCG	Xba I		
11	pRISE	uro	F	URO pRISE B2	GCAAAAAGGATTACTACCAGGGC			
12	pRISE	uro	R	URO pRISE F3	**CACC**ACCACGGTGCTAAAGATGCG			
13	pRISE	ry	F	ry_pRISE F1	CTACACAGATGACATTCCCCGC			
14	pRISE	ry	R	ry_pRISE B1	**CACC**AAACGCTTGGCACGACAGAC			
			F	M13 Forward	5'-GTAAAACGACGGCCAG-3'			
			R	M13 Reverse	5'-CAGGAAACAGCTATGAC-3'			

8.4 Metabolomics of *cho*, an uncharacterized mutant

The field of metabolomics has proven to give more insights in mutants for either novel or unknown metabolites (Kamleh, 2008). Previous studies have been done on *Drosophila* were done based on observational analysis, like variation in eye color pigmentation. This time we tried to use the metabolomic profiling in a way to reveal the cover for historically known mutants without exactly knowing what is the genetic lesion, like the *cho* mutant fly. In this contest, we tested the *cho* mutant against the Oregon R to elucidate the genetic lesion causing this pigmentation variation.

8.4.1 *Cho* Phenotypes

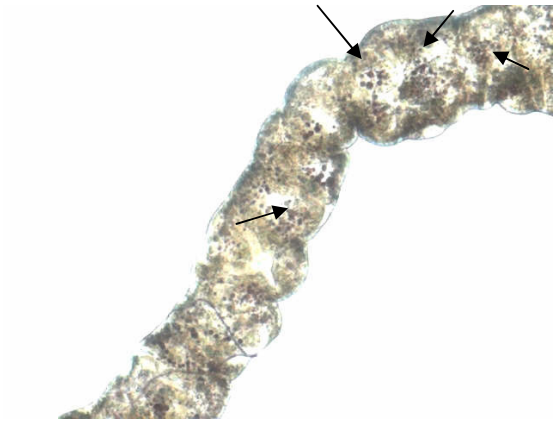

Figure 8-1 Part of Malpighian tubule from *cho* mutant.This picture shows the pigmentations in the MT in the *cho* mutant.

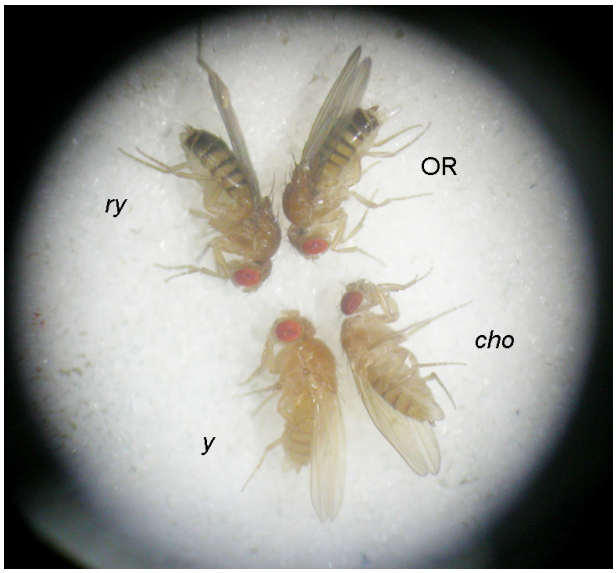

Figure 8-2 Four different flies showing different phenotypes.

8.4.2 Metabolomic comparisons between *cho* and Oregon R

Table 8-1 The major metabolite differences between *cho* and OR.

Sampled on two occasions (n=5) separated by five months (*cho*/OR).

Compound	m/z	Ratio 1	P value 1	Ratio 2	P value 2
Hydroxyproline	132.0656	1.92	0.010003	9.10	0.002113
Proline betaine	144.102	0.17	0.000793	0.17	0.000094
N-acetyl histamine	154.0976	0.42	0.011233	0.31	0.027323
Xanthurenic acid	206.045	0.60	0.008469	0.43	0.000107
Kynurenine	209.0923	0.49	0.001686	0.46	0.001774
Hydroxytryptophan	221.0922	0.19	0.009653	0.28	0.000405
Pyrimidodiazepine	222.0988	2.20	0.000021	1.50	0.024299
Hydroxykyurenine	225.0872	0.27	0.000457	0.43	0.000116
Dehydrobiopterin	236.078	3.06	0.000365	2.73	0.000104
Formylkynurenine	237.087	0.34	0.007335	0.46	0.029471
Biopterin 1	238.0937	1.72	0.013539	1.40	0.042726

Biopterin 2	238.0937	3.73	0.000013	2.68	0.001068
Drosopterin	369.1533	0.37	0.002922	0.19	0.000215
Xanthomattin	424.0647	1.61	0.157908	3.33	0.001808

8.5 Metabolites List

Formula	Compounds	MZ	Time	Ionization mode
C2H3NO2	Iminoglycine	74.02365	19.47	positive
C2H5NO2	Glycine	76.03931	19.92	positive
C4H6O2	butanedione	87.04408	16.3	positive
C4H6O2	butanedione	87.04409	18.82	positive
C4H8O2	Butanoic acid	89.05979	8.299	positive
C3H7NO2	Alanine	90.05495	19.85	positive
C3H7NO2	Alanine	90.05498	18.84	positive
C4H9NO2	GABA	104.0706	18.82	positive
C5H14NO	Choline	104.107	19.4	positive
C3H7NO3	L-Serine	106.0499	19.92	positive
C4H11NO2	Diethanolamine	106.0863	20.91	positive
C8H10	Ethylbenzene	107.0856	5.152	positive
C6H4O2	p-Benzoquinone	109.0284	19.08	positive
C4H5N3O	Cytosine	112.0506	20.22	positive
C5H9N3	Histamine	112.087	29.12	positive
CH5O4P	Hydroxymethylphosphonate	112.9999	17.44	positive
C4H4N2O2	Uracil	113.0346	11.63	positive
C6H8O2	cis-1,2-Dihydrobenzene-1,2-diol	113.0598	8.223	positive

C5H9NO2	L-Proline	116.0704	17.75	positive
C8H7N	Indole	118.0652	14.67	positive
C5H11NO2	valine	118.0862	18.03	positive
C5H11NO2	glycine betaine	118.0863	16.56	positive
C4H9NO3	L-Threonine	120.0655	18.94	positive
C8H9N	Indoline	120.0808	14.4	positive
C3H7NO2S	L-Cysteine	122.0271	17.08	positive
C8H11N	Phenethylamine	122.0966	14.86	positive
C6H5NO2	Niacin/Nicotinate	124.0394	8.266	positive
C2H7NO3S	Taurine	126.0218	18.28	positive
C6H6O3	1,2,3-Trihydroxybenzene	127.039	20.34	positive
C6H9NO2	2,3,4,5-Tetrahydropyridine-2-carboxylate	128.0708	6.455	positive
C5H7NO3	Pyrroline-4-hydroxy-2-carboxylate	130.0499	18.49	positive
C5H7NO3	Pyrroline-4-hydroxy-2-carboxylate	130.05	19.52	positive
C6H11NO2	methylproline3	130.0863	25.43	positive
C5H11N3O	guanidino butanal	130.0974	17.47	positive
C6H10O3	beta-Ketoisocaproate	131.0703	8.223	positive
C5H9NO3	Glutamate 5-semialdehyde	132.0656	18.42	positive
C6H13NO2	L-Leucine	132.1018	14.92	positive
C6H13NO2	L-Leucine	132.1019	15.96	positive
C4H8N2O3	L-Asparagine	133.0608	19.92	positive
C4H7NO4	L-Aspartate	134.0448	19.14	positive
C4H7NO4	L-Aspartate	134.0449	5.472	positive
C5H5N5	Adenine	136.0618	14.66	positive
C5H4N4O	Hypoxanthine	137.0458	11.82	positive
C5H4N4O	Hypoxanthine	137.0459	17.84	positive
C8H8O2	Phenylacetic acid	137.0597	8.049	positive
C10H16	alpha-Pinene	137.1326	5.028	positive
C7H7NO2	4-Aminobenzoate	138.055	17.75	positive
C6H6N2O2	Urocanate	139.0503	15.99	positive

C2H8NO4P	Ethanolamine phosphate	142.0264	21.28	positive
C7H13NO2	Proline Betaine	144.1019	16.58	positive
C8H16O2	Octanoic acid	145.1224	5.964	positive
C6H11NO3	Amino-3-oxohexanoic acid	146.0812	25.45	positive
C5H11N3O2	guanidino butyric acid	146.0923	17.17	positive
C7H16NO2+	acetylcholine 1+	146.1176	17.28	positive
C7H16NO2+	acetylcholine 1+	146.1177	16.27	positive
C5H10N2O3	Glutamine	147.0764	19.48	positive
C6H14N2O2	L-Lysine	147.1129	25.41	positive
C5H9NO4	glutamate	148.0604	18.62	positive
C5H9NO4	N-Acetyl-L-serine	148.0606	5.364	positive
C6H12O4	(R)-Pantoate	149.0806	19.48	positive
C8H7NO2	Indole-5,6-quinone	150.055	14.65	positive
C5H11NO2S	L-Methionine	150.0583	15.82	positive
C6H7N5	Methyladenine	150.0774	17.67	positive
C6H6N4O	Methylhypoxanthine	151.0617	15.82	positive
C5H5N5O	Guanine	152.0567	13.3	positive
C8H9NO2	(Z)-4-Hydroxyphenylacetaldehyde-oxime	152.0706	16.19	positive
C5H4N4O2	Xanthine	153.0407	11.23	positive
C7H11N3O	N-acetylhistamine	154.0974	18.21	positive
C6H9N3O2	L-Histidine	156.0766	24.7	positive
C6H7NO4	2-Aminomuconate	158.0448	9.729	positive
C6H12N3O2+	Guanidine proline+	158.0925	16.48	positive
C4H6N4O3	(S)(+)-Allantoin	159.0513	15.31	positive
C8H17NO2	2-amino octanoic acid 1	160.1332	16.56	positive
C8H17NO2	2-amino octanoic acid 2	160.1332	12.85	positive
C9H7NO2	indole carboxylic acid1	162.055	10.01	positive
C6H11NO4	O-Acetyl-L-homoserine	162.0762	15.9	positive
C7H16NO3	Carnitine	162.1123	18.42	positive
C6H10O3S	Dihydroxy-5-(methylthio)pent-1-en-3-one	163.0423	9.162	positive

C6H10O5	3,3-Dimethylmalate	163.0601	18.29	positive
C6H5N5O	pterin	164.0566	13.09	positive
C5H11NO3S	L-Methionine S-oxide	166.0532	19.44	positive
C9H11NO2	L-Phenylalanine	166.0863	14.38	positive
C5H4N4O3	Urate	169.0356	14.33	positive
C7H11N3O2	1-Methylhistidine	170.0925	24.9	positive
C3H9O6P	Glycerolphosphate	173.0209	18	positive
C10H8NO2	Quinaldic acid	174.0551	14.65	positive
C6H14N4O2	L-Arginine	175.1187	25.47	positive
C6H9NO5	N-Formyl-L-glutamate	176.0554	9.753	positive
$C_7H_{13}NO_4$	Spermidic acid	176.0918	15.85	positive
C6H13N3O3	L-Citrulline	176.1029	20.19	positive
C6H5N5O2	Isoxanthopterin	180.0517	13.16	positive
C6H13NO5	D-Galactosamine	180.0867	20.39	positive
C6H7N5O2	Dihydroxanthopterin	182.0673	13.25	positive
C9H11NO3	L-Tyrosine	182.0811	16.61	positive
C5H15NO4P+	Choline phosphate+	184.0734	24.33	positive
C8H14N2O3	Ala-Pro	187.1078	19.08	positive
C9H21N3O	N-acetylspermidine	188.1758	28.15	positive
C8H16N2O3	N6-Acetyl-L-lysine	189.1233	15.62	positive
C9H20N2O2	7,8-Diaminononanoate	189.1597	25.89	positive
C10H7NO3	Kynurenic acid	190.0499	8.743	positive
C7H11NO5	N-Acetyl-L-glutamate	190.0711	8.793	positive
C7H14N2O4	meso-2,6-Diaminoheptanedioate	191.1027	19.15	positive
C10H9NO3	5-Hydroxyindoleacetate	192.0656	14.73	positive
C9H11NO4	DOPA	198.0761	18.94	positive
C12H25NO	Dodecanamide	200.201	5.401	positive
C12H25NO	Dodecanamide	200.201	12.9	positive
C9H17NO4	O-Acetylcarnitine	204.1227	15.43	positive
C11H12N2O2	L-Tryptophan	205.0973	15.07	positive

C8H16N2O4	Val Ser	205.1183	19.04	positive
C8H16N2O4	Val Ser	205.1184	23.99	positive
C10H7NO4	Xanthurenic acid	206.0447	10.18	positive
C10H12N2O3	L-Kynurenine	209.0921	14.73	positive
C10H11NO4	4-Hydroxyphenylacetylglycine	210.0761	17.11	positive
C13H10O3	Dihydroxyfluorene-9-one	215.0696	18.7	positive
C2H8NO4P	phosphoethanolamine	216.0633	19.44	positive
C9H16N2O4	gamma-Glutamyl-gamma-aminobutyraldehyde	217.1185	8.269	positive
C8H16N4O3	Acetylarginine	217.1295	18.62	positive
C10H19NO4	Propionyl carnitine	218.1388	14.43	positive
C9H17NO5	Pantothenate	220.1177	8.169	positive
C9H17NO5	Pantothenate	220.1181	6.523	positive
C11H12N2O3	5-Hydroxy-L-tryptophan	221.0921	14.63	positive
C8H15NO6	Pyrimidodiazopterin	222.0985	12.09	positive
C7H14N2O4S	L-Cystathionine	223.0747	23.35	positive
C10H12N2O4	3-Hydroxy-L-kynurenine	225.087	16.2	positive
C13H20O3	Methyl jasmonate	225.1487	5.266	positive
C14H29NO	Myristamide	228.2322	5.372	positive
C11H20N2O3	Leu-Pro	229.1547	16.56	positive
C11H20N2O3	Leu-Pro	229.1547	15.19	positive
C11H20N2O3	Leu-Pro	229.1548	14.14	positive
C14H31NO	Dodecyldimethylamine oxide	230.2479	11.62	positive
C11H21NO4	Butyrylcarnitine	232.1544	13.72	positive
C10H22N2O4	1,1,3-tris(ethoxymethyl)urea	235.1653	17.98	positive
C9H9N5O3	dehydrosepiapterin	236.0777	10.75	positive
C11H12N2O4	N-Formylkynurenine	237.087	14.86	positive
C9H11N5O3	Biopterin1	238.0936	14.33	positive
C9H11N5O3	Biopterin2	238.0936	11.21	positive
C9H13N5O3	Dihydrobiopterin	240.1091	15.21	positive
C12H20N2O3	Pirbuterol	241.1547	16.69	positive

C6H11O8P	Inositol cyclic phosphate	243.0265	19.14	positive
C6H11O8P	Inositol cyclic phosphate	243.0265	20.32	positive
C9H13N3O5	Cytidine	244.0929	20.28	positive
C9H12N2O6	Uridine	245.0769	11.63	positive
C10 H20O3 N4	Ethyl-Acetyl-Arginine	245.1609	16.45	positive
C14H31NO2	N,N-bis(butoxymethyl)-2-methylpropan-2-amine	246.2429	12.64	positive
C6H15N4O5P	phosphoarginine	255.0854	23.7	positive
C11H14N2O5	glycyl-dopa	255.0977	19.86	positive
C16H33NO	palmitamide	256.2632	5.315	positive
$C_8H_{20}NO_6P$	GPC	258.1098	21.35	positive
C6H14NO8P	D-Glucosamine 6-phosphate	260.0531	19.17	positive
C6H13O9P	Glucose phosphate	261.0371	19.22	positive
C6H13O9P	Fructose phosphate	261.0371	20.29	positive
C11H20N2O5	Glutamyl-leucine	261.1445	14.35	positive
$C_9H_{12}NO_6P$	Tyrosine phosphate	262.0475	20.68	positive
C12H17N4OS+	thiamine(+) 2	265.1116	28.17	positive
C10H13N5O4	Adenosine	268.104	14.59	positive
C10H13N5O4	Deoxyguanosine	268.1041	13.59	positive
C10H12N4O5	Inosine	269.0881	12.85	positive
C15H12O5	narigenin	273.0752	18.45	positive
$C_{10}H_{17}N_3O_6$	Glu-gln	276.1189	19.3	positive
C18H28O2	Stearidonic acid	277.2161	5.057	positive
C18H30O2	(9Z,12Z,15Z)-Octadecatrienoic acid	279.2322	5.031	positive
C11H15N5O4	Methyl adenosine	282.1198	18.88	positive
C18H35NO	Oleamide	282.2794	5.286	positive
C10H13N5O5	Guanosine1	284.099	14.91	positive
C10H13N5O5	Guanosine2	284.099	15.93	positive
C17H37NO2	C17 sphinganine	288.2897	11.83	positive
C18H30O3	17-Hydroxylinolenic acid	295.2271	5.031	positive
C11H15N5O3S	5'-Methylthioadenosine	298.0967	11.92	positive

C18H37NO2	Dehydrosphinganine(Sphingosine)	300.2893	11.93	positive
C10H17N3O6S	GSH	308.0908	17.55	positive
C12H24N2O7	Fructosyllysine	309.1657	25.4	positive
C12H18N6O4	2-aminodimethyladenosine	311.1465	24.85	positive
C16H29NO5	Butoctamide semisuccinate	316.2113	12.99	positive
C16H29NO5	Butoctamide semisuccinate	316.2119	14.01	positive
C19 H43 O2 N	C19 sphinganine	316.3209	11.65	positive
C9H14N3O8P	cytidine monophosphate	324.0593	21.01	positive
C9H13N2O9P	uridine monophosphate	325.0434	17.15	positive
C12H20O10	Difructose anhydride isomer	325.113	17.71	positive
C12H20O10	Difructose anhydride isomer	325.1131	19.22	positive
C10H12N5O6P	c AMP	330.0602	16.34	positive
C11H15N2O8P	Nicotinamide D-ribonucleotide	335.0638	20	positive
C10H15N4O7P	2'-Deoxyinosine 5'-phosphate	335.0738	19.09	positive
C9H14N5O7P	Dihydroneopterin phosphate	336.0695	19.9	positive
C18 H29O3 N3	Histidine lipid	336.2282	12.48	positive
C11H19N3O7S	S-(Hydroxymethyl)glutathione	338.1016	18.08	positive
C18 H29 O3 N3	Hisitidine lipid	338.2437	12.38	positive
$C_{22}H_{44}ON$	Dodecamide	338.3414	5.152	positive
C12H22O11	Sucrose	343.1234	18.3	positive
C10H13O7N5P	cGMP	346.0547	16.2	positive
C10H14N5O7P	AMP isomer 2	348.0703	20.14	positive
C10H14N5O7P	AMP isomer 2	348.0703	19.11	positive
C10H13N4O8P	IMP	349.0544	17.9	positive
C19H34O5N	C19H34O5N	356.2432	5.434	positive
C18H37N4O3	C18H37N4O3	358.2952	6.526	positive
C20 H31 O3 N3	guanidinosphingolipid	362.2434	12.29	positive
C10H14N5O8P	GMP	364.0654	19.66	positive
C20 H33 O3 N3	C20-guanidino phytosphingolipid	364.2586	12.13	positive
C15H16N10O2	drosopterin	369.1531	20.4	positive

C17H20N4O6	Riboflavin	377.1455	10.42	positive
C12H21PN5O7	C12H20PN5O7	378.1159	19.71	positive
C14H17N5O8	Succinyladenosine	384.1151	11.89	positive
C28H42O	Ergosta-5,7,22,24(28)-tetraen-3beta-ol	395.3311	5.697	positive
C23H45NO4	L-Palmitoylcarnitine	400.3422	11.6	positive
C20H13N3O8	Xanthomattin	424.0776	14.57	positive
C25H45NO4	Linolenylcarnitine	424.342	11.59	positive
C25H47NO4	Linolylcarnitine	426.3575	11.56	positive
C13H22N4O8S2	S-Glutathionyl-L-cysteine	427.0951	22.68	positive
C10H15N5O10P2	ADP	428.0368	24.42	positive
C25H49NO4	Oleoylcarnitine	428.3733	11.47	positive
C11H20N4O11P2	CDP-ethanolamine	447.0678	22.04	positive
C14H18N5O11P	N6-(1,2-Dicarboxyethyl)-AMP	464.0813	17.1	positive
$C_{21}H_{41}O_7P$	DHAP(18:0)	478.2923	10.85	positive
C18H32O16	Raffinose	505.1765	18.32	positive
C17H27N3O17P2	UDP-N-acetyl-D-glucosamine	608.0888	20.95	positive
C21H28N7O14P2+	NAD+	664.1163	20.58	positive
C24H42O21	Stachyose	667.229	18.32	positive
$C_{37}H_{72}NO_8P$	PE(18:0/14:1(9Z))	690.5064	9.469	positive
$C_{37}H_{72}NO_8P$	PE(18:0/14:1(9Z))	690.5067	6.503	positive
$C_{40}H_{75}O_{10}P$	PG(16:0/18:2(9Z,12Z))	747.5167	8.266	positive
C30H52O26	Cellopentaose	829.2809	20.43	positive
$C_3H_4O_3$	pyruvic acid	87.00881	7.547	Negative
$C_3H_6O_3$	Lactic acid	89.02444	7.774	Negative
$C_3H_6O_3$	beta lactic acid	89.02446	6.755	Negative
C3 H6 O4	Glycolic acid	105.0194	7.285	Negative
$C_4H_4O_4$	Fumaric acid	115.0038	7.513	Negative
$C_4H_6O_4$	Succinic acid	117.0193	8.096	Negative
$C_4H_8O_4$	Erythrose	119.0351	16.72	Negative
$C_5H_6O_4$	Glutaconic acid	129.0194	12	Negative

C_5H8O_4	pentanedioic acid	131.0351	6.239	Negative
$C_4H_7NO_4$	2-aminobutanedioic acid	132.0303	19.04	Negative
$C_4H_6O_5$	malic acid	133.0143	10.62	Negative
$C_5H_{10}O_4$	Deoxyribose	133.0507	8.16	Negative
$C_4H_8O_5$	Erythronic acid	135.03	6.829	Negative
$C_5H_6O_5$	Oxoglutaric acid	145.0143	8.493	Negative
C6 H10O4	Adipic acid	145.0507	6.359	Negative
$C_5H_8O_5$	Citramalic acid	147.0299	9.055	Negative
$C_6H_{12}O_4$	Mevalonic acid	147.0663	8.158	Negative
$C_5H_{10}O_5$	pentose	149.0457	12.47	Negative
$C_8H_8O_3$	3,4-Dihydroxyphenylacetaldehyde	151.0401	5.445	Negative
$C_5H_{12}O_5$	D-Xylitol	151.0613	15.15	Negative
$C_7H_{12}N_2O_3$	Glycylproline	153.067	6.378	Negative
$C_5H_4N_2O_4$	Orotic acid	155.01	12.4	Negative
$C_7H_{11}NO_3$	Tiglylglycine	156.0667	24.82	Negative
$C_5H_4O_3$	Furoic acid	157.0143	9.632	Negative
$C_6H_8O_5$	Oxoadipic acid	159.03	11.92	Negative
$C_8H_{16}O_3$	(R)-2-Hydroxycaprylic acid	159.1027	5.557	Negative
$C_5H_6O_6$	Hydroxyoxoglutaric acid	161.0092	6.415	Negative
$C_5H_{10}O_6$	Arabinonic acid	165.0406	15.56	Negative
$C_9H_{10}O_3$	Homovanillin	165.0558	5.774	Negative
$C_8H_8O_4$	3,4-Dihydroxymandelaldehyde	167.035	5.686	Negative
$C_3H_6O_6P$	Glyceraldehyde phosphate	168.991	17.8	negative
$C_3H_9O_6P$	Glycerol 3-phosphate	171.0064	17.81	Negative
$C_6H_6O_6$	-Aconitic acid	173.00925	10.166	Negative
$C_6H_8O_6$	Ascorbic acid	175.0248	9.632	Negative
$C_6H_{10}O_6$	3-Keto-b-D-galactose	177.04051	11.915	Negative
$C_6H_{12}O_6$	hexose	179.05612	16.717	Negative
$C_6H_{12}N_2O_3$	D-Alanyl-D-alanine	181.06035	16.717	Negative
C6H14O6	hexitol	181.07184	15.92	Negative

$C_4H_9NO_5S$	Homocysteic acid	182.01288	9.449	Negative
$C_7H_8O_6$	cis-2-Methylaconitate	187.02487	8.392	Negative
$C_6H_8O_7$	Isocitric acid	191.01979	12.073	Negative
$C_7H_{12}O_6$	Quinic acid	191.05626	13.916	Negative
C6H12O7	Gluconic acid	195.05104	16.507	Negative
$C_{10}H_{11}NO$	Tryptophanol	196.05437	16.378	Negative
$C_8H_{15}N_3O_4$	N-a-Acetylcitrulline	198.08852	18.437	Negative
$C_8H_{16}N_2O_5$	N-Acetyl-b-glucosaminylamine	201.08812	9.219	Negative
$C_8H_7NO_4$	2-Methyl-3-hydroxy-5-formylpyridine-4-carboxylate	202.01241	19.827	Negative
$C_7H_{10}O_7$	Homocitric acid	205.03539	10.442	Negative
C13 H20 O2	4-heptoxyphenol	207.13905	5.244	Negative
$C_6H_{13}NO_5$	Fructosamine	214.04868	19.37	Negative
$C_4H_{11}O_3PS$	Diethylthiophosphate	215.01419	11.972	Negative
C5 H13 O7 P	2-C-methyl-D-erythritol 4-phosphate	215.03276	16.147	Negative
$C_5H_{14}NO_6P$	Glycerylphosphorylethanolamine	215.05588	8.008	Negative
$C_9H_9NO_4$	3-Hydroxyhippuric acid	216.02798	19.049	Negative
$C_3H_9O_6P$	Glycerol 3-phosphate	217.01196	17.828	Negative
$C_{10}H_{12}O_4$	Homoveratric acid	217.04832	15.969	Negative
$C_6H_{10}N_3O_4P$	4-Amino-2-methyl-5-phosphomethylpyrimidine	218.03294	16.147	Negative
$C_9H_{17}NO_5$	Pantothenic acid	218.10339	8.135	Negative
$C_9H_{11}N_5O_2$	2'-Deoxysepiapterin	220.08405	10.98	Negative
$C_{11}H_{13}NO_3$	N-Acetyl-L-phenylalanine	228.06442	23.292	Negative
$C_3H_8NO_8P$	Glycero Phosphoserine	230.00722	19.04	Negative
$C_4H_{10}NO_8P$	Glycero Phosphothreonine	244.0229	18.604	Negative
$C_{15}H_{22}O_3$	2-Ethylhexyl 4-hydroxybenzoate	249.14967	5.123	Negative
$C_{10}H_{14}N_2O_6$	3-Methyluridine	257.07813	7.862	Negative
$C_{15}H_{14}O_6$	Epicatechin	271.06067	18.41	Negative
$C_{12}H_{15}NO_5$	Acetylvanilalanine	274.06995	23.288	Negative
$C_{16}H_{22}O_4$	Alpha-CEHC	277.14453	4.688	Negative
$C_7H_{15}O_{10}P$	Sedoheptulose 7-phosphate	289.03314	19.235	Negative

$C_{17}H_{26}O_4$	Gingerol	293.1759	5.266	Negative
$C_{10}H_{16}NO_3PS$	Aminoparathion	306.05798	11.504	Negative
$C_9H_{19}O_{11}P$	1-(sn-Glycero-3-phospho)-1D-myo-inositol	333.05933	18.967	Negative
$C_{11}H_{16}N_2O_8$	N-Acetylaspartylglutamic acid	349.08893	9.445	Negative
$C_{15}H_{20}O_{10}$	3-Methoxy-4-hydroxyphenylglycol glucuronide	359.09836	8.14	Negative
$C_{12}H_{23}NO_{10}$	Lactosamine	376.1015	19.595	Negative
$C_{18}H_{38}NO_5P$	Sphingosine 1-phosphate	424.24701	11.056	Negative
$C_{20}H_{30}O_5$	15-Keto-prostaglandin E2	387.15781	8.115	Negative
$C_{21}H_{18}O_8$	7-Deoxyadriamycinone	397.09323	16.154	Negative
$C_{23}H_{37}NO_5$	Columbiananin	406.25998	5.311	Negative
$C_{22}H_{37}NO_3$	Leukotriene B4 dimethylamide	408.27533	5.255	Negative
$C_{28}H_{42}O_2$	(R)-gamma-Tocotrienol	409.31128	5.023	Negative
$C_{23}H_{43}NO_6$	Hexadecanedioic acid mono-L-carnitine ester	410.2908	5.216	Negative
$C_{30}H_{44}O_2$	Demethylphylloquinone	436.33414	3.995	Negative
$C_{21}H_{42}NO_7P$	LysoPE(16:1(9Z)/0:0)	450.26251	10.86	Negative
$C_{21}H_{44}NO_7P$	LysoPE(16:0/0:0)	452.27805	10.946	Negative
$C_{22}H_{44}NO_7P$	LysoPC(14:1(9Z))	464.27829	10.82	Negative
$C_{23}H_{42}NO_7P$	LysoPE(18:3(9Z,12Z,15Z)/0:0)	474.26263	10.86	Negative
$C_{23}H_{46}NO_7P$	LysoPE(18:1(9Z)/0:0)	478.29315	10.724	Negative
$C_{26}H_{22}Cl_2N_2O_3$	Doconazole	479.09366	18.953	Negative
$C_{29}H_{42}O_4$	Ubiquinone Q4	489.2774	3.742	Negative
$C_{12}H_{23}NO_4$	Isovalerylcarnitine	489.31845	13.843	Negative
$C_{18}H_{32}O_{16}$	trihexose	503.16193	19.143	Negative
c ADP	$C_{15}H_{21}N_5O_{13}P_2$	540.05359	20.522	Negative
$C_{36}H_{71}NO_3$	Ceramide (d18:1/18:0)	600.51221	5.124	Negative
$C_{30}H_{60}NO_6P$	CerP(d18:1/12:0)	606.41406	9.572	Negative
$C_{20}H_{32}N_6O_{12}S_2$	Oxidized glutathione	611.14362	21.851	Negative
$C_{33}H_{66}NO_8P$	PE(14:0/14:0)	634.44574	9.228	Negative
$C_{24}H_{42}O_{21}$	tetrahexose	665.21472	19.558	Negative
C43 H44O19	pentahexose	863.2428	20.56	Negative

C31 H50 O19 N7 P3 S	3-Isopropenylpimelyl-CoA	948.20209	19.01	Negative
$C_{43}H_{83}O_{13}P$	PI(16:0/18:0)	859.53168	8.212	Negative
$C_{41}H_{75}O_{13}P$	PI(16:2(9Z,12Z)/16:0)	805.48651	8.252	Negative
$C_{42}H_{70}NO_{10}P$	PS(22:6(4Z,7Z,10Z,13Z,16Z,19Z)/14:0)	778.46576	8.324	Negative
$C_{42}H_{74}NO_{10}P$	PS(20:4(5Z,8Z,11Z,14Z)/16:0)	782.49701	8.324	Negative
$C_{45}H_{76}NO_8P$	PE(22:6(4Z,7Z,10Z,13Z,16Z,19Z)/18:1(9Z))	788.52441	5.564	Negative
$C_{45}H_{78}NO_8P$	PE(22:6(4Z,7Z,10Z,13Z,16Z,19Z)/18:0)	790.53967	5.557	Negative
$C_{45}H_{76}NO_7P$	PE(22:6(4Z,7Z,10Z,13Z,16Z,19Z)/P-18:1(9Z))	808.5061	8.272	Negative
$C_{14}H_{25}NO_{11}$	N-Acetyllactosamine	811.284	19.439	Negative
$C_{44}H_{78}NO_8P$	PC(18:4(6Z,9Z,12Z,15Z)/18:1(9Z))	824.54431	11.238	Negative
$C_{43}H_{81}O_{13}P$	PI(18:1(9Z)/16:0)	857.51697	8.212	Negative
$C_{43}H_{82}O_{16}P_2$	PIP(18:1(9Z)/16:0)	897.48956	10.044	Negative
$C_{45}H_{82}O_{16}P_2$	PIP(18:3(6Z,9Z,12Z)/18:0)	921.48926	9.83	Negative
$C_{47}H_{83}O_{13}P$	PI(22:4(10Z,13Z,16Z,19Z)/16:0)	923.50531	10.061	Negative

Chapter 9 Index

R

S

T

U

W

X

Chapter 10 Publications

10.1 Papaers

10.1.1 Paper 1

Kamleh, M. A., **Hobani, Y**., Dow, J. A. and Watson, D. G. (2008). Metabolomic profiling of *Drosophila* using liquid chromatography Fourier transform mass spectrometry. *FEBS Lett* 582, 2916-22.

10.1.2 Paper 2

Kamleh, M. A., **Hobani, Y**., Dow, J. A., Zheng, L. and Watson, D. G. (2009). Towards a platform for the metabonomic profiling of different strains of *Drosophila melanogaster* using liquid chromatography-Fourier transform mass spectrometry. *Febs J* 276, 6798-809.

10.1.3 Paper 3

Bratty, M. A., **Hobani, Y**., Dow, J. A. T. and Watson, D. G. (2011) Metabolomic profiling of the effects of allopurinol on *Drosophila melanogaster*. *Metabolomics*, 1-7

10.2 Posters

10.2.1 Poster 1

Hobani, Y. H., Kamleh, A., Watson, D. G. and Dow, J. A. (2009). Taking a *rosy* look at the *Drosophila* metabolome by mass spectrometry. *Comparative Biochemistry and Physiology-Part A: Molecular & Integrative Physiology* 153, S83-S83.

10.2.2 Poster 2

Hobani, Y., Kamleh, A., Watson, D. and Dow, J. (2008). Mapping the *Drosophila* metabolome using liquid chromatography Fourier transform mass spectrometry. *Comparative Biochemistry and Physiology-Part A: Molecular & Integrative Physiology* 150, S135-S136.

Chapter 11 References

Adams MD, C. S., Holt RA, Evans CA, Gocayne JD, Amanatides PG, Scherer SE, Li PW, Hoskins RA, Galle RF, George RA, Lewis SE, Richards S, Ashburner M, Henderson SN, Sutton GG, Wortman JR, Yandell MD, Zhang Q, Chen LX,Brandon RC, Rogers YH, Blazej RG, Champe M, Pfeiffer BD, Wan KH, Doyle C, Baxter EG, Helt G, Nelson CR, Gabor GL, Abril JF, Agbayani A, An HJ, Andrews-Pfannkoch C, Baldwin D, Ballew RM, Basu A, Baxendale J, Bayraktaroglu L, Beasley EM,Beeson KY, Benos PV, Berman BP, Bhandari D, Bolshakov S, Borkova D, Botchan MR, Bouck J, Brokstein P, Brottier P, Burtis KC, Busam DA, Butler H, Cadieu E, Center A, Chandra I, Cherry JM, Cawley S, Dahlke C, Davenport LB, Davies P, de Pablos B, Delcher A, Deng Z, Mays AD, Dew I, Dietz SM, Dodson K, Doup LE, Downes M, Dugan-Rocha S, Dunkov BC, Dunn P, Durbin KJ, Evangelista CC, Ferraz C, Ferriera S, Fleischmann W, Fosler C, Gabrielian AE, Garg NS, Gelbart WM,Glasser K, Glodek A, Gong F, Gorrell JH, Gu Z, Guan P, Harris M, Harris NL, Harvey D, Heiman TJ, Hernandez JR, Houck J, Hostin D, Houston KA, Howland TJ, Wei MH, Ibegwam C, Jalali M, Kalush F, Karpen GH, Ke Z, Kennison JA, Ketchum KA,Kimmel BE, Kodira CD, Kraft C, Kravitz S, Kulp D, Lai Z, Lasko P, Lei Y, Levitsky AA, Li J, Li Z, Liang Y, Lin X, Liu X, Mattei B, McIntosh TC, McLeod MP, McPherson D, Merkulov G, Milshina NV, Mobarry C, Morris J, Moshrefi A, Mount SM, Moy M, Murphy B, Murphy L, Muzny DM, Nelson DL, Nelson DR, Nelson KA, Nixon K, Nusskern DR, Pacleb JM, Palazzolo M, Pittman GS, Pan S, Pollard J, Puri V, Reese MG, Reinert K, Remington K, Saunders RD, Scheeler F, Shen H, Shue BC, Sidén-Kiamos I,Simpson M, Skupski MP, Smith T, Spier E, Spradling AC, Stapleton M, Strong R, Sun E, Svirskas R, Tector C, Turner R, Venter E, Wang AH, Wang X, Wang ZY, Wassarman DA, Weinstock GM, Weissenbach J, Williams SM, WoodageT, Worley KC,Wu D, Yang S, Yao QA, Ye J, Yeh RF, Zaveri JS, Zhan M, Zhang G, Zhao Q, Zheng L, Zheng XH, Zhong FN, Zhong W, Zhou X, Zhu S, Zhu X, Smith HO, Gibbs RA, Myers EW, Rubin GM, Venter JC. (2000). The genome sequence of *Drosophila melanogaster. Science* **287**, 2185.

Ainsworth, C., Wan, S. and Skaer, H. (2000). Coordinating cell fate and morphogenesis in *Drosophila* renal tubules. *Philos Trans R Soc Lond B Biol Sci* **355**, 931-7.

Akbari, O. S., Oliver, D., Eyer, K. and Pai, C. Y. (2009). An Entry/Gateway cloning system for general expression of genes with molecular tags in *Drosophila melanogastre*. *BMC Cell Biol* **10**, 8.

Al-Gazali, L., Hamamy, H. and Al-Arrayad, S. (2006). Genetic disorders in the Arab world. *British Med J* **333**, 831-4.

Al-Odaib, A. N., Abu-Amero, K. K., Ozand, P. T. and Al-Hellani, A. M. (2003). A new era for preventive genetic programs in the Arabian Peninsula. *Saudi Med J* **24**, 1168-75.

Alpert, A. J. (1990). Hydrophilic-interaction chromatography for the separation of peptides, nucleic acids and other polar compounds. *J Chromatogr* **499**, 177-96.

Ames, B. N., Cathcart, R., Schwiers, E. and Hochstein, P. (1981). Uric acid provides an antioxidant defense in humans against oxidant- and radical-caused aging and cancer: a hypothesis. *Proc Natl Acad Sci U S A* **78**, 6858-62.

Appelblad, P., Jonsson, T., Pontén, E., Viklund, C. and Jiang, W. (2008). A Practical Guide to HILIC., vol. 5 th issue (ed. T. Jonsson). Sweden: Merck SeQuant AB, Box 7956, 907 19 Umeå, Sweden. .

Ashburner, M. (1989). *Drosophila*: a laboratory manual: Cold Spring Harbour Laboratory Press.

Ashburner, M. (1990). Puffs, genes and hormones revisited. *Cell* **61**, 1-3.

Bach, G., Tomczak, J., Risch, N. and Ekstein, J. (2001). Tay Sachs screening in the Jewish Ashkenazi population: DNA testing is the preferred procedure. *American Journal of Medical Genetics* **99**, 70-75.

Baker, B. S. (1973). The maternal and zygotic control of development by cinnamon, a new mutant in *Drosophila melanogastre*. *Developmental Biology* **33**, 429-40.

Bateman, K. P., Kellmann, M., Muenster, H., Papp, R. and Taylor, L. (2009). Quantitative-qualitative data acquisition using a benchtop Orbitrap mass spectrometer. *J Am Soc Mass Spectrom* **20**, 1441-50.

Bennett, W. M. (2009). Autosomal dominant polycystic kidney disease: 2009 update for internists. *Korean J Intern Med* **24**, 165-8.

Berg, P. and Lehman, I. R. (2007). Retrospective: Arthur Kornberg (1918-2007). *Science* **318**, 1564.

Berry, C. E. and Hare, J. M. (2004). Xanthine oxidoreductase and cardiovascular disease: molecular mechanisms and pathophysiological implications. *J Physiol* **555**, 589-606.

Bier, E. (2005). *Drosophila*, the golden bug, emerges as a tool for human genetics. *Nat Rev Genet* **6**, 9-23.

Boy, A. L., Zhai, Z., Habring-Muller, A., Kussler-Schneider, Y., Kaspar, P. and Lohmann, I. (2010). Vectors for efficient and high-throughput construction of fluorescent *Drosophila* reporters using the PhiC31 site-specific integration system. *Genesis* **48**, 452-6.

Brand, A. H. and Perrimon, N. (1993). Targeted gene expression as a means of altering cell fates and generating dominant phenotypes. *Development* **118**, 401-15.

Breitling, R., Pitt, A. R. and Barrett, M. P. (2006). Precision mapping of the metabolome. *Trends Biotechnol* **24**, 543-8.

Brindle, J. T., Antti, H., Holmes, E., Tranter, G., Nicholson, J. K., Bethell, H. W. L., Clarke, S., Schofield, P. M., McKilligin, E. and Mosedale, D. E. (2002). Rapid and noninvasive diagnosis of the presence and severity of coronary heart disease using 1H-NMR-based metabonomics. *Nature Medicine* **8**, 1439-1445.

Cabrero, P., Pollock, V. P., Davies, S. A. and Dow, J. A. (2004). A conserved domain of alkaline phosphatase expression in the Malpighian tubules of dipteran insects. *J Exp Biol* **207**, 3299-305.

Chace, D. H., Kalas, T. A. and Naylor, E. W. (2003). Use of tandem mass spectrometry for multianalyte screening of dried blood specimens from newborns. *Clin Chem* **49**, 1797-817.

Chapman, R. F. and Chapman, R. F. (1998). The insects: structure and function: Cambridge Univ Pr.

Chintapalli, V. R., Wang, J. and Dow, J. A. (2007). Using FlyAtlas to identify better *Drosophila melanogastre* models of human disease. *Nat Genet* **39**, 715-20.

Chung, H. Y., Baek, B. S., Song, S. H., Kim, M. S., Huh, J. I., Shim, K. H., Kim, K. W. and Lee, K. H. (1997). Xanthine dehydrogenase/xanthine oxidase and oxidative stress. *Age* **20**, 127-140.

Collins, F. S. and Mansoura, M. K. (2001). The human genome project. *Cancer* **91**, 221-225.

Collins, J. F., Duke, E. J. and Glassman, E. (1970). Nutritional control of xanthine dehydrogenase. I. The effect in adult *Drosophila melanogastre* of feeding a high protein diet to larvae. *Biochimica et biophysica acta* **208**, 294.

Consortium, G. P. (2010). A map of human genome variation from population-scale sequencing. *Nature* **467**, 1061-73.

Courtright, J. B. (1967). Polygenic control of aldehyde oxidase in *Drosophila*. *Genetics* **57**, 25-39.

Daviss, B. (2005). Growing pains for metabolomics. *The Scientist* **19**, 25-28.

Dent, C. E. and Philpot, G. R. (1954). Xanthinuria, an inborn error (or deviation) of metabolism. *Lancet* **266**, 182-5.

Dettmer, K., Aronov, P. A. and Hammock, B. D. (2007). Mass spectrometry-based metabolomics. *Mass Spectrom Rev* **26**, 51-78.

Dettmer, K. and Hammock, B. D. (2004). Metabolomics--a new exciting field within the" omics" sciences. *Environmental Health Perspectives* **112**, A396.

Dietzl, G., Chen, D., Schnorrer, F., Su, K. C., Barinova, Y., Fellner, M., Gasser, B., Kinsey, K., Oppel, S., Scheiblauer, S. et al. (2007). A genome-wide transgenic RNAi library for conditional gene inactivation in *Drosophila*. *Nature* **448**, 151-6.

Dow, J. A. (2007). Model organisms and molecular genetics for endocrinology. *Gen Comp Endocrinol* **153**, 3-12.

Dow, J. A., Maddrell, S. H., Gortz, A., Skaer, N. J., Brogan, S. and Kaiser, K. (1994). The Malpighian tubules of *Drosophila melanogastre*: a novel phenotype for studies of fluid secretion and its control. *J Exp Biol* **197**, 421-8.

Dow, J. T. and Davies, S. A. (2003). Integrative physiology and functional genomics of epithelial function in a genetic model organism. *Physiol Rev* **83**, 687-729.

El Mouzan, M. I., Al Salloum, A. A., Al Herbish, A. S., Qurachi, M. M. and Al Omar, A. A. (2008). Consanguinity and major genetic disorders in Saudi children: A community-based cross-sectional study. *Annals of Saudi Medicine* **28**, 169-173.

Ellaway, C. J., Wilcken, B. and Christodoulou, J. (2002). Clinical approach to inborn errors of metabolism presenting in the newborn period. *J Paediatr Child Health* **38**, 511-7.

Evans, B. A. and Howells, A. J. (1978). Control of drosopterin synthesis in *Drosophila melanogastre*: mutants showing an altered pattern of GTP cyclohydrolase activity during development. *Biochemical Genetics* **16**, 13-26.

Fiehn, O., Kloska, S. and Altmann, T. (2001). Integrated studies on plant biology using multiparallel techniques. *Current Opinion in Biotechnology* **12**, 82-86.

Fire, A., Xu, S., Montgomery, M. K., Kostas, S. A., Driver, S. E. and Mello, C. C. (1998). Potent and specific genetic interference by double-stranded RNA in Caenorhabditis elegans. *Nature* **391**, 806-11.

Fodor, S. P., Read, J. L., Pirrung, M. C., Stryer, L., Lu, A. T. and Solas, D. (1991). Light-directed, spatially addressable parallel chemical synthesis. *Science* **251**, 767.

Forrest, H. S., Glassman, E. and Mitchell, H. K. (1956). Conversion of 2-amino-4-hydroxypteridine to isoxanthopterin in *D. Melanogaster*. *Science* **124**, 725-6.

Forrest, H. S., Hanly, E. W. and Lagowski, J. M. (1961). Biochemical differences between the mutants *Rosy*-2 and *maroon-like* of *Drosophila melanogaster*. *Genetics* **46**, 1455-63.

Franco, R., Li, S., Rodriguez-Rocha, H., Burns, M. and Panayiotidis, M. I. (2010). Molecular mechanisms of pesticide-induced neurotoxicity: Relevance to Parkinson's disease. *Chem Biol Interact* **188**, 289-300.

Friedman, T. B. (1973). Observations on the regulation of uricase activity during development of *Drosophila melanogaster*. *Biochem Genet* **8**, 37-45.

Friedman, T. B. and Johnson, D. H. (1977). Temporal control of urate oxidase activity in *Drosophila*: evidence of an autonomous timer in Malpighian tubules. *Science* **197**, 477-9.

Garattini, E., Fratelli, M. and Terao, M. (2008). Mammalian aldehyde oxidases: genetics, evolution and biochemistry. *Cell Mol Life Sci* **65**, 1019-48.

Gates, P. (2004). Electrospray Ionisation (ESI). Last updated 20th January 2004: The University of Bristol, School of Chemistry. http://www.chm.bris.ac.uk/ms/theory/esi-ionisation.html.

Ghneim, H. (2010). IEMs in Saudi Arabia compared to Europe and USA. *Personal communications.*

Glassman, E. and Mitchell, H. K. (1959). Mutants of *Drosophila Melanogaster* deficient in xanthine dehydrogenase. *Genetics* **44**, 153-62.

Goh, K. I., Cusick, M. E., Valle, D., Childs, B., Vidal, M. and Barabasi, A. L. (2007). The human disease network. *Proc Natl Acad Sci U S A* **104**, 8685-90.

Gok, F., Ichida, K. and Topaloglu, R. (2003). Mutational analysis of the xanthine dehydrogenase gene in a Turkish family with autosomal recessive classical xanthinuria. *Nephrol Dial Transplant* **18**, 2278-83.

Guo, Y. (1996). Cloning, characterization and site-selected mutagenesis of genes encoding V-ATPase in *Drosophila*. PhD thesis, Glasgow University.

Hadorn, E. and Schwinck, I. (1956). A Mutant of *Drosophila* without Isoxanthopterine which is Non-Autonomous for the Red Eye Pigments. *Nature* **177**, 940 - 941.

Harrison, R. (2002). Structure and function of xanthine oxidoreductase: where are we now? *Free Radic Biol Med* **33**, 774-97.

Harrison, R. (2004). Physiological roles of xanthine oxidoreductase. *Drug Metab Rev* **36**, 363-75.

Hazelrigg, T., Levis, R. and Rubin, G. M. (1984). Transformation of white locus DNA in *Drosophila*: dosage compensation, zeste interaction, and position effects. *Cell* **36**, 469-481.

Hilliker, A. J., Duyf, B., Evans, D. and Phillips, J. P. (1992). Urate-null *rosy* mutants of *Drosophila melanogastre* are hypersensitive to oxygen stress. *Proc Natl Acad Sci U S A* **89**, 4343-7.

Horning, E. C. and Horning, M. G. (1971). Metabolic profiles: gas-phase methods for analysis of metabolites. *Clinical chemistry* **17**, 802.

Houten, S. M. (2009). Metabolomics: Unraveling the chemical individuality of common human diseases. *Ann Med*, 1-6.

Hu, Q., Noll, R. J., Li, H., Makarov, A., Hardman, M. and Graham Cooks, R. (2005). The Orbitrap: a new mass spectrometer. *J Mass Spectrom* **40**, 430-43.

Ichida, K., Matsumura, T., Sakuma, R., Hosoya, T. and Nishino, T. (2001). Mutation of human molybdenum cofactor sulfurase gene is responsible for classical xanthinuria type II. *Biochemical and Biophysical Research Communications* **282**, 1194-200.

Invitrogen. (2002). Gateway® Recombination Cloning: Entry Clones. . In *Instruction Manual*, vol. Catalog no. 11813-011, pp. 17. Carlsbad, USA: www.invitrogen.com.

Invitrogen. (2010). Gateway® Technology with Clonase™ II. In *A universal technology to clone DNA sequences for functional analysis and expression in multiple systems*, vol. Catalog nos 12535-029, pp. 4. Carlsbad, USA: www.invitrogen.com.

Jackson, F. R. (1978). Autonomous timer in Malpighian tubules. *Science* **200**, 1185-6.

Kaback, M., Lim-Steele, J., Dabholkar, D., Brown, D., Levy, N. and Zeiger, K. (1993). Tay-Sachs Disease--Carrier screening, prenatal diagnosis, and the molecular era: an international perspective, 1970 to 1993. *Jama* **270**, 2307.

Kaback, M. M. (2000). Population-based genetic screening for reproductive counseling: the Tay-Sachs disease model. *European Journal of Pediatrics* **159**, 192-195.

Kamdar, K. P., Primus, J. P., Shelton, M. E., Archangeli, L. L., Wittle, A. E. and Finnerty, V. (1997). Structure of the molybdenum cofactor genes in *Drosophila*. *Biochemical Society Transactions* **25**, 778-83.

Kamleh, M. A., Hobani, Y., Dow, J. A. and Watson, D. G. (2008). Metabolomic profiling of *Drosophila* using liquid chromatography Fourier transform mass spectrometry. *FEBS Lett* **582**, 2916-22.

Kamleh, M. A., Hobani, Y., Dow, J. A., Zheng, L. and Watson, D. G. (2009). Towards a platform for the metabonomic profiling of different strains of *Drosophila melanogastre* using liquid chromatography-Fourier transform mass spectrometry. *Febs J* **276**, 6798-809.

Katzen, F. (2007). Gateway recombinational cloning: a biological operating system. *Expert Opinion on Drug Discovery* **2**, 571-589.

Kawase, H., Hasegawa, T., Hashimoto, H., Noto, T. and Nakajima, T. (1994). A study on the metabolism of spermidine in mammals: purification and identification of a newly identified metabolite, 2-oxo-1-pyrrolidinepropionic acid, in rat urine. *J Biochem* **115**, 356-61.

Keller, E. C., Jr. and Glassman, E. (1965). Phenocopies of the *ma-l* and *ry* mutants of *Drosophila melanogastre*: inhibition in vivo of xanthine dehydrogenase by 4-hydroxypyrazolo(3,4-d)pyrimidine. *Nature* **208**, 202-3.

Kennerdell, J. R. and Carthew, R. W. (2000). Heritable gene silencing in *Drosophila* using double-stranded RNA. *Nat Biotech* **18**, 896-898.

Kerr, M. K., Martin, M. and Churchill, G. A. (2000). Analysis of variance for gene expression microarray data. *J Comput Biol* **7**, 819-37.

Kind, T. (2010). Mass Spectrometry Adduct Calculator, vol. 2011. Davis, California: Metabollomics Fiehn Lab.

Kondo, T., Inagaki, S., Yasuda, K. and Kageyama, Y. (2006). Rapid construction of *Drosophila* RNAi transgenes using pRISE, a P-element-mediated transformation vector exploiting an *in vitro* recombination system. *Genes and Genetic Systems* **81**, 129-34.

Kral, L. G., Johnson, D. H., Burnett, J. B. and Friedman, T. B. (1986). Cloning a cDNA for *Drosophila melanogastre* urate oxidase. *Gene* **45**, 131-7.

Kronn, D., Jansen, V. and Ostrer, H. (1998). Carrier screening for cystic fibrosis, Gaucher disease, and Tay-Sachs disease in the Ashkenazi Jewish population: the first 1000 cases at New York University Medical Center, New York, NY. *Archives of internal medicine* **158**, 777.

Lamy, P., Grove, J. and Wiuf, C. (2011). A review of software for microarray genotyping. *Hum Genomics* **5**, 304-9.

Lanpher, B., Brunetti-Pierri, N. and Lee, B. (2006). Inborn errors of metabolism: the flux from Mendelian to complex diseases. *Nat Rev Genet* **7**, 449-60.

Lee, Y. S. and Carthew, R. W. (2003). Making a better RNAi vector for *Drosophila*: use of intron spacers. *Methods* **30**, 322-9.

Leung, Y. F. and Cavalieri, D. (2003). Fundamentals of cDNA microarray data analysis. *TRENDS in Genetics* **19**, 649-659.

Levskaya, A., Chevalier, A. A., Tabor, J. J., Simpson, Z. B., Lavery, L. A., Levy, M., Davidson, E. A., Scouras, A., Ellington, A. D. and Marcotte, E. M. (2005). Synthetic biology: engineering Escherichia coli to see light. *Nature* **438**, 441-442.

Lewin, R. (1986). First success with reverse genetics. *Science* **233**, 159-60.

Lindon, J. C., Holmes, E. and Nicholson, J. K. (2006). Metabonomics techniques and applications to pharmaceutical research & development. *Pharmaceutical research* **23**, 1075-1088.

Lipshutz, R. J., Fodor, S. P. A., Gingeras, T. R. and Lockhart, D. J. (1999). High density synthetic oligonucleotide arrays. *Nature genetics* **21**, 20-24.

Makarov, A., Denisov, E., Lange, O. and Horning, S. (2006). Dynamic range of mass accuracy in LTQ Orbitrap hybrid mass spectrometer. *J Am Soc Mass Spectrom* **17**, 977-82.

Maloley, P. A. and R.Westfall, G. (2000). Gout and hyperurecimia. In *Textbook Of Therapeutics: Drug And Disease Management*, (ed. D. R. G. Eric T. Herfindal). USA: Lippincott Williams.

Mamer, O. A., Crawhall, J. C. and Tjoa, M. S. S. (1971). The identification of urinary acids by coupled gas chromatography-mass spectrometry. *Clinica Chimica Acta* **32**, 171-184.

Martin, H. M., Hancock, J. T., Salisbury, V. and Harrison, R. (2004). Role of xanthine oxidoreductase as an antimicrobial agent. *Infection and immunity* **72**, 4933.

Martins, A. M. (1999). Inborn errors of metabolism: a clinical overview. *Sao Paulo Medical Journal* **117**, 251-265.

Mashego, M. R., Rumbold, K., De Mey, M., Vandamme, E., Soetaert, W. and Heijnen, J. J. (2007). Microbial metabolomics: past, present and future methodologies. *Biotechnology letters* **29**, 1-16.

McGall, G., Labadie, J., Brock, P., Wallraff, G., Nguyen, T. and Hinsberg, W. (1996). Light-directed synthesis of high-density oligonucleotide arrays using semiconductor photoresists. *Proc Natl Acad Sci U S A* **93**, 13555-60.

McKay, C. M. (1972). Quantitative measurement of pteridines. *Drosophila Information Service* **48**, 62.

McLuckey, S. A. and Wells, J. M. (2001). Mass analysis at the advent of the 21st century. *Chem. Rev* **101**, 571-606.

Meneshian, A. and Bulkley, G. B. (2002). The physiology of endothelial xanthine oxidase: from urate catabolism to reperfusion injury to inflammatory signal transduction. *Microcirculation* **9**, 161-75.

Myerowitz, R. and Costigan, F. C. (1988). The major defect in Ashkenazi Jews with Tay-Sachs disease is an insertion in the gene for the alpha-chain of beta-hexosaminidase. *Journal of Biological Chemistry* **263**, 18587.

Nauli, S. M., Alenghat, F. J., Luo, Y., Williams, E., Vassilev, P., Li, X., Elia, A. E., Lu, W., Brown, E. M., Quinn, S. J. et al. (2003). Polycystins 1 and 2 mediate mechanosensation in the primary cilium of kidney cells. *Nat Genet* **33**, 129-37.

Ngu, L. H., Afroze, B., Chen, B. C., Affandi, O. and Zabedah, M. Y. (2009). Molybdenum cofactor deficiency in a Malaysian child. *Singapore Med J* **50**, e365-7.

O'Donnell, M. J., Dow, J. A., Huesmann, G. R., Tublitz, N. J. and Maddrell, S. H. (1996). Separate control of anion and cation transport in Malpighian tubules of *Drosophila* Melanogaster. *J Exp Biol* **199**, 1163-75.

O'Donnell, M. J., Rheault, M. R., Davies, S. A., Rosay, P., Harvey, B. J., Maddrell, S. H., Kaiser, K. and Dow, J. A. (1998). Hormonally controlled chloride movement across *Drosophila* tubules is via ion channels in stellate cells. *Am J Physiol* **274**, R1039-49.

O'Hare, K. and Rubin, G. M. (1983). Structures of P transposable elements and their sites of insertion and excision in the *Drosophila melanogastre* genome. *Cell* **34**, 25-35.

O'Kane, C. J. and Gehring, W. J. (1987). Detection in situ of genomic regulatory elements in *Drosophila*. *Proc Natl Acad Sci U S A* **84**, 9123-7.

Oldiges, M., Lutz, S., Pflug, S., Schroer, K., Stein, N. and Wiendahl, C. (2007). Metabolomics: current state and evolving methodologies and tools. *Appl Microbiol Biotechnol* **76**, 495-511.

Oliver, S. G., Winson, M. K., Kell, D. B. and Baganz, F. (1998). Systematic functional analysis of the yeast genome. *Trends Biotechnol* **16**, 373-8.

Olsen, J. V., de Godoy, L. M., Li, G., Macek, B., Mortensen, P., Pesch, R., Makarov, A., Lange, O., Horning, S. and Mann, M. (2005). Parts per million mass accuracy on an Orbitrap mass spectrometer via lock mass injection into a C-trap. *Mol Cell Proteomics* **4**, 2010-21.

Orkin, S. H. (1986). Reverse genetics and human disease. *Cell* **47**, 845-50.

Pacher, P., Nivorozhkin, A. and Szabo, C. (2006). Therapeutic effects of xanthine oxidase inhibitors: renaissance half a century after the discovery of allopurinol. *Pharmacol Rev* **58**, 87-114.

Patel, G. K., Davies, W. L., Price, P. P. and Harding, K. G. (2010). Ulcerated tophaceous gout. *International Wound Journal*.

Patel, V., Chowdhury, R. and Igarashi, P. (2009). Advances in the pathogenesis and treatment of polycystic kidney disease. *Curr Opin Nephrol Hypertens* **18**, 99-106.

Pauling, L., Robinson, A. B., Teranishi, R. and Cary, P. (1971). Quantitative analysis of urine vapor and breath by gas-liquid partition chromatography. *Proc Natl Acad Sci U S A* **68**, 2374.

Pea, F. (2005). Pharmacology of drugs for hyperuricemia. Mechanisms, kinetics and interactions. *Contrib Nephrol* **147**, 35-46.

Pinksy, L. (1972). Inborn errors of metabolism: principles and their applications. *Can Med Assoc J* **106**, 677-690.

Ramazzina, I., Folli, C., Secchi, A., Berni, R. and Percudani, R. (2006). Completing the uric acid degradation pathway through phylogenetic comparison of whole genomes. *Nature chemical biology* **2**, 144-148.

Rashed, M. S., Bucknall, M. P., Little, D., Awad, A., Jacob, M., Alamoudi, M., Alwattar, M. and Ozand, P. T. (1997). Screening blood spots for inborn errors of metabolism by electrospray tandem mass spectrometry with a microplate batch process and a computer algorithm for automated flagging of abnormal profiles. *Clin Chem* **43**, 1129-41.

Reaume, A. G., Clark, S. H. and Chovnick, A. (1989). Xanthine dehydrogenase is transported to the *Drosophila* eye. *Genetics* **123**, 503-9.

Reiter, L. T., Potocki, L., Chien, S., Gribskov, M. and Bier, E. (2001). A systematic analysis of human disease-associated gene sequences in *Drosophila melanogastre*. *Genome Research* **11**, 1114-25.

Revesz, K. M., Landwehr, J. M. and Keybl, J. (2002). Delta13C and delta18O isotopic composition of CaCO3 measured by continuous flow isotope ratio mass spectrometry: statistical evaluation and verification by application to Devils Hole core DH-11 calcite. *Rapid Commun Mass Spectrom* **16**, 2102-14.

Rossetti, S., Consugar, M. B., Chapman, A. B., Torres, V. E., Guay-Woodford, L. M., Grantham, J. J., Bennett, W. M., Meyers, C. M., Walker, D. L. and Bae, K. (2007). Comprehensive molecular diagnostics in autosomal dominant polycystic kidney disease. *Journal of the American Society of Nephrology* **18**, 2143.

Rubin, G. M. and Spradling, A. C. (1983). Vectors for P element-mediated gene transfer in *Drosophila*. *Nucleic Acids Research* **11**, 6341-51.

Ruddle, F. H. (1982). Reverse genetics as a means of understanding and treating genetic disease. *Advances in Neurology* **35**, 239-42.

Saadallah, A. A. and Rashed, M. S. (2007). Newborn screening: experiences in the Middle East and North Africa. *Journal of Inherited Metabolic Disease* **30**, 482-9.

Sachidanandam, R., Weissman, D., Schmidt, S. C., Kakol, J. M., Stein, L. D., Marth, G., Sherry, S., Mullikin, J. C., Mortimore, B. J. and Willey, D. L. (2001). A map of human genome sequence variation containing 1.42 million single nucleotide polymorphisms. *Nature* **409**, 928-933.

Salek, R. M., Maguire, M. L., Bentley, E., Rubtsov, D. V., Hough, T., Cheeseman, M., Nunez, D., Sweatman, B. C., Haselden, J. N. and Cox, R. D. (2007). A metabolomic comparison of urinary changes in type 2 diabetes in mouse, rat, and human. *Physiological Genomics* **29**, 99.

Sambrook, J. and Russell, D. (2001). Molecular cloning: A laboratory manual. . New York: Cold Spring Harbor Laboratory Press, Cold Spring Harbor, .

Schwarz, G. and Mendel, R. R. (2006). Molybdenum cofactor biosynthesis and molybdenum enzymes. *Annu Rev Plant Biol* **57**, 623-47.

Sentry, J. W. and Kaiser, K. (1992). P-element transposition and targeted manipulation of the *Drosophila* genome. *Trends in Genetics* **8**, 329-331.

Shinozaki, K., Kashiwagi, A., Nishio, Y., Okamura, T., Yoshida, Y., Masada, M., Toda, N. and Kikkawa, R. (1999). Abnormal biopterin metabolism is a major cause of impaired endothelium-dependent relaxation through nitric oxide/O2- imbalance in insulin-resistant rat aorta. *Diabetes* **48**, 2437-45.

Shulaev, V. (2006). Metabolomics technology and bioinformatics. *Briefings in bioinformatics* **7**, 128.

Singh, S. R., Liu, W. and Hou, S. X. (2007). The adult *Drosophila* Malpighian tubules are maintained by multipotent stem cells. *Cell Stem Cell* **1**, 191-203.

Sozen, M. A., Armstrong, J. D., Yang, M., Kaiser, K. and Dow, J. A. (1997). Functional domains are specified to single-cell resolution in a *Drosophila* epithelium. *Proc Natl Acad Sci U S A* **94**, 5207-12.

Spector, T. (1988). Oxypurinol as an inhibitor of xanthine oxidase-catalyzed production of superoxide radical. *Biochemical pharmacology* **37**, 349-352.

Stayner, C. and Zhou, J. (2001). Polycystin channels and kidney disease. *Trends Pharmacol Sci* **22**, 543-6.

Sturtevant, A. H. (1955). [New mutants report.]. *Drosophila Information Service* **29**, 75.

Sullivan, D. T. and Sullivan, M. C. (1975). Transport defects as the physiological basis for eye color mutants of *Drosophila melanogastre*. *Biochem Genet* **13**, 603-13.

Tadmouri, G. O., Nair, P., Obeid, T., Al Ali, M. T., Al Khaja, N. and Hamamy, H. A. (2009). Consanguinity and reproductive health among Arabs. *Reprod Health* **6**, 17.

Terhzaz, S., Finlayson, A. J., Stirrat, L., Yang, J., Tricoire, H., Woods, D. J., Dow, J. A. and Davies, S. A. (2010). Cell-specific inositol 1,4,5 trisphosphate 3-kinase mediates epithelial cell apoptosis in response to oxidative stress in *Drosophila*. *Cell Signal* **22**, 737-48.

Thibault, S. T., Singer, M. A., Miyazaki, W. Y., Milash, B., Dompe, N. A., Singh, C. M., Buchholz, R., Demsky, M., Fawcett, R., Francis-Lang, H. L. et al. (2004). A complementary transposon tool kit for Drosophila melanogaster using P and piggyBac. *Nat Genet* **36**, 283-7.

Thony, B., Auerbach, G. and Blau, N. (2000). Tetrahydrobiopterin biosynthesis, regeneration and functions. *Biochem J* **347 Pt 1**, 1-16.

Tipton, P. A. (2006). Urate to allantoin, specifically (S)-allantoin. *Nature chemical biology* **2**, 124-125.

Torrie, L. S., Radford, J. C., Southall, T. D., Kean, L., Dinsmore, A. J., Davies, S. A. and Dow, J. A. (2004). Resolution of the insect ouabain paradox. *Proc Natl Acad Sci U S A* **101**, 13689-93.

Vast_Scientific_Inc. (2010). SIEVE Software ver 1.3 (online). Available from http://www.vastscientific.com/sieve/index.html Last accessed on 5 December 2010.

Vogels, G. D. and Van der Drift, C. (1976). Degradation of purines and pyrimidines by microorganisms. *Bacteriol Rev* **40**, 403-68.

Vorbach, C., Harrison, R. and Capecchi, M. R. (2003). Xanthine oxidoreductase is central to the evolution and function of the innate immune system. *Trends Immunol* **24**, 512-7.

Vorbach, C., Scriven, A. and Capecchi, M. R. (2002). The housekeeping gene xanthine oxidoreductase is necessary for milk fat droplet enveloping and secretion: gene sharing in the lactating mammary gland. *Genes Dev* **16**, 3223-35.

Wahl, R. C., Warner, C. K., Finnerty, V. and Rajagopalan, K. V. (1982). *Drosophila melanogastre ma-l* mutants are defective in the sulfuration of desulfo Mo hydroxylases. *Journal of Biological Chemistry* **257**, 3958.

Wallrath, L. L., Burnett, J. B. and Friedman, T. B. (1990). Molecular characterization of the *Drosophila melanogastre urate oxidase* gene, an ecdysone-repressible gene expressed only in the Malpighian tubules. *Mol. Cell. Biol.* **10**, 5114-5127.

Wallrath, L. L. and Friedman, T. B. (1991). Species differences in the temporal pattern of *Drosophila* urate oxidase gene expression are attributed to trans-acting regulatory changes. *Proc Natl Acad Sci U S A* **88**, 5489-93.

Wang, J., Kean, L., Yang, J., Allan, A. K., Davies, S. A., Herzyk, P. and Dow, J. A. (2004). Function-informed transcriptome analysis of *Drosophila* renal tubule. *Genome Biol* **5**, R69.

Wang, Q., Zhao, C., Bai, L., Deng, X. and Wu, C. (2008). Reduction of drosopterin content caused by a 45-nt insertion in Henna pre-mRNA of *Drosophila melanogastre*. *Sci China C Life Sci* **51**, 702-10.

Watson, D. G. (2010). The potential of mass spectrometry for the global profiling of parasite metabolomes. *Parasitology* **137**, 1409-23.

Weavers, H., Prieto-Sanchez, S., Grawe, F., Garcia-Lopez, A., Artero, R., Wilsch-Brauninger, M., Ruiz-Gomez, M., Skaer, H. and Denholm, B. (2009). The insect nephrocyte is a podocyte-like cell with a filtration slit diaphragm. *Nature* **457**, 322-6.

Wessing, A., D. Eichelberg. (1978). Malpighian tubules, rectal papillae and excretion. London: Academic Press.

Wessing, A. and Eichelberg, D. (1978). Malpighian tubules, rectal papillae and excretion. *The genetics and biology of Drosophila* **2**, 1-42.

Wieczorek, H., Putzenlechner, M., Zeiske, W. and Klein, U. (1991). A vacuolar-type proton pump energizes K+/H+ antiport in an animal plasma membrane. *J Biol Chem* **266**, 15340-7.

Wishart, D. S. (2008). Applications of metabolomics in drug discovery and development. *Drugs in R&# 38; D* **9**, 307-322.

Wu, X., Wakamiya, M., Vaishnav, S., Geske, R., Montgomery, C., Jr., Jones, P., Bradley, A. and Caskey, C. T. (1994). Hyperuricemia and urate nephropathy in urate oxidase-deficient mice. *Proc Natl Acad Sci U S A* **91**, 742-6.

Wu, Z. and Irizarry, R. A. (2004). Preprocessing of oligonucleotide array data. *Nat Biotechnol* **22**, 656-8; author reply 658.

Yoder, B. K. (2007). Role of primary cilia in the pathogenesis of polycystic kidney disease. *J Am Soc Nephrol* **18**, 1381-8.

Yokomizo, H., Yoshimatsu, K., Hashimoto, M., Ishibashi, K., Umehara, A., Yoshida, K., Fujimoto, T., Watanabe, K. and Ogawa, K. (2004). Prophylactic efficacy of allopurinol ice ball for leucovorin/5-fluorouracil therapy-induced stomatitis. *Anticancer Res* **24**, 1131-4.

Zhang, Q., Taulman, P. D. and Yoder, B. K. (2004). Cystic kidney diseases: all roads lead to the cilium. *Physiology (Bethesda)* **19**, 225-30.